

# **Reservoir prognosis of the Gassum Formation and the Karlebo Member within two areas of interest in northern Copenhagen**

The EUDP project "Geothermal pilot hole, phase 1b"

Henrik Vosgerau, Ulrik Gregersen, Morten Leth Hjuler,  
Hanne Dahl Holmslykke, Lars Kristensen, Sofie Lindström,  
Anders Mathiesen, Carsten Møller Nielsen, Mette Olivarius,  
Gunver Krarup Pedersen & Lars Henrik Nielsen



# **Reservoir prognosis of the Gassum Formation and the Karlebo Member within two areas of interest in northern Copenhagen**

The EUDP project "Geothermal pilot hole, phase 1b"

Henrik Vosgerau, Ulrik Gregersen, Morten Leth Hjuler, Hanne Dahl Holmslykke,  
Lars Kristensen, Sofie Lindström, Anders Mathiesen, Carsten Møller Nielsen,  
Mette Olivarius, Gunver Krarup Pedersen & Lars Henrik Nielsen

# Contents

<b>Preface</b>	<b>6</b>
<b>Résumé</b>	<b>8</b>
<b>1. Geological setting</b>	<b>19</b>
<b>2. Data basis</b>	<b>23</b>
<b>3. Sequence stratigraphic framework</b>	<b>26</b>
<b>4. Biostratigraphy</b>	<b>29</b>
4.1 Palynostratigraphic framework.....	29
4.1.1 Dinoflagellate cyst zonation of the Danish Basin .....	32
4.1.2 Spore-pollen zonation of the Danish Basin .....	32
4.2 Methods.....	35
4.3 Stratigraphic breakdown of the investigated wells.....	36
4.3.1 Margretheholm-1 .....	36
4.3.2 Karlebo-1A.....	40
4.3.3 Höllviksnäs-1/Höllviken-2 .....	45
4.3.4 Lavø-1.....	49
4.3.5 Stenlille-1 .....	51
4.3.6 Stenlille-2.....	55
4.3.7 Stenlille-5.....	57
4.3.8 Stenlille-6.....	58
4.3.9 Stenlille-15.....	59
4.4 Concluding remarks .....	59
<b>5. Seismic interpretation and mapping</b>	<b>60</b>
5.1 Database and workflow.....	60
5.2 Seismic stratigraphy and facies .....	60
5.2.1 Regional well tie, stratigraphy and overall unit thicknesses.....	61
5.2.2 Seismic facies.....	61
5.2.3 Faults and folds .....	63
5.3 Concluding remarks .....	63
<b>6. Reservoir properties</b>	<b>69</b>
6.1 Petrography and diagenesis .....	69
6.1.1 Samples and methods.....	69
6.1.2 Detrital components.....	70
6.1.3 Authigenic phases .....	71
6.1.4 Porosity and permeability .....	72
6.1.5 Discussion .....	72
6.1.6 Conclusions .....	73

6.2	Provenance analysis .....	79
6.2.1	Samples and methods.....	79
6.2.2	Zircon ages.....	79
6.2.3	Discussion .....	80
6.2.4	Conclusions.....	82
6.3	Reservoir prognosis .....	85
6.3.1	Reservoir prognosis for the western area.....	87
6.3.2	Reservoir prognosis for the eastern area.....	90
6.3.3	Geothermal potential .....	92
6.3.4	Estimation of reservoir parameters .....	92
<b>7.</b>	<b>Production capacity</b> .....	<b>101</b>
7.1	Static and dynamic modelling .....	101
7.1.1	Input data.....	101
7.1.2	Static modelling procedure.....	102
7.1.3	Dynamic modelling procedure.....	103
7.1.4	Simulations cases .....	104
7.1.5	Results.....	105
7.2	Productivity evaluation .....	106
<b>8.</b>	<b>Mineral composition of mudstones</b> .....	<b>113</b>
8.1	Introduction.....	113
8.2	Methods.....	113
8.2.1	Bulk mineralogy .....	113
8.2.2	Clay mineralogy.....	114
8.3	Results .....	115
8.3.1	TOC content .....	115
8.3.2	Silt content.....	115
8.3.3	Bulk mineralogy .....	117
8.3.4	Clay mineralogy.....	122
8.4	Discussion .....	123
8.5	Main results.....	124
<b>9.</b>	<b>Formation damage control</b> .....	<b>125</b>
9.1	Introduction.....	125
9.2	Formation damage .....	125
9.2.1	Clay swelling.....	125
9.2.2	Fines migration .....	126
9.3	Formation damage control .....	127
9.3.1	Identification of formation damage .....	128
9.3.2	Quantification of reservoir formation damage.....	129
9.3.3	Remediation of formation damage .....	129
9.3.4	Prevention of formation damage .....	130
9.4	Concluding remarks .....	130
	<b>References</b> .....	<b>132</b>

**Appendices 1–5:** Stratigraphic summary charts of wells.

**Appendix 6:** Description of mudstone cuttings selected for bulk mineralogy analysis.

**Appendix 7:** Drilling problems reported in completion reports of selected wells.

**Enclosure 1:** Log plot - lithostratigraphy, sequence stratigraphy and bio events.

**Enclosure 2:** Log plot - lithostratigraphy, sequence stratigraphy and samples for bulk- and clay mineralogy analysis

## Preface

The present report documents and outlines the results of Work Package 2 (WP2), dealing with the subsurface, of Phase 1b of the project “Geothermal pilot hole” which is financially supported by EUDP (Energiteknologisk udvikling og demonstration) of the Danish Energy Agency. The main purpose of WP2 is to provide a well-constrained prognosis of relevant reservoir parameters (depth, thickness, transmissivity, production capacity etc.) of the Upper Triassic – Lower Jurassic Gassum Formation and secondary the overlying Lower Jurassic Karlebo Member within two areas of interest in northern Copenhagen, which were pointed out in the first phase of the project (Phase 1a). The obtained results in WP2 will form the geological basis for a decision on the location of an exploration well to be drilled in Phase 2 of the project (yet to be granted).

A comprehensive résumé of the outcome of WP2 is given in the following which also forms an input to the overall reporting of Phase 1b (compiled by Ross Engineering). Chapter 1 provides an introduction to the regional geological setting and the general structure of the subsurface in the Danish onshore area whereas the succeeding chapters document the data foundation and the work and results of the various tasks which have been undertaken in WP2. The various tasks are reported in details by the specialists involved, and include:

- Establishing of a sequence stratigraphic framework for the Gassum Formation–Fjerritslev Formation interval based on a log correlation of selected wells from Stenlille and eastern and northern Zealand and data on biostratigraphy, lithology and depositional environments. The sequence stratigraphic framework elucidates the variation in the lithological composition of the Gassum Formation, the Karlebo Member and the overlying parts of the Fjerritslev Formation in eastern Zealand and indicates to which degree their composition can be predicted at a future drilling location. Furthermore, it has formed an important basis for the selection of representative core data from existing wells (in particular the Stenlille wells) for the evaluation of reservoir values and associated uncertainties in the areas of interest.
- Palynological analysis of the Upper Triassic–Lower Jurassic succession on Zealand, encompassed by the Gassum and Fjerritslev Formations in deep wells. The results, which combine new and previously analyzed data, are used to establish a biostratigraphic breakdown of the succession, based on stratigraphic ranges and quantitative abundances of spores and pollen and marine dinoflagellate cysts. The palynology also provides information on the depositional environments of the sedimentary succession. The improved biostratigraphy has helped to constrain the sequence stratigraphic framework.
- Detailed analysis of existing seismic data collected closest to the two areas of interest for the purpose of identifying and defining the Gassum Formation and the Karlebo Member and to estimate their depth and thickness as well as interpreting possible internal seismic facies.
- Characterizing and estimating reservoir quality based on petrography, diagenesis and provenance analysis, petrophysical log interpretations and porosity, permeability and temperature data.
- Preliminary estimates (modeling) of production capacities for potential drilling sites based on input values (e.g. reservoir values) obtained in the various studies above.

- Evaluation of drilling risks related to the clayey overburden of the Fjerritslev Formation based on clay mineralogical analysis and an examination of completion reports of deep wells at Zealand in order to list drilling problems encountered in the Fjerritslev Formation.
- A literature study on how to prevent formation damage, which is a well-known phenomenon in geothermal as well as oil bearing reservoirs, as this leads to reduced productivity in the reservoirs.

# Résumé

## Background of Work Package 2 (WP2)

The present study provides a prognosis of the geothermal potential for the Gassum Formation and the Karlebo Member<sup>1</sup> in two areas of interest within northern Copenhagen. The two areas were selected as being relevant for geothermal heat exploration in Phase 1a of the project based on infrastructure considerations (e.g. positions of existing district heating plants, current and future district heat networks and coupling points) as well as the composition of the subsurface in the larger Copenhagen area.

The Gassum Formation and the Karlebo Member were treated as a composite unit in Phase 1a of the project as the boundary between them is difficult to define in existing seismic data. However, the recognition of a boundary between the two units has been possible in the present phase of the project, based on a detailed and comprehensive interpretation of the seismic lines closest to the two areas of interest, guided by a sequence stratigraphic interpretation of the composite succession. As a consequence of this, more accurate estimates of depth, thickness and reservoir properties are given for both the Gassum Formation and the Karlebo Member in the present report. The Karlebo Member consists of sandstone beds that are petrographically very similar to those in the Gassum Formation, but are in general separated by thicker mudstone intervals than the sandstones are in the Gassum Formation. The Karlebo Member forms the lower part of the Fjerritslev Formation in northern and eastern Zealand. The remaining upper part of the Fjerritslev Formation in Zealand, as well as the entire Fjerritslev Formation in Jutland, consists almost entirely of mudstones and claystones. Petrophysical log data from deep wells shows that the Gassum Formation in general contains the largest amount of reservoir sandstones and is thus considered to be the main target for geothermal recovery in the two areas of interest.

A secondary scope of WP2 is to evaluate if the clay mineralogy in mudstone intervals of the Gassum Formation, the Karlebo Member, and especially in the thick mudstone-dominated part of the Fjerritslev Formation (i.e. the overburden of the potential sandstone reservoirs) may cause a particular drilling risk, e.g. due to a high content of reactive clay minerals. Finally, the geological data form input for considerations about development of drilling equipment, selection of well completion techniques and logging tools and for financial assessment of the profitability of incorporating a geothermal plant in the district heating system; all subjects which are reported in other work packages and/or are to be dealt with in Phase 2 of the project.

---

<sup>1</sup>Named "Lower Jurassic unit" in the Phase 1a report, but a formal definition of the Karlebo Member of the Fjerritslev Formation is planned as a future publication. The Karlebo Member encompasses the Lower Jurassic sandstones overlying the Gassum Formation.

## Areas of interest

The two areas of interest are separated by a NNW–SSE striking fault, the Amager Fault, which form part of a major fault zone running from north of Zealand into the HGS license area as outlined in Phase 1a of the project. GEUS’ standard “rule of thumb” is to place a geothermal well at a distance of minimum 2 km from a recognized fault as modelling indicates that the reservoir flow is not influenced if such a distance is kept, even if the fault is modelled as a non-permeable barrier (which it seldom is). The distance of 2 km from the areas of interest to the fault is thus a very conservative precaution. The detailed seismic mapping undertaken in the present phase of the project reveals that the fault should instead be described as a fault zone, approximately 1 km wide and containing a number of faults with different displacement. The Gassum Formation and the Karlebo Member are thicker and occur at a deeper level in the eastern area compared to the western area, indicating that down-faulting towards the east took place during deposition (Fig. 1). In contrast, the overlying, mudstone-dominated part of the Fjerritslev Formation shows no marked thickness variation across the fault, thereby indicating that faulting had ceased when this part of the succession was deposited. The fault zone was most likely affected by a later compressional tectonic phase of Cretaceous age or younger as seen by the occurrence of vertical faults which separate minor inversion ridges and extend up into the Cretaceous chalk. Minor progradational seismic reflectors and subtle troughs are observed within the Gassum Formation and the Karlebo Member and point towards a dynamic depositional regime. Based on GEUS’ general knowledge of the Upper Triassic–Lower Jurassic succession in the rim of the Norwegian-Danish Basin, such features may be interpreted as reflecting depositional and erosional processes within near-coastal and fluvial environments.

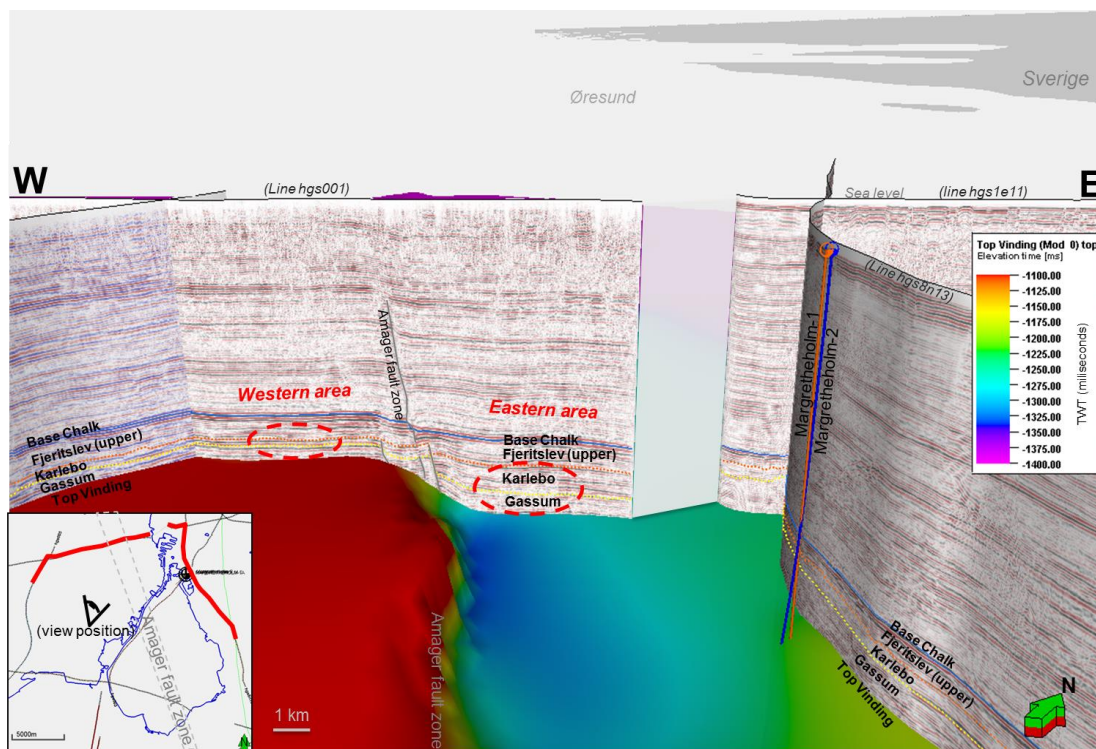


**Figure 1.** Seismic lines in 3D view seen towards northern Copenhagen and Margretheholm in northern Amager. View position and direction are marked on the inserted location map in lower left corner of the figure as is the overall trend of the Amager Fault zone. The colored surface reflects the depth to and morphology of the Top Vinding surface corresponding to the base of the Gassum Formation. The surface clearly illustrates the fault controlled deeper position of the eastern area compared to the western area. It is also evident that the thickness of the Gassum Formation and the Karlebo Member, marked on the seismic profiles, becomes considerably thicker from the western area across the Amager Fault zone to the eastern area. In contrast, the overlying, mudstone-dominated part of Fjeritslev Formation shows no marked thickness variation across the fault, indicating that faulting had ceased when this part of the succession was formed. Depths to the Top Vinding surface is given in TWT (see inserted scale).

The Gassum Formation is around 200 m thick and has its top c. 2000 m below sea level in the eastern area whereas it is around 150 m thick and has its top c. 1750 m below sea level in the western area (Table 1). The porosity and permeability values for the Gassum Formation are estimated to be slightly lower in the eastern area compared to the western area, perhaps related to the deeper burial depth of the eastern area as permeability and porosity in general decrease with increasing depth. The mean porosity and permeability of the reservoir sandstones in the eastern area are thus estimated to 21% and 313 mD, respectively, whereas they are estimated to 25% and 375 mD for the western area (Table 1). The proportion of reservoir sandstone in the formation (Potential reservoir sand in Table 1) is estimated to 80 m and 75 m for the eastern area and western area, respectively. In addition, the reservoir transmissivity for the Gassum Formation is estimated to 25 Darcy-meter for the eastern area and 28 Darcy-meter for the western area. The reservoir transmissivity is an important parameter as it expresses the performance of the reservoir, given by multiplying the estimated thickness of potential reservoir sand with the estimated reservoir permeability. As a rule of thumb, the reservoir transmissivity of a sandstone interval should be

greater than 10 Darcy-meter<sup>2</sup> in order to constitute a potential geothermal reservoir in the Danish area. Thus, the Gassum Formation is considered suitable for geothermal exploitation in both areas.

Although the estimated porosity, permeability and transmissivity values are slightly higher in the western area this does not necessary qualify the reservoir properties of the Gassum Formation as being best in this area. This is because the geothermal water of the Gassum Formation in the eastern area benefits from having higher temperatures than in the western area (65 °C contra 57 °C, respectively, in the middle of the Gassum Formation, Table 1) as consequence of the deeper subsurface location of the Gassum Formation in this area.

The secondary reservoir target, the Karlebo Member, is c. 200 m thick and has its top c. 1800 m below sea level in the eastern area whereas it is around 100 m thick and has its top c. 1650 m below sea level in the western area (Table 1). These depths imply that temperatures of 54 °C and 59 °C are attributed to the middle of the Karlebo Member in the western area and eastern area, respectively. The depth difference of 150 m between the western area and the eastern area is not reflected by the estimated porosity and permeability values. In fact, the permeability is estimated to be higher in the eastern area than the western area, 375 mD contra 300 mD, whereas the porosity is almost the same; 23% for the eastern area and 22% for the western area (Table 1). Furthermore, the proportion of reservoir sandstone in the member is estimated to be twice as high in the eastern area compared to the western area (40 m contra 20 m as shown in Table 1). This has a major impact on the reservoir transmissivity, which is estimated to be 15 Darcy-meter for the eastern area whereas it is 6 Darcy-meter for the western area. Seen in isolation, the Karlebo Member can therefore not be considered as a suitable geothermal reservoir in the western area based on the present assessments and calculations, which are outlined in the following chapters. Nevertheless, it may contribute to the geothermal production if geothermal energy is produced simultaneously from the Gassum Formation and the directly overlying Karlebo Member. This is also the case in the eastern area where the Karlebo Member furthermore forms a secondary geothermal reservoir target in its own.

The reservoir estimates in Table 1 largely build on petrophysical evaluations of relevant log-data from deep wells combined with porosity and permeability measurements on core material. With respect to the western area, primarily data from Lavø-1 along with data from the Stenlille and Margretheholm wells were used, whereas the reservoir properties of the eastern area were predicted mainly on the basis of data from the Margretheholm wells and the Karlebo-1A well.

---

<sup>2</sup> *The mean gas transmissivity of the reservoir is considered reasonable if it exceeds 8 Darcy-meter according to Mathiesen et al. (2013). GEUS estimates that this value corresponds approximately to a fluid transmissivity of 10 Darcy-meter.*

**Table 1.** Estimated reservoir values for the Gassum Formation and the Karlebo Member in the two areas of interest. Uncertainty estimates of the shown parameter values are given in section 6.3.

	Gassum Fm		Karlebo Mb	
	Western area	Eastern area	Western area	Eastern area
<b>Macro reservoir parameters</b>				
Depth to top [MBSL]	1750	2000	1650	1800
Thickness [m]	150	200	100	200
<b>Sandstone proportion</b>				
Thickness of Gross sand [m]	101	100	40	80
Thickness of potential reservoir sand <sup>1</sup> [m]	75	80	20	40
Potential reservoir sand/formation <sup>2</sup>	0.5	0.4	0.2	0.2
Potential reservoir sand/Gross sand <sup>3</sup>	0.7	0.8	0.5	0.5
<b>Water conducting properties (reservoir sand)</b>				
Porosity [%]	25	21	23	22
Gas-permeability [mD]	300	250	240	300
Reservoir-permeability <sup>4</sup> [mD]	375	313	300	375
Reservoir-transmissivity (Kh) <sup>5</sup> [Dm]	28	25	6	15
<b>Temperature</b>				
Temperature <sup>6</sup> [°C]	57	65	54	59
<b>Texture (sandstone)</b>				
Dominating grain size /sorting/roundness	Fine to medium, well sorted, subrounded		Very fine to fine, moderately to well sorted, subrounded	

<sup>1</sup> Thickness of Potential reservoir sand is estimated on the basis of cut-off values on Vshale (< 30%) and log-porosity (> 15%).

<sup>2</sup> Thickness of Potential reservoir sand divided with thickness of lithostratigraphic unit.

<sup>3</sup> Thickness of Potential reservoir sand divided with thickness of Gross sand.

<sup>4</sup> Reservoir-permeability is the permeability which is expected to be measured in connection to a pump test or well test. The reservoir-permeability is estimated by multiplying the Gas-permeability with an upscaling factor of 1.25.

<sup>5</sup> Reservoir-transmissivity is estimated on the basis of an interpretation of log data and analysis core data. The Reservoir-transmissivity is upscaled to reservoir conditions.

<sup>6</sup> Temperature is the estimated temperature in the middle of the Gassum Fm/Karlebo Mb.

## Composition of the reservoir sandstones

In general, the sandstones in the Gassum Formation are mainly fine- to medium-grained and well sorted, whereas they are very fine- to fine-grained and moderately to well sorted in the Karlebo Member. Individual sand grains are generally subrounded in both the Gassum Formation and the Karlebo Member. Thin section and scanning electron microscopy (SEM) analysis of sandstone material from Stenlille cores and cutting samples from the Margretheholm-1 well furthermore reveals that sandstones from the Gassum Formation and the Karlebo Member have a comparable and very mature mineralogy with detrital quartz being the dominant component (on average constituting 81% of sand grains). Feldspar is a minor to common component (averaging 6%) and the feldspar content is on average twice as high in the Karlebo Member as in the Gassum Formation. Mica, organic matter, clay and heavy minerals are usually rare. The overall content of authigenic minerals is rather low

(averaging 8%) and includes among others small scattered siderite rhombs in the Karlebo Member and rare to minor kaolinite, mainly in the Gassum Formation. However, kaolinite infilled all sandstone pores in a single cutting fragment from the Gassum Formation in the Margrethholm-1 well, indicating that in certain levels this mineral may reduce porosity and permeability. Carbonate cementation is rare but may be pronounced in certain intervals as a cutting fragment from the Gassum Formation showed a calcite content of 45%. Quartz overgrowths are volumetrically minor but slightly more pronounced in sandstone material from the Margrethholm-1 well than from the Stenlille wells, in accordance with an approximately 300 m deeper burial depth of the succession in the Margrethholm area than the Stenlille area. Differences in depth and diagenesis, influencing the reservoir properties, were therefore taken into account when predicting the reservoir properties of the two areas of interest on the basis of Stenlille data.

## Reservoir model

The reservoir data in Table 1 and regional mapping of the depth to the top and base of the Gassum Formation and the Karlebo Member, compiled on the basis of seismic data, have been used to set up a reservoir model in order to simulate flow rates and the timespan before cooled water from injection wells reach the production wells. In these simulations, geothermal plants are considered which have two deviated production wells and two deviated injection wells together with a vertical spud well, which is also used for injection. The reservoir simulations were run for a location in each of the prognosis areas. A well spacing of 1500 m was used for initial screening but simulation runs with different well spacing (done in Work Package 3) showed that distances could be kept as low as 900 m without a cold-water breakthrough at the production wells within the simulation run of 25 years. Short distances are preferred as it implies a smaller inclination of the wells in order to obtain the necessary distance at reservoir level, if the wells of the geothermal plant emanate from the same surface location. This may lower drilling risks as drilling in general becomes more complicated with increasing angle of drilling.

For the initial simulations, a constant production rate of 100 m<sup>3</sup>/h pr. production well and 66.66 m<sup>3</sup>/h pr. injection well was simulated in order to give a total production/injection of 4800 m<sup>3</sup>/day for the two production wells and the three injection wells. In deployment, higher well rates can be obtained, as long as the injection pressure is kept below the formation fracture pressure. This can be optimized by well completion and well inclination.

The production-/injection-index (WPI) was calculated in order to compare the productivity and injectivity for the two locations. The WPI is the ratio between fluid rate and the effective drawdown in the well, and is a measure of the fluid output/input to the reservoir pr. bar applied overpressure to the well. The WPI is a normalized number, which makes it easy to compare the productivity/injectivity for wells operated at different rates. In general, WPI's for the eastern location are approximately 30% higher relative to the western location, which means that production and injection rates are 30% higher for the same pressure drawdown. The difference in WPI is a combination of differences in reservoir parameter values and reservoir thickness.

For both locations the simulated injection bottom hole pressure (BHP), which is the necessary pressure in the bottom of the well to force the fluid volume from the well into the reservoir, never exceeded the formation fracture pressure. The eastern location has a more favorable production temperature profile due to the deeper position of the reservoir.

To illustrate the influence of the Amager Fault, a simulation case was run for the western location (located c. 2 km west of the fault). Although the fault was set to be closed for flow and pressure communication in the simulation, this did not reveal any effect on the WPI's or on the production temperature profile.

Overall, the model simulations showed suitable production capacities for both locations but with the eastern location being most favorable because of higher WPI's and temperature and thicker reservoir intervals, which delays cold-water breakthrough as the cold-water front is divided over a higher reservoir interval.

## Clay mineralogy

Clay mineralogical analysis of mudstone intervals in the Gassum Formation, the Karlebo Member, and the overlying mudstone-dominated part of the Fjerritslev Formation show a largely uniform clay mineralogical composition with kaolinite as the dominant clay mineral followed by mixed-layer minerals, which appear to be interstratified illite and vermiculite. Smectite and chlorite are not detected in any of the samples. Kaolinite may occur both as a detrital mineral and as an authigenic mineral formed during diagenesis. The latter is reported below from some sandstone samples. Previous studies show that kaolinite is commonly a dominant clay mineral in the Upper Triassic and Lower Jurassic deposits in the Danish Basin. There are slight differences in the clay mineral assemblage between Margrethholm-1 and Karlebo-1A (the wells representing a fairly close position to the palaeo-shoreline) and Kvols-1 and -2A, where the sediments were deposited in deeper water farther from the coastline. The data suggest that kaolinite decreases and the other minerals increase in amount away from the coastline (Table 2).

In the samples used for clay-mineral analysis the amount of clay-sized particles has been determined (right column in Table 2). The data values show that most of the mudstones contain more silt than clay. The samples from Kvols-1 and -2A are bulk samples, whereas those from Karlebo-1A and Margrethholm-1 are picked cuttings. This difference in methods produces a bias towards more fine-grained lithologies for the latter method.

The bulk-mineralogy has been examined in all the samples used for clay mineral analysis, as well as several additional samples. The bulk-mineralogy provides information on the minerals in the sand- and silt-fractions. The analyses show that quartz is the most common mineral and that traces of feldspar (microcline and albite) occur in many samples. Kaolinite and illite, or mica, is present in most samples and are probably detrital minerals to a large extent. Calcite appears to originate mainly from caving of overlying Cretaceous chalk. The minerals pyrite, siderite, and ankerite are interpreted as formed during diagenesis, and occur in varying, but small amounts.

**Table 2.** The average content of clay minerals in the Fjerritslev Formation, the Karlebo Member and the Gassum Formation is shown. The data values demonstrate the very small variation in the clay mineral assemblage between the units. More detailed information is provided in Chapter 8. Please note the low number of analyses, which means that average values in the table may change if just a few more analyses were added. The right-hand columns show the content of clay-sized particles (mostly clay minerals) and the amount of silt and very fine-grained sand in the samples.

Lithostratigraphy	Well	Number of analyses	Clay content (wt-%)			Grain-size fraction (wt-%)	
			Kaolinite	Vermiculite + mixed layer min.	Illite, mica	Clay	Silt and very fine sand
Fjerritslev Fm above Karlebo Mb	Margretheholm-1A	3	35-39	40-44	15-19	50	50
	Karlebo-1A	4	35-39	40-44	15-19	55	45
	Kvols-1, Kvols-2A	10	35-39	45-49	10-14	45	55
Karlebo Mb	Margretheholm-1A	4	40-44	35-39	10-14	32	68
	Karlebo-1A	2	40-44	40-44	15-19	44	44
Gassum Fm	Margretheholm-1A	3	45-40	30-34	10-14	40	60
	Karlebo-1A	3	30-34	45-49	15-19	52	48

The clay mineralogical composition in itself does not give rise to particular drilling risk concerns, since clay swelling during drilling in general is attributed to smectite, a very reactive clay mineral which has not been encountered in the present analysis. A review of completion reports of selected wells reveals that drilling problems related to swelling, sticking, caving and solubility in water do occur in the Fjerritslev Formation and locally in clayey intervals of the Gassum Formation. An overview of this information has been compiled from the completion reports and made available as Appendix 7 in the present report. However, it has not been possible to link a specific clay mineralogical composition to the intervals where these phenomena have been observed. Intervals of reactive clays, not covered by the present sampling, may of course be present. However, it is also possible that the observed drilling problems should be linked to an inappropriate composition of the drilling mud in relation to the clay mineralogy. A minor literature study on formation damage control emphasizes the importance of having a proper brine concentration of the fluids used during drilling and completion of wells and workover operations. Swelling of clay particles is more likely to occur when the clay is exposed to aqueous solutions with brine concentrations below a critical salt concentration. Furthermore, a low salt concentration and/or high fluid velocities may cause a release of fine-grained minerals, primarily kaolinite, which may lead to plugging of pore throats and thus reduced permeability in the reservoir sandstones.

The obtained knowledge of the clay mineralogy may therefore provide important information concerning the composition of drilling mud etc. when the muddy intervals of the Fjerritslev Formation, the Karlebo Member and the Gassum Formation are to be drilled in the future.

## Stratigraphic framework and offset data

The number of wells in eastern Zealand is limited to Margretheholm-1/1A/2, Karlebo-1/1A and Lavø-1 from which no cores of reservoir sandstones exist. Furthermore, the petrophysical log data from Lavø-1 are of poor quality. However, a large amount of petrophysical log

data of good quality, as well as core data, exist from the Stenlille area which is situated in the central part of Zealand, c. 60 km west of the areas of interest. Twenty deep wells in the area provide information of the Karlebo Member and Gassum Formation. The wells were drilled to test the Gassum Formation (reservoir) and Fjerritslev Formation (seal) prior to and during the establishment of the gas storage facility site at Stenlille. As outlined above, comprehensive analyses have been undertaken on the high-quality data from Stenlille and extrapolated to eastern Zealand in order to prognosticate the reservoir properties in the two areas of interest.

Prior to these analyses, an important task was to substantiate the relevance of the Stenlille data as an analogue for the Gassum Formation and the Karlebo Member in the two areas of interest. Several factors pointed towards this being the case. A sequence stratigraphic subdivision of the Gassum Formation – Fjerritslev Formation interval, based primarily on vertical log motifs from deep wells combined with comprehensive biostratigraphic analyses, showed that several packages of sandstones and intervening mudstones can be correlated between the wells from Stenlille and the wells in eastern Zealand. Consequently, these sedimentary packages are of regional extent and it is therefore likely that they are also present in the subsurface of the prognosis areas. In the selection of relevant analogue data from Stenlille (especially core data), emphasis has in particular been placed on those data which cover the regional sedimentary packages. The base of the Gassum Formation is regional mapped based on seismic data and appears as a northward, down-dipping flank along which both the Stenlille area and the western prognosis area occur at a comparable down-flank position (Fig. 2). This indicates an overall similar paleogeographic setting and probably some similar depositional environments for the Stenlille area and the western prognosis area during the deposition of the Gassum Formation and Karlebo Member thereby stressing the relevance of the Stenlille data for especially the western prognosis area. The presence of cysts from marine phytoplankton (dinoflagellates, acritarchs, prasino-phytes) in nearly all of the palynological samples shows that the sedimentary succession (Gassum Formation, Karlebo Member, Fjerritslev Formation) was deposited in a marine to marginal marine environment; lateral continuity of sedimentary packages is in general large in marine settings.

Furthermore, radiometric dating based on U–Pb in detrital zircon grains from the Gassum Formation and Karlebo Member indicate that these sediments in the Stenlille area and in northeastern Zealand (the Karlebo-1A, Lavø-1 and Margretheholm-1 wells) have a largely similar provenance. The sediments were sourced by reworking of the Lower Triassic Bunter Sandstone Formation on the Ringkøbing–Fyn High and to a lesser degree from erosion of crystalline rocks in Fennoscandia.

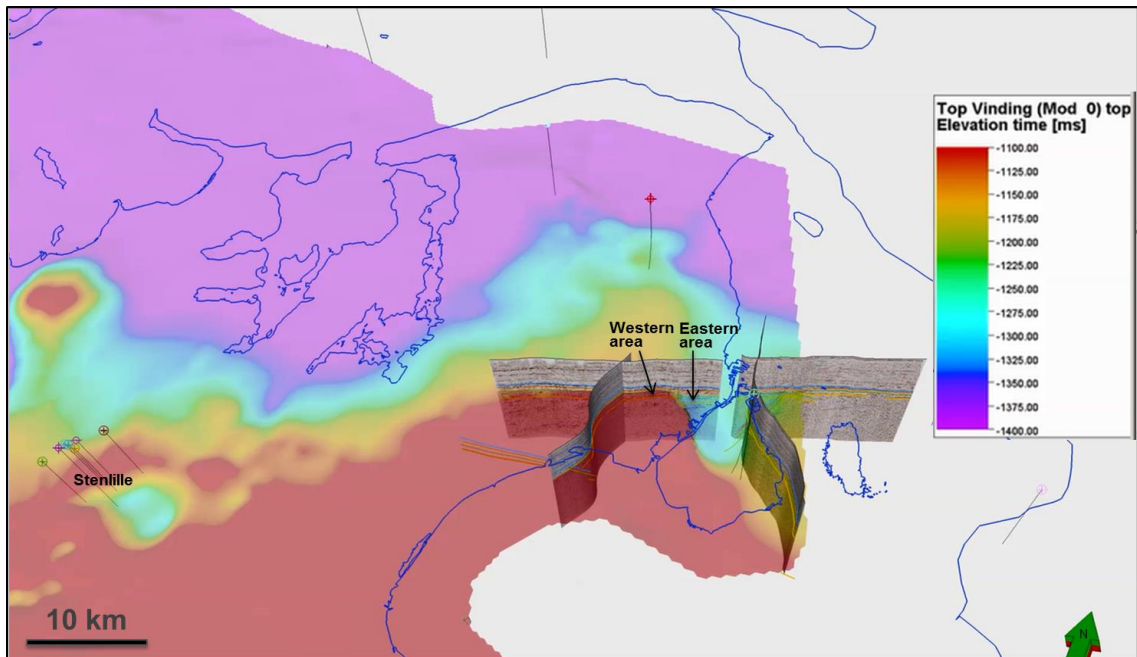


**Figure 2.** The figure illustrates the depth to and morphology of the Top Vinding surface, corresponding to the base of the Gassum Formation, in central and eastern Zealand. Vertical “needles” mark the position of existing wells. The surface appears as a northward, down-dipping flank along which both the Stenlille area and the western prospect area occur in a comparable down-flank position, thereby indicating an overall similar paleogeographic and depositional setting. Depths to the Top Vinding surface is given in two-way time (TWT, see inserted scale).

As outlined above, the relevance of the Stenlille data was confirmed by the outcome of the petrographic analysis of sandstone material from the Gassum Formation and the Karlebo Member in the Stenlille wells and the Margrethholm-1 well, which show an overall similar mature mineralogy with high quartz content and low feldspar content. Compared to the Gassum Formation in Jutland, both the Gassum Formation and the Karlebo Member in Zealand have a much more mature mineralogy. They are therefore expected to be less reactive to water injection, which may induce feldspar alteration and dissolution after slight changes in brine composition and flux (Milliken et al. 1989).

For the final selection of a borehole location, considerations of flow rate versus temperature, differences in drilling costs related to different drilling depths etc. as well as non-geological related parameters such as optimal position in relation to district heating infrastructure has to be taken into account. The present report of WP2 compiles and documents relevant subsurface data and analysis of these and thereby forms a solid foundation for delivering the geological input for selection of the final location of an exploration well in Phase 2 of the project.

Although the present analyses suggest that the many detailed well data from the Stenlille area can be used to predict the reservoir properties in the two areas of interest, extrapolation of the Stenlille data as far as to eastern Zealand is associated with some uncertainties. A new well in the Copenhagen area, from which cores, petrophysical log data and hydraulic test data of high quality are collected and subsequently analysed, will considerably increase our ability to predict the reservoir properties of the Gassum Formation and the

Karlebo Member in the greater Copenhagen area. Hence, the economic risk associated with the establishment of a geothermal plant will be reduced - not only in the Copenhagen area but in eastern Zealand as a whole. Furthermore, a new well will enable comparison of obtained core analyses data (including direct porosity and permeability measurements) with petrophysical log data and hydraulic test data from intervals of penetrated reservoir sandstone, and will thus provide a unique possibility to verify to what extent traditional petrophysical log data can be used to estimate the reservoir properties of geothermal sandstones of the Gassum Formation and the Karlebo Member in eastern Zealand. This knowledge is important for evaluation of the geothermal potential in a given area based on log data from existing wells, and for selecting suitable log tools for estimating porosity, permeability and injectivity of reservoir sandstones in connection to the performance of geothermal wells in the future.

# 1. Geological setting

The Copenhagen area is located in the Danish Basin which constitutes the southeastern part of the Norwegian-Danish Basin, formed by stretching of the crust in Early Permian time. To the south the basin is restricted from the North German Basin by the Ringkøbing–Fyn High, which forms part of a regional elevated basement ridge, striking WNW–ESE. To the northeast and east the basin is bounded by the Fennoscandian Border Zone, consisting of the Sorgenfrei–Tornquist Zone and Skagerrak–Kattegat Platform which form the transition to the shallow basement of the Baltic Shield (Fig. 1.1).

After initial deposition of Rotliegend coarse clastic sediments in the Danish Basin and the North German Basin a long period of subsidence followed during which thick deposits of Zechstein salt were formed in the basins followed by the deposition of sand, mud, carbonate and to a lesser degree salt deposits in the Triassic and Early Jurassic. Regional uplift in early Middle Jurassic led to a significant erosion of the underlying sediments, especially against the flanks and above the shallow basement in the Ringkøbing–Fyn High. However, fault related subsidence continued in the Sorgenfrei–Tornquist Zone with the deposition of sand and mud. Regional subsidence took place again during the later part of the Middle Jurassic and continued generally until Late Cretaceous–Paleogene time when subsidence was succeeded by uplift and erosion related to the Alpine deformation and opening of the North Atlantic. The deposits of the last period of subsidence consist of Upper Jurassic – Lower Cretaceous sandstones and in particular mudstones and siltstones followed by a thick succession of Upper Cretaceous chalk which form the upper part of the Mesozoic strata in the basins. The substantial amounts of sediments that were deposited through the Mesozoic, led at times to plastic deformation and vertical mobilization of underlying Late Permian salt deposits. In some places the overlying strata were thereby lifted up (on salt pillows) or penetrated by the rising salt (by salt diapirs). However, salt movement is less pronounced in Zealand compared to Jutland and southern Denmark, and Permian salt is not present in the subsurface in eastern Zealand.

The two areas of interest in the present study are located on each side of the Amager Fault, a significant NNW–SSE trending fault, which forms part of a set of right-stepping normal extensional faults forming the western boundary of the Øresund Sub-basin - a marginal sub-basin in the Danish Basin (Fig. 1.2). The faults die out along their strike and separate gently dipping transfer zones or relay ramps (Erlström et al. 2013). A reverse fault, the Romeleåsen Fault zone in Figure 1.2, constitutes the north-eastern margin of the sub-basin and the transition to the Sorgenfrei-Tornquist zone. The eastern area of interest is situated in the Øresund Sub-basin implying that the Gassum Formation occurs in a down-faulted position in the subsurface relatively to the western area. Hence, the reservoir sandstones of the formation are to be found at a deeper level in the eastern area and differences in temperature and possibly reservoir properties are accordingly to be expected between the two areas of interest.

The Mesozoic succession is around 2700 m and 3500 m thick in the western and eastern areas of interest, respectively. As a rule of thumb, geothermal sandstone reservoirs should be present within a depth interval of 800–3000 meters; the upper depth limit to ensure that

the formation water has sufficiently high temperatures to be a relevant heat component in district heating plants, and the lower limit due to an increasing risk of insufficient porosity and permeability at increasing reservoir depths (Kristensen et al. 2016). In both areas of interest, several sandstone reservoirs may fulfill this depth criterion, including those which the present project focusses on; the Upper Triassic–Lower Jurassic Gassum Formation and secondary the overlying Lower Jurassic Karlebo Member. The latter is only present in eastern Zealand where it represents a proximal setting to the offshore mudstones of the Fjerritslev Formation. The Gassum Formation and the Karlebo Member resembles each other lithologically, and the sediments reflect similar depositional environments.

Deeper lying sandstones of the Lower Triassic Bunter Sandstone Formation may also form a geothermal reservoir in the western area whereas the formation occurs below 3000 meters in the eastern area. However, the formation is present at shallower depths further south in the Øresund Sub-basin, e.g. at Margrethholm where the geothermal plant exploits c. 73 °C warm water from the formation at a depth of around 2.6 km. Finally, Lower Cretaceous sandstones may form potential geothermal reservoirs in both areas of interest but the present knowledge of these sandstones is limited as well as data are few and because the Lower Cretaceous unit, containing the potential geothermal reservoir sandstones, cannot be mapped on the seismic data.

The Gassum Formation constitutes the best known sandstone reservoir in Denmark and is exploited for geothermal extraction in Thisted and Sønderborg and for gas storage in Stenlille. The formation is widespread in the Danish Basin and partly also in the Danish part of the North German Basin with an overall thickness of 30–150 meters and with thicknesses of up to more than 300 meters in Sorgenfrei–Tornquist zone (Nielsen 2003). However, the formation is generally not present above the Ringkøbing–Fyn High and may furthermore be absent locally due to uplift and erosion related to vertical salt movement in the subsurface.

The Gassum Formation and the overlying Karlebo Member are dominated by fine to medium-grained, local coarse, light gray sandstones, alternating with darker-colored mudstones and siltstones and locally thin coal seams (Bertelsen 1978, Michelsen & Bertelsen 1979, Michelsen et al. 2003). The sediments reflect deposition during repeated sea level changes in the last part of the Triassic Period and early Jurassic Period (Nielsen 2003). During this time interval, the main part of the subsiding Danish area formed a shallow sea to which rivers transported large amounts of sand eroded from the Scandinavian basement area and locally from the Ringkøbing–Fyn High in periods when this was exposed. Large amounts of sand was deposited as marine shoreface sand, forming relatively continuous and widely distributed sandstone bodies, but sand was furthermore deposited in river channels, estuaries and lagoons. Succeeding fault activity has in places split up the sandstone bodies as well as subsequent compaction and mineral precipitation (diagenesis) has modified the reservoir properties of the sandstones. In western Skåne, time equivalent deposits to the Gassum Formation and the Karlebo Member are present. In general, these reflect a more proximal setting in tidal and river channels, washover fans, coastal and deltaic environments etc. (Ahlberg 1994). Although the sediments in western Skåne reflect more varying depositional environments, their overall occurrence and distribution was probably largely governed by the same relative sea level changes as recorded in the Danish Basin (Hjuler et al. 2014).

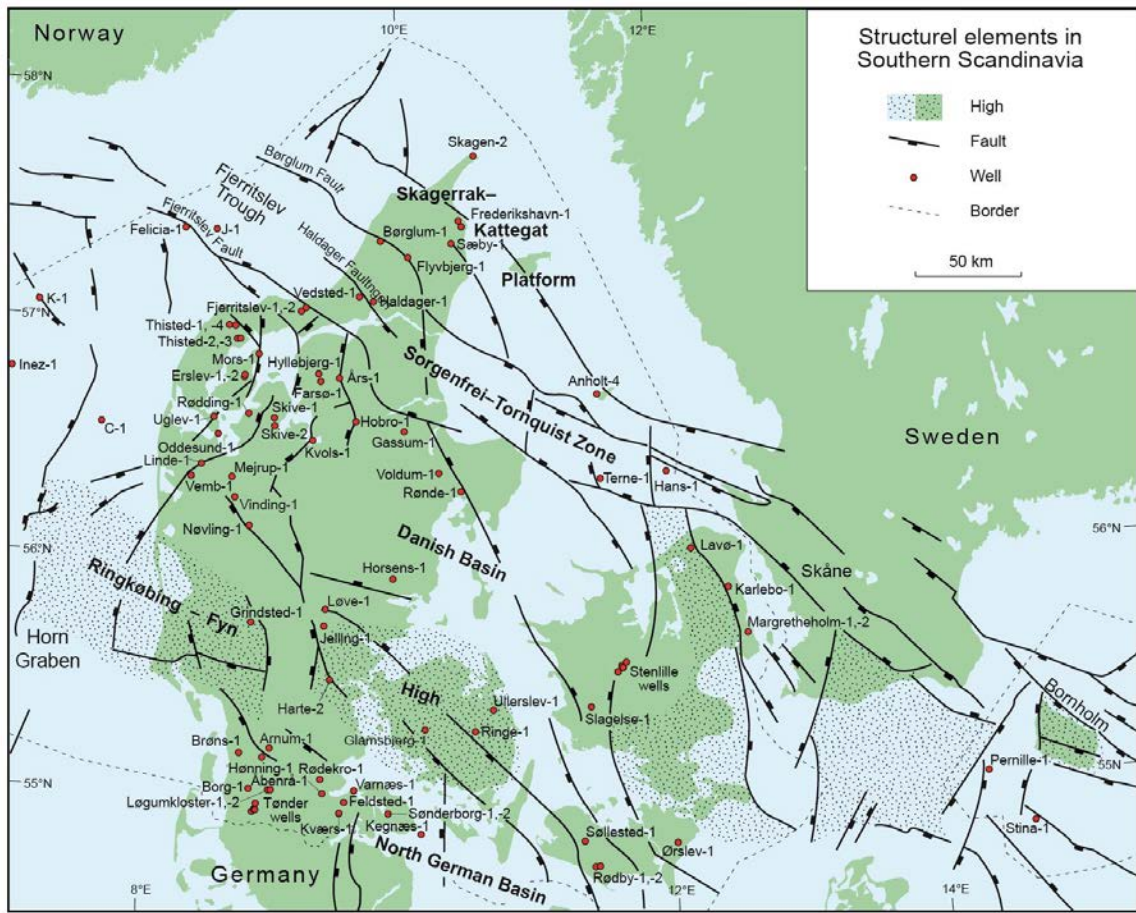


**Figure 1.1.** Well locations and principal structural elements in southern Scandinavia. Based on Nielsen (2003).

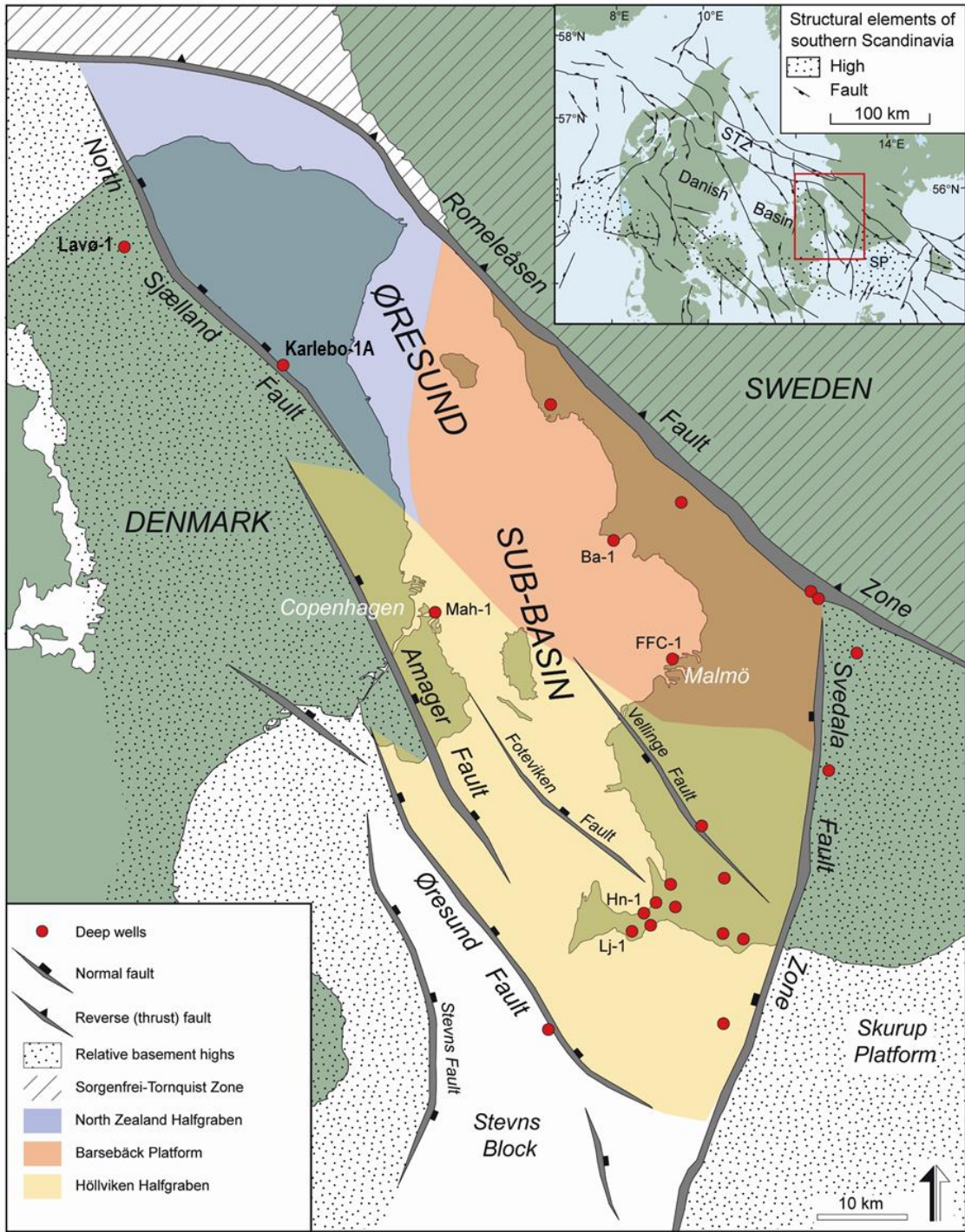


**Figure 1.2.** The Øresund region and the Danish Basin (inserted map in upper right corner) with main structural elements marked. Deep wells in the Øresund region are marked and onshore Denmark these comprise Lavø-1, Karlebo-1 and Margrethesholm-1 (Mah-1). The Swedish well Höllviken-1 (Hn-1) is included in the log-plot in Enclosure 1. Abbreviations on inserted map of the Danish Basin: RFH: Ringkøbing–Fyn High, STZ: Sorgenfrei–Tornquist Zone, SKP: Skagerak–Kattegat Platform. After Erlström et al. (2013).

## 2. Data basis

The available database in Zealand is shown in Figure 2.1 in terms of the location of deep wells and where seismic data have been collected. In addition, the quality of the data is indicated. From the map it is evident that the density of data varies considerably. The nearest wells, situated around 5 km away from the areas of interest, are Margrethholm-1/1A and -2. Karlebo-1A and Lavø-1 are located in northern Zealand, roughly 25 km and 40 km from the areas of interest, respectively. In Stenlille, around 60 km southwest from the areas of interest, twenty deep wells in the area provide information of the Karlebo Member and Gassum Formation. The many wells in Stenlille are a consequence of sandstones in the Gassum Formation being used for gas storage in the area. As gas is only injected in the upper half of the formation, most of the Stenlille wells do not penetrate the lower half of the formation. For clarity, only Stenlille-1 and Stenlille-19 are marked in Figure 2.1. Further to the southwest the Slagelse-1 well is situated in a distance of c. 85 km from the areas of interest

From Margrethholm-1/1A and several of the Stenlille wells, including Stenlille-1 and Stenlille-19, a complete petrophysical log suite of high quality exist, implying that it is possible to give reliable estimates of the porosity of penetrated sandstones. In addition, several cores exists from the Gassum Formation in the Stenlille wells, giving very valuable reservoir information based on porosity and permeability measurements, thin section analysis etc. of the cored sandstones . A complete log suite does not exist from the Karlebo-1/1A well but the recorded gamma-ray, sonic and resistivity logs are of reasonable quality and allow determination of most of the reservoir parameters. Unfortunately, log data from the lower part of Gassum Formation do not exist from this well due to technical problems during log recording of this part of the formation. The log suites from Margrethholm-2, Slagelse-1 and Lavø-1 are incomplete and the interpretation of several relevant reservoir parameters is therefore not possible.

The well data are not equally relevant in the setting up reservoir prognosis for the Gassum Formation and the Karlebo Member in the two areas of interest. Those well data that are supposed to be most representative for the prospect areas should thus be given the greatest significance in the reservoir evaluations. This demands considerations about similarities in structural settings, depositional environments, distance from paleo-shoreline, sediments sources, petrography, burial depths, diagenetic alternations etc. These parameters are elucidated by the various geological analyses undertaken in the project and form the basis for choosing representative data, e.g. core data, in the prognosis evaluations.

Data from the Margrethholm wells and Karlebo-1/1A well are thus considered most relevant for the eastern prospect area as these wells also occur within the Øresund Sub-basin. The western prospect area is situated west of the Amager Fault zone, and hence west of the Øresund Sub-basin. This justifies a higher weighting of data from the Lavø-1 and the Stenlille wells in the prognosticating of the western prognosis area.

In Table 4.2 depth intervals and thicknesses are shown for the Gassum Formation and Karlebo Member for those wells from which log-data contribute to the reservoir evaluations

of the prospects. In addition, depth interval and thickness is shown for the Fjerritslev Formation and the Chalk Group. Depth interval and thicknesses of these overburdens have also been estimated for prospect areas and are relevant as they can be included in the assessment of the costs for the drilling phase.

The quality of the seismic lines collected in the region is marked with colors in Figure 2.1 and indicates to which degree the seismic data can be used for mapping lithostratigraphic units (e.g. formations and members) in the deep geothermal depth interval (800–3000 m). It is a general quality indication that greatly reflects in what year the seismic data was collected (obviously the younger the data are the better the quality). The seismic coverage is reasonable around the prospect areas, especially because a roughly West–East trending seismic line of very good quality is running through the areas. An important task in this phase of the project has been to undertake a detailed analysis of seismic data from this line and the other lines occurring closest to the prospect areas, for identifying and defining the Gassum Formation and the Karlebo Member and estimating their depth and thickness etc., as outlined in Chapter 5.

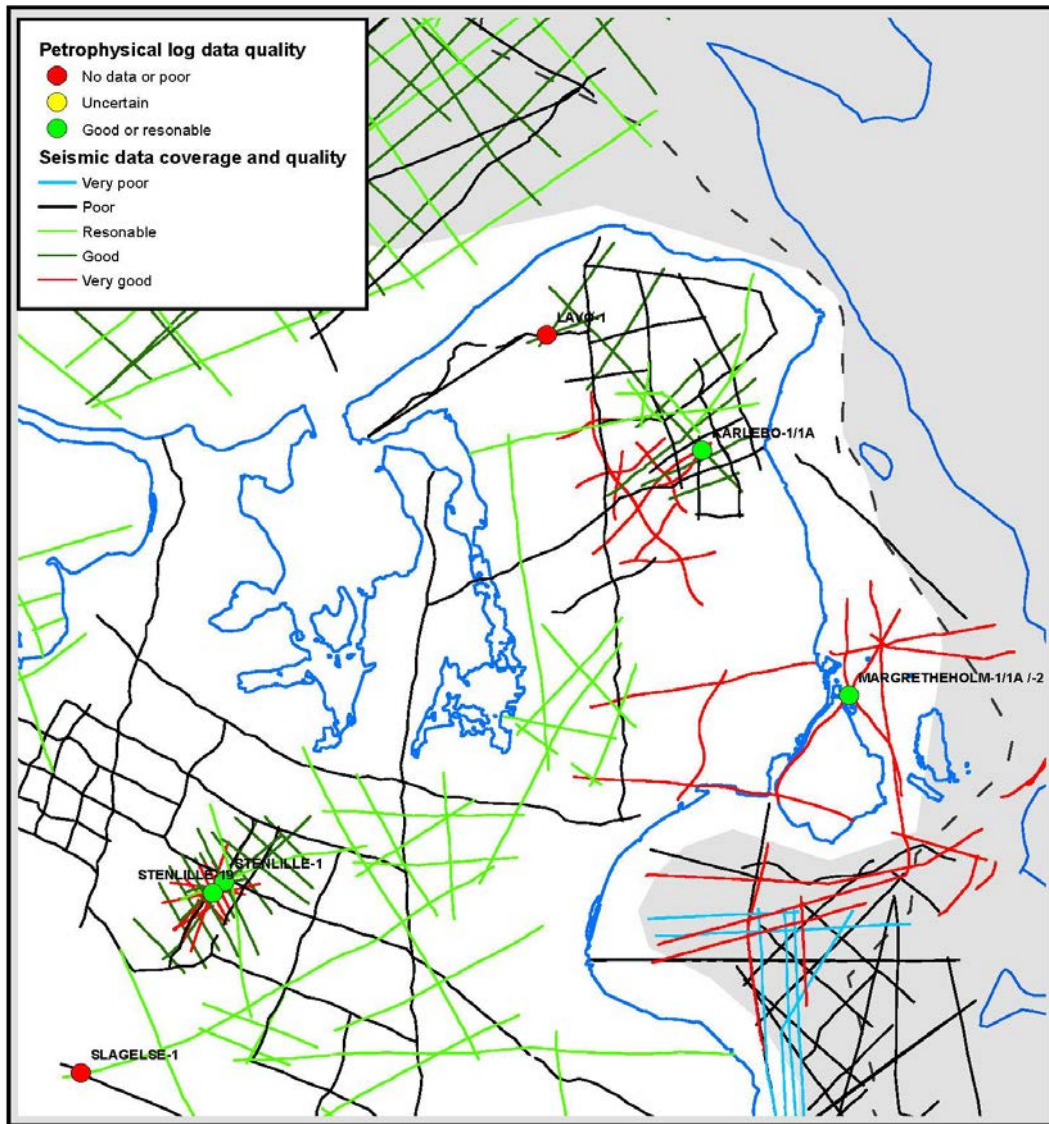


**Figure 2.1.** Coverage and quality of seismic and petrophysical log data from deep wells. The quality indexes reflect to which degree the data can be used to extract information about geo-thermal relevant lithostratigraphic units in the deep subsurface.

**Table 2.1.** Wells from which petrophysical log-data of the Gassum Formation and the Karlebo Member contribute to the reservoir evaluations of the prospects. The approximate locations of the wells are seen in Figure 2.1. Thicknesses are given in meters and depth intervals in meters below sea level (mbsl).

		Margretheholm-1/1A	Karlebo-1/1A	Lavo-1	Stenlille-1	Stenlille-19
<b>Chalk Group</b>	Depth interval (mbsl)	111–1591	147–1668	42–1995	150–1158	151–1138
	Thickness (m)	1480	1521	1873	1008	987
<b>Fjerritslev Fm</b> (above Karlebo Mb)	Depth interval (mbsl)	1639–1704	1753–1830	2045–2106	1205–1327	1178–1315
	Thickness (m)	65	77	61	122	137
<b>Karlebo Mb</b> (basal Fjerritslev Fm)	Depth interval (mbsl)	1704–1833	1830–1991	2106–2265	1327–1465	1315–1458
	Thickness (m)	129	161	159	138	143
<b>Gassum Fm</b>	Depth interval (mbsl)	1833–2017	1991–2118	2265–2340	1465–1609	1458–1603
	Thickness (m)	184	127	75	144	145

### 3. Sequence stratigraphic framework

A sequence stratigraphic subdivision of the Gassum Formation – Fjerritslev Formation interval is established for an overall SE–NW transect through Zealand based primarily on correlations of vertical well log motifs (essentially gamma ray (GR) and sonic (DT) logs) combined with biostratigraphic data (Enclosure 1). The sequence stratigraphic panel elucidates among others the distribution of sand and mud in space and time related to variations in relative sea level. The lithology is marked by the fill pattern between the GR and DT log tracks of each well and is based on an interpretation of petrophysical log data combined with information about the lithological composition of cutting samples etc., given in well completion reports. Significant vertical shifts in lithology, which can be correlated from well to well over large distances, commonly reflect marked changes in the depositional environments related to relative sea-level variations. For instance, sand was supplied to the Danish Basin from the crystalline basement in Fennoscandia in Late Triassic–Jurassic time and deposited as fluvial and coastal sand at the rim of the basin whereas silt and clay sedimentation gradually took over basinwards with increasing distance from the coast. However, during periods of relative sea-level fall the coast, and rivers behind it, prograded into the basin and sand was consequently deposited in the central parts of the basin. During succeeding relative sea-level rises the sand-rich coastal and fluvial depositional systems were flooded and forced back to the rim of basin, and deposition of offshore mud returned in the central parts of the basin. Repeated relative sea level variations through Late Triassic–Jurassic times, and the associated progradation and retreating of the coast line, are thus the main reason why the Gassum Formation and the Karlebo Member consist of alternating thick successions of mudstone and sandstone deposited in various environments.

Combined with a general knowledge of the structural setting and palaeogeography, a sequence stratigraphic subdivision of subsurface strata can be used to predict if sandstones are present at a given location, and thus if one of the basal prerequisites for a geothermal production is fulfilled. The sequence stratigraphic scheme given in Enclosure 1 has thus been used to evaluate if sandstones, like the ones which are penetrated in existing wells, can be expected to be found in the areas of interest and hence if data from these wells (e.g. porosity and permeability data from Stenlille cores) are representative for the prognosis areas. This is discussed below followed by a comprehensive presentation and documentation of the biostratigraphic data which formed an important input for subdividing the subsurface strata into depositional sequences.

The numbering of sequence boundaries (SB) and maximum flooding surfaces (MFS), given in the sequence stratigraphic panel in Enclosure 1, follows and is correlative to the well-established sequence stratigraphic subdivision in Nielsen (2003). However, the sequence stratigraphic framework in Nielsen (2003) was mainly based on well data from Jutland and did not incorporate data from the Margretheholm-1/1A, Margretheholm-2 and Karlebo-1/1A wells since these wells were drilled after the framework was established. The new wells from eastern Zealand provide important input for evaluating the subsurface, and hence the geothermal potential, in this region.

Nielsen (2003) and Hamberg & Nielsen (2000) demonstrated that it is possible to subdivide depositional sequences within the Gassum Formation – Fjerritslev Formation interval into lowstand, transgressive, highstand and falling stage systems tracts based on an interpretation of depositional environments reflected by vertical well log motifs, palynofacies data and sedimentological descriptions and interpretations of cores. This has not yet been done for the wells on eastern Zealand as this is a comprehensive and hence very resource demanding task. However, the identification of correlatable sequence boundary and maximum flooding surfaces is sufficient to substantiate if the sandstones penetrated in the wells (or similar sandstones) can be expected to be present in the areas of interest and hence if reservoir data from the existing wells form relevant analogue data.

The Kvols-1 well, drilled in central Jutland, has been included in the sequence stratigraphic panel in order to make a link to the sequence stratigraphic subdivision of strata in a well included in Nielsen (2003). In addition, the Swedish well Höllviknäs-1 is included in order to visualize the lithological composition of strata which are time equivalent to the Gassum and Fjerritslev formations and which represent a very proximal depositional setting in the Danish Basin. The latest Rhaetian maximum flooding event (MFS 7) has been used as datum line for the wells in the panel. The surface represents a significant flooding which influenced the entire basin including the basin margin in southern Sweden and the Skagerrak-Kattegat Platform (Enclosure 1). It is expected to be traceable over most of the Danish Basin as a thin unit of marine mudstones, in places intercalated with thin sandstone beds. In the present study this mudstone interval has largely been picked out in the wells on the basis of biostratigraphic data (see Chapter 4).

From the sequence stratigraphic panel it is evident that no clear lateral variation in the amount of sandstone and mudstones is obvious in the Gassum Formation below MFS 7. In contrast, an overall lateral decrease in the sandstone proportion on behalf of an increasing mudstone proportion is seen within several sequences from the Höllviknäs-1 well in east towards the Kvols-1 well in west. For example, sequence 9 consists almost entirely of sandstone in the Höllviknäs-1 well whereas it passes into interbedded sandstone and mudstone of the Gassum Formation in Margretheholm-1 and Kalebo-1A, with a further increase in the mudstone proportion in the Kalebo Member in Lavø-1 and Stenlille-1, and finally consisting almost entirely of mudstones of the Fjerritslev Formation in the Kvols-1 well. Furthermore, the sequences above MFS7 reflect an overall backstepping pattern of the sandy depositional systems culminating with the deposition of offshore mud of the Fjerritslev Formation in the entire region at around MFS 15 (in late Early Jurassic time).

The overall SW–NE transect through Zealand reveals that the basal part of the Gassum Formation in the Stenlille area, consisting almost entirely of extremely permeable sandstones, is not expected to be present in the areas of interest as this part of the formation has not been encountered in the deep wells in eastern Zealand (Enclosure 1). Core data from this part of the formation in Stenlille are thus not included in prognosticating the reservoir properties of the Gassum Formation in the areas of interest (see section 6.3). The sequences which subdivide the Gassum Formation and Karlebo Member above SB 5 are correlatable between the Stenlille wells and the wells on eastern Zealand (Enclosure 1). Some of the internal sandstone intervals may likewise be correlatable, or at least representing similar depositional environments as indicated by the presence of comparable vertical

log motifs and furthermore supported by an overall similar sandstone petrography of analyzed sandstone material from cores from the Stenlille wells and cutting samples from the Margretheholm-1 well (see section 6.1).

In summary, it can be concluded that the sequences above SB 5, and many of their internal sandstones, have a regional extent and thus can be expected to be present also in the subsurface at the prognosis areas. It is therefore relevant to include core data from the Gassum Formation (above SB 5) and the Karlebo Member from the Stenlille wells in a prognosis of the reservoir properties of sandstones at the areas of interest. However, adding considerations about structural settings and burial depths implies that the Stenlille core data are most relevant for the western area as outlined in Chapters 2 and 6.

## 4. Biostratigraphy

Palynology is one of the most useful biostratigraphic tools for correlating the sedimentary succession in deep wells. Because palynomorphs represent both spores and pollen from land plants, and microalgae from freshwater and marine environments, they allow correlation between the marine and the terrestrial environments. In this study, palynology have been used to correlate the Upper Triassic to Lower Jurassic succession of several deep wells on Zealand, in order to establish a sequence stratigraphic framework for the Gassum Formation – Fjerritslev Formation interval. The palynological study encompasses nine wells: Margretheholm-1, Karlebo-1A, Stenlille-1, -2, -5, -6, -15, and Lavø-1 situated on Zealand, and Höllviksnäs-1/Höllviken-2 situated in SW Scania (Figs. 1.1 and 1.2, and Enclosure 1). The study includes both new data and revision of previously analysed data.

### 4.1 Palynostratigraphic framework

The biostratigraphic results of this study have been compared with established palynostratigraphic schemes for the uppermost Triassic to Lower Jurassic of western Europe. The terrestrial palynostratigraphy is primarily based on the works of Lund (1977; 2003), Batten & Koppelhus (1996), Dybkjær (1991), Kürschner & Herngreen (2010), Koppelhus (1991), Koppelhus & Nielsen (1994), Herngreen et al. (2003), and Lindström & Erlström (2006, 2007, 2011). The spore-pollen zonation used herein is that of Lund (1977), with revisions of Dybkjær (1991), and Koppelhus & Nielsen (1994), and supplemented by data from Kürschner & Herngreen (2010). The dinoflagellate cyst stratigraphy used herein is that of Poulsen & Riding (2003). The Rhaetian dinocyst biostratigraphy was further supplemented by Lindström (2002) and Lindström & Erlström (2006, 2007). Important biostratigraphic events, used in this study, are shown in Figures 4.1–4.2, and the dinoflagellate cyst and spore-pollen zonations applied to the wells are briefly described in sections 4.1.1. and 4.1.2. below.

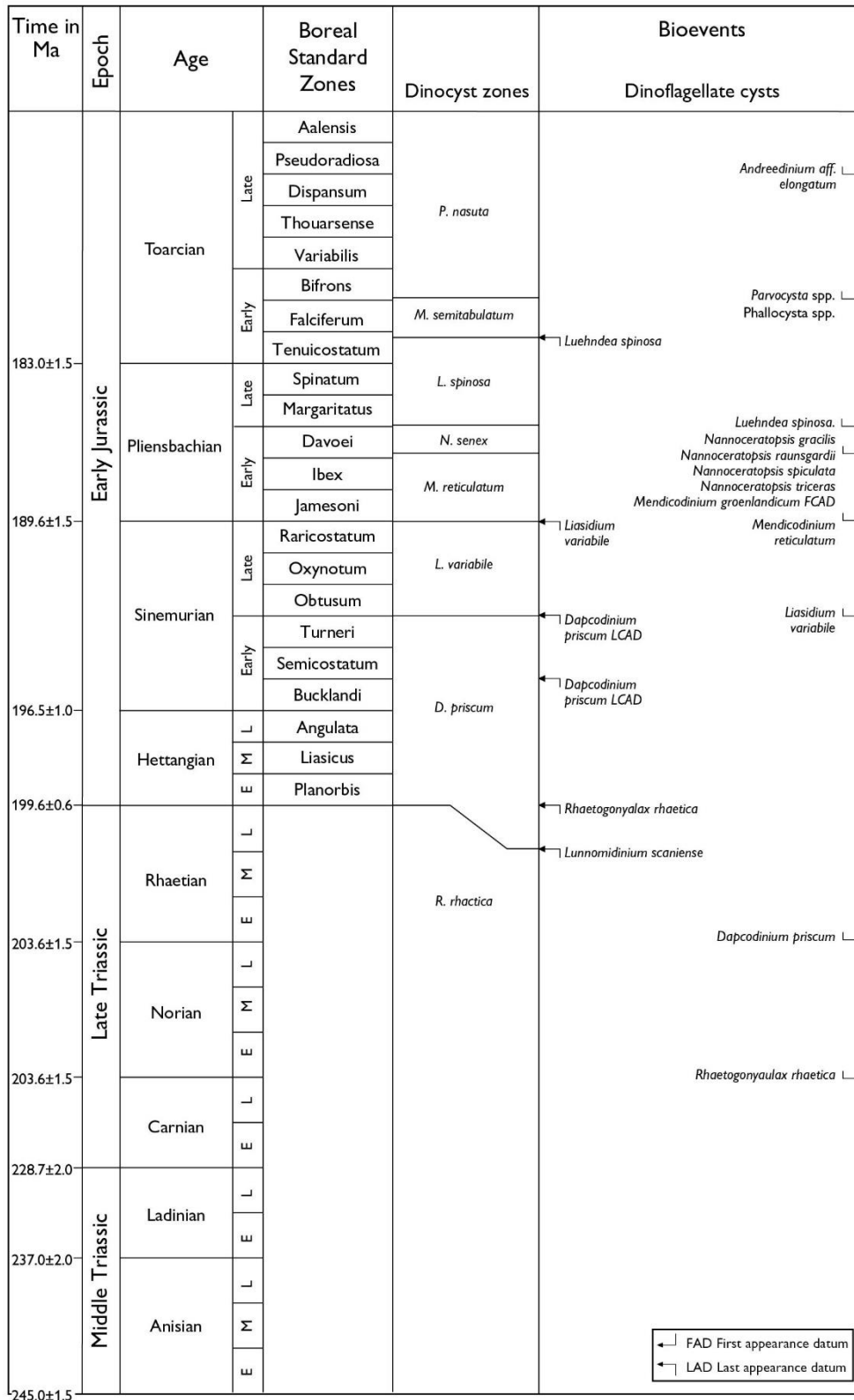


Fig. 4.1. Dinoflagellate cyst biostratigraphy for the Danish Basin (based mainly on Poulsen & Riding 2003).

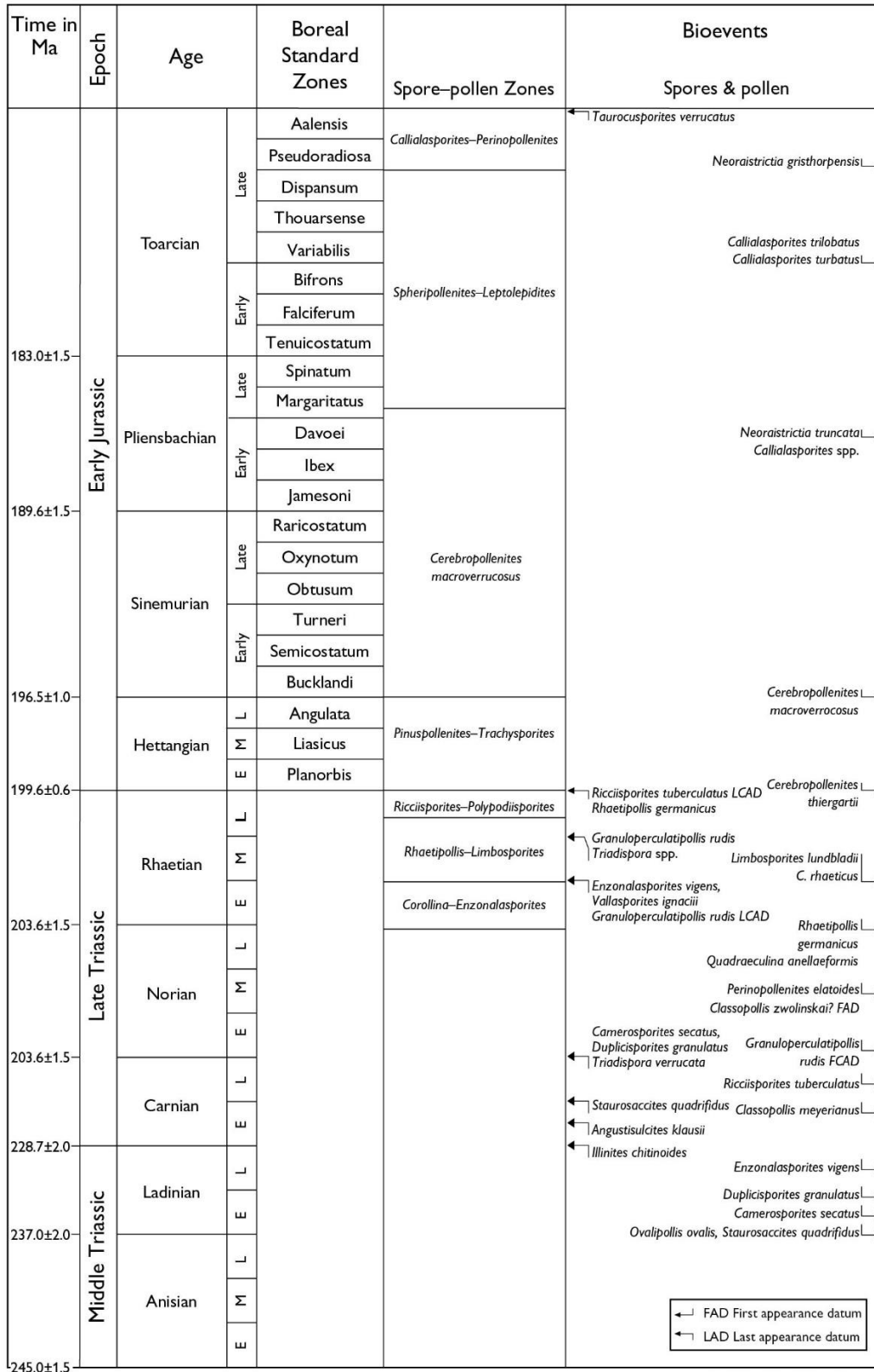


Fig. 4.2. Spore-pollen biostratigraphy for the Danish Basin (based mainly on Lund, 1977; Dybkjær 1991; Batten & Koppelhus 1996).

#### 4.1.1 Dinoflagellate cyst zonation of the Danish Basin

The dinoflagellate cyst zonation used herein was erected by Poulsen & Riding (2003) (Fig. 4.1). They subdivided the Rhaetian–Lower Jurassic into seven zones, partly based on the zonation for the English Jurassic by Woollam & Riding (1983) and Riding & Thomas (1992). The oldest zone in their zonation is the *Rhaetogonyaulax rhaetica* Zone, which was suggested to be restricted to the Rhaetian. Several dinoflagellate cyst taxa are present in this zone, and because the zone straddles the end-Triassic mass extinction, the majority of the taxa including the nominate taxon have their last occurrences within or at the top of this zone, e.g. *Beaumontella caminuspinia*, *Lunnomidinium scaniense* and *Suessia swabiana*. One of the dinoflagellates that survived the end-Triassic mass extinction was the one that produced the cyst referred to as *Dapcodinium priscum*. This taxon is the nominate species for the succeeding Hettangian to early Sinemurian *Dapcodinium priscum* Zone (Fig. 4.1). Poulsen & Riding (2003) subdivided the *D. priscum* Zone into two subzones: subzones a and b. Subzone a is characterized by the presence of *D. priscum* and the top of the subzone is marked by the last occurrence of this taxon. Subzone b is devoid of the index taxon and also of younger dinoflagellate cysts (Poulsen & Riding 2003). The succeeding zone is the late Sinemurian *Liasidium variabile* Zone, which is characterized by the presence of the nominate species, the range of which is restricted to this zone (Poulsen & Riding 2003).

The following zone, the early Pliensbachian *Mendicodinium reticulatum* Zone, is according to Poulsen & Riding (2003) characterised either by the presence of *Mendicodinium reticulatum*, or by an absence of dinoflagellate cysts. In the wake of the end-Triassic mass extinction, cyst-forming dinoflagellates were of low diversity, hence, the nominate taxa for these zones are quite often the only recognized dinoflagellate cysts in assemblages from the Hettangian to early Pliensbachian. The *Mendicodinium reticulatum* Zone is succeeded by the late Pliensbachian *Nannoceratopsis senex* Zone, defined as the interval between the first occurrence of the nominate taxon and the first occurrence of *Luehndea spinosa*, corresponding to the Davoei Ammonite Zone (Poulsen & Riding 2003). The range of *L. spinosa* defines the Pliensbachian to earliest Toarcian *Luehndea spinosa* Zone. The lower boundary of this zone reflects the first major diversification of dinoflagellate cysts after the end-Triassic mass extinction. Several taxa appear for the first time, including *Nannoceratopsis gracilis*, *N. raunsgaardii*, *N. ridingii*, *N. tricerias*, *Mancodinium semitabulatum*. This zone corresponds to the Margaritatus, Spinatum and Tenuicostatum Ammonite zones (Fig. 4.1). The early Toarcian Falciferum and lower Bifrons zones are encompassed by the *Mancodinium semitabulatum* Zone, which is characterised by an absence of both *L. spinosa* and elements typical for the succeeding *Parvocysta nasuta* Zone. The latter is of late Toarcian to earliest Aalenian age and encompasses the upper Bifrons, Variabilis, Thouarsence, Levesquei and Opalinum ammonite zones. In the Danish Basin the lower boundary of the *P. nasuta* Zone is marked by the first occurrence of *Parvocysta* spp. Later within the zone, members of the dinoflagellate cyst genera *Susadinium* and *Phallocysta* appear for the first time (Poulsen & Riding 2003).

#### 4.1.2 Spore-pollen zonation of the Danish Basin

Lund (1977) erected spore-pollen zones for the Late Triassic to Early Jurassic succession in Denmark and northern Germany. Based primarily on core material from the Rødby-1 well

he subdivided the late Norian to Rhaetian succession into four zones, in ascending order: the late Norian–early Rhaetian *Corollina–Enzonalasporites* Zone (the spore genus *Corollina* is a junior synonym of *Classopollis*, which is used herein), the late early Rhaetian–early middle Rhaetian *Ricciisporites–Conbaculatisporites* Zone, the middle Rhaetian *Rhaetipollis–Limboisporites* Zone, and the late Rhaetian *Ricciisporites–Polypodiisporites* Zone (Fig. 4.2). In additions, he established one Hettangian zone, the *Pinuspollenites–Trachysporites* Zone (Fig. 4.2), and also suggested that the succeeding Sinemurian spore-pollen flora belonged to a new, but un-named zone. The latter zone was later defined and named the *Cerebropollenites macroverrucosus* Zone by Dybkjær (1991), covering the Sinemurian–Pliensbachian spore-pollen floras. Dybkjær (1991) further erected the *Spheripollenites–Leptolepidites* Zone and the *Perinopollenites elatoides* Zone, for the Toarcian and Aalenian–Bathonian spore-pollen floras, respectively. Based on palyno-assemblages from Bornholm, Koppelhus & Nielsen (1994) erected the Pliensbachian *Chasmatosporites* Zone for assemblages corresponding to the upper C. macroverrucosus Zone. They further emended the definition of the *P. elatoides* Zone of Dybkjær (1991) so that it is also defined by the presence of *Callialasporites*, and renamed it the *Callialasporites–Perinopollenites* Zone (Koppelhus & Nielsen 1994). The definitions and characteristics of the zones are shown in Table. 4.1.

Spore-pollen zones often reflect variations in palaeoclimate, but their recognition is sensitive to variations in depositional environment, as spores and pollen may be affected by sorting related to grain-size of the sediments, and depending on whether they are dispersed by wind or water. In order to be readily recognized at least regionally, the individual zones need to have well-defined lower and upper boundaries. Preferably these boundaries should be marked by first or last occurrences of multiple taxa to ensure recognition regardless of depositional environment. Table 4.1 clearly shows that several of the zones are weakly defined. For example, the two lowermost zones defined by Lund (1977), the *Corollina–Enzonalasporites* and the *Ricciisporites–Conbaculatisporites* zones, could not readily be separated in this study. Assignment to the *Corollina–Enzonalasporites* Zone was made solely on the occurrence of *Enzonalasporites*, *Patinasporites* or *Vallasporites*. The sometime difficulty in separating the zones erected by Lund (1977) lead Lindström (2016) to present an informal, alternative zonation for the middle Rhaetian to Hettangian of the Stenlille wells. These informal zones are referred to where appropriate.

**Table 4.1.** Definitions and characteristics of the latest Triassic to earliest Middle Jurassic spore-pollen zones for the Danish Basin (mainly after Lund, 1977; Dybkjær, 1991).

Spore-pollen zone	Lower boundary	Characteristics	Upper boundary	Suggested age, and comments
<b>Callialasporites–Perinopollenites (C–P) Zone</b> (Dybkjær 1991 emend. Koppelhus & Nielsen 1994)	FO of <i>Callialasporites</i> spp. according to Koppelhus & Nielsen (1994)	Dominated by <i>Perinopollenites elatoides</i> , while <i>Classopollis</i> and <i>Spheripollenites</i> are less prominent	Not defined	Aalenian–Bathonian. However, according to Batten & Koppelhus (1996) the FAD of <i>Callialasporites</i> spp. is in the late early Toarcian.
<b>Spheripollenites – Leptolepidites (S–L) Zone</b> (Dybkjær 1991).	Distinct increase in <i>Spheripollenites</i> , FO of <i>Leptolepidites</i> and/or <i>Ischyosporites</i> .			Toarcian. <i>Ischyosporites</i> has its first appearance datum close to the Triassic–Jurassic boundary, but is virtually absent until it becomes more common again in the Toarcian.
<b>Cerebropollenites macroverrucosus (C.m.) Zone</b> (Dybkjær 1991)	First occurrence of <i>Cerebropollenites macroverrucosus</i> .		Immediately below a distinct increase in <i>Spheripollenites</i> and the first occurrence of <i>Leptolepidites</i> .	Sinemurian to Pliensbachian. This zone is difficult to recognize if the nominate taxon is absent.
<b>Pinuspollenites–Trachysporites (P–T) Zone</b> (Lund 1991)	Marked by a distinct increase in <i>Pinuspollenites minimus</i> .	Common presence of <i>Pinuspollenites minimus</i> . Absence of <i>C. macroverrucosus</i> .	Immediately below the first occurrence of <i>Cerebropollenites macroverrucosus</i> .	Hettangian. <i>Trachysporites</i> spp. is not always a prominent constituent within this zone.
<b>Transition zone</b> (Lund 1977; Larsson 2009)		The palynoflora is transitional in character, containing many Rhaetian elements, but also many typical Hettangian ones.		Latest late Rhaetian to earliest Hettangian, according to Lund (1977). Probably equates to the CCM and PDS zones of the Stenlille area (Lindström 2016).
<b>Ricciisporites–Polypodiisporites (R–P) Zone</b> (Lund 1977)	Distinct increase in <i>Polypodiisporites polymicroforatus</i> .		Distinct decrease in <i>P. polymicroforatus</i> .	Late Rhaetian. Corresponds to the RPD zone of Lindström (2016).
<b>Rhaetipollis–Limbosporites (R–L) Zone</b> (Lund 1977)	First occurrence of <i>Limbosporites lundbladiae</i> .	Co-occurrence of <i>Limbosporites lundbladiae</i> and <i>Rhaetipollis germanicus</i> , and common <i>Ricciisporites tuberculatus</i> .		Middle Rhaetian. Corresponds to the GCP zone of Lindström (2016).
<b>Ricciisporites–Conbaculatisporites (R–C) Zone</b> (Lund 1977)		Absence of <i>Enzonasporites</i> spp. and <i>Limbosporites lundbladiae</i> . <i>Ricciisporites tuberculatus</i> is usually common.		Early Rhaetian
<b>Corollina–Enzonasporites (C–E) Zone</b> (Lund 1977)	Co-occurrence of <i>Classopollis (Corollina)</i> and <i>Enzonasporites</i> .	Presence of <i>Eucommiidites major</i> . According to Lund (1977) <i>Echinosporites iliacooides</i> is present in the lower part of the zone. This taxon has its known LAD in the earliest Carnian (Schulz & Heunisch 2005), hence, the specimens registered by Lund (1977) were most likely reworked.	Last occurrence of <i>Enzonasporites</i> spp.	Norian to early Rhaetian

## 4.2 Methods

The palynological samples in this study were processed according to standard palynological preparation methods at the palynological laboratory at GEUS. The method largely follows that described in Poulsen et al. (1990). The present study includes palynological analysis of core samples and side wall core samples from the Stenlille wells, and Lavø-1, and complemented with analyses from the Swedish Höllviken-2 core for comparison. Core samples and side wall core samples enables the use of both first (FO) and last (LO) occurrences of stratigraphically important taxa. However, the majority of the assemblages investigated in this study are from ditch cuttings samples, primarily from the Margretheholm-1 and Karlebo-1A wells. A common and well-known minor complication for biostratigraphers working on ditch cuttings samples is contamination of assemblages due to caving from higher stratigraphical levels. However, it needs to be pointed out that in some stratigraphic intervals caving can be extra problematic. One example of this that relates to this study is caving of Jurassic strata within a Jurassic interval, i.e. in Lavø-1 caving of Pleinsbachian–Toarcian into lower units complicated the biostratigraphic dating made by Poulsen (1996; compare with Table 4.5 herein). Because many Jurassic spore-pollen taxa are long-ranging, the existing biostratigraphic schemes of NW Europe are largely based on quantitative data (Lund 1977; Dybkjær 1991; Koppelhus 1991). Medium-large amounts of caving (or reworking, for that matter) will distort the quantitative signals rendering accurate assignment to biozones difficult or even impossible. Hence, for ditch cutting samples the last occurrence (LO) of a taxon in a section (unless reworked) is considered a more reliable datum than a first occurrence (FO). However, the LO of a taxon within a succession does not always correspond to its known last appearance datum (LAD), e.g. due to lack of samples, or there may be a hiatus within the succession, or the taxon may be extremely rare or absent due to palaeoenvironmental factors. In this study, a quantitative analysis has been carried out on the majority of the samples. Between 150 and 300 specimens have been counted in most assemblages in order to assess abundance variations in various groups of palynomorphs. Increased abundances of spores and pollen, so called acmes, are often used for characterization of a specific spore-pollen zone, or certain events within a zone (see e.g. Table 4.1). Often, the first (FCO) or last (LCO) common occurrence of a taxon is a better marker than its FO or LO, as the latter two can be difficult to pinpoint if a taxon is very rare at the start or end of its range.

The presence of reworked palynomorphs can provide interesting information about the local geology of an area, and its environmental and tectonic development. Increased reworking is usually connected to tectonic uplift or periods of increased erosion. If the reworked material is similar in age to the material deposited in situ, interpretations of the true age of an assemblage can be made very difficult. Further, if the reworked palynomorphs dominate an assemblage, the true age of that sample will be much harder to assess and is easily missed.

### 4.3 Stratigraphic breakdown of the investigated wells

The palynostratigraphic breakdown of the Gassum and Fjerritslev formations in each respective well is presented below in Tables 4.2–4.10. Most commonly, each sample is presented on its own, however, in some cases it has been necessary to combine samples into intervals (i.e. in Stenlille-1 where a majority of the data is of high resolution). In most cases, each sample/interval is assigned to a dinoflagellate cyst zone and a spore-pollen zone (see Figs. 4.1 and 4.2). In some rare cases, assignment to both a dinoflagellate cyst zone and a spore-pollen zone has not been possible. Any considerations regarding the zonal assignment, age or depositional environment can be found within these tables. In a few instances there are no comments to the zonal assignment simply because the zonal assignment is constrained by under- or overlying samples. The consensus of the palynostratigraphic breakdown and the sequence stratigraphy of the wells is presented in Enclosure 1. In addition, stratigraphic summary charts of Margrethholm-1, Karlebo-1A, Höllviken-2, Lavø-1 and Stenlille-1 are presented in Appendices 2–6.

#### 4.3.1 Margrethholm-1

The palynology of the Upper Triassic to Lower Jurassic succession of the Margrethholm-1 well has previously been studied by Dybkjær et al. (2002), Mathiesen et al. 2007, and Lindström & Erlström (2011).

Dybkjær et al. (2002) analysed 12 samples palynologically, and their stratigraphic breakdown is presented in Table 4.2. Lindström in Mathiesen et al. (2007) and Lindström & Erlström (2011) revised the stratigraphic breakdown of the well for the Upper Triassic to Lower Cretaceous succession by analysing the same samples, as well as additional ones, and the results are also incorporated in Table 4.2. For this study, additional cuttings samples were analysed from the interval 1670–2032 m, and these have helped to further refine the stratigraphic breakdown as shown in Table 4.2 below, and in Appendix 1.

**Table 4.2.** Stratigraphic breakdown of Margrethholm-1 based on palynology. Previous age assessments by <sup>1</sup>Dybkjær et al. (2002), <sup>2</sup>Lindström in Mathiesen et al. (2007), <sup>3</sup>Lindström & Erlström (2011).

Depth in meter	Sample type	Previous age assessment	Age assessment (this study)	Palynozone, dominant taxa and/or marker taxa, depositional environment
1655		Early Toarcian <sup>1</sup>	Late Pliensbachian–earliest Toarcian	<b>Spheripollenites–Leptolepidites Zone.</b> Presence of <i>Parvocysta</i> sp. indicates occurrence of strata of late Toarcian to earliest Aalenian age, above this interval. Major acme <i>Spheripollenites</i> . Abundant <i>Classopollis</i> spp. <b>Luehndea spinosa Zone</b> of Poulsen & Riding (2003). FO/LO <i>Luehndea spinosa</i> indicates Margaritatus to uppermost Tenuicostatum Zones; Late Pliensbachian to earliest Toarcian (Poulsen &

				Riding 2003). <b>Shallow marine environment:</b> 8% dinocysts, 11% marine acritarchs.
1665–1670	CU		Late Pliensbachian	<b>Nannoceratopsis senex Zone.</b> <b>Spheripollenites–Leptolepidites Zone.</b> Abundant <i>Classopollis</i> spp. Rare <i>Callialasporites</i> spp. may (if <i>in situ</i> ) indicate an age younger than late early Pliensbachian (Davoei Zone; Herngreen et al. 2003) or late early Toarcian (Batten & Koppelhus 1996). <b>Marginal marine environment:</b> 5% dinocysts, 2% marine acritarchs.
1680–1685	CU		Late Pliensbachian	<b>Nannoceratopsis senex Zone.</b> <b>Spheripollenites–Leptolepidites Zone.</b> Marked increase in <i>Spheripollenites</i> spp. and decrease in <i>Pinuspollenites</i> spp. Abundant <i>Classopollis</i> spp. <b>Marine environment:</b> 17% dinocysts, 5% marine acritarchs.
1695	CU	Late Pliensbachian <sup>2</sup>	Late Pliensbachian	<b>Nannoceratopsis senex Zone.</b> <b>Cerebropollenites macroverrucosus Zone.</b> Marked decrease in <i>Deltoidospora</i> spp. and marked increase in <i>Classopollis</i> spp. <i>Acme Micrhystridium</i> spp. <b>Marine environment:</b> 14% dinocysts, 10% marine acritarchs.
1700	CU	Late Pliensbachian – Early Toarcian <sup>1</sup>	Late Pliensbachian	<b>Nannoceratopsis senex Zone</b> <b>Cerebropollenites macroverrucosus Zone</b> of Dybkjær (1991) <b>Shallow marine environment:</b> dinocysts present in low numbers (semiquantitative assessment only).
1710–1715	CU		Late Pliensbachian	<b>Nannoceratopsis senex Zone</b> of Poulsen & Riding (2003). FOs of <i>Nannoceratopsis ridingi</i> , <i>N. spiculata</i> , and <i>N. senex</i> are here regarded as being <i>in situ</i> due to an acme of <i>N. senex</i> which is not recorded above this level. <b>Cerebropollenites macroverrucosus Zone</b> of Dybkjær (1991). Increase in <i>Spheripollenites</i> spp. may be due to caving. <b>Marginal marine environment:</b> 6% dinocysts, 6% marine acritarchs.
1720	CU	(Hettangian <sup>1</sup> ) Pliensbachian <sup>2,3</sup>		<b>C. macroverrucosus Zone</b> of Dybkjær (1991) No quantitative assessment.
1730	CU	Late Pliensbachian <sup>2</sup>		FO <i>Dissiliodinium</i> sp. <b>C. macroverrucosus Zone</b> of Dybkjær (1991) FO of <i>Neoraistrickia</i> sp. may indicate a late early Pliensbachian age (Davoei; Herngreen et al. 2003).

				<b>Shallow marine environment:</b> 14% dinocysts, 5% marine acritarchs.
1750	CU	Sinemurian–Pliensbachian <sup>2</sup>		<b>C. macroverrucosus Zone</b> of Dybkjær (1991) <b>Marginal marine environment:</b> 9% dinocysts, 2% marine acritarchs.
1790	CU	(Sinemurian <sup>2</sup> ), latest Sinemurian <sup>3</sup>		<b>C. macroverrucosus Zone</b> of Dybkjær (1991) <b>Shallow marine environment:</b> 11% dinocysts, <1% marine acritarchs, <1% fresh/brackish water <i>Botryococcus braunii</i> .
1817.5	CU	Early Sinemurian <sup>2</sup>	Early Sinemurian	<b>D. priscum Zone.</b> LCO of <i>D. priscum</i> indicates this zone. <b>C. macroverrucosus Zone.</b> FO of <i>C. macroverrucosus</i> allows assignment to this zone (Dybkjær 1991). <b>Shallow marine environment:</b> 14% dinocysts, <1% marine acritarchs.
1842.5	CU	?Late Hettangian <sup>2</sup>	Late Hettangian	<b>Dapcodinium priscum Zone.</b> Presence of <i>D. priscum</i> allows recognition of this zone (Poulsen & Riding 2003). <b>Pinuspollenites-Trachysporites Zone</b> of Lund (1977) <b>Shallow marine environment:</b> 10% dinocysts, <1% marine acritarchs.
1870–1872.5	CU		Early Hettangian	<b>Dapcodinium priscum Zone.</b> Presence of <i>D. priscum</i> allows recognition of this zone (Poulsen & Riding 2003). <b>Pinuspollenites-Trachysporites Zone</b> FCO of <i>P. minimus</i> allows assignment to this zone (Lund 1977). Probably equates to the <b>DPPi zone</b> of the Stenlille area (Lindström 2016). <b>Marginal marine environment:</b> 9% dinocysts, <1% marine acritarchs.
1920–1925	CU		latest Rhaetian–earliest Hettangian	<b>Dapcodinium priscum Zone.</b> Presence of <i>D. priscum</i> allows recognition of this zone (Poulsen & Riding 2003). <b>Transition zone.</b> Dominance of <i>Deltoidospora</i> and <i>P. elatoides</i> , common <i>Stereisporites</i> and aberrant <i>Deltoidospora</i> . LOs: <i>C. rhaeticus</i> , <i>L. rhaeticus</i> , <i>S. gothae</i> . LCO of <i>R. tuberculatus</i> indicate latest Rhaetian–earliest Hettangian. Equates to the <b>PDS-Zone</b> of Stenlille area (Lindström 2016). <b>Marginal marine environment:</b> 1% dinocysts, <1% marine acritarchs.
1930	CU	Late Rhaetian <sup>1, 2, 3</sup>	Late Rhaetian	<b>R. rhaetica Zone.</b> LCO and LO of <i>R. rhaetica</i> . <b>Rhaetipollis–Limboisporites Zone.</b> Equivalent to the <b>GCP interval</b> of the Stenlille area (Lindström 2016). LOs of <i>G. rudis</i> , <i>T. reticulatus</i> .

				<b>Marine environment:</b> 33% dinocysts, 9% marine acritarchs.
1945–1950	CU		Middle Rhaetian	<b>R. rhaetica Zone.</b> <b>Rhaetipollis–Limbosporites Zone.</b> Equivalent to the <b>GCP interval</b> of the Stenlille area (Lindström 2016). LOs of <i>L. lundbladiae</i> , <i>O. ovalis</i> , <i>P. polymicroforatus</i> . <b>Marginal marine environment:</b> 3% dinocysts, <1% marine acritarchs.
1980–1985	CU		Middle Rhaetian	<b>R. rhaetica Zone.</b> <b>Rhaetipollis–Limbosporites Zone.</b> Equivalent to the <b>GCP interval</b> of the Stenlille area (Lindström 2016). LOs: <i>R. germanicus</i> , <i>D. cavernatus</i> . <b>Marginal marine environment or lagoonal:</b> 3% dinocysts, <1% marine acritarchs, 6% fresh/brackish water <i>Botryococcus braunii</i> .
2015–2020	CU		Middle Rhaetian	<b>R. rhaetica Zone.</b> <b>Rhaetipollis–Limbosporites Zone.</b> Equivalent to the <b>GCP interval</b> of the Stenlille area (Lindström 2016). <b>Marginal marine environment:</b> 3% dinocysts, <1% marine acritarchs.
2025	CU	(Rhaetian <sup>1</sup> ) Early Rhaetian <sup>3</sup>	Middle Rhaetian	<b>R. rhaetica Zone.</b> <b>Rhaetipollis–Limbosporites Zone.</b> Equivalent to the <b>GCP interval</b> of the Stenlille area (Lindström 2016). <b>Marginal marine environment:</b> common dinocysts (semi-quantitative assessment only).
2030–2035	CU		Early Rhaetian	<b>R. rhaetica Zone.</b> <b>Corollina–Enzonasporites Zone</b> of Lund (1977). FO <i>Limbosporites lundbladiae</i> , may be due to caving. LOs: <i>Patinasporites densus</i> , <i>Triadispora</i> spp., <i>Rimaesporites aquilonalis</i> (LADs early Rhaetian) <b>Marine environment:</b> 22% dinocysts.
2075	CU	(Rhaetian <sup>1</sup> ) Norian <sup>3</sup>	Early Rhaetian	<b>R. rhaetica Zone.</b> <b>Corollina–Enzonasporites Zone</b> of Lund (1977). LO <i>L. scaniense</i> . <b>Marginal marine environment:</b> 8% dinocysts.

### 4.3.2 Karlebo-1A

The palynology of the Upper Triassic to Lower Jurassic succession of the Karlebo-1A well has previously been studied by Mathiesen et al. 2007, and Lindström & Erlström (2011). The stratigraphic breakdown presented by Mathiesen et al. (2007) and Lindström & Erlström (2011) is shown in Table 4.3. For this study, the previous data was re-assessed and some additional ditch cuttings samples were analysed. This resulted in a revision of the stratigraphic breakdown and this is presented in Appendix 2 and in Table 4.3.

**Table 4.3.** Stratigraphic breakdown of Karlebo-1A based on palynology. Previous age assessments by <sup>1</sup>Lindström in Mathiesen et al. (2007), <sup>2</sup>Lindström & Erlström (2011).

Depth in meter	Sample type	Previous age assessment	Age	Palynozone, dominant taxa and/or marker taxa
1865	CU	Aalenian <sup>1,2</sup>	Aalenian-Bajocian?	<b>Parvocysta nasuta Zone</b> of Poulsen & Riding (2003), or possibly as young as late early Bajocian, based on LAD of <i>Nannoceratopsis gracilis</i> . <b>Callialasporites–Perinopollenites Zone.</b> <b>Depositional environment:</b> No quantitative assessment made.
1875	CU	Late Toarcian <sup>1,2</sup>	Late Toarcian	<b>Parvocysta nasuta Zone</b> of Poulsen & Riding (2003), as indicated by the LO of <i>Mendicodinium reticulatum</i> suggesting an earliest Aalenian age (Opalinum Zone) or older. <b>Callialasporites–Perinopollenites Zone.</b> Increase in <i>Perinopollenites elatoides</i> along with consistent occurrence of <i>Callialasporites</i> spp. indicates C–P Zone. LO of <i>Taurocusporites verrucatus</i> indicates a Late Toarcian age (LAD late Toarcian; Batten & Koppelhus 1996). <b>Marginal marine environment:</b> 5% dinocysts, 1% marine acritarchs.
1900	CU	Late Early Toarcian <sup>1,2</sup>	Late Toarcian	<b>Parvocysta nasuta Zone</b> of Poulsen & Riding (2003). The LO <i>Limbicysta bjaerkei</i> (FAD late Early Toarcian, Bifrons Zone; Bjærke 1980; Riding & Thomas 1992; Koppelhus & Dam, 2003; LAD early Aalenian, Opalinum Zone; Feist-Burkhardt & Pross, 2010) suggests an age younger than late Early Toarcian (Poulsen & Riding, 2003), and the co-occurrence of and <i>Parvocysta</i> sp. and <i>Susadinium</i> sp. suggests a Late Toarcian, Levesquei Zone, to earliest Aalenian, Opalinum Zone (Poulsen & Riding 2003). <b>Spheripollenites–Leptolepidites Zone.</b> <b>Shallow marine environment:</b> 12% dinocysts, 6% marine acritarchs.

1925	CU	Toarcian <sup>1,2</sup>	Late Pliensbachian to earliest Toarcian	<p><b>Luehndea spinosa Zone</b> of Poulsen &amp; Riding (2003). LO/FO <i>Luehndea spinosa</i> indicates a late Pliensbachian to earliest Toarcian age; the Margaritatus, Spinatum and Tenuicostatum Zones.</p> <p><b>Spheripollenites–Leptolepidites Zone.</b> Marked increase in <i>Spheripollenites</i> spp. and decrease in <i>Pinuspollenites</i> spp.</p> <p><b>Shallow marine environment:</b> 12% dinocysts, 3% marine acritarchs.</p>
1942.5	CU	Toarcian <sup>1,2</sup>	late Pliensbachian Early	<p><b>Nannoceratopsis senex Zone.</b> FO of <i>Nannoceratopsis</i> spp. which have their FADs in the Davoei Zone (Poulsen &amp; Riding 2003), indicates a late Early Pliensbachian.</p> <p><b>Spheripollenites–Leptolepidites Zone.</b> <i>Perinopollenites elatoides</i> and <i>Pinuspollenites minimus</i> dominate. Rare <i>Callialasporites</i> spp. may (if <i>in situ</i>) indicate an age younger than late early Pliensbachian (Davoei Zone; Herngreen et al. 2003) or late early Toarcian (Batten &amp; Koppelhus 1996).</p> <p><b>Marginal marine environment:</b> 6% dinocysts, 2% marine acritarchs.</p>
1955	CU	?late Toarcian <sup>1</sup> , Early Pliensbachian <sup>2</sup>	late Pliensbachian Early	<p><b>Mendicodinium reticulatum Zone.</b></p> <p><b>Cerebropollenites macroverrucosus Zone.</b> <i>Perinopollenites elatoides</i> and <i>Pinuspollenites minimus</i> dominate. Marked decrease in <i>Deltoidospora</i> spp. Increase in <i>Classopollis</i> spp. Rare <i>Callialasporites</i> spp. may (if <i>in situ</i>) indicate an age younger than late early Pliensbachian (Davoei Zone; Herngreen et al. 2003) or late early Toarcian (Batten &amp; Koppelhus 1996).</p> <p><b>Marginal marine environment:</b> 6% dinocysts, 3% marine acritarchs.</p>
1970–2030	CU	Late Pliensbachian <sup>1</sup> , Pliensbachian <sup>2</sup>	Pliensbachian	<p><b>Mendicodinium reticulatum Zone.</b></p> <p><b>Cerebropollenites macroverrucosus Zone.</b> <i>Perinopollenites elatoides</i> and <i>Deltoidospora</i> dominate.</p> <p><b>Shallow to marginal marine environment:</b> 6–11% dinocysts, 0–3% marine acritarchs.</p>
2042.5 m	CU	Late Pliensbachian <sup>1</sup> , Pliensbachian <sup>2</sup>	Early Pliensbachian	<p><b>Mendicodinium reticulatum Zone.</b> Unless caved, FO of <i>Mendicodinium reticulatum</i> (FAD early Pliensbachian; Poulsen &amp; Riding 2003) may indicate <i>M. reticulatum</i> Zone. Absence of <i>Liasidium variabile</i> (LAD top Sinemurian) may also indicate an early Pliensbachian age or younger (Poulsen &amp; Riding 2003).</p> <p><b>Cerebropollenites macroverrucosus Zone.</b></p> <p><b>Depositional environment.</b> No quantitative</p>

				assessment made in this study.
2062.5	CU	Late Pliensbachian <sup>1</sup> , Pliensbachian <sup>2</sup>	Pliensbachian	<b>?<i>Liasidium variable</i>–<i>Mendicodinium reticulatum</i> zones.</b> Absence of <i>Liasidium variable</i> (LAD top Sinemurian) indicates an early Pliensbachian age or younger (Poulsen & Riding 2003). <b><i>Cerebropollenites macroverrucosus</i> Zone.</b> <b>Depositional environment.</b> No quantitative assessment made in this study.
2080	CU	Late Pliensbachian <sup>1</sup> , Pliensbachian <sup>2</sup>	Pliensbachian	<b>?<i>Liasidium variable</i>–<i>Mendicodinium reticulatum</i> zones.</b> Absence of <i>Liasidium variable</i> (LAD top Sinemurian) indicates an early Pliensbachian age or younger (Poulsen & Riding 2003). <b><i>Cerebropollenites macroverrucosus</i> Zone.</b> <i>Kekryphalospora distincta</i> (FO ?early, late Pliensbachian; Batten & Koppelhus 1996) and <i>Manumia delcourtii</i> (FO late Pliensbachian; Batten & Koppelhus 1996) are considered to be caved. <b>Marine environment:</b> 22% dinocysts, marine acritarchs present.
2107.5	CU	Sinemurian <sup>1,2</sup>	Late Sinemurian	<b>?<i>Liasidium variable</i>–<i>Mendicodinium reticulatum</i> zones,</b> however the nominate taxa have not been encountered. Absence of both <i>D. priscum</i> and <i>Mendicodinium reticulatum</i> may indicate a late Sinemurian age. <b><i>Cerebropollenites macroverrucosus</i> Zone.</b> <b>Marginal marine environment:</b> 4% dinocysts, 1% marine acritarchs.
2125	CU	Early Sinemurian <sup>1,2</sup>	Early Sinemurian	<b><i>Dapcodinium priscum</i> Zone.</b> LO <i>D. priscum</i> indicates an early Sinemurian age (LAD top early Sinemurian; Poulsen & Riding 2003). <b><i>Cerebropollenites macroverrucosus</i> Zone.</b> FO of <i>Cerebropollenites macroverrucosus</i> (FAD early Sinemurian; Batten & Koppelhus 1996). <b>Shallow marine environment:</b> 17% dinocysts, 2% marine acritarchs.
2130–2150	CU	Hettangian <sup>1</sup> , Early Sinemurian <sup>2</sup>	Hettangian	<b><i>Dapcodinium priscum</i> Zone.</b> Presence of <i>D. priscum</i> indicates this zone (Poulsen & Riding 2003). <b><i>Pinuspollenites-Trachysporites</i> Zone.</b> LCO of <i>Trachysporites</i> spp. at 2130 m. The reason this sample is re-assessed as Hettangian is that identification of <i>C. macroverrucosus</i> is doubtful. Early specimens of this taxon are sometimes difficult to separate from <i>C. thiergartii</i> , and in this case it is not clear whether the specimen belongs to <i>C. macroverrucosus</i> or <i>C. thiergartii</i> . <b>Shallow to marginal marine environment:</b> 6–14% dinocysts, <1% marine acritarchs.

2160–2163	CU		Hettangian	<p><b>Dapcodinium priscum Zone.</b> Presence of <i>D. priscum</i> indicates this zone (Poulsen &amp; Riding 2003).</p> <p><b>Pinuspollenites-Trachysporites Zone.</b></p> <p><b>Marginal marine environment:</b> 3% dinocysts, 1% marine acritarchs.</p>
2185-2190	CU		Early Hettangian	<p><b>Dapcodinium priscum Zone.</b> Presence of <i>D. priscum</i> indicates this zone (Poulsen &amp; Riding 2003).</p> <p><b>Pinuspollenites-Trachysporites Zone.</b> <i>Trachysporites</i> spp. is rare. The assemblage is dominated by <i>Perinopollenites elatoides</i>, <i>Pinuspollenites minimus</i> and <i>Deltoidospora</i> spp. It can be correlated with the early Hettangian DPPi zone of the Stenlille wells (Lindström 2016).</p> <p><b>Marginal marine environment:</b> 6% dinocysts, 4% marine acritarchs.</p>
2195	CU	Early Hettangian <sup>1,2</sup>	Early Hettangian	<p><b>Dapcodinium priscum Zone.</b> Presence of <i>D. priscum</i> indicates this zone (Poulsen &amp; Riding 2003).</p> <p><b>Pinuspollenites-Trachysporites Zone.</b> FCO <i>Pinuspollenites minimus</i> allows assignment to the <i>P-T</i> Zone. <i>Trachysporites</i> spp. is rare. The assemblage is dominated by <i>Perinopollenites elatoides</i>, <i>Pinuspollenites minimus</i> and <i>Deltoidospora</i> spp. It can be correlated with the early Hettangian DPPi zone of the Stenlille wells (Lindström 2016).</p> <p><b>Marginal marine environment:</b> 10% dinocysts, 2% marine acritarchs.</p>
2215	CU	Latest Rhaetian <sup>1,2</sup>	Late Rhaetian	<p><b>Rhaetogonyaulax rhaetica Zone.</b> The LO, but also acme of <i>R. rhaetica</i> suggests that this sample is located close to MFS7 of Nielsen (2003).</p> <p><b>Rhaetipollis-Limbosporites Zone,</b> although <i>Limbosporites lundbladiae</i> was not registered.</p> <p><b>Shallow marine environment:</b> 15% dinocysts, 3% of the fresh/brackish water alga <i>Botryococcus braunii</i> suggests nearby input of freshwater.</p>
2232.5–2255	CU	Middle Rhaetian <sup>1,2</sup>	Middle Rhaetian	<p><b>Rhaetogonyaulax rhaetica Zone.</b> 2232.5 m: LO <i>Lunnomidinium scaniense</i>. 2255 m: LO <i>Suessia</i> sp. A</p> <p><b>Rhaetipollis-Limbosporites Zone.</b> ?FO of <i>Limbosporites lundbladiae</i> possibly indicates base of the <i>R-L</i> Zone (Lund 1977). The LCO of <i>Rhaetipollis germanicus</i> is noteworthy.</p>
2280–2292.5	CU	Middle Rhaetian <sup>1,2</sup>	?early Rhaetian–Middle Rhaetian	<p><b>Rhaetogonyaulax rhaetica Zone.</b> Acme <i>Dapcodinium priscum</i>.</p> <p>Based on the absence of <i>L. lundbladiae</i>, this</p>

				sample could tentatively be assigned to the <b><i>Ricciisporites–Conbaculatisporites</i> Zone</b> of Lund (1977), which could suggest an early Rhaetian age. An acme in <i>Granuloperculatipollis rudis</i> is noted in this interval.
2333–2335 black frag- ments	CU			The majority of this assemblage is considered to be caved. Triassic palynomorphs are present, but may be caved from Rhaetian strata above. <b>Depositional environment</b> has not been assessed due to the large amount of caving.
2333–2335 green frag- ments	CU			The majority of this assemblage is considered to be caved. Triassic palynomorphs are present, but may be caved from Rhaetian strata above. Presence of <i>Retisulcites perforates</i> and <i>Echinosporites iliacooides</i> (LADs in the earliest Carnian; Schulz & Heunisch 2005), is noteworthy. <b>Depositional environment</b> has not been assessed due to the large amount of caving.
2333–2335 red frag- ments	CU		?Mid Norian–early Rhaetian	<b><i>Rhaetogonyaulax rhaetica</i> Zone.</b> FO/LO <i>Suessia swabiana</i> (FAD mid Norian–top Rhaetian; Riding et al. 2010). <b>?<i>Corollina–Enzonasporites</i> Zone.</b> LO <i>Triadispora</i> sp. and <i>Cordaitina minor</i> may indicate an early Rhaetian age or older. The majority of this assemblage is considered to be caved. Triassic palynomorphs are present, but may be caved from Rhaetian strata above. Dominated by bisaccate pollen: unidentified, <i>Alisporites</i> spp. and <i>Pinuspollenites minimus</i> . <i>Deltoidospora</i> spp., <i>Classopollis</i> spp., <i>Calamospora tener</i> and <i>Quadraeculina anellaeformis</i> are common. <b>Depositional environment</b> has not been assessed due to the large amount of caving, but the presence of the marine dinoflagellate cyst <i>Suessia swabiana</i> indicates a marine environment.

### 4.3.3 Höllviksnäs-1/Höllviken-2

The biostratigraphic data is from core samples from the cored the Höllviken-2 well, and are compiled from Lindström & Erlström (2011), and the stratigraphic breakdown is shown in Table 4.4. As there are no geophysical logs for Höllviken-2, it has been correlated with the logs from the nearby Höllviksnäs-1 well, and these are the logs used on Appendix 3. The data has been revised herein, mainly in regards to the Pliensbachian–Toarcian interval. Vajda (2001), who primarily focused on the Lower Cretaceous succession in the Höllviken-2 core, assigned the interval from 1319–1296 m to the Aalenian. The Rhaetian–earliest Sinemurian interval was recently revised and described in detail in Lindström et al. (in press), and this is also shown in Appendix 3, and in Table 4.4 below.

**Table 4.4.** *Palynostratigraphic breakdown of the cored Höllviken-2 well, southwest Scania, based on Lindström & Erlström (2011), and Lindström et al. (in press).*

Depth in meter (Depth in brackets refers to corresponding depth in Höllviksnäs-1)	Sample type	Previous age assessment	Age	Palynozone, dominant taxa and/or marker taxa
1305.15–1294.35	CO	Aalenian <sup>1,2</sup>	Aalenian	<b>Callialasporites-Perinopollenites Zone</b> (Koppelhus & Nielsen 1994). Decrease in <i>Deltoidospora</i> spp. and in <i>Pinuspollenites minimus</i> . <b>Marginal marine environment:</b> <2 % dinoflagellate cysts, <1 % marine acritarchs.
1308.95	CO	Late Toarcian <sup>1</sup> , Aalenian <sup>2</sup>	Aalenian	<b>Callialasporites-Perinopollenites Zone</b> (Koppelhus & Nielsen 1994). LO <i>Taurocusporites verrucatus</i> may indicate a late Toarcian age (Batten and Koppelhus, 1996). FO <i>Tigrisporites scurrandus</i> . <b>Marginal marine environment:</b> 2 % dinoflagellate cysts, 1 % marine acritarchs.
1316.50	CO	Late Toarcian <sup>1</sup> , Aalenian <sup>2</sup>	Late Toarcian-earliest Aalenian	<b>Parvocysta nasuta Zone</b> of Poulsen & Riding (2003). FO <i>Parvocysta</i> sp., <i>Andreedinium</i> aff. <i>elongatum</i> (late Toarcian-earliest Aalenian; Levesquei to Opalinum Zones; Feist-Burkhardt & Monteil 1994). <b>Callialasporites-Perinopollenites Zone</b> (Koppelhus & Nielsen 1994). <b>Marginal marine environment:</b> 6 % dinoflagellate cysts, marine acritarchs rare but present.
1319.60	CO	Late Toarcian <sup>1</sup>	Late Toarcian	<b>Callialasporites-Perinopollenites Zone</b> (Koppelhus & Nielsen 1994). Increase in <i>Perinopollenites elatoides</i> . Minor increase in <i>P. minimus</i> , <i>Cerebropollenites</i> spp., and <i>Spheripollenites</i> spp.

				<b>Marginal marine environment:</b> 6 % dinoflagellate cysts, <1 % marine acritarchs.
1326.60–1329.80	CO	Late Toarcian <sup>1</sup>	Late Toarcian	<b>Spheripollenites–Leptolepidites Zone.</b> 1329.80 m: FO <i>Callialasporites turbatus</i> (FAD Late Toarcian, Batten & Koppelhus 1996). <i>Leptolepidites</i> spp. are present but rare. <b>Marginal marine environment:</b> 2–4 % dinoflagellate cysts, 0–<1 % marine acritarchs.
1333.40–1342.78	CO	Pliensbachian–Early Toarcian <sup>1</sup>	Latest Pliensbachian	<b>Dinoflagellate zone not assigned.</b> The majority of the dinoflagellate cysts within this interval belong to <i>Mendicodinium</i> spp. or “Rotundus granulatus” sensu Koppelhus. A specimen that can possibly be assigned to <i>Mendicodinium morgenrothum</i> at 1340.0 m is noteworthy. Butler (1995) suggests an Aalenian to Early Bajocian range for <i>M. morgenrothum</i> . It is confirmed to occur sporadically from 1327 m in the Höllviken-2 succession, indicating that its stratigraphic range needs revision. <b>Spheripollenites–Leptolepidites Zone.</b> 1342.78 m: first consistent occurrence of <i>Leptolepidites</i> spp. suggests assignment to this zone. According to Batten & Koppelhus (1996) <i>Leptolepidites</i> spp. has its FAD in the latest Pliensbachian. <b>Shallow marine environment, shallowing upwards to marginal marine environment, possibly terrestrial environment:</b> 0–15 % dinoflagellate cysts, <1 % marine acritarchs. A dominance of <i>Deltoidospora</i> spp. at 1333.40 m may signal fern colonization on newly exposed surfaces.
1347.92 (1357)	CO	Pliensbachian–Early Toarcian <sup>1</sup>	late Early Pliensbachian	<b>Cerebropollenites macroverrucosus Zone.</b> FO <i>Neoraistrickia truncata</i> (FAD late Toarcian, Batten & Koppelhus 1996; FAD late Early Pliensbachian, Davoei Zone, Hengreen et al. 2003). <b>Marginal marine environment:</b> 1 % dinoflagellate cysts.
1366.10 (1376)	CO	Pliensbachian–Early Toarcian <sup>1</sup>	Late Pliensbachian	The FO of <i>Mendicodinium groenlandicum</i> suggests assignment to the <b>Nannoceratopsis senex Zone</b> , however, no <i>Nannoceratopsis</i> spp. were recorded in this sample. <b>Cerebropollenites macroverrucosus Zone.</b> <b>Marginal marine environment:</b> 3 % dinoflagellate cysts.
1368.50 (1377.5)	CO	Pliensbachian–Early Toarcian <sup>1</sup>	Early Pliensbachian	<b>Mendicodinium reticulatum Zone.</b> FO <i>Mendicodinium reticulatum</i> (FAD late Sinemurian; Poulsen & Riding 2003). Absence of <i>Liasidium</i>

				<p><i>variabile</i> (LAD top Sinemurian) indicates an early Pliensbachian age (Poulsen &amp; Riding 2003).</p> <p><b>Cerebropollenites macroverrucosus Zone.</b></p> <p><b>Marginal marine environment:</b> 9 % dinoflagellate cysts, &lt;1 % marine acritarchs.</p>
1371– 1372.65 (1382)	CO	Late Sinemurian <sup>1</sup>	Early Sinemurian      Late Sinemurian	<p><b>Dapcodinium priscum Zone/Liasidium variable Zone.</b> 1372.65 m: LO <i>Dapcodinium priscum</i>, FO <i>Liasidium variable</i>. Normally these two taxa do not occur together, possibly indicating a hiatus or condensed level.</p> <p><b>Cerebropollenites macroverrucosus Zone.</b> 1371 m, <b>Marginal marine, probably lagoonal environment:</b> &lt;1 % dinoflagellate cysts, 3 % fresh/brackish water alga <i>Botryococcus braunii</i>, &lt;1 % other freshwater cysts.</p> <p>1372.65 m, <b>Marginal marine environment:</b> 4 % dinoflagellate cysts, marine acritarchs present but rare.</p>
1380.16 (1388)	CO	Early Sinemurian <sup>1</sup>	Early Sinemurian	<p><b>Dapcodinium priscum Zone.</b> Continued presence of <i>D. priscum</i> allows assignment to this zone.</p> <p><b>Cerebropollenites macroverrucosus Zone.</b> FO <i>Cerebropollenites macroverrucosus</i> allows assignment to this zone (Dybkjær 1991).</p> <p><b>Marginal marine environment:</b> 5 % dinoflagellate cysts.</p>
1393.78– 1428.0 (1430)	CO	Hettangian <sup>1</sup> –Late Hettangian <sup>1</sup>	Hettangian–Late Hettangian	<p><b>Dapcodinium priscum Zone.</b> Presence of <i>D. priscum</i> allows assignment to this zone.</p> <p><b>Pinuspollenites–Trachysporites Zone.</b> Increase in <i>Chasmatosporites</i> spp. at 1404 m indicates a Late Hettangian age from this level. FO of <i>Cerebropollenites thiergartii</i> indicates proximity to the Triassic-Jurassic boundary.</p> <p>1428 m: marked increase in <i>Pinuspollenites minimus</i> allows assignment to this zone.</p> <p><b>Marginal marine environment:</b> 0–6 % dinoflagellate cysts, &lt;1 % fresh/brackish water alga <i>Botryococcus braunii</i>.</p>
1433.90– 1439.20	CO	Latest Rhaetian <sup>1</sup>	Latest Rhaetian	<p><b>Transition Zone.</b> 1439.20 m: FO <i>Kraeuselisporites reissingerii</i>, FO <i>Ischyosporites variegatus</i>,</p> <p><b>Terrestrial environment:</b> &lt;1 % dinoflagellate cysts, marine acritarchs present but very rare, &lt;1 % fresh/brackish water alga <i>Botryococcus braunii</i>.</p>
1439.60– 1446	CO	Latest Rhaetian <sup>1</sup>	Latest Rhaetian	<p><b>Rhaetogonyaulax rhaetica Zone.</b> LO <i>Rhaetogonyaulax rhaetica</i> at 1439.60 m allows assignment to this zone.</p> <p><b>Ricciisporites–Polypodiisporites Zone.</b> This</p>

				interval is assigned to the <i>Deltoidospora</i> spp. – <i>Ricciisporites tuberculatus</i> – <i>Polypodiisporites polymicroforatus</i> (DRP) interval (Lindström et al. in press). LCO of <i>Polypodiisporites polymicroforatus</i> occurs at 1439.60 m. <b>Marginal marine environment:</b> <1 % dinoflagellate cysts, <1–8 % marine acritarchs.
1469.94	CO		Middle Rhaetian	<b>Rhaetipollis–Limbosporites Zone.</b> <b>Terrestrial environment, forest mire:</b> <1 % marine acritarchs, <1 % fresh/brackish water alga <i>Botryococcus braunii</i> .
1475.50– 1477.75	CO		Middle Rhaetian	<b>Rhaetogonyaulax rhaetica Zone.</b> <b>Rhaetipollis–Limbosporites Zone.</b> <b>Marginal marine environment:</b> <1–5 % marine acritarchs, <1 % fresh/brackish water alga <i>Botryococcus braunii</i> .

#### 4.3.4 Lavø-1

Palynological slides from Lavø-1, originally reported by Poulsen (1996), were re-examined herein. The majority of the cuttings samples were found to contain large amounts of caved material, to such an extent that it was not possible to assess the age of those samples. However, slides from the cored intervals in Lavø-1 were re-examined and these were found to provide interesting new information that have helped to further constrain the stratigraphic breakdown of the Gassum to Fjerritslev formations (Table 4.5; Appendix 4). One ditch cuttings sample from the Rhaetian was also checked for palynomorphs, but not quantitatively assessed due to the large amounts of caved material. The new stratigraphic breakdown differs significantly from that of Poulsen (1996) as is shown in Table 4.5.

**Table 4.5.** *Palynostratigraphic breakdown of selected core and cuttings samples from the Lavø-1 well. Previous age assignments are from Poulsen (1996).*

Depth in meter	Sample type	Previous age assessment	Age	Palynozone, dominant taxa and/or marker taxa
2077	CO		Toarcian	<b><i>Mancodinium semitabulatum</i> Zone–<i>Parvocysta nasuta</i> Zone.</b> See the sample below <b>?<i>Spheripollenites–Leptolepidites</i> Zone.</b> <i>Manumia delcourtii</i> indicates late Pliensbachian or younger (Batten & Koppelhus 1996). Dominance of <i>Deltoidospora</i> and <i>Classopollis</i> . <i>Perinopollenites elatoides</i> only present in low numbers. <i>Nevesisporites vallatus</i> , <i>Alisporites</i> spp. and <i>Punctatisporites</i> spp. are common to abundant. <i>Spheripollenites</i> spp. present in low number. Rare <i>Ischyosporites variegatus</i> . <b>Marine environment:</b> 23 % dinoflagellate cysts, 10 % marine acritarchs.
2078	CO	Early Toarcian	Toarcian	<b><i>Mancodinium semitabulatum</i> Zone–<i>Parvocysta nasuta</i> Zone.</b> Co-occurrence of <i>N. gracilis</i> , <i>M. groenlandicum</i> , <i>M. semitabulatum</i> , and absence of <i>Luehndea spinosa</i> and dinoflagellates of the <i>Parvocysta</i> and <i>Susadinium</i> , indicates this zone (Poulsen & Riding 2003), i.e. top Tenuicostatum, Falciferum, and lower Bifrons Zones. The presence of <i>Wallodinium laganum</i> suggests a somewhat younger age, Late Toarcian to earliest Aalenian (Aalensis to Opalinum zones; Feist-Burkhardt & Pross 2010).

				<p><b>Spheripollenites–Leptolepidites Zone.</b>  <i>Manumia delcourtii</i> indicates late Pliensbachian or younger (Batten &amp; Koppelhus 1996). Dominance of <i>Deltoidospora</i> and <i>Classopollis</i>. <i>Perinopollenites elatoides</i> only present in low numbers. <i>Nevesisporites vallatus</i>, <i>Alisporites</i> spp. and <i>Punctatisporites</i> spp. are common to abundant.  <b>Shallow marine environment:</b> 12 % dinoflagellate cysts, 5 % marine acritarchs.</p>
2163	CO	Late Pliensbachian- Early Toarcian	Early Pliensbachian	<p><b>Mendicodinium reticulatum Zone.</b> Presence of rare specimens of <i>Mendicodinium groenlandicum</i> and <i>M. reticulatum</i> along with an absence of <i>Liasidium variable</i> and <i>Nannoceratospis senex</i>, suggests assignment to this zone, and an early Pliensbachian age; Jamesoni, Ibex and early Davoei zones (Poulsen &amp; Riding 1996).  <b>Cerebropollenites macroverrucosus Zone.</b> Dominated by <i>Perinopollenites elatoides</i> and <i>Deltoidospora</i>. <i>Classopollis</i> present in low numbers. Presence of <i>C. macroverrucosus</i> and absence of <i>Manumia delcourtii</i> indicates an early Sinemurian to early Pliensbachian age (Batten &amp; Koppelhus 1996).  <b>Marginal marine environment:</b> 4 % dinoflagellate cysts, &lt;1 % marine acritarchs.</p>
2277.5	CO	?Early Pliensbachian	Late Rhaetian	<p><b>Ricciisporites–Polypodiisporites Zone.</b>  Mass occurrence of sphaeromorphs, equivalent to the end-Triassic event beds, the grey siltstone interval of Lindström et al. (2012).  <b>Depositional environment:</b> No quantitative assessment made.</p>
2283	CO	?Late Sinemurian	Late Rhaetian	<p><b>Ricciisporites–Polypodiisporites Zone.</b>  Mass occurrence of sphaeromorphs, suggests equivalent to the end-Triassic event beds, the grey siltstone interval of Lindström et al. (2012).  <b>Depositional environment:</b> No quantitative assessment made.</p>
2307-2310	CU		Middle Rhaetian	<p><b>Rhaetogonyaulax rhaetica Zone,</b> based on the co-occurrence of <i>Lunnomidinium scaniense</i> and <i>Dapcodinium priscum</i>.  <b>Depositional environment:</b> No quantitative assessment made due to the overwhelming amount of caved material.</p>

### 4.3.5 Stenlille-1

The palynological data from the interval from 1411.90–1523.46 m in the cored Stenlille-1 well, were obtained within a Geocenter Denmark funded research project, and has been reported in Lindström et al. (2012) and Lindström (2016). The stratigraphic breakdown is presented in Appendix 5 and in Table 4.6 below.

**Table 4.6.** Stratigraphic breakdown of the cores and sidewall cores in Gassum and Fjerritslev formations of Stenlille-1. Palynostratigraphy includes data from Lindström et al. (2012) and Lindström (2016).

Depth in meter	Sample type	Age	Palynozone, dominant taxa and/or marker taxa
1221.11-1221.13	CO	Late Toarcian or Early Cretaceous	<b>Inconclusive.</b> Assemblage of Early-Middle Jurassic character. Presence of <i>Tauocusporites verrucosus</i> indicates an age not younger than the Toarcian. A single specimen of <i>Cleistosphaeridium</i> sp. suggests an Early Cretaceous age. <b>Marine environment:</b> 11% dinocysts, 14% marine acritarchs, 3% fresh/brackish water <i>Botryococcus braunii</i> .
1226.51-1226.52	CO	Late Toarcian–earliest Aalenian	<b>Spheripollenites–Leptolepidites Zone.</b> Dominated by spores; <i>Deltoidospora</i> spp. and <i>Aratrisporites minimus</i> . Abundant <i>Nevesisporites vallatus</i> <i>Leptolepidites</i> spp. and <i>Foraminisporites jurassicus</i> . Common <i>Classopollis</i> spp. and <i>Spheripollenites</i> spp. allows assignment to this zone. <b>Parvocysta nasuta Zone.</b> Presence of <i>Parvocysta</i> sp. indicates a Late Toarcian (Levesquei Zone) to earliest Aalenian age (Opalinum Zone). This interval most likely correlates with the “reworking interval” in the Anholt borehole (Nielsen et al. 2003; Seidenkrantz et al. 1993). <b>Marine environment:</b> 2% dinocysts, 10% marine acritarchs.
1376.5, 1386.5	SW C	Late Hettangian	<b>Dapcodinium priscum Zone.</b> LO <i>Dapcodinium priscum</i> indicates an early Sinemurian age at the youngest (Poulsen & Riding 2003). <b>Pinuspollenites–Trachysporites Zone.</b> Dominance of <i>Perinopollenites elatoides</i> and <i>Deltoidospora</i> spp. <b>Marginal marine environment:</b> <1-2% dinocysts, 3% marine acritarchs. 0–2% fresh/brackish water <i>Botryococcus braunii</i> .
1411.90, 1418.95	CO	Late Hettangian	<b>Dapcodinium priscum Zone.</b> Continued common presence of <i>Dapcodinium priscum</i> allows assignment to this zone (Poulsen & Riding 2003). <b>Pinuspollenites–Trachysporites Zone, Uppermost PPI Zone</b> (Lindström 2016). Dominance of <i>Perinopollenites elatoides</i> along with <i>Deltoidospora</i> spp. and <i>Classopollis</i> spp. <i>Pinuspollenites minimus</i> is rare to common only. Absence of <i>Cerebropollenites macroverrucosus</i> suggests a Hettangian age (Dybkjær 1991). <b>Marine environment:</b> 16–22% dinocysts, <1% marine acritarchs.

1455	CO	Hettangian	<p><b>Dapcodinium priscum Zone.</b> Presence of <i>Dapcodinium priscum</i> allows assignment to this zone (Poulsen &amp; Riding 2003). <b>Pinuspollenites –Trachysporites Zone, Upper PPI zone</b> (Lindström 2016). Dominance of <i>Perinopollenites elatoides</i> and <i>Deltoidospora</i> spp. <i>Pinuspollenites minimus</i> are abundant.</p> <p><b>Marine environment:</b> 18% dinocysts, &lt;1% marine acritarchs.</p>
1489.28– 1483.25	CO	Hettangian	<p><b>Dapcodinium priscum Zone.</b></p> <p><b>Pinuspollenites–Trachysporites Zone, PPI zone</b> (Lindström 2016). Dominance of <i>Perinopollenites elatoides</i>, and high abundances of <i>Pinuspollenites minimus</i> and <i>Deltoidospora</i> spp. Common <i>Stereisporites</i> spp. and <i>Classopollis</i> spp. LOs of <i>P. polymicroforatus</i>, <i>R. tuberculatus</i>, <i>L. lundbladiae</i>, <i>Triancoraesporites reticulatus</i>, <i>Rhaetipollis germanicus</i> and <i>Lunatisporites rhaeticus</i>. <i>Perinopollenites</i> increase in abundance while <i>Pinuspollenites</i> decreases towards the top of the zone.</p> <p><b>Marine environment:</b> 7–29% dinocysts, &lt;1–6% marine acritarchs, only sporadic &lt;1% <i>Botryococcus braunii</i> or <i>Lecaniella</i>.</p>
1491.42– 1489.90	CO	Early Hettangian	<p><b>Dapcodinium priscum Zone.</b></p> <p><b>DPPi Zone, Pinuspollenites–Trachysporites Zone.</b> <i>Deltoidospora</i> spp. Dominates. <i>Perinopollenites elatoides</i> and <i>Pinuspollenites minimus</i> are abundant. <i>Stereisporites</i> spp. and <i>Trachysporites</i> spp. are common. Increase in <i>Aratrisporites minimus</i> in the middle of the zone. LOs of <i>Semiretisporis gothae</i>, <i>Ovalipollis ovalis</i>, <i>Triancoraesporites ancorae</i>, <i>Densoisporites fissus</i> and <i>Cingulizonates rhaeticus</i>, within this zone.</p> <p><b>Marine with input of freshwater:</b> 2–23% dinocysts, ≤1% marine acritarchs, 0–5% of the fresh water alga <i>Lecaniella</i>.</p>
1494.90– 1491.42	CO	Latest Rhaetian to earliest Hettangian	<p><b>Dapcodinium priscum Zone</b>, from 1492.82 m.</p> <p><b>Rhaetogonyaulax rhaetica Zone</b>, top 1492.82 m. LO of <i>R. rhaetica</i>.</p> <p><b>PDS Zone, Transition zone.</b> Dominance of <i>Perinopollenites elatoides</i>, together with abundant <i>Deltoidospora</i> spp. Increase in <i>Classopollis</i> spp. <i>Stereisporites</i> spp. common to abundant. FO of <i>Ischyosporites variegatus</i> is in the middle of this zone.</p> <p><b>Marine with major input of fresh water:</b> &lt;1–22% dinocysts, &lt;1–9% marine acritarchs, &lt;1–30% of the fresh water alga <i>Lecaniella</i>.</p>
1495.51– 1495.10	CO	Late Rhaetian	<p><b>Rhaetogonyaulax rhaetica Zone.</b></p> <p><b>CCM Zone, Transition zone.</b> Dominance of <i>Calamospora tener</i>, <i>Conbaculatisporites</i> spp. and monosulcate pollen.</p> <p><b>Marginal marine or lagoonal:</b> 0–&lt;1% dinocysts, &lt;1–10% marine acritarchs, &lt;1–18% fresh/brackish water <i>Botryococcus braunii</i>.</p>
1503.35– 1495.51	CO	Late Rhaetian	<p><b>Rhaetogonyaulax rhaetica Zone.</b></p> <p><b>PRD Zone, Ricciisporites–Polypodiisporites Zone.</b> Dominance of <i>Polypodiisporites polymicroforatus</i>, <i>Deltoidospora</i> spp. (predominantly <i>D. toralis</i>), and <i>Ricciisporites tuberculatus</i>. FO of <i>Cerebropollenites thiergartii</i> at the top of the zone.</p> <p><b>Marginal marine:</b> &lt;2% dinocysts, 2–14% marine acritarchs, ≤1% fresh/brackish water <i>Botryococcus braunii</i>.</p>
1523.46–	CO	Middle – Late Rhae-	<p><b>Rhaetogonyaulax rhaetica Zone.</b></p>

1503.70		tian	<p><b>GCP Zone, Rhaetipollis–Limbosporites Zone.</b> Dominance of <i>Classopollis</i> and <i>Perinopollenites elatoides</i>. Consistent and often common <i>Granuloperculatipollis rudis</i>. <i>Ricciisporites tuberculatus</i> is common to abundant.</p> <p>Predominantly <b>Marine environment</b>.</p> <p>1523.46 m: <b>Marine environment</b>, 21% dinocysts, 6% marine acritarchs.</p> <p>1522.89–1520.80 m: <b>Marginal marine environment</b>, 3–7% dinocysts, &lt;1% marine acritarchs.</p> <p>1518.74–1506.02 m: <b>Marine environment</b>, 25–77% dinocysts, 0–11% marine acritarchs, &lt;1% fresh/brackish water <i>Botryococcus braunii</i>.</p> <p>1505.81–1504.21 m: <b>Marine environment, fluctuating but declining values</b>, 6–35% dinocysts, &lt;1–11% marine acritarchs, ≤1% fresh/brackish water <i>Botryococcus braunii</i>.</p> <p>1503.70 m: &lt;1% dinocysts, 2% marine acritarchs, 1% fresh/brackish water <i>Botryococcus braunii</i>.</p>
1532.79	CO		<p><b>Rhaetogonyaulax rhaetica Zone.</b></p> <p><b>GCP Zone:</b> Dominance of <i>Classopollis</i>, <i>Perinopollenites</i> with common to abundant <i>Ricciisporites tuberculatus</i>. <i>G. rudis</i> is rare.</p> <p><b>Marginal marine environment:</b> 9% marine dinocysts, &lt;1% marine acritarchs, &lt;1% fresh/brackish water <i>Botryococcus braunii</i>.</p>
1542.29	CO	Late Early Rhaetian	<p><b>Rhaetogonyaulax rhaetica Zone.</b></p> <p><i>Dapcodinium priscum</i> (dominant), <i>Beaumontella caminuspina</i>, and <i>Suessia swabiana</i>.</p> <p><b>GCP Zone:</b> <i>Classopollis zwolinskai</i> and <i>Granuloperculatipollis rudis</i> are abundant, which may indicate a late Early Rhaetian age (see Lund 2003).</p> <p>FO <i>Quadraeculina anellaeformis</i> (FAD base Rhaetian; Kürschner and Hengreen, 2010). LO <i>Camerosporites secatus</i> may indicate an Early Rhaetian age.</p> <p><b>Marine environment:</b> 41% marine dinocysts, &lt;1% marine acritarchs.</p>
1542.38	CO	Middle Rhaetian	<p><b>Rhaetogonyaulax rhaetica Zone.</b></p> <p><b>Rhaetipollis–Limbosporites Zone, CPR Zone:</b> Dominance of <i>Classopollis</i>, <i>Perinopollenites</i> with common to abundant <i>Ricciisporites tuberculatus</i>. <i>G. rudis</i> is rare.</p> <p>FO <i>Limbosporites lundbladiae</i> (FAD base mid Rhaetian; Lund 2003; Schulz &amp; Heunisch 2005).</p> <p><b>Marine environment:</b> 47% marine dinocysts, 2% marine acritarchs.</p>
1556.0 and 1576.0	CO and SC	Early-Middle Rhaetian	<p><b>Rhaetogonyaulax rhaetica Zone.</b> Presence of common <i>Dapcodinium priscum</i> at 1576.0 m.</p> <p><b>?Rhaetipollis–Limbosporites Zone.</b> <i>Ricciisporites tuberculatus</i>, <i>Perinopollenites elatoides</i> and <i>Classopollis</i> spp. dominate.</p> <p>FO <i>Cingulizonates rhaeticus</i> (FAD base mid Rhaetian; Lund 2003; Schulz &amp; Heunisch 2005). LO <i>Triadisporea crassa</i> and <i>Triadisporea</i> sp. indicate an Early Rhaetian age. (LAD <i>Triadisporea</i> spp.</p> <p><b>Marginal marine environment:</b> 5–6% marine dinocysts, &lt;1%</p>

			marine acritarchs, 0–4% fresh/brackish water <i>Botryococcus braunii</i> .
1602.0	SC	Early Rhaetian	<p><b><i>Rhaetogonyaulax rhaetica</i> Zone.</b></p> <p><b>?<i>Corollina–Enzonasporites</i> Zone.</b> FO <i>Rhaetipollis germanicus</i> (FAD base Rhaetian; Schulz &amp; Heunisch 2005; Kürschner &amp; Hergreen 2010) indicates an Early Rhaetian age, at the oldest.</p> <p><b>Depositional environment:</b> No quantitative assessment was made. Rare occurrence of marine acritarchs point to marginal marine environment.</p>
1637.5	SC		<p><b><i>Rhaetogonyaulax rhaetica</i> Zone.</b> Presence of <i>R. rhaetica</i> (FAD base Norian; Riding et al. 2010).</p> <p><b>?<i>Corollina–Enzonasporites</i> Zone.</b></p> <p><b>Depositional environment:</b> No quantitative assessment was made. Rare occurrence of dinoflagellate cysts point to marginal marine environment.</p>

### 4.3.6 Stenlille-2

The Lower Jurassic succession of the Stenlille-2 well was studied by Dybkjær (1991), and is briefly reviewed herein, because it partly overlaps with the Stenlille-1 succession.

**Table 4.7.** Stratigraphic breakdown of the cores and sidewall cores in Gassum and Fjerritslev formations of Stenlille-2. Palynostratigraphic data from Dybkjær (1991).

Depth in meter	Sample type	Previous age assessment	Age	Palynozone, dominant taxa and/or marker taxa
1228	SW	Early Toarcian	Late Pliensbachian–early Toarcian	<p><b>Luehndea spinosa Zone.</b> Presence of <i>Nannoceratopsis gracilis</i> indicates an age younger than late Pliensbachian (Poulsen &amp; Riding, 2003).</p> <p><b>Spheripollenites–Leptolepidites Zone.</b> FO <i>Manumia delcourtii</i> indicates a late Pliensbachian/Toarcian age (Batten &amp; Koppelhus 1996). Abundant <i>Spheripollenites</i> spp. and FO of <i>Leptolepidites</i> spp. allows assignment to this zone (Dybkjær 1991).</p> <p><b>Marginal marine environment:</b> dinoflagellate cysts present but rare, 3 % marine acritarchs.</p>
1234	SW	Early Toarcian	Late Pliensbachian–early Toarcian	<p><b>Luehndea spinosa Zone.</b> Presence of <i>Nannoceratopsis gracilis</i> indicates an age younger than late Pliensbachian (Poulsen &amp; Riding 2003).</p> <p><b>Spheripollenites–Leptolepidites Zone.</b> FO <i>Manumia delcourtii</i>. Marked increase in <i>Spheripollenites</i> spp. and marked decrease in <i>Pinuspollenites minimus</i>. Abundant <i>Spheripollenites</i> spp. indicates assignment to this zone (Dybkjær 1991), but <i>Leptolepidites</i> spp. was not recorded.</p> <p><b>Marginal marine environment:</b> &lt;1 % dinoflagellate cysts, 6 % marine acritarchs.</p>
1240–1258	SW			<p><b>Luehndea spinosa Zone.</b> Presence of <i>Nannoceratopsis gracilis</i>, FO at 1258 m, indicates an age younger than late Pliensbachian (Poulsen &amp; Riding 2003).</p> <p><b>Cerebropollenites macroverrucosus Zone.</b> Samples dominated by <i>Classopollis</i> spp., <i>Perinopollenites elatoides</i>, <i>Pinuspollenites minimus</i> and <i>Deltoidospora</i> spp.</p> <p><b>Shallow marine environment:</b> ≤1 % dinoflagellate cysts, 16–20 % marine acritarchs, decreasing upwards.</p>
1390–1392	SW	Early Sinemurian	Early Sinemurian	<p><b>Dapcodinium priscum Zone.</b> Last common</p>

				<p>occurrence of <i>Dapcodinium priscum</i> at 1390 m allows assignment to this zone (Poulsen &amp; Riding 2003).</p> <p><b>Cerebropollenites macroverrucosus Zone.</b> First occurrence of <i>C. macroverrucosus</i> at 1393 m marks the lower boundary of this zone (Dybkjær 1991).</p> <p><b>Marginal marine environment:</b> &lt;1–3 % dinoflagellate cysts, 3–7 % marine acritarchs.</p>
1401–1494	SC, CO		Hettangian	<p><b>Dapcodinium priscum Zone.</b> <i>D. priscum</i> is present, but generally rare, except at 1460 m where it constitutes 19 % of the total palynofloral.</p> <p><b>Pinuspollenites–Trachysporites Zone.</b> 1494 m: FCO <i>Pinuspollenites minimus</i>. FCO of <i>Chasmatosporites</i> spp. at 1491.78 m. FCO of <i>Leiofusa jurassica</i> at 1491 m.</p> <p><b>Shallow to marginal marine environment:</b> 1–19 % dinoflagellate cysts, &lt;1–25 % marine acritarchs.</p>
1496	CO		Latest Rhaetian/earliest Hettangian	<p><b>Dapcodinium priscum Zone.</b> <i>D. priscum</i> is present, but generally rare.</p> <p><b>Transition zone.</b> Dominance of <i>Deltoidospora</i> spp. and <i>Calamospora tener</i>, with abundant <i>Perinopollenites elatoides</i> and <i>Punctatisporites</i> spp., and common <i>Marattisporites punctatus</i> and <i>Stereisporites</i> spp. Probably corresponds to the PDS zone of Lindström (2016).</p> <p><b>Marginal marine environment:</b> 1 % dinoflagellate cysts, 6 % marine acritarchs.</p>
1510–1513	CO	Late Rhaetian	Late Rhaetian	<p><b>Rhaetogonyaulax rhaetica Zone.</b> 1510 m: LO <i>Rhaetogonyaulax rhaetica</i>. 1512 m: LCO and acme of <i>Rhaetogonyaulax rhaetica</i> probably equates to MFS7 of Nielsen (2003).</p> <p><b>Rhaetipollis–Limboisporites Zone.</b> <i>Clasopollis</i> spp. dominates, with abundant <i>Ricciisporites tuberculatus</i>, and common <i>Deltoidospora</i> spp. and <i>Perinopollenites elatoides</i>. Most likely equates to the <b>GCP Zone</b> of Stenlille-1.</p> <p><b>Marine to marginal marine environment:</b> &lt;1–24 % dinoflagellate cysts, &lt;1–24 % marine acritarchs.</p>

### 4.3.7 Stenlille-5

The palynological data from Stenlille-5 are included as it complements the palynostratigraphic data from Stenlille-1 and -2. The data was generated within a Geocenter Denmark financed project (Lindström et al. 2012).

**Table 4.8.** Stratigraphic breakdown of the cores and sidewall cores in Gassum and Fjerritslev formations of Stenlille-5. Palynology from Lindström et al. (2012) and this report.

Depth in meter	Sample type	Previous age assessment	Age	Palynozone, dominant taxa and/or marker taxa
1419.86	CO	Early Sinemurian	Early Sinemurian	<b>Dapcodinium priscum Zone.</b> Continued presence of <i>Dapcodinium priscum</i> allows assignment to this zone (Poulsen & Riding 2003). <b>Cerebropollenites macroverrucosus Zone.</b> First occurrence of <i>Cerebropollenites macroverrucosus</i> allows recognition of this zone (Dybkjær 1991). <b>Marginal marine environment:</b> 8 % dinoflagellate cysts, <1 % marine acritarchs.
1422.15–1430.08	CO	Late Hettangian	Late Hettangian	<b>Dapcodinium priscum Zone.</b> <b>Pinuspollenites–Trachysporites Zone.</b> Dominance of <i>Perinopollenites elatoides</i> and <i>Deltoidospora</i> spp. <i>Pinuspollenites minimus</i> is common to rare. <b>Marginal marine environment:</b> 6–10 % dinoflagellate cysts, <1 % marine acritarchs.
1545.00	CO		Late Rhaetian	<b>Rhaetogonyaulax rhaetica Zone.</b> LO of <i>R. rhaetica</i> allows assignment to this zone (Poulsen & Riding 2003). <i>D. priscum</i> is also present. Common Sphaeromorphs indicates proximity to Grey siltstone interval. <b>Ricciisporites–Polypodiisporites Zone.</b> Dominance of <i>R. tuberculatus</i> , <i>P. polymicroforatus</i> , and <i>Deltoidospora</i> spp. This corresponds to the <b>PRD zone</b> of Lindström (2016). <b>Marginal marine environment:</b> 3 % dinoflagellate cysts, 6 % marine acritarchs.
1550.94	CO		Late Rhaetian	<b>Rhaetogonyaulax rhaetica Zone.</b> Acme of <i>Rhaetogonyaulax rhaetica</i> suggests MFS7 of Nielsen (2003). <b>Rhaetipollis–Limbosporites Zone.</b> Dominance of <i>R. tuberculatus</i> , <i>Deltoidospora</i> spp., <i>P. elatoides</i> dominating. <i>Classopollis</i> abundant, while <i>P. polymicroforatus</i> is absent suggests assignment to this zone and the equivalent <b>GCP Zone</b> of Lindström (2016).

				<b>Marine environment:</b> 68 % dinoflagellate cysts, 1 % marine acritarchs.
1612	SC		?early Rhaetian	<b>Rhaetogonyaulax rhaetica Zone.</b> Presence of <i>Lunnomidinium scaniense</i> . <b>?Ricciisporites–Conbaculatisporites or Corollina–Enzonasporites Zone.</b> FO <i>Quadraeculina anellaeformis</i> (FAD base Rhaetian; Kürschner & Hergreen 2010) and presence of <i>Triadispora</i> sp. may indicate early Rhaetian or older. <b>Depositional environment:</b> No quantitative assessment made.

#### 4.3.8 Stenlille-6

Three cuttings samples were analysed from Stenlille-6 in order to obtain additional information regarding the age of the lower part of the Gassum Formation. However, the samples were severely affected by caving, thus no quantitative assessments were made. Common caved *Liasidium variable* demonstrates the presence of the Late Sinemurian *Liasidium variable* Zone of Poulsen & Riding (2003) at a higher stratigraphical level within this well. The very meagre information obtained from the cuttings samples are presented in Table 4.9.

**Table 4.9.** *Palynological comments on three cuttings samples from Stenlille-6.*

Depth in meter	Sample type	Age	Palynozone, dominant taxa and/or marker taxa
1671–1677	CU	Early Rhaetian	? <b>Corollina–Enzonasporites Zone.</b> Presence of <i>Rhaetipollis germanicus</i> and <i>Quadraeculina anellaeformis</i> (FADs basal Rhaetian; Batten & Koppelhus 1996; Kürschner & Hergreen 2010), along with an absence of <i>Limbosporites lundbladiae</i> and other younger Rhaetian elements, suggests an Early Rhaetian age.
1677–1683	CU	Early Rhaetian	A few possible specimens of <i>Sverdrupiella</i> sp. suggests a Norian to early Rhaetian age (Riding et al. 2010).
1713–1716	CU	?Early Rhaetian	Presence of LO <i>Lunnomidinium scaniense</i> (alfa). Common <i>Granuloperculatipollis rudis</i> may suggest an early Rhaetian age.

### 4.3.9 Stenlille-15

Three core samples from the lower Gassum Formation were analysed. The uppermost sample contained very few palynomorphs. The composition of the palynoflora differs from typical middle Rhaetian ones; hence these samples may be older. The lowermost sample appears to represent a fully terrestrial setting. Additional studies are needed to enable more accurate age assignments.

**Table 4.10.** *Palynological comments on three core samples from Stenlille-15.*

Depth in meter	Sample type	Age	Palynozone, dominant taxa and/or marker taxa
1535.67–1535.69	CO	Rhaetian	Presence of <i>Dapcodinium priscum</i> and <i>Rhaetipollis germanicus</i> suggest a Rhaetian age (see Figs. 4.1. and 4.2.). <b>Depositional environment.</b> No assessment made, but probably marginal marine.
1572.21–1572.22	CO	?middle Rhaetian	<b><i>Rhaetogonyaulax rhaetica</i> Zone.</b> <i>Dapcodinium priscum</i> totally dominant. Co-occurrence of this taxon with <i>Lunnonidinium scaniense</i> and <i>Suessia swabiana</i> allows recognition of this zone. <b>?<i>Rhaetipollis</i>–<i>Limbosporites</i> Zone.</b> Presence of <i>Rhaetipollis germanicus</i> indicates a Rhaetian age. <i>Classopollis</i> spp. and <i>Perinopollenites elatooides</i> are dominant. <b>Marine environment:</b> 68 % dinoflagellate cysts, 2 % marine acritarchs.
1613.64–1613.65	CO	?early Rhaetian	<b>?<i>Ricciisporites</i>–<i>Conbaculatisporites</i> Zone.</b> Common <i>Ricciisporites tuberculatus</i> and <i>Conbaculatisporites</i> spp. may indicate this zone. The presence of <i>Cingulatisporites rhaeticus</i> suggests a middle Rhaetian age. <b>Terrestrial environment:</b> No dinoflagellate cysts or marine acritarchs were encountered.

## 4.4 Concluding remarks

The palynological analysis of the subsurface uppermost Triassic to Lower Jurassic succession on Zealand have resulted in a revised palynostratigraphic framework for the interval covering the Gassum and Fjerritslev formations. The analysis, which includes new and existing data, allows recognition of both spore-pollen and dinoflagellate cyst biozones. The analysis further shows that the succession was deposited in a predominantly marine to marginal marine setting. The lack of core samples within major parts of the Fjerritslev Formation hinders a more high resolution biostratigraphic breakdown. It is clear from the present report that there are certain problems with the recognition of in particular, the early Rhaetian, and Sinemurian to Pliensbachian spore-pollen zones. A fully biostratigraphic breakdown of the Gassum Formation – Fjerritslev Formation interval demands a new core covering this interval.

## 5. Seismic interpretation and mapping

The aim of this subtask is to tie key horizons on seismic sections, interpret seismic facies and details of the Gassum Formation and lithostratigraphic units above from seismic data at Copenhagen (mainly the HGS lines in Fig. 5.1) and the Margretheholm-1/1A &-2 wells (abbreviated below as MAH-1/1A and MAH-2). This study was carried out to improve the understanding of the Gassum Formation and lithostratigraphic units above.

### 5.1 Database and workflow

Figure 5.1 shows the database with used seismic reflection lines and position of the MAH-1/1A,-2 wells. First, the project area, the seismic and well data and useful seismic stratigraphic horizons were identified. Regional interpreted seismic stratigraphic horizons, maps, seismic data and well data from a previously project were loaded into a new Petrel™ project on a PC workstation. The MAH-1/1A,-2 wells were tied with seismic lines and important stratigraphic boundaries from the wells were tied to the seismic data including formation boundaries (Figs. 5.2 and 5.3).

Seismic stratigraphic key horizons were studied in the area. Thickness variations and faults were reviewed with loop-ties through the data and with maps in 2D and 3D views (Fig. 5.2). Then seismic facies between different well sites in the region were studied and compared (Figs. 5.4 and 5.5). Finally details of seismic data and facies near possible pilot hole locations at the western and eastern prognosis areas were studied but also at the Margretheholm wells for comparison (Figs. 5.6 and 5.7).

### 5.2 Seismic stratigraphy and facies

The seismic stratigraphic key horizons used in the present study are: “Top Vinding”, “Top Gassum”, “Top Karlebo”, “Top Fjerritslev” and “Base Chalk” (see Figs. 5.2 and 5.3). The seismic horizons do not always exactly correspond to the lithostratigraphic unit tops defined in wells which are defined based on a characteristic change in lithology. Consequently, more informal seismic stratigraphic names are usually used for the lithostratigraphic units. For example, “Gassum” is the name for the seismic unit which roughly corresponds to the lithostratigraphic defined Gassum Formation. Likewise, “Top Gassum” is the name for the seismic horizon which closely corresponds to the top of the Gassum Formation.

Some of the important questions to address in the present study relate to details and characteristics of seismic facies and their possible relations to the drilled lithostratigraphic units. Other important questions are related to lateral correlation ties of interpreted seismic horizons and units – especially the Gassum Formation and overlying units from the MAH-1/1A,-2 wells to the prognosis areas in northern Copenhagen.

### 5.2.1 Regional well tie, stratigraphy and overall unit thicknesses

Figure 5.2 shows a consistent tie of the regional key horizons (dotted horizontal lines) from the Margretheholm wells (vertical red and blue lines) to the seismic cross section with the position of the two prognosis areas marked (western and eastern area). The Top Vinding surface is marked and clearly illustrates that the basin is markedly deeper in the eastern area, east of the Amager Fault. The figure also illustrates that the seismic stratigraphic unit Gassum thickens across the fault towards east. Furthermore, the tentative TWT thickness of both the Gassum and the overlying Karlebo units thickens considerably from west to east across the Amager Fault and may nearly double in thickness at some locations east of the fault (Fig. 5.2). The seismic interpretation of horizons and ties from wells in the region, including correlation across faults/fault zones, is subject to uncertainties, due to the open data grid with only a few seismic lines (Fig. 5.1), data gaps between seismic lines, displacements due to faults and because seismic facies comparison between each side of faults/fault zones are difficult. The presented interpretation is considered as the most likely with the present data. An alternative interpretation was done which, however, only gave a slightly thicker development of the Gassum and Karlebo units on the east side of the Amager Fault/fault zone. The thicknesses (in milliseconds Two-Way-Time) of the seismic units Gassum and Karlebo have been calculated for specific points in the western and eastern area (at preliminary prognosis sites) and were converted to possible thickness in meter. These thicknesses have been included as input for reservoir prognoses (see Section 6.3).

The seismic stratigraphic unit, named “Fjerritslev (upper)” in Figure 5.2, most likely corresponds to the upper, mudstone dominated part of the Fjerritslev Formation. It seems almost to keep its TWT thickness across the fault and show no marked displacement. In contrast, the Top Vinding, Top Gassum and Top Karlebo show disconnected reflectors across the fault with displacements of up to c. 250 m, as well as marked increased seismic unit thicknesses across the fault. This indicates that larger movements took place across the fault until Early Jurassic time (until the Karlebo unit was deposited). The Amager Fault actually appears as an approximately 1 km wide fault zone consisting of a number of faults (Fig. 5.7). Some minor mounds with disturbed reflectors and onlap toward the fault on its east side might reflect mass movements related to fault activity (Fig. 5.7). Seismic sub-units of the Gassum unit seem to thicken eastward of the fault which may indicate that some extra accommodation space was created in the basin, possibly due to subsidence. It has not been possible to identify which specific internal parts of the Gassum Formation are present on both side of the fault zone. A later compressional tectonic phase seems to have affected the Amager Fault zone and created minor inversion/ridges in the Gassum unit, Fjerritslev unit and into the Chalk unit above, indicating a Cretaceous or younger compression/inversion tectonic phase.

### 5.2.2 Seismic facies

In order to investigate the seismic units with their boundaries and seismic facies in more detail, different seismic lines and wells have been studied and compared.

Figure 5.3 shows two SW-NE striking seismic sections with seismic stratigraphic interpretations and the Margrethholm-1/1A,-2 wells added. The inserted litho-log is from Margrethholm-1/1A (yellow colour: sandstone; brown colour: claystone dominated). The seismic facies within sandstone intervals, forming part of the Gassum Formation, show slightly increased reflectivity (stronger colored reflectors) than immediately above and below in both the seismic sections. Increased reflectivity often indicates a change in physical parameters through the section, normally related to changes in acoustic impedance (density and/or seismic velocity). In some cases, such changes could be related to changes in lithology, but they can also reflect a number of other factors such as changes in compaction, fluid content, faults, overlying units, seismic noise, processing issues, etc. As explained below it appears that lithological differences may have some significance to the seismic facies (mounds and reflectivity differences) near the Margrethholm wells.

### **Mounds and reflectivity differences**

Some of the internal reflections of the Gassum unit seem to have a slightly mounded appearance at the Margrethholm wells (Figs. 5.3 and 5.4). Increased reflectivity downwards in the Gassum unit is observed at the Karlebo-1A well (Fig. 5.4) as is slightly mounded, downward increased reflectivity in seismic sections at the Stenlille-1 well (Fig. 5.5). Figure 5.3 shows a correlation of the litho-log of the MAH-1/1A with sandstone dominated (yellow) intervals of the Gassum Formation with tentatively ties to the seismic facies described above. Thus, it is concluded that these seismic facies characteristics at these locations likely reflect the transitions to sand rich intervals of the Gassum Formation.

The mounded appearance may from the well correlation be partly due to:

- the sand content
- differential compaction around more competent lithology (e.g. sandstones)
- depositional features
- faults
- other causes

However, it is also seen from Figure 5.3 that the seismic facies with mounded, continuous strong reflections only continues for a short distance towards SW before it changes into discontinuous weaker reflections. This may not necessarily reflect a change in lithology as other factors (some mentioned above; e.g. faults, noise) may disturb/alter the appearance of the seismic facies. The W–E seismic section through the northern Copenhagen, with the prognosis areas indicated, does not clearly show such mounds and only in the western area stronger reflections are observed at the top of the Gassum unit (Fig. 5.7). However, the absence of clear mounds in this seismic cross-section does not rule out the possible presence of sandy deposits.

### **Progradation & troughs**

Minor progradational features and subtle troughs are observed within and near the Gassum and Karlebo units (Figs. 5.6 and 5.7). Interpretations of such minor progradational reflectors and subtle troughs in the Gassum unit and above are uncertain, but may in some cases be related to depositional systems and erosional events, respectively. Knowing the overall depositional setting of the Vinding Formation, Gassum Formation and the Karlebo Member

near the Sorgenfrei-Tornquist zone, such features may be interpreted as relating to large scale depositional and erosional morphology/processes within near coastal and fluvial systems. The regional interpreted Top Vinding surface (corresponding to the Base Gassum surface) shows that the area from the Stenlille wells to the western prognosis site appears as a northward dipping flank/ridge, possible with some similar depositional setting along this area (Fig. 5.8).

### 5.2.3 Faults and folds

A closer look of the seismic data in Figure 5.3 shows that the marked reflector at the Base Chalk horizon, as well the underlying interpreted reflectors (including Top Gassum), must have a considerable dip or fault displacement in the white gap area without seismic data (where the litho-log of MAH-1/1A is placed). The Top of the Gassum Formation in MAH-2 is at 1830 m TVD and at 1832 m TVD in MAH-1/1A and thus at nearly the same level, indicating no or little fault displacement between these wells. Consequently, the marked dip/displacement, mentioned above, is expected to occur east of the wells. Further analyses of offsets or bends of seismic reflectors patterns in line hgs003 (Fig. 5.3) reveal patterns of minor fault displacements and folds, such as shown in Figure 5.6. The faults both indicate extension and more dominant younger (Cretaceous) compressional related tectonics with subtle thrust faults and folds and a flower like structure central in line hgs8n13, bounded by the two shallowest drawn faults (Fig. 5.6). The seismic section hgs001 in Figure 5.7 apparently shows less faults/folds than in Figure 5.6, except than in the Amager Fault zone (around the Amager Fault marked by the blue vertical line). Furthermore, it seems that the section also illustrates less faults are present west of the fault zone. A review of seismic sections from Øresund, Amager and the greater Copenhagen area generally indicates that the northern Copenhagen area is less affected by such faults/folds (especially west of the Amager Fault zone) compared to the offshore areas and Amager. Faults can have impact on reservoir/production related issues, including reservoir connectivity (depending on displacement, clay-smearing in fault and other factors). Faults can also in some cases conduct fluids between formations. Considerations related to faults thus could be important from the view of production planning.

## 5.3 Concluding remarks

This study of well data from the Margrethholm wells and seismic data from Amager, Øresund and Copenhagen area has resulted in a review of the seismic stratigraphic interpretation using different display methods and study of seismic facies. It seems likely that the stratigraphic interval corresponding to the Gassum Formation and the overlying Karlebo Member (lower part of the Fjerritslev Formation) thickens considerably and nearly doubles in total thickness at some locations from west towards east across the Amager Fault zone in northern Copenhagen. However, the low data density and disturbed data implies that interpretation/correlation is associated with uncertainty, and it cannot be excluded that the thickness variations are less. Thickness estimates based on seismic interpretation converted from Two-Way-Time to meter were used for reservoir prognoses (see section 6.3). In contrast, the mudstone dominated upper part of the Fjerritslev Formation appears approxi-

mately to keep its thickness across the fault zone. It seems that the number of faults increases from northern Copenhagen and towards east across the Amager Fault zone, being especially abundant in Øresund and on Amager. A comparison of the seismic facies at the location of the Stenlille, Karlebo and Margrethholm wells indicates increased reflectivity from the Fjerritslev Formation (including the Karlebo Member) and into the Gassum Formation. Such a facies transition is less clear in the seismic section across the northern Copenhagen at the two prognosis areas (Fig. 5.7). However, the Top Gassum horizon seems to be located near at a marked reflector in the western area, whereas the horizon is not as clearly associated with a reflector in the eastern area. The fact that the Top Gassum is not so well defined in the eastern area may reflect a less well defined contrast in density/seismic velocity and possible less lithology contrast/differences etc. Interpretation of minor progradational reflectors and subtle troughs in the Gassum Formation and above are uncertain, but may in some cases be related to depositional systems and erosion. Knowing the overall depositional setting of the Vinding Formation, Gassum Formation and the Karlebo Member of the Fjerritslev Formation near the Sorgenfrei-Tornquist zone, such features may be related to depositional and erosional processes within near coastal and fluvial systems. Furthermore, the use of Petrel software has provided improved facilities for both visualization analyses of the seismic data combined with well data, which has contributed to the interpretation of the geophysical data. It has not been part of the study to use the seismic data to give any specific lithology prognoses in the areas of interest.

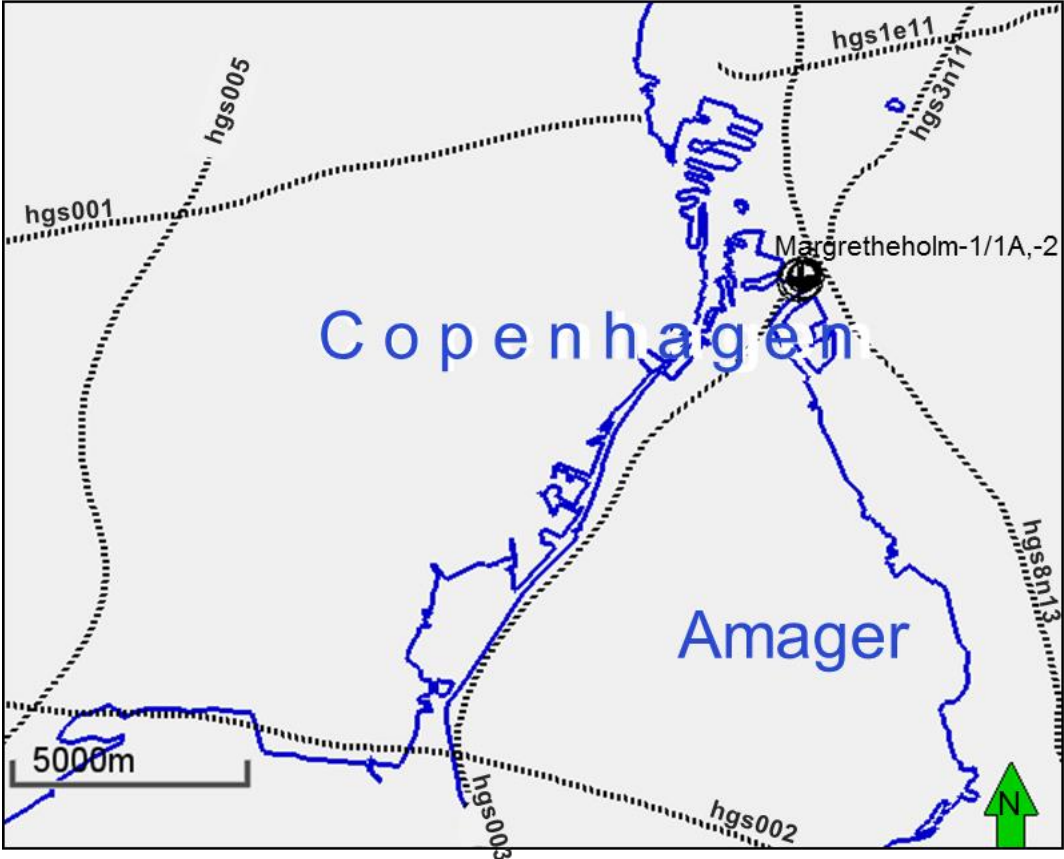


**Figure 5.1.** Map with position of the Margrethholm-1/1A & -2 wells and seismic lines used in the project.

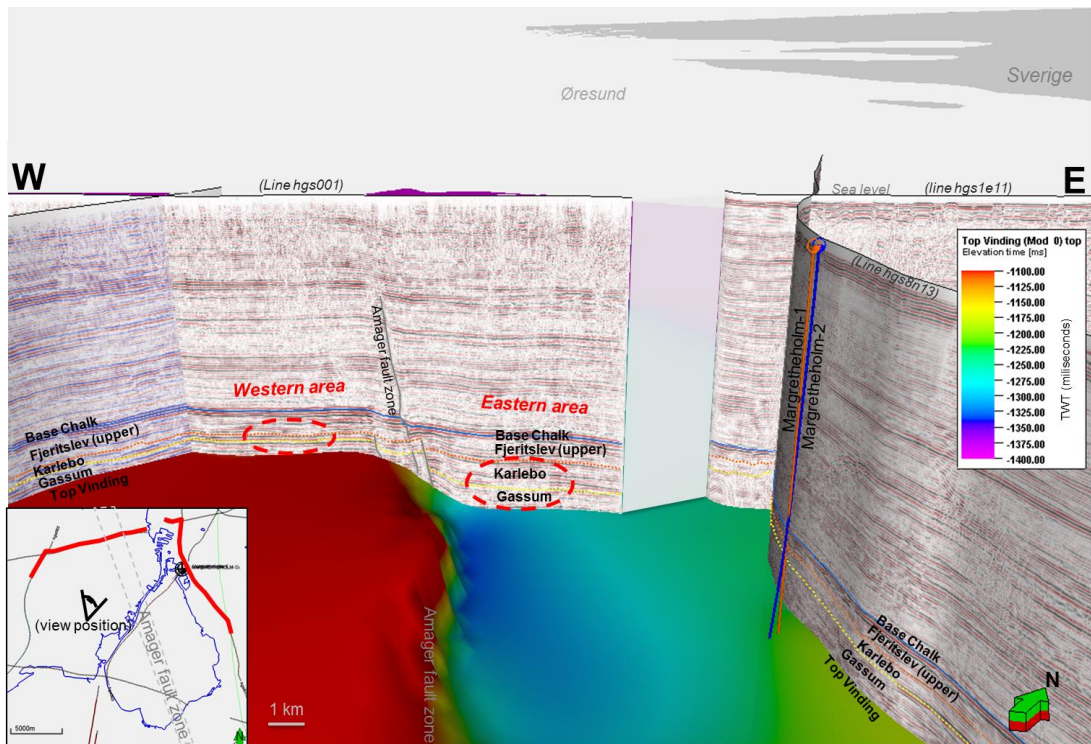


**Figure 5.2.** Seismic lines in 3D view seen towards northern Copenhagen (left) and towards Margretheholm in northern Amager (right) (see inserted location map to the left). The colored surface is a depth map (TWT – see scale to the right) of the Top Vinding/Base Gassum. The map illustrates the morphological variations with the fault-controlled deeper basin east of the Amager Fault zone. The seismic stratigraphic Gassum unit and Karlebo unit thickens across the fault towards east, below the mudstone dominated Fjeritslev (upper) unit.

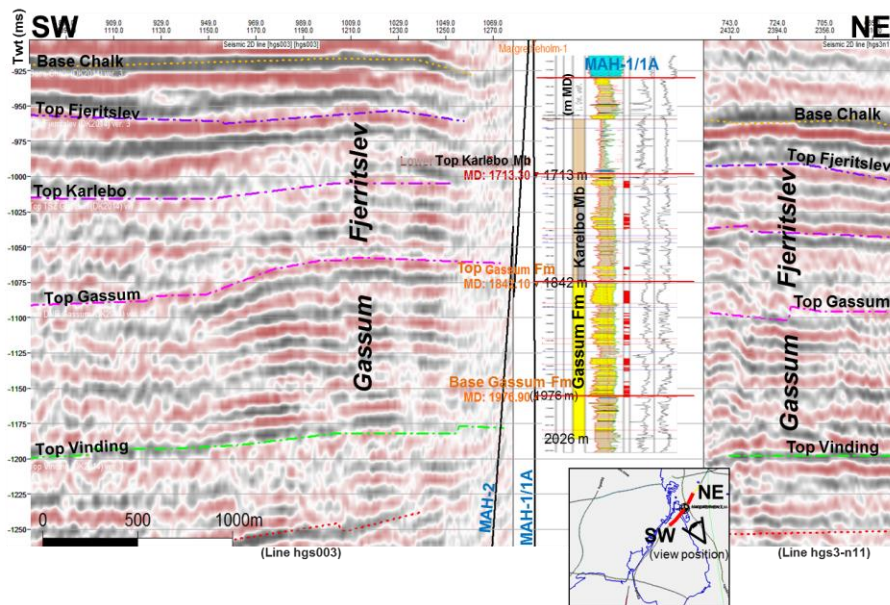


**Figure 5.3.** Seismic lines (hgs003 and hgs3-n11) and the Margrethholm-1/A & -2 wells. The small inserted litho-log is from the Margrethholm-1/A well, with sandstones in yellow color, claystones in brown color and the Chalk group in blue color. The depth scale of the litho-log is in meter (MD) and is not scaled exact to the seismic section (in TWT), but a tentatively match is made. The MD depths (meter) in orange and red colors are so called "well tops" used for calibration to the seismic section.

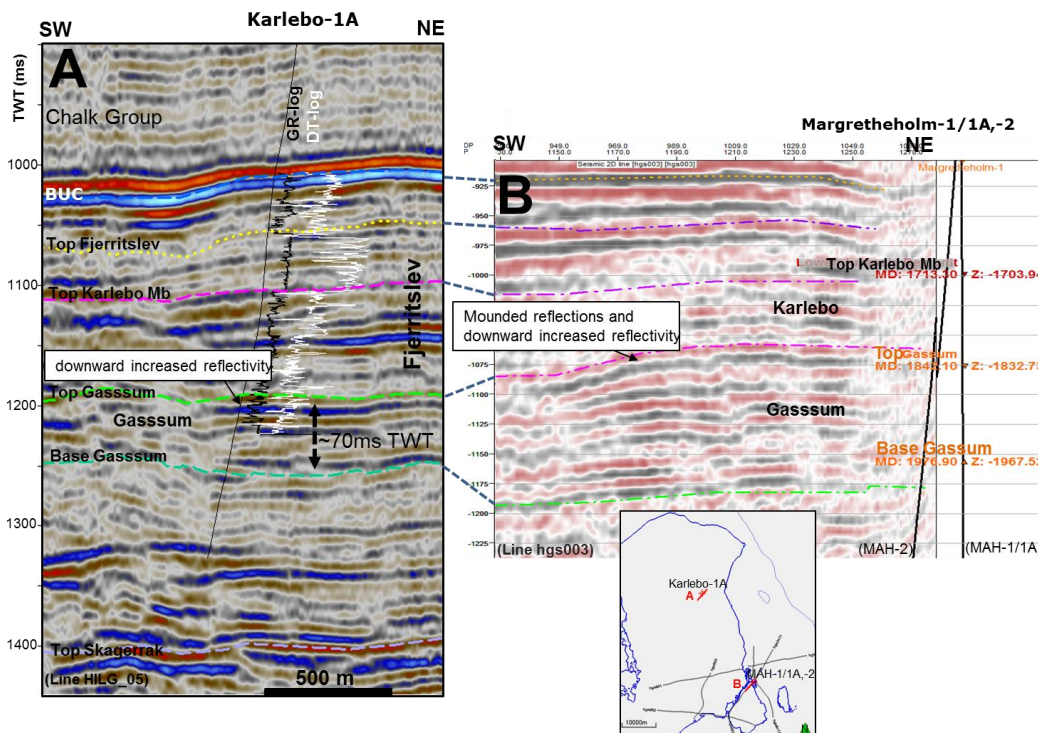


**Figure 5.4.** Seismic sections at well sites. A: Seismic line HILG-05 with the Karlebo-1A well and B: Seismic line hgs003 with the Margrethholm-1/A & -2 wells. Note the slightly mounded, downward increased reflectivity at the Top Gassum, reflecting the marked contrast between mudstones of the Fjerritslev Formation and sandstones of the Gassum Formation.

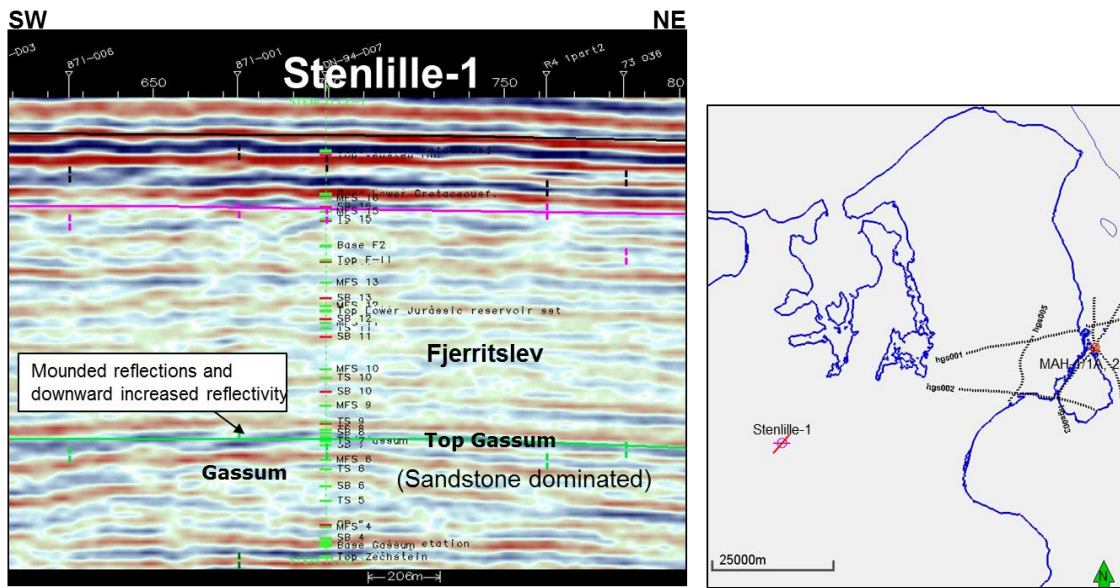


**Figure 5.5.** Seismic line DN-94-D01 with the Stenlille-1 well in central Zealand, c. 60 km WSW from the study area. Note the slightly mounded, downward increased reflectivity at the Top Gassum reflecting the marked contrast between the Fjerritslev Formation and the more sandstone rich Gassum Formation.

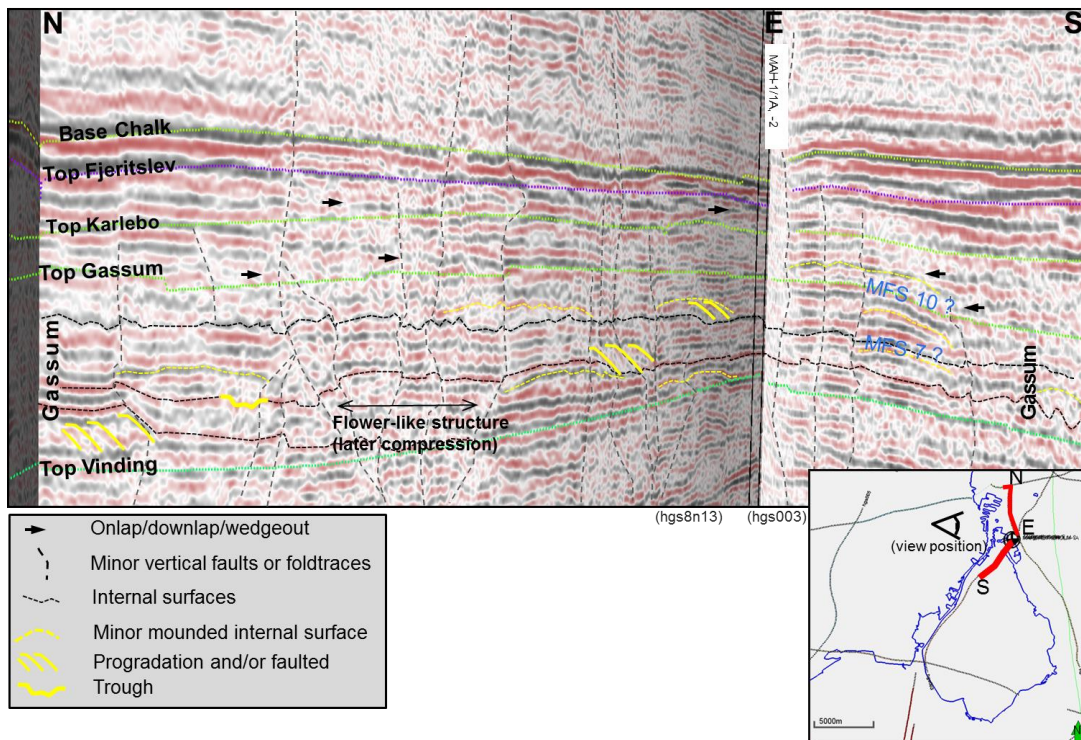


**Figure 5.6.** Seismic tie and facies near the Margretheholm-1/1A & -2 wells, with interpretation of horizons and subtle faults, mounds, progradation and troughs features.

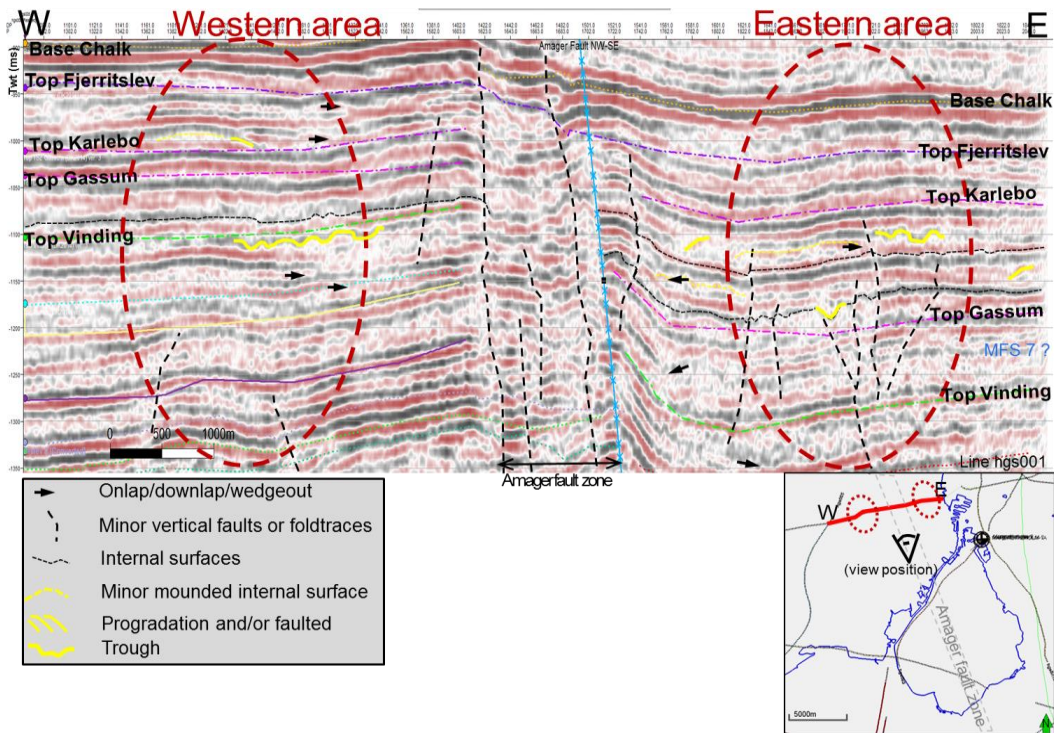


**Figure 5.7.** Seismic line hgs001, with interpretation of horizons and subtle faults, mounds, progradation and troughs features. The approximate positions of the proposed western and eastern areas for a pilot hole are shown with dashed red circles on each side of the Amager Fault (blue vertical line).

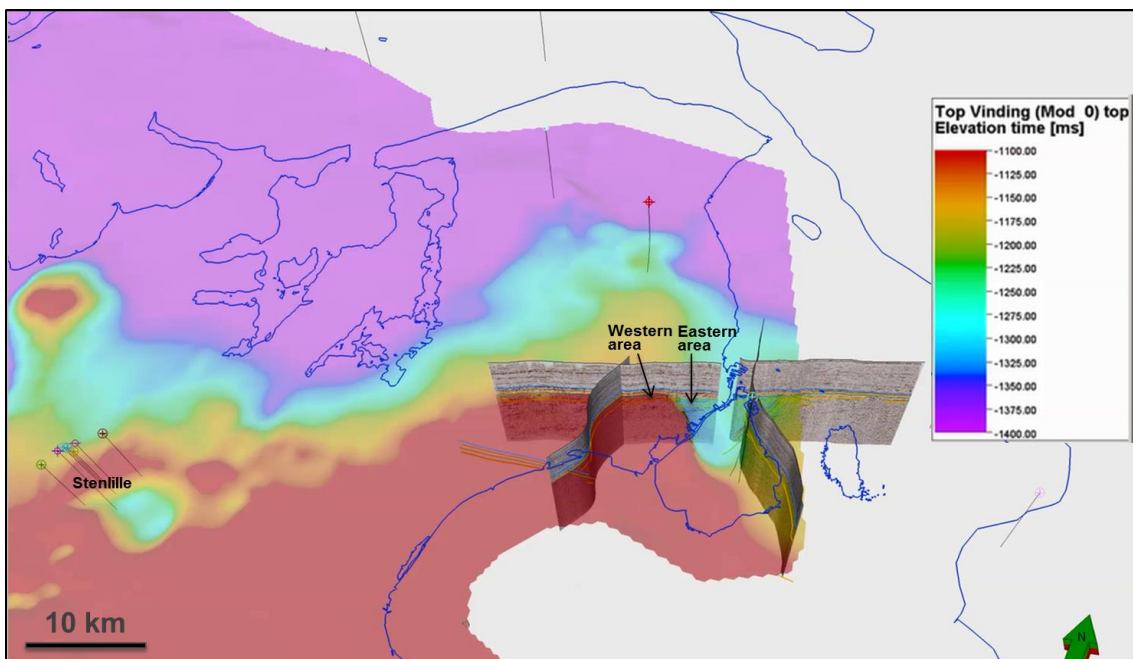


**Figure 5.8.** Depth to and morphology of the Top Vinding surface, corresponding to the Base Gassum surface, in central and eastern Zealand. Vertical “needles” mark the position of existing wells. The surface appears as a northward, down-dipping flank along which both the Stenlille area and the western prospect area occur in a comparable down-flank position. Depths to the Top Vinding surface is given in two-way time (TWT, see inserted scale).

## 6. Reservoir properties

### 6.1 Petrography and diagenesis

The petrography and diagenesis of sandstones from the Gassum Formation and Karlebo Member in the Margrethholm and Stenlille areas are studied to identify which factors control the reservoir quality and whether a mature mineralogy is diagnostic for eastern Denmark. Sandstones from the Stenlille area were included since they are the nearest available cores. Studying cores give a better petrographic determination than using cuttings, and permeability measurements are only possible in core plugs. However, cutting samples from the Margrethholm-1 well are in general of good quality, meaning that some larger fragments and even some of the fragile fragments have been preserved in some samples. Thus, the results can be used to indicate whether the Stenlille area is a good analogue for the Margrethholm area.

#### 6.1.1 Samples and methods

Sampling was conducted in the Gassum Formation and Karlebo Member in the Margrethholm-1, Stenlille-1 and Stenlille-5 wells (Fig. 6.1). The raw cutting material from the Margrethholm-1 well was washed to separate the cutting fragments, which were then dried and sieved to remove the clay fraction. The cuttings were collected in intervals of between 2.5 and 5.0 meters length, so the indicated depths are averages of the sampled intervals. A total of 18 new thin sections were prepared, of which 13 are from cuttings from the Margrethholm-1 well and 5 are from cores from the Stenlille-1 and Stenlille-5 wells. The mineralogy was quantified by point counting of 14 thin sections from the Margrethholm-1, Stenlille-1, Stenlille-5, Stenlille-15 and Stenlille-19 wells. Of these, 4 old thin sections were point counted from the Stenlille-15 and Stenlille-19 wells since matching porosity-permeability data exist. Data from the Stenlille-18 well are used for comparison (Weibel et al. 2017). Porosity determinations were performed on large cutting fragments from 3 samples from the Gassum Formation in the Margrethholm-1 well. Porosity-permeability measurements were conducted on 5 core plugs from the Karlebo Member in the Stenlille-1 and Stenlille-5 wells. Data from conventional core analyses of sandstone samples from the Gassum Formation are used for comparison, comprising 1398 analyses of cores from the Stenlille wells (Weibel et al. 2017) and 10 analyses of sidewall cores from the Margrethholm-2 well (Springer 2003).

Thin sections of sandstone samples were made with blue epoxy impregnation to make open pore space visible. Half of each thin section was etched and stained with sodium cobaltinitrite for K-feldspar and plagioclase identification. Mineralogy and petrographic relationships were described for each thin section. The detrital and authigenic phases were quantified by point counting using transmitted and reflected optical microscopy. The point counting technique involves automatic sliding of a thin section on a stage which moves in fixed steps. Petrographic determination of up to 500 minerals was performed in each thin

section. The porosity was counted additionally and was identified as primary or secondary. Cutting fragments consisting of sandstone were selected for point counting of samples from the Margrethholm-1 well.

Grain size and sorting was measured in the point counted thin sections. The mean grain diameter was determined by measurement of 100 grains intersecting a number of straight lines. The mean diameter was recalculated to mean area since grain-size analysis in thin sections underestimates the dimensions relative to sieving analysis (Johnsen 1994). The grain size nomenclature is from Wentworth (1922). Sorting was calculated from the grain-size distribution in thin sections as graphic standard deviation (Folk 1966). The sorting classes are defined for eight relative phi classes that range from very well to poorly sorted. The relative mineral abundances are described as dominant (>50%), abundant (15–50%), common (5–15%), minor (1–5%) and rare (<1%).

Scanning electron microscopy (SEM) analyses were conducted to evaluate the petrographic relationships. They were performed on carbon-coated thin sections and gold-coated rock chips glued on stubs. A Philips XL40 SEM equipped with a ThermoNoran energy dispersive X-ray spectrometry (EDX) detector was used for the analyses. A qualitative identification of the minerals was achieved by elemental analyses of the grains using EDX.

Porosity and permeability measurements were conducted by conventional core analysis (American Petroleum Institute 1998). NaCl was removed by cleaning the samples in methanol prior to analysis. Permeability was determined on core plugs using N<sub>2</sub>-gas. The permeability was not measured for the samples that were extremely porous, had large fractures or were too small to fit the holder. Only porosity could be measured on cutting samples, and it was only possible in the samples with centimeter-large cutting fragments. A total of 5 fragments were analyzed from each sample and the porosity results were averaged from those analyses for which the calculated density was in the expected interval.

### **6.1.2 Detrital components**

The sandstones in the Gassum Formation are mostly fine- to medium-grained, whereas the sandstones in the Karlebo Member are very fine- to fine-grained (Table 6.1; Fig. 6.2). The sandstones in the Gassum Formation are well sorted, except for the uppermost part in which they are moderately well sorted. The sandstones in the Karlebo Member are mostly moderately well sorted. The grains are in general subrounded in both the Gassum Formation and Karlebo Member. Sandstones from the Stenlille area are on average coarser-grained and more well sorted than sandstones from the Margrethholm-1 well, and this trend is found both within the Gassum Formation and Karlebo Member (Table 6.1). The sandstones of the Karlebo Member are subarkoses, whereas quartz arenites and subarkoses are about equally abundant in the Gassum Formation.

The Karlebo Member and the Gassum Formation in eastern Denmark have comparable mineralogy. Quartz is dominant in all samples (average: 81%) (Fig. 6.3) and 6% of the quartz grains are polycrystalline on average. Feldspar is minor to common (average: 6%) and consists primarily of K-feldspar whereas plagioclase is less common or absent and

perthite is rare. The feldspar grains often have dissolution features. The average feldspar content is twice as high in the Karlebo Member as in the Gassum Formation. Some of the cutting samples contain cutting fragments of several different grain sizes and there are more feldspars in the finest-grained fragments. Especially one sample from the lower part of the Gassum Formation (Margrethholm-1, 2001.25 m) has large variation in feldspar abundance between the cutting fragments, and the grain size and sorting are highly variable.

Mica is by far most common in the Karlebo Member, but mica, organic matter, clay clasts and heavy minerals are usually rare in both stratigraphic units (Fig. 6.3). Mica and organic matter are oriented parallel to the bedding and are concentrated in layers, often together with clay clasts. Likewise, heavy minerals are concentrated in certain laminae. Detrital clays can be difficult to identify due to drilling mud, but they are quantified as minor to rare except in the Stenlille-18 well where they are common to minor (Fig. 6.3). Rock fragments are minor to rare constituents and are mainly of sedimentary and plutonic origin. Glauconite grains are rare and abraded. Centimeter-long calcitic shell fragments are sometimes present in the Karlebo Member and are oriented parallel to bedding. Trace fossils lined by clay are present in some intervals of the Karlebo Member.

### 6.1.3 Authigenic phases

The amount of authigenic minerals is typically higher in the Margrethholm-1 well than in the Stenlille wells, but is overall rather low in both wells (average: 8%) (Fig. 6.3). Pyrite is rare, but occurs scattered in the sandstones both as framboids, which are most abundant within organic matter, and as euhedral crystals. Rare anatase is present in a few samples. Partial dissolution of K-feldspar, plagioclase and perthite is common (Fig. 6.4A) and secondary porosity is present within the grains, except where they are filled with clay or carbonate. Albite overgrowths occur occasionally on detrital albite, radiating illite-chlorite coatings occur locally in a few samples and mica alteration is rare. Small scattered siderite rhombs are present in amounts of 1–2% in most of the studied sandstones from the Karlebo Member, whereas they are largely absent in the Gassum Formation. The siderite has formed after beginning K-feldspar dissolution and prior to calcite cement and quartz overgrowths (Fig. 6.4B). Siderite occurs as spheroids besides rhombs in one of the samples (Margrethholm-1, 1723.75 m).

Kaolinite is in general a minor to rare phase (average: 2%), but is apparently more common in the Gassum Formation in the Margrethholm-1 well (Fig. 6.3) where it even fills all pores in a single cutting fragment from one of the samples (Margrethholm-1, 1932.50 m). Kaolinite mostly occurs in patches where it is sometimes evident that it has formed as partial replacement of a feldspar grain. Kaolinite booklets have formed prior to quartz overgrowths and calcite (Fig. 6.4B). Quartz overgrowths are thin in most samples (average: 3%), but are more common in the Margrethholm-1 well (Fig. 6.4C) than in the Stenlille wells (Fig. 6.3). Quartz overgrowths are in places enclosed in calcite and ankerite (Figs. 6.4B, 6.4D).

Carbonate cementation is rare but one sandstone, cemented with 45% poikilotopic calcite, has been point counted (Margrethholm-1, 1972.50 m) in order to quantify the amount of

pervasive cement (Fig. 6.3). Here the quartz and feldspar remnants in calcite-cemented oversized pores show that the cement has replaced some of the detrital grains (Fig. 6.4D). Some of the feldspar lamellae have been preferentially replaced, and the feldspar grains appear to have been most susceptible to replacement. Thin quartz overgrowths are enclosed in the pervasive calcite cement. Pervasive carbonate cement seems to be most common in the finest-grained sandstones. Calcite is present as scattered rhombs in some samples (Fig. 6.4B). Ankerite is patchy in the only sample where it has been identified (Margrethholm-1, 1856.25 m), and here it has partly replaced quartz and K-feldspar grains.

#### **6.1.4 Porosity and permeability**

High porosities of about 22–30% and high permeabilities of about 100–1000 mD are dominant in the Gassum Formation sandstones in the Stenlille wells (Fig. 6.5) (Weibel et al. 2017). Very high permeabilities of about 1000–6000 mD are present in some of the coarsest-grained sandstones. High porosities of 23–25% are found in cutting fragments from the Gassum Formation sandstones in the Margrethholm-1 well (Table 6.2). Porosity-permeability analyses of sidewall cores from the Margrethholm-2 well show that the Gassum Formation in the Margrethholm area may have a similar porosity-permeability range as in the Stenlille area, although the very high permeabilities found in some of the Stenlille sandstones may not be present in the Margrethholm area (Fig. 6.5). High porosities and permeabilities of 28–31% and 484–662 mD, respectively, are found in the Karlebo Member in the Stenlille wells (Table 6.2, Fig. 6.5). Secondary porosity amounts to a maximum of 4% in the studied sandstones (average: 1%) and has formed from feldspar dissolution and from feldspar replacement with microporous clay.

#### **6.1.5 Discussion**

The Gassum Formation in eastern Denmark has formerly been studied in a core from the Stenlille-18 well in which the sandstone mineralogy was shown to be more mature than in the Gassum Formation in western Denmark (Weibel et al. 2017). In the present study, it is shown that a comparable mature mineralogy is present in other wells in the Stenlille area and in the Margrethholm-1 well (Fig. 6.3). Furthermore, it is shown that the Karlebo Member in the Stenlille and Margrethholm areas has a mineralogy that is quite similar to the Gassum Formation in Zealand, although the Karlebo Member is more feldspar-rich on average. However, the Karlebo Member is much more mature than the Gassum Formation in Jutland. Thus, it may be presumed that a mature mineralogy with high quartz content and low feldspar content is diagnostic for the sandstones of the Gassum Formation and Karlebo Member in eastern Denmark, which means they are less reactive to water injection (Holmslykke et al. in prep). This is because feldspar alteration and dissolution can be induced by slight changes in brine composition and flux (Milliken et al. 1989).

The diagenetic alterations are limited in the studied sandstones (Fig. 6.2), resulting in high porosities and permeabilities (Fig. 6.5). The only phase that decreases the reservoir quality significantly is pervasive carbonate cement, which only occurs in few thin intervals (Fig.

6.4D). Carbonate cement appears to be slightly more abundant in the Margretheholm area than in the Stenlille area, but this may be an artefact caused by the carbonate-cemented cutting fragments being overrepresented in the samples. This is because the fragile sandstones are more easily crushed during drilling.

The sandstones in the Gassum Formation are overall more well-sorted and coarser-grained than those in the Karlebo Member (Table 6.1), so presumably the Gassum Formation had higher initial permeability than the Karlebo Member. Kaolinite is more abundant in the Gassum Formation than in the Karlebo Member, whereas siderite is most common in the Karlebo Member. The high maturity of the sandstones in the Gassum Formation is evident by the high quartz content (Fig. 6.3). The higher feldspar content in the Karlebo Member than in the Gassum Formation may be related to its finer grain size or to a slight difference in sediment supplies.

The sediments in the Stenlille area have been buried to a maximum depth of about 600 meters deeper than today prior to uplift, whereas sediments in the Margretheholm area may have been buried about 600–700 meters deeper than their present depth (Japsen & Bidstrup 1999; Japsen et al. 2007). Thus, the deepest sediments in the Gassum Formation in the Margretheholm area have been buried to depths of up to about 2.7 km.

The Stenlille area is overall a good analogue for the Margretheholm area since the mineralogy is quite similar (Figs. 6.2, 6.3). However, the diagenesis is further developed within the Gassum Formation and Karlebo Member in the Margretheholm area than in the Stenlille area, which has mainly affected the abundance of the quartz cement. This is because the sediments in the Margretheholm area are buried about 300 meters deeper than in the Stenlille area and the amount of structural inversion is presumably largest in the Margretheholm area. Thus, the Stenlille data may be most suitable as analogue for the western proposed drilling area in Copenhagen, since the sandstones west of the Amager Fault zone are shallower than those in the eastern proposed drilling area. However, sufficiently large pores are still present in the Margretheholm area (Fig. 6.4C), and the core analysis data from sidewall cores in the Margretheholm-2 well confirm that good reservoir quality is probably present in most of the Gassum Formation in the eastern area (Fig. 6.5).

### **6.1.6 Conclusions**

- Good reservoir quality with high porosities and permeabilities is presumably present in the Gassum Formation and Karlebo Member sandstones in the Copenhagen area, except within occasional concretions of pervasive carbonate cement.
- The detrital mineralogy is uniform in the Stenlille and Margretheholm wells and data from the Stenlille area is therefore regarded as a good analogue for the Copenhagen area.
- The diagenesis is further developed in the Margretheholm area than in the Stenlille area because the sediments are deeper buried east of the Amager Fault zone, but overall the diagenetic alterations are limited since the sediments have only been exposed to maximum burial depths of about 2.1–2.7 km.

- The high mineralogical maturity of the sandstones in the Gassum Formation and Karlebo Member in the Stenlille and Margrethholm areas implies that the reaction potential of sandstone flushed with geothermal brine may be lower than in western Denmark where the higher feldspar content may imply a higher risk for scaling.

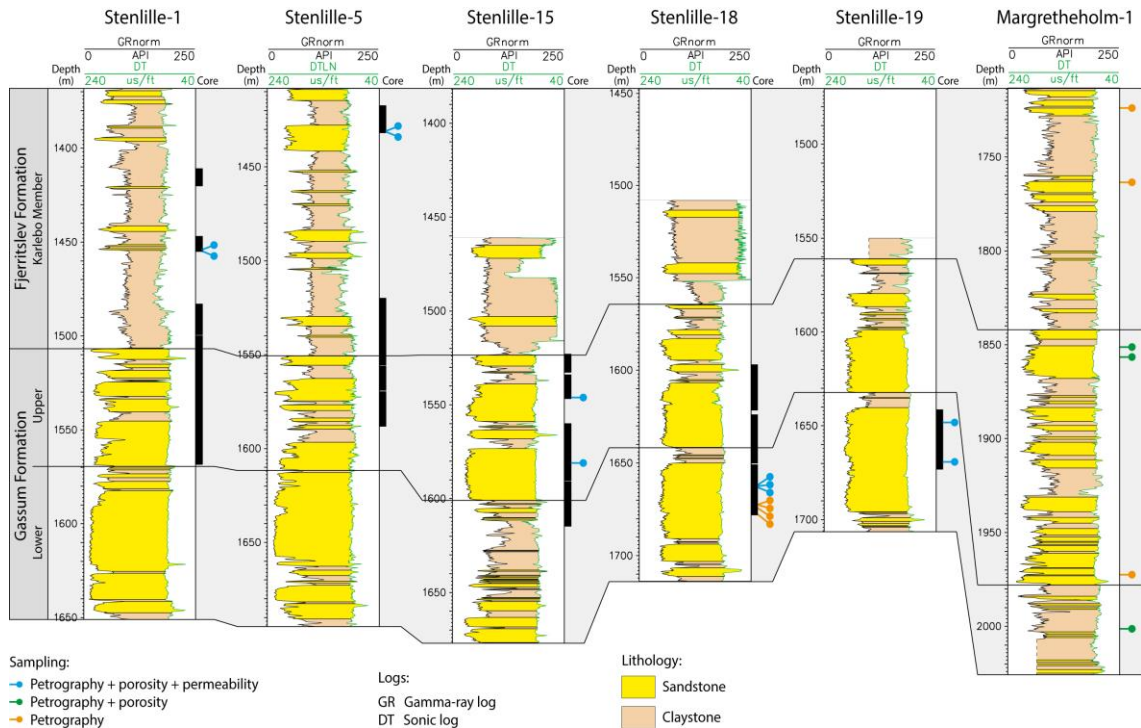


**Figure 6.1.** Lithological columns and wireline logs of the wells that have been sampled for petrographic analysis. The sampling depths and types of analyses are indicated. The sampled material comprises cuttings from the Margrethholm-1 well and cores from the remaining wells. The well-sections are aligned to the top of the Karlebo Member. See Figure 1.1 for well locations.

**Table 6.1.** Average grain size and sorting of sandstones from the Karlebo Member and Gassum Formation in eastern Denmark. The grain size is smaller and the sorting is poorer in the Margrethholm area than in the Stenlille area within both stratigraphic units. The Karlebo Member is finer-grained and poorer sorted than the Gassum Formation.

Stratigraphy	Area	Grain size ( $\mu\text{m}$ )	Sorting ( $\phi$ )	n
Karlebo Member	Margrethholm	95	0.55	2
	Stenlille	140	0.53	4
Gassum Formation	Margrethholm	203	0.51	4
	Stenlille	280	0.49	4

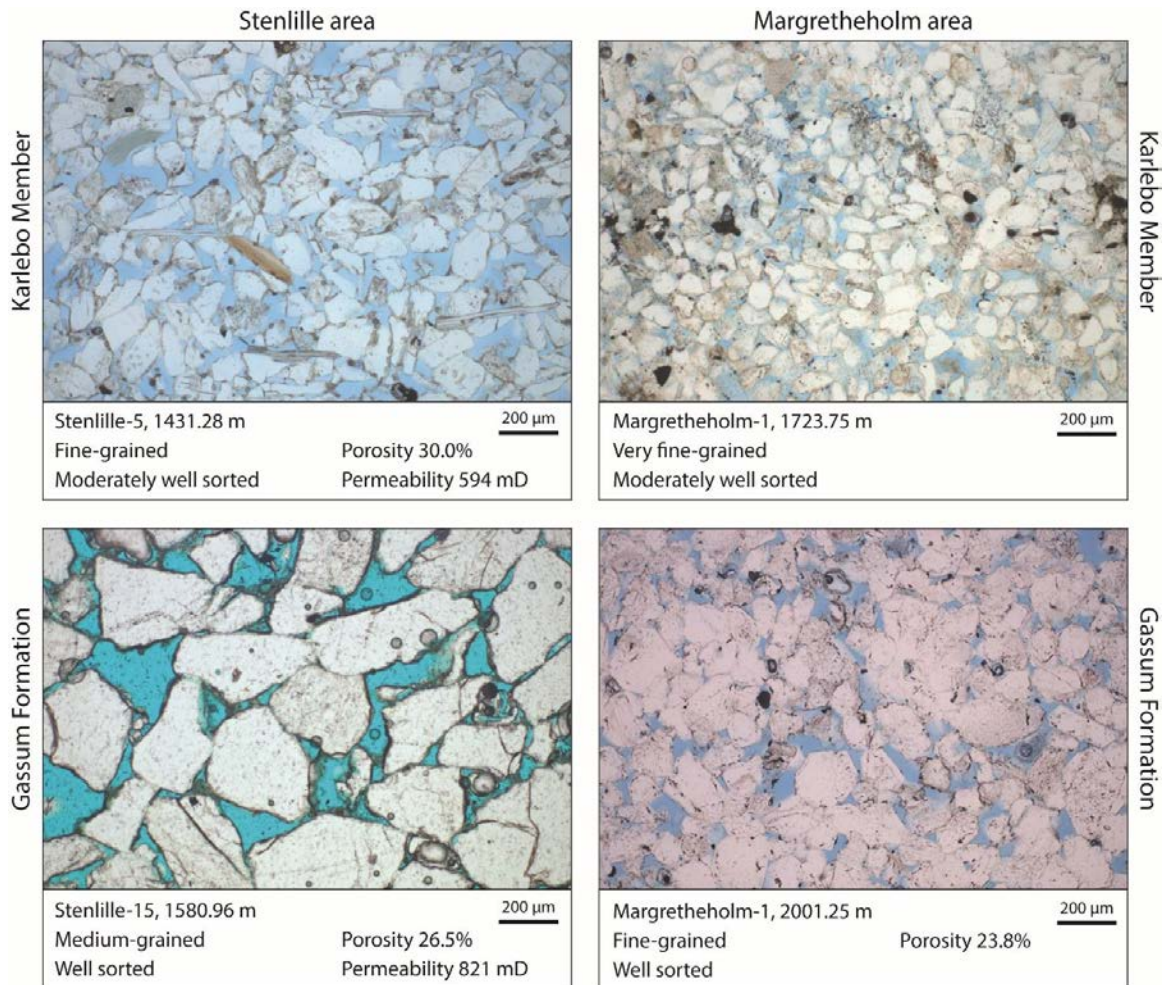


**Figure 6.2.** Typical textures of the Karlebo Member and Gassum Formation in the Stenlille and Margretheholm areas. The sandstones in the Margretheholm area are finer grained and deeper buried than in the Stenlille area. Open pore space is marked by blue color. Porosity could only be measured on the largest cutting fragments from the Margretheholm-1 well.

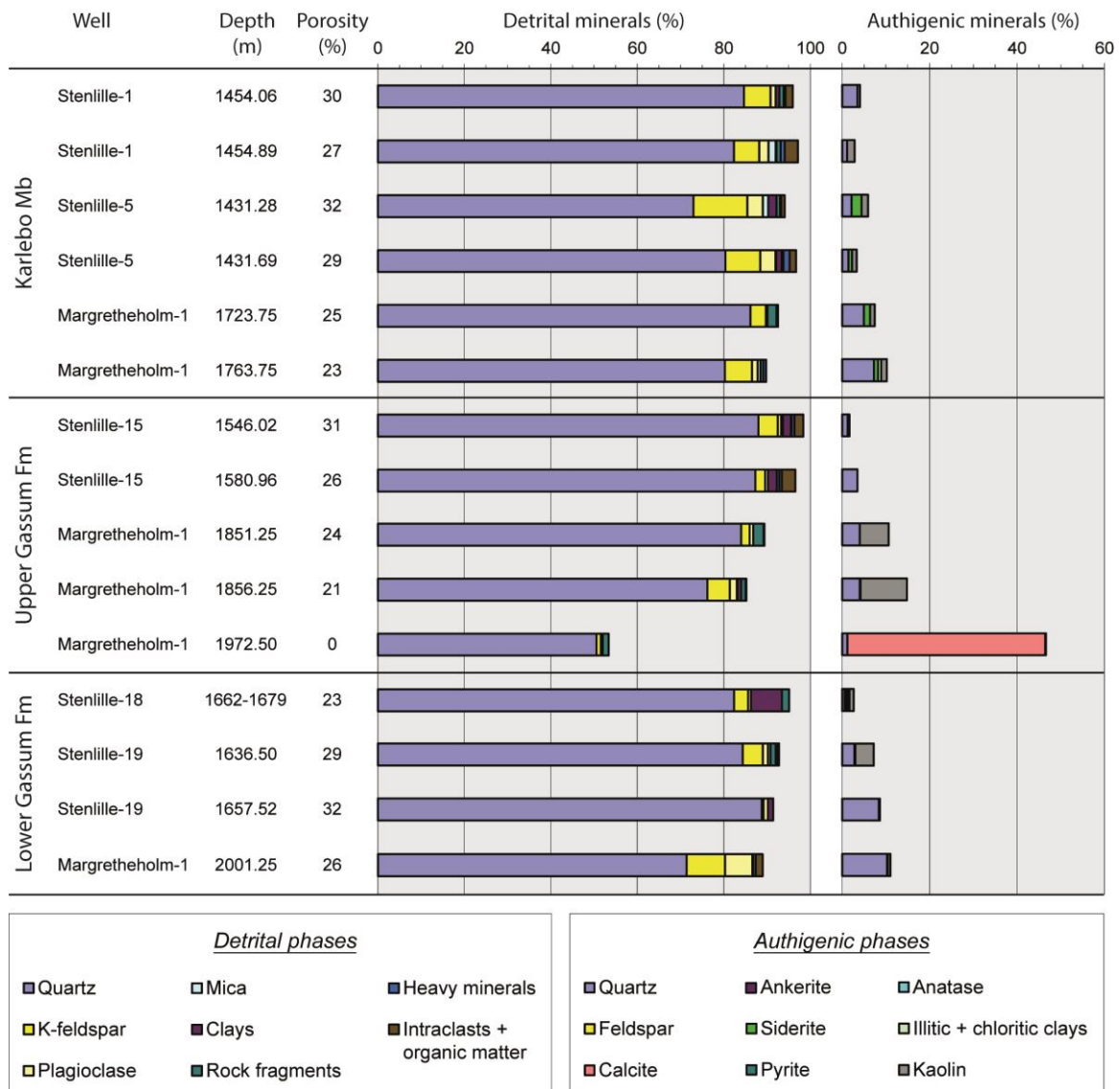


**Figure 6.3.** Detrital and authigenic mineral phases quantified by point counting of thin sections. The point counted porosities are listed. The data from the Stenlille-18 well is an average of 7 samples from Weibel et al. (2017).

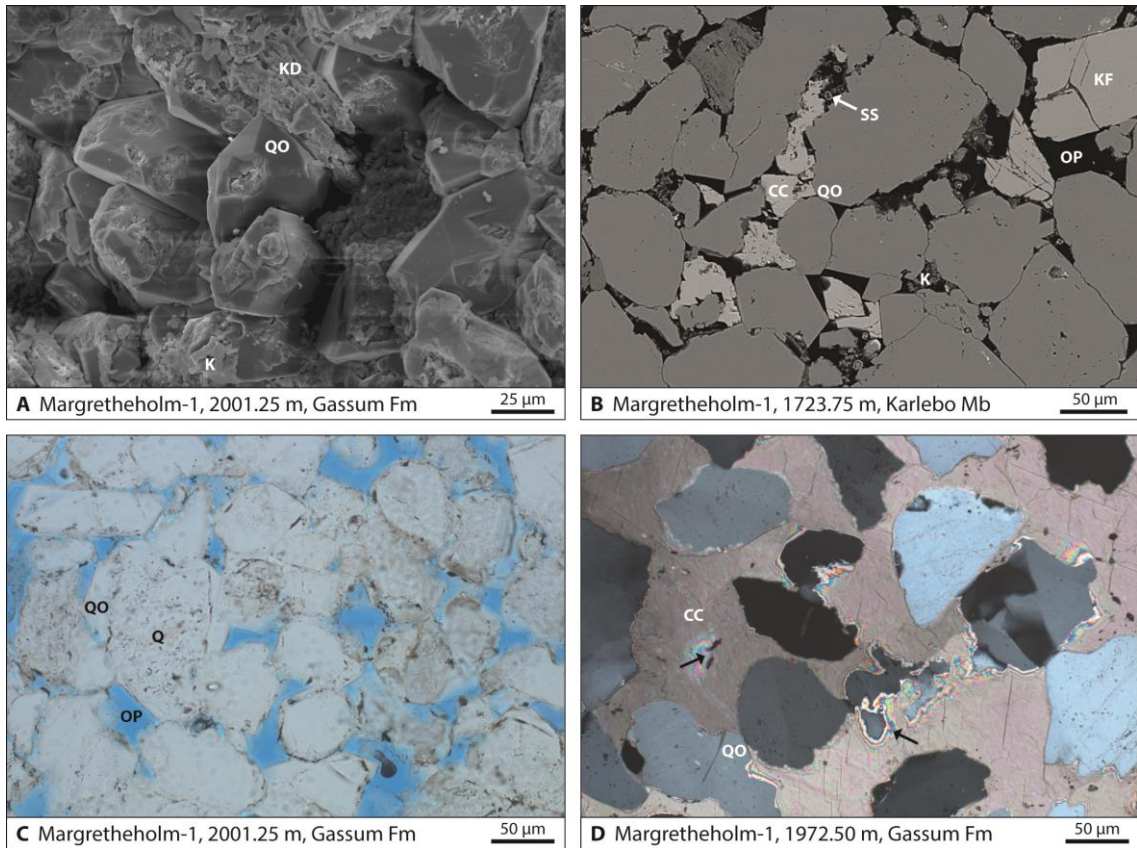


**Figure 6.4.** Dominant diagenetic changes in the Gassum Formation and Karlebo Member in the Margretheholm area. A: Quartz overgrowths enclose kaolinite booklets, and a K-feldspar grain has been partly dissolved; secondary electron image. B: Quartz overgrowths enclose kaolinite and siderite spheroids, and patchy calcite cement encloses all authigenic phases; backscatter electron image. C: Open pores are present between quartz overgrowths; transmitted light image. D: Remnants of quartz and feldspar are present within poikilotopic calcite cement (see arrows) in the few core intervals where it is pervasive and show that the cement has partly replaced some of the framework grains; crossed nicols image. Abbreviations: CC calcite cement, K kaolinite, KF K-feldspar grain, KD K-feldspar dissolution, OP open pore, Q quartz grain, QO quartz overgrowth, SS siderite spheroid.

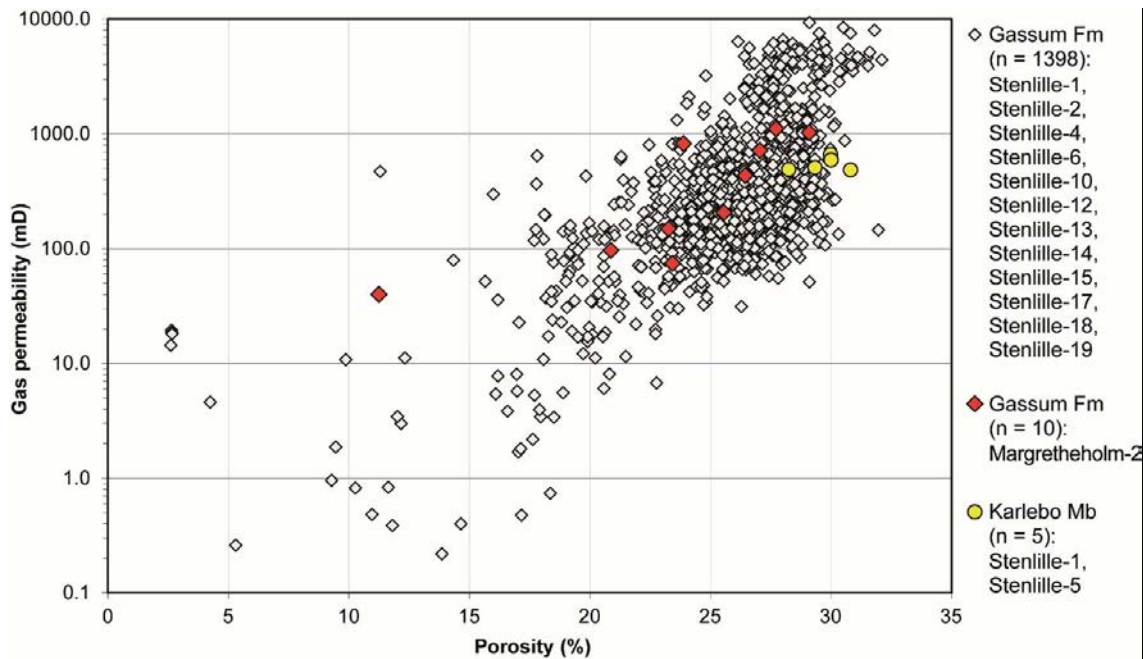


**Figure 6.5.** Porosity-permeability data from sandstones in the Stenlille and Margretheholm areas. High porosities and permeabilities are found in most samples from the Gassum Formation and in the few samples from the Karlebo Member. Data from the Gassum Formation in the Stenlille area are from Weibel et al. (2017). Data from the Margretheholm-2 well are from sidewall cores and compiled by Springer (2003).

**Table 6.2.** Core analysis data produced in this study, comprising the first porosity-permeability analyses of the Karlebo Member and the first porosity analyses of cuttings from the Gassum Formation in the Margretheholm-1 well.

Stratigraphy	Well	Depth (m)	Permeability (mD)	Porosity (%)	Grain density (g/cc)
Karlebo Mb	Stenlille-1	1454.06	662	30.0	2.63
		1454.62	484	30.8	2.64
		1454.89	491	28.2	2.63
	Stenlille-5	1431.28	594	30.0	2.64
		1431.69	510	29.3	2.65
Gassum Fm	Margretheholm-1	1851.25		23.2	2.62
		1856.25		24.9	2.64
		2001.25		23.8	2.66

## 6.2 Provenance analysis

Zircon U–Pb geochronometry is applied to determine the sediment source areas of the Gassum Formation and Karlebo Member in eastern Denmark. This is done to investigate the cause of their mature mineralogy (Fig. 6.3) and to interpret the sediment transport directions which can help constrain the geographical distribution of the reservoir sandstones.

### 6.2.1 Samples and methods

Eight sandstones were sampled for U–Pb age dating of detrital zircon grains (Fig. 6.6), of which three are from the upper part of the Gassum Formation (sampled in the Karlebo-1A, Margrethholm-1 and Stenlille-4 wells) and five are from the Karlebo Member (sampled in the Karlebo-1A, Lavø-1, Margrethholm-1 and Stenlille-5 well). A zircon age dating of a sandstone from the lower part of the Gassum Formation (sampled in the Stenlille-19 well) is available from another study (Olivarius 2015) and is here included for comparison.

The cutting samples from the Karlebo-1A and Margrethholm-1 wells were collected from 5 to 20 meter thick intervals to get sufficient material. The cuttings were washed, all samples were crushed, and the zircon grains were separated on a water-shaking Wilfley table. Zircon grains in all types of shapes and sizes were included by random hand-picking. Zircon U–Pb ages were obtained by laser-ablation inductively coupled plasma mass spectrometry (LA-ICP-MS) at GEUS following the general procedures of Frei & Gerdes (2009). A Thermo Finnigan Element2 mass spectrometer coupled to a NewWave NWR213 laser ablation system was used for the analyses.  $^{207}\text{Pb}/^{206}\text{Pb}$  ages were used for zircons older than 800 Ma and  $^{206}\text{Pb}/^{238}\text{U}$  ages for younger zircons because a gap between populations is present at this age and  $^{206}\text{Pb}/^{238}\text{U}$  ages are more precise for younger ages. About 120 zircon grains were analyzed from each sample, but some of the samples contained many discordant grains. The Lolite software was used for the data reduction (Paton et al. 2011). Ages with a discordance <10% are plotted in the age distributions. Common Pb correction was applied to the ages when necessary, which includes 2–34% of the grains in each sample.

### 6.2.2 Zircon ages

The zircon age distributions of the Gassum Formation and Karlebo Member in Zealand have many similarities and are not statistically different from each other, except from the Karlebo Member sample from the Karlebo-1A well which is significantly different from the Gassum Formation samples from the Stenlille wells. A number of small age peaks are present in the 3.0–1.7 Ga interval, of which most represent single grains (Fig. 6.7). The dominant ages are in the 1.7–1.5 Ga interval. Abundant ages are present in the 1.5–1.0 and 0.6–0.3 Ga intervals, whereas ages in the 1.0–0.6 Ga interval are less common.

Concordant zircon grains with ages that correspond to the basement in the Fennoscandian Shield in Norway and Sweden (1.9–0.9 Ga) comprise 68–74% of the zircons from the Stenlille wells, 81–86% of those from the Margrethholm-1 well, 85–95% of those from the

Karlebo-1A well and 78–90% of those from the Lavø-1 well. Concordant zircons with ages matching the basement in the Variscan Orogen in central Europe (650–280 Ma) constitute 16–23% in the Stenlille wells, 7–11% in the Margretheholm-1 well, 2–12% in the Karlebo-1A well and 5–15% in the Lavø-1 well.

### 6.2.3 Discussion

Different zircon age distributions are found in the Gassum Formation in Zealand (Fig. 6.7) and Jutland (Olivarius et al. in prep), which show that different provenance areas were the dominant sediment suppliers in the eastern and western part of the Norwegian-Danish Basin during the Late Triassic – Early Jurassic. Zircons with Variscan ages are not encountered in Jutland, but are common in all samples from the Stenlille and Margretheholm areas and are minor to common in the samples from the Karlebo-1A and Lavø-1 wells (Fig. 6.7). Basement rocks with such ages are not present in the Fennoscandian Shield (except for 0.5–0.4 Ga old rocks in the Caledonian Orogen), so these zircons must originate from the Variscan Orogen in central Europe. The zircons have presumably been deposited earlier and then reworked during deposition of the Gassum Formation and Karlebo Member. The Ringkøbing-Fyn High was exposed and eroded at the time, at least during lowstand episodes (Nielsen 2003), so it is likely that erosion of older sediments on the Ringkøbing-Fyn High has supplied much of the sediment in the southeastern part of the Norwegian-Danish Basin.

The two samples with the lowest contents of zircon grains with Variscan ages (Karlebo-1A at 2000.00 m and Lavø-1 at 2280.24 m) are from the Karlebo Member in the two northernmost of the studied wells. These are the only samples that are collected above a maximum flooding surface, whereas the remaining samples are collected above or at a sequence boundary. This indicates that sediment supply dominantly came from southern Norway during episodes of maximum flooding, which is probably because the Ringkøbing-Fyn High was flooded in periods of highstand.

Zircons with Variscan ages were transported northwards by wind across the North German Basin during the Early Triassic when the sediments of the Bunter Sandstone Formation were deposited in southern Denmark (Olivarius et al. in press). Comparison with the zircon age distributions in these sediments shows that erosion of the Bunter Sandstone Formation on the Ringkøbing-Fyn High is a very probable source of the young zircons in the eastern part of the Norwegian-Danish Basin. The lower content of zircons with Variscan ages in the Karlebo-1A, Lavø-1 and Margretheholm-1 wells than in the Stenlille wells (Fig. 6.7) suggests that less sediment was supplied by erosion on the Ringkøbing-Fyn High to northeastern Zealand than to the Stenlille area. This may be a result of the short distance from the Ringkøbing-Fyn High to the Stenlille area. According to the sequence stratigraphy, the sample from the Stenlille-4 well and the lower sample from the Karlebo-1A well have been deposited at about the same time (after SB 7), but contain 23 and 12% Variscan zircons, respectively.

The Bunter Sandstone Formation also contains zircons with a wide spectrum of Fennoscandian ages (Olivarius et al. in press), which must have been incorporated in the Gas-

sum Formation and Karlebo Member along with the Variscan zircons. Thus, the simultaneous sediment input to the Norwegian-Danish Basin from direct erosion of the Fennoscandian basement is unknown, but the high quartz content and low content of rock fragments in the sediment (Fig. 6.3) indicate that it may primarily be reworked from older sediments. The Paleozoic sediments that had covered the basement in southern Sweden were removed during the Triassic prior to deposition of the Gassum Formation, and a largely flat-relief peneplain was formed (Japsen et al. 2016). Sediment supply from southern Sweden is therefore presumed to have been limited, as also seen by the rather small content of zircons with ages matching the Swedish basement of the Eastern Segment (Figs. 6.7 and 6.8).

The number of zircons with ages in the 3.0–1.9 Ga interval is high in the studied sediments (Fig. 6.7) compared to the Gassum Formation in western Denmark (Olivarius et al. in prep), so these old zircons must have been supplied from another source which could be reworking of the Bunter Sandstone Formation where such ages are present. The only basement areas in Sweden and Norway where such ages are present are the Svecofennian Orogen and Transscandinavian Igneous Belt (TIB), but their distinctive 1.9–1.8 Ga ages are not abundant in the Gassum Formation and Karlebo Member which show that sediment was not transported westwards in significant amounts across southern Sweden (Fig. 6.8).

The prominent 1.67–1.62 Ga age peak in the Gassum Formation and Karlebo Member in eastern Denmark (Fig. 6.7) is not pronounced in the Bunter Sandstone Formation, but it is dominant in the upper part of the Gassum Formation in Jutland and almost missing in the lower part. This age peak is not found in the older Triassic deposits of the Skagerrak Formation in the Norwegian-Danish Basin (Olivarius & Nielsen 2016), but occurs in the Caledonian Orogen in central southern Norway that may have been elevated when the Gassum Formation and Karlebo Member were deposited. Therefore, it seems likely that such zircons were transported directly from the Caledonian Orogen to eastern Denmark at the time (Fig. 6.8).

Seismic interpretations in the present study show that the Gassum Formation and Karlebo Member are thinning out southwards towards the Ringkøbing-Fyn High. This may indicate that the high formed an elevated landmass exposed to erosion at the time when sediments of the Gassum Formation and Karlebo Member were deposited in the subsiding Norwegian-Danish Basin. Sediment inputs from the north and the south may have mixed in the narrow basin, and their long-travelled nature is in accordance with the high mineralogical maturity of the Gassum Formation and Karlebo Member in eastern Denmark. Heavy reworking in the shoreface zone at the time of deposition may have caused additional breakdown of feldspar grains and added to the high mineralogical maturity. This explains why the mineralogy in Zealand is more mature than in Jutland, and it shows that the distribution of the Gassum Formation in eastern Denmark is mainly controlled by local erosion. Thus, sandstones with good reservoir quality are present north of the Ringkøbing-Fyn High, but it is not well understood to which degree the Amager Fault zone had an influence on the sediment distribution in the easternmost part of the basin. Well data, including core material, from nearby Swedish wells may constitute appropriate reservoir analogues for the Gassum Formation and Karlebo Member in the eastern proposed drilling area in Copenhagen, especially if the time-equivalent sediments from Sweden have a similar provenance.

## 6.2.4 Conclusions

- The sediment supply to the eastern part of the Norwegian-Danish Basin during deposition of the Gassum Formation and Karlebo Member came from at least two source areas, comprising primarily the Ringkøbing-Fyn High and secondarily the Caledonian Orogen.
- The local sediment contribution from erosion on the Ringkøbing-Fyn High consisted presumably of recycled sediments of the Bunter Sandstone Formation, as shown by the content of zircon grains with Variscan ages, and this explains the high mineralogical maturity of the sediments.
- Sediment was also supplied from the north where the basement of the Caledonian Orogen presumably was exposed and uplifted in central southern Norway, and this sediment input became mixed with the reworked sediments in the eastern part of the Norwegian-Danish Basin.

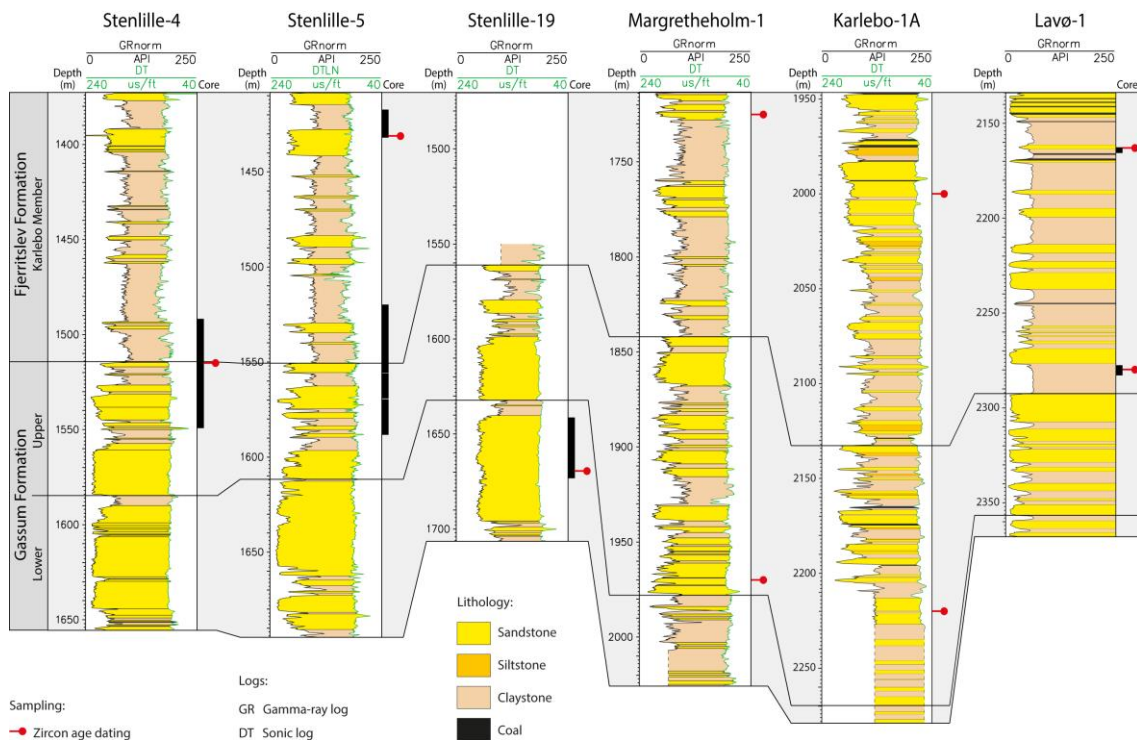


**Figure 6.6.** Lithological columns and wireline logs of the wells that have been sampled for radiometric age dating. The sampled material comprises cuttings from the Karlebo-1A and Margretheholm-1 wells and cores from the remaining wells. The well-sections are aligned to the top of the Karlebo Member. See Figure 1.1 for well locations.

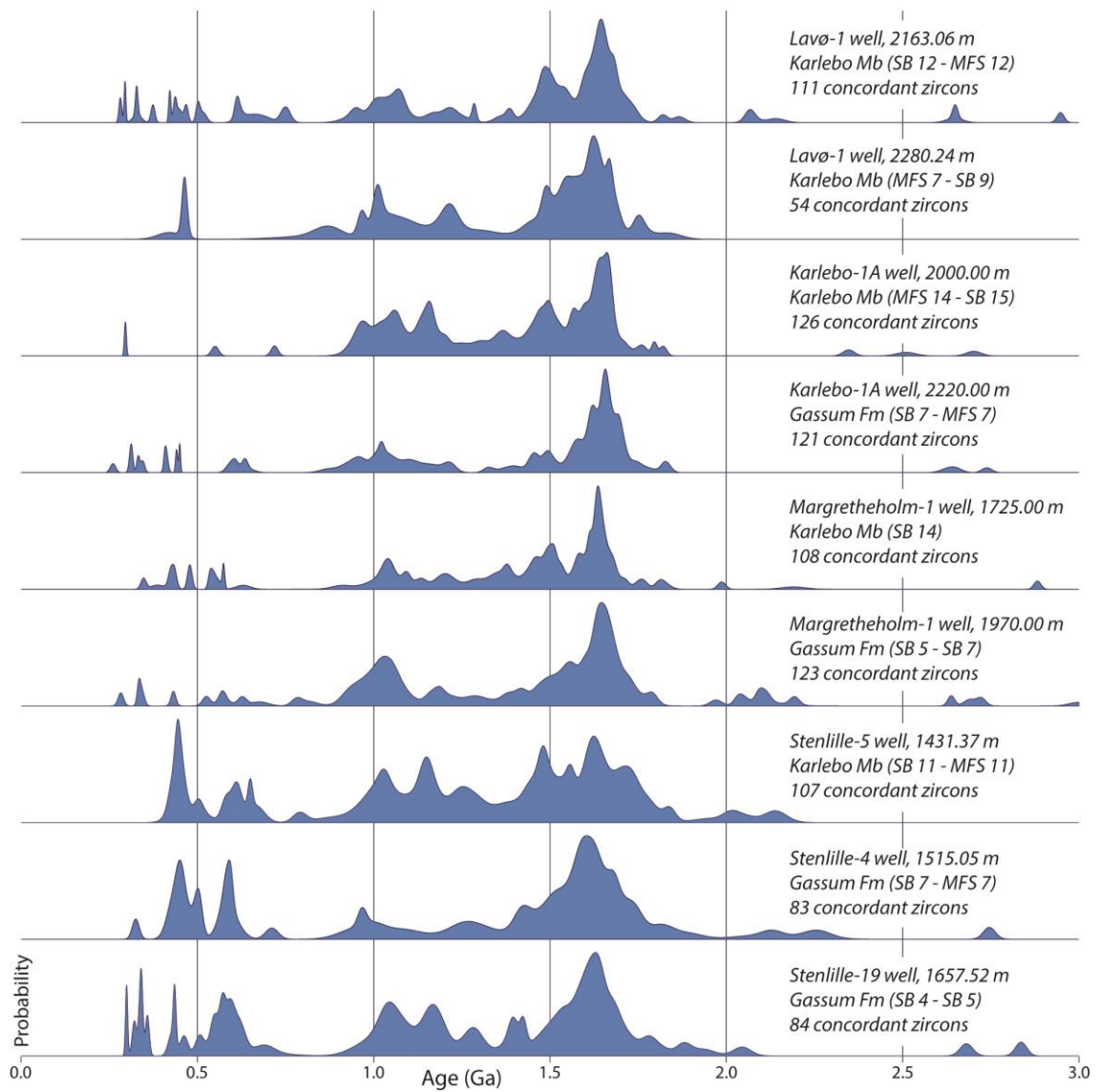


**Figure 6.7.** Zircon U–Pb age distributions of the Gassum Formation and Karlebo Member in eastern Denmark. The position of the samples in relation to the sequence stratigraphic surfaces is indicated. SB: Sequence boundary. MFS: Maximum flooding surface. The ages are in billion years (Ga).

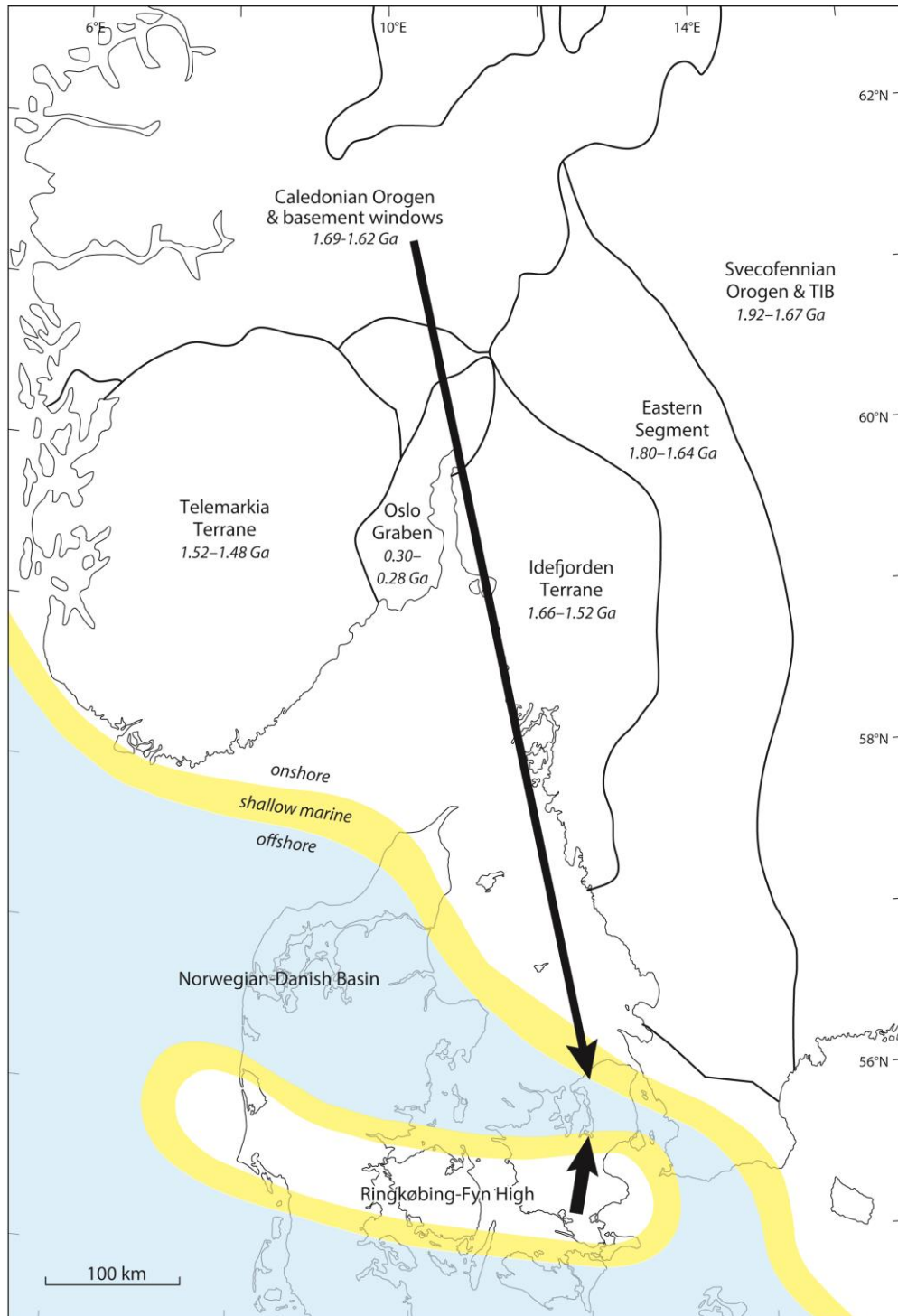


**Figure 6.8.** Schematic sediment supplies to eastern Denmark during deposition of the Gassum Formation and Karlebo Member. Zircon ages in the Stenlille-4, -5, -19, Margrethholm-1, Karlebo-1A and Lavø-1 wells show that most of the sediment probably was supplied from reworking of the Bunter Sandstone Formation on the Ringkøbing-Fyn High and from erosion of the Caledonian Orogen in central southern Norway. The outline of the Norwegian-Danish Basin is tentative; the northern coastline is from Hettangian (Michelsen et al. 2003) and some of the Ringkøbing-Fyn High coastline is based on the seismic interpretations in the present study. The basement ages are compiled by Bingen & Solli (2009).

### 6.3 Reservoir prognosis

A prognosis of relevant reservoir parameters, i.e. depth, thickness, net sand, porosity, permeability and transmissivity, is established for the two target successions: the Gassum Formation and the overlying Karlebo Member. The prognosis takes in reservoir parameters related to two geothermal prospects located close to the HGS-1 seismic line and situated west and east of the Amager fault Zone, respectively (Fig. 5.2). The Amager Fault Zone represents a pronounced synsedimentary fault system that affects both formation and net sand thicknesses and which form the western boundary of the Øresund Sub-basin. The basis data for the prognoses are:

1. **Interpreted seismic data.** The seismic data has been depth-converted, and the data provides formation tops and thicknesses. The seismic interpretation corresponds to the regional seismic interpretation recently completed at GEUS. The depth-converted surfaces correlate to information about formation tops available from offset wells, e.g. Margretheholm-1.
2. **Well data.** The well data consist primarily of calculated reservoir parameters in relevant wells. Data from the Margretheholm wells and the Karlebo-1A well are particularly important for assessing the eastern prospect as these wells also are situated in the Øresund Sub-basin. The Western prospect area is situated west of the Amager Fault, and hence west of the Øresund Sub-basin, and this, together with more comparable burial depths, justifies the use of data from Lavø-1 and the Stenlille wells for this prospect.
3. **Porosity-permeability models.** A direct measurement of permeability is not possible on the basis of petrophysical logs. Instead “indirect permeability logs” are derived based on porosity logs combined with porosity-permeability models (poro-perm models). The latter derives from porosity and permeability measurements on core material of sandstones (Fig. 6.9). One poro-perm model is established using conventional core analysis data from several Stenlille wells (‘Stenlille model’ in Fig. 6.9), and another poro-perm model originates from porosity and permeability measurements performed on sidewall cores from the Margretheholm-2 well (‘Copenhagen model’ in Fig. 6.9). These two poro-perm models are, in fact, based on rather scattered datasets as the sandstone permeability depends on factors other than porosity, e.g. grain size, clay content and sediment source area. In 2016, three additional porosity measurements were performed on cuttings samples from the Gassum Formation in the Margretheholm-1 well. These data show porosities in range 23–25%, i.e. the extra dataset confirms the porosity range given by the sidewall core (SWC) data.

Tables 6.3 and 6.4 list the specific well data dealing with the Gassum Formation and the Karlebo Member, respectively. The Karlebo-1A, Margretheholm-1, Lavø-1 and the Stenlille wells are considered. The tabulated data act as input data for reservoir prognoses. Based on previous works within the geothermal and oil industry, GEUS defined the two terms ‘Potential reservoir sand’ and ‘Gross sand’. The term ‘Potential reservoir sand’ corresponds herein to sandstones having minimum 15% porosity and a shale content less than 30%.

These cut-off values are applied to relevant log-derived curves in order to separate out proper reservoir intervals suitable for geothermal water production. 'Gross sand' is the total thickness of sandstones, and includes all sandstone intervals having a shale content less than 30%.

The porosity-permeability models described above are based on core analysis data measured at laboratory conditions, and thus up-scaling to reservoir conditions is needed prior to addressing the geothermal potential. Up-scaling of the permeability from laboratory to reservoir conditions is subject to discussion, because the geology, fractures and the different fluids affect the up-scaling process. Herein an up-scaling factor of 1.25 is applied. The scaling factor originates from an in-house GEUS study (see section 6.3.3).

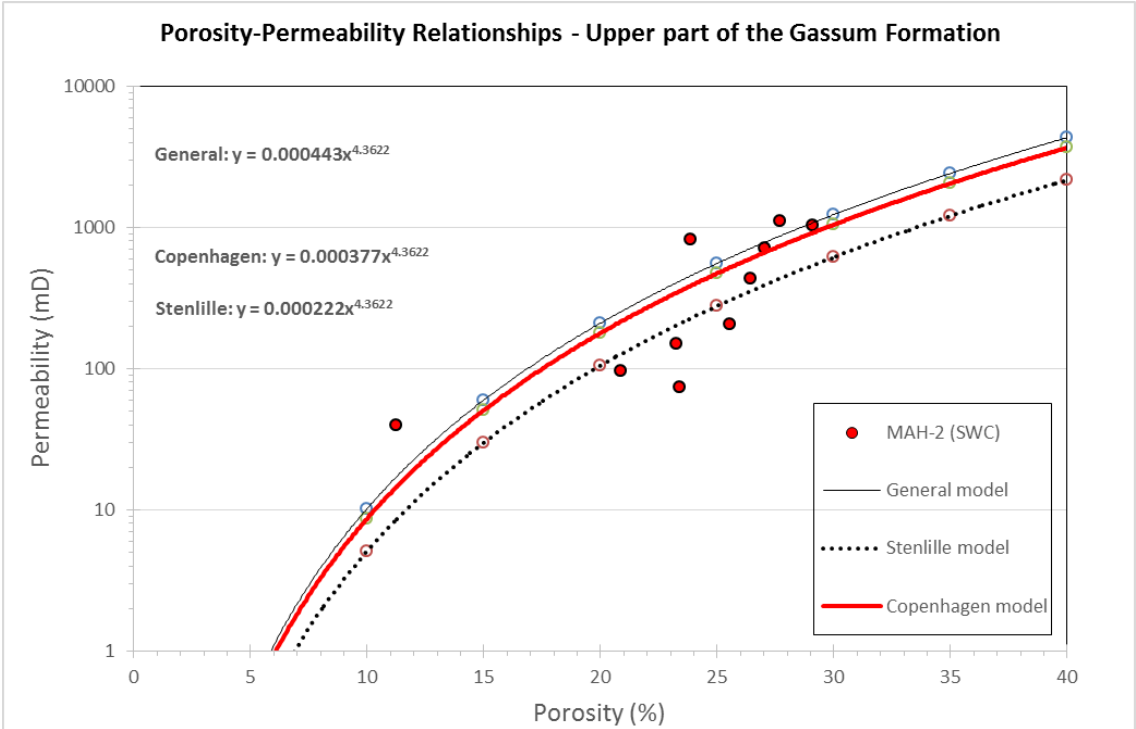


**Figure 6.9.** The two permeability models suggested for permeability prognoses: the Stenlille model and the Copenhagen model. Note that the permeability is gas permeability, i.e. the models are based on core analysis data measured at laboratory conditions. The methodology of establishing local porosity-permeability models, like the Stenlille and Copenhagen models, using a General model as a template, is outlined in Kristensen et al. (2016).

**Table 6.3.** Reservoir values for the Gassum Formation in selected wells. Both Gross sand thickness and Potential reservoir sand thickness refer to the accumulated thickness of individual layers. The data from the Stenlille wells are based on data from Stenlille-1, -2, -4, -6, -10, -12, -14, -15 and -18. Several reservoir parameters cannot be estimated for the formation in Lavø-1 due to a lack of relevant log data.

Gassum Formation	Karlebo-1A	MAH-1	Lavø-1	Stenlille wells
Depth to top (m bsl)	1991	1832	2265	1500
Thickness of formation (m)	127	184	75	150
Temperature in middle (°C)	57	54	65	48
Gross sand thickness/formation thickness	0.47	0.47	0.67	0.83
Gross sand (m)	60	63	50	124
Potential reservoir sand thickness/ formation thickness	0.31	0.40		0.80
Potential reservoir sand (m)	40	54		120
Porosity (%)	20	22		27
Gas permeability (mD)	290	300		400
Reservoir permeability (mD)	363	375		500
Reservoir transmissivity (Dm)	15	20		60

**Table 6.4.** Reservoir values for the Karlebo Member in selected wells. Both Gross sand thickness and Potential reservoir sand thickness refer to the accumulated thickness of individual layers. The data from the Stenlille wells are based primarily on data from Stenlille-1, -4 and -5 wells, but also information from the Gassum Formation have been extrapolated to the Karlebo Member (in this context data from Stenlille-2, -6, -10, -12, -14, -15 and -18 have been considered). Several reservoir parameters cannot be estimated for the formation in Lavø-1 due to a lack of relevant log data.

Karlebo Member	Karlebo-1A	MAH-1	Lavø-1	Stenlille wells
Depth to top (m bsl)	1830	1704	2106	1300
Thickness of formation (m)	161	129	160	140
Temperature in middle (°C)	57	54	65	48
Gross sand thickness/formation thickness	0.50	0.22	0.28	0.15
Gross sand (m)	81	28	44	21
Potential reservoir sand thickness/ formation thickness	0.27	0.17		0.14
Potential reservoir sand (m)	44	22		20
Porosity (%)	21	22		24
Gas permeability (mD)	310	325		240
Reservoir permeability (mD)	388	406		300
Reservoir transmissivity (Dm)	17	9		6

### 6.3.1 Reservoir prognosis for the western area

Table 6.5 presents a prognosis of relevant reservoir parameters for the western prospect. The regional seismic interpretation provides thickness and depth estimates for the Gassum Formation and the Karlebo Member. Data from nearby wells give information about reservoir properties, and the general GEUS temperature model provides information about formation temperatures.

### **Gassum Formation**

The basic data for the prognosis is reservoir parameters listed on a well-to-well basis in Table 6.3. High 'Gross sand thickness/formation thickness' ratios of 0.67 and 0.83 characterize the Gassum Formation in Lavø-1 and the Stenlille wells, respectively, whereas a ratio of 0.47 is attributed to the formation in both Karlebo-1A and Margretheholm-1 (Table 6.3). The ratio of 0.67 from Lavø-1 is used to estimate the Gross sand thickness of the Gassum Formation in the western prognosis area, as it is the nearest of the wells occurring west of the Amager Fault zone. As the formation thickness is estimated to 150 m in the western prognosis area, the expected Gross sand thickness then becomes 101 m (given by  $0.67 \times 150$  m).

A ratio for 'Potential reservoir sand thickness/formation thickness' has been calculated, if possible. The ratio is presumably higher than found in Margretheholm-1 (0.40) but lower than the ratio of 0.80 which characterize the Gassum Formation in the Stenlille wells. Consequently, GEUS consider the ratio to be in the range of 0.40–0.80 for the western area, and has chosen to use a ratio value of 0.50 in estimating the accumulated thickness of Potential reservoir sand. The Potential reservoir sand in the Gassum Formation in the western prognosis area is thus estimated to 75 m (given by  $0.50 \times 150$  m).

Interpreted porosity logs from Margretheholm-1, Karlebo-1A and Stenlille-1 deliver porosity-depth relationships that provide the porosity of the prospect, since the seismic interpretation points out the expected reservoir depth. When dealing with the Gassum Formation, especially the Stenlille porosity data are considered representative for the western prognosis area. A porosity of 25% is assigned to the reservoir sandstones of the Gassum Formation in the western prognosis area (Table 6.5).

The Stenlille permeability model provides reasonable permeability estimates for the western area. The model relates porosity to gas permeability (core permeability's measured at laboratory conditions). A gas permeability of 300 mD is assigned to the reservoir sandstones of the Gassum Formation in the western prognosis area (Table 6.5). The gas permeability is up-scaled to reservoir conditions using a scaling factor of 1.25 implying that the reservoir permeability becomes 375 mD (given by  $1.25 \times 300$  mD = 375 mD).

Finally, the transmissivity is calculated as the reservoir permeability multiplied by the Potential reservoir sand thickness. The transmissivity is thus estimated to 28 Darcy-meter (given by  $0.375$  Darcy  $\times$  75 m).

### **Karlebo Member**

The basic data for the prognosis is reservoir parameters listed on a well-to-well basis in Table 6.4. The seismic data suggest that the Karlebo Member is c. 100 m thick in the western prospect area. The Gross sand thickness of 40 m, given in Table 6.5, relies primarily on data from the Lavø-1 well. The 'Gross sand thickness/formation thickness' ratio is 0.4 (given by  $40$  m/ $100$  m). This ratio is largely in accordance with an average ratio calculated for Karlebo-1A and Margretheholm-1.

The estimated 'Potential reservoir sand thickness/formation thickness' ratio relies on data from Margrethholm-1 and Karlebo-1A. A weight factor of two is applied to data representing the closest well (Margrethholm-1) and the ratio thus become 0.20 for the Karlebo Member in the western prognosis area (given by  $(2 \times 0.17 + 0.27)/3$ ). The 'Potential reservoir sand thickness/formation thickness' ratio of 0.2 forms the basis of estimating the accumulated thickness of Potential reservoir sandstones. This is estimated to 20 m (given by  $0.20 \times 100$  m).

Interpreted porosity logs from Margrethholm-1, Karlebo-1A and Stenlille-1 deliver porosity-depth relationships that provide the porosity of the prospect, since the seismic interpretation points out the expected reservoir depth. Especially the Stenlille porosity data are considered representative for the western area. A porosity of 23% is assigned to the reservoir sandstones of the Karlebo Member in the western prognosis area (Table 6.5).

The permeability is estimated from the Stenlille permeability model, which relates porosity to gas permeability (gas permeability measured on core plug samples at laboratory conditions). A gas permeability of 240 mD is assigned to the reservoir sandstones of the Karlebo Member in the western prognosis area (Table 6.5). The gas permeability is up-scaled to reservoir conditions using a scaling factor of 1.25 implying that the reservoir permeability becomes 300 mD (given by  $1.25 \times 240$  mD).

Finally, the transmissivity is calculated as the reservoir permeability multiplied by the Potential reservoir sand thickness. The transmissivity is thus estimated to 6 Darcy-meter (given by  $0.3$  Darcy  $\times$  20 m).

As part of this study, GEUS analyzed five additional core samples originating from rather clean sandstone intervals within the Karlebo Member in the Stenlille-1 and Stenlille-5 wells (in the depth interval 1430–1455 m). These core data show high sandstone porosities and gas permeabilities; around 29% and 500 mD, respectively. The extra dataset confirms the rather high average porosity and permeability estimates for the Karlebo Member listed in Table 6.5.

**Table 6.5.** *Estimated reservoir parameters and associated uncertainty ranges for the Gassum Formation and the Karlebo Member in the western prognosis area. The parameters are constrained by the regional seismic interpretation and well data from nearby wells.*

Western prognosis area	Gassum Fm		Karlebo Mb	
	Estimated value	Uncertainty range	Estimated value	Uncertainty range
Depth to top (m bsl)	1750	1662-1838	1650	1665-1735
Thickness of unit or formation (m)	150	135-165	100	90-110
Temperature in middle (°C)	57	54-59	54	51-57
Gross sand thickness/formation thickness	0.67	0.63-0.70	0.4	0.38-0.42
Gross sand (m)	101	95-107	40	38-42
Potential reservoir sand thickness/formation thickness	0.50	0.47-0.53	0.20	0.19-0.21
Potential reservoir sand (m)	75	68-83	20	18-22
Porosity (%)	25	24-26	23	21-24
Gas permeability (mD)	300	150-600	240	120-480
Reservoir permeability (mD)	375	188-750	300	150-600
Reservoir transmissivity (Dm)	28	14-56	6	3-12

### 6.3.2 Reservoir prognosis for the eastern area

Table 6.6 presents a prognosis of relevant reservoir parameters for the eastern prospect. The regional seismic interpretation provides thickness and depth estimates for the Gassum Formation and the Karlebo Member. Data from nearby wells give information about reservoir properties, and the general GEUS temperature model provides information about formation temperatures.

#### Gassum Formation

The basic data for the prognosis is reservoir parameters listed on a well-to-well basis in Table 6.3. The Karlebo-1A and Margrethholm-1 wells point to a 'Gross sand thickness/formation thickness' ratio of 0.47, but a slightly higher ratio of 0.50 is suggested for the prospect (round off value). The estimated formation thickness is 200 m, and the expected Gross sand thickness then becomes 100 m (given by  $0.50 \times 200$  m).

The ratio 'Potential reservoir sand thickness/formation thickness' is presumed to be similar to the ratio estimated for the Gassum Formation in Margrethholm-1. A ratio of 0.40 is thus used to estimate the accumulated thickness of Potential reservoir sand. The Potential reservoir sand in the Gassum Formation in the eastern prospect area is thus estimated to be 80 m (given by  $0.40 \times 200$  m).

Interpreted porosity logs from Margrethholm-1, Karlebo-1A and Stenlille-1 deliver porosity-depth relationships that provide the porosity of the prospect, since the seismic interpretation points out the expected reservoir depth. When dealing with the Gassum Formation, especially porosity data from the Margrethholm-1 and Karlebo-1A wells are considered representative of eastern area. A porosity of 21% is assigned to the reservoir sandstones of the Gassum Formation in the eastern prognosis area (Table 6.6).

The Copenhagen permeability model provides reasonable permeability estimates for the eastern prospect area. The model relates porosity to gas permeability (i.e. a core permeability measured at laboratory conditions). A gas permeability of 250 mD is assigned to the reservoir sandstones of the Gassum Formation in the eastern prognosis area (Table 6.6). The gas permeability is up-scaled to reservoir conditions using a scaling factor of 1.25 implying that the reservoir permeability becomes 313 mD (given by  $1.25 \times 250$  mD).

Finally, the transmissivity is calculated as the reservoir permeability multiplied by the Potential reservoir sand thickness. The transmissivity is thus estimated to 25 Darcy-meter (given by  $0.313$  Darcy  $\times$  80 m).

### **Karlebo Member**

The basic data for the prognosis is reservoir parameters listed on a well-to-well basis in Table 6.4. The seismic data suggest that the Karlebo Member is 200 m thick and thus twice as thick as in the western prospect area. The 'Gross sand thickness/formation thickness' ratio is estimated to be c. 0.4 based on a mean of the ratio values from Karlebo-1A and Margrethholm-1. Expected Gross sand thickness is estimated to be 80 m (given by  $0.4 \times 200$  m).

The estimated 'Potential reservoir sand thickness/formation thickness' ratio relies on data from Margrethholm-1 and Karlebo-1A. A weight factor of two is applied to data representing the closest well (Margrethholm-1) and the ratio thus becomes 0.20 (given by  $(2 \times 0.17 + 0.27)/3$ ). The Potential reservoir sand thickness/formation thickness' ratio of 0.20 forms the basis for estimating the accumulated thickness of Potential reservoir sandstones. This estimated to 40 m (given by  $0.20 \times 200$  m).

Interpreted porosity logs from Margrethholm-1, Karlebo-1A and Stenlille-1 deliver porosity-depth relationships that provide the porosity of the prospect, since the seismic interpretation points out the expected reservoir depth. With respect to the Karlebo Member, especially porosity data from the Margrethholm-1 and Karlebo-1A wells are considered representative of eastern area. A porosity of 22% is assigned to the reservoir sandstones of the Karlebo Member in the eastern prognosis area (Table 6.6).

The permeability is estimated from the Copenhagen permeability model, which relates porosity to gas permeability (i.e. a core permeability measured at laboratory conditions). A gas permeability of 300 mD is assigned to the reservoir sandstones of the Karlebo Member in the eastern prognosis area (Table 6.6). The gas permeability is up-scaled to reservoir conditions using a scaling factor of 1.25 implying that the reservoir permeability becomes 375 mD (given by  $1.25 \times 300$  mD).

Finally, the transmissivity is calculated as the reservoir permeability multiplied by the potential reservoir sand thickness. The transmissivity is thus estimated to 15 Darcy-meter (given by  $0.375$  Darcy  $\times$  40 m).

**Table 6.6.** *Estimated reservoir parameters and associated uncertainty ranges for the Gassum Formation and the Karlebo Member in the eastern prognosis area. The parameters are constrained by the regional seismic interpretation and well data from nearby wells.*

Eastern prognosis area	Gassum Fm		Karlebo Mb	
	Estimated value	Uncertainty range	Estimated value	Uncertainty range
Depth to top (m bsl)	2000	1900-2100	1800	1710-1890
Thickness of unit or formation (m)	200	180-220	200	180-220
Temperature in middle (°C)	65	61-68	59	56-62
Gross sand thickness/formation thickness	0.50	0.47-0.53	0.4	0.38-0.42
Gross sand (m)	100	95-105	80	76-84
Potential reservoir sand thickness/formation thickness	0.40	0.38-0.42	0.20	0.19-0.21
Potential reservoir sand (m)	80	72-88	40	36-44
Porosity (%)	21	20-22	22	21-23
Gas permeability (mD)	250	125-500	300	150-600
Reservoir permeability (mD)	313	156-625	375	187-750
Reservoir transmissivity (Dm)	25	12-50	15	8-30

### 6.3.3 Geothermal potential

A reservoir is considered to have a geothermal potential if the transmissivity is greater than 10 Darcy-meter as a general rule of thumb. Based on this criterion, the Gassum Formation can be considered as forming a suitable geothermal reservoir in both the western and eastern prognosis areas where the transmissivity is estimated to 28 Darcy-meter and 25 Darcy-meter, respectively (Tables 6.5 and 6.6). Core analysis data from the Stenlille-19 well indicate that an extremely permeable zone exists in the lower part of the Gassum Formation in the Stenlille area. Presumably, this zone pinches out towards the western prospect area, but comparable facies with good reservoir properties cannot be excluded also to be present at higher stratigraphic levels in the Gassum Formation in the western prospect area, and would then provide an upside potential.

The transmissivity is estimated to 15 Darcy-meter for the Karlebo Member in the eastern prospect and can thus be considered as forming a suitable geothermal reservoir. This is not the case in the western prospect where the transmissivity is estimated to be only 6 Darcy-meter. However, the uncertainty range, associated to this value, do allow transmissivity values up to 12 Darcy-meter (Table 6.5).

### 6.3.4 Estimation of reservoir parameters

Figures 6.10–6.13 show a lithological interpretation along with a petrophysical evaluation of the log data from the Margrethholm-1, Karlebo-1A, Lavø-1 and Stenlille-1 wells. The evaluation includes porosity and permeability determination, and red bars illustrate intervals of potential reservoir sandstones.

### Interpretation of lithology

Well-log data and cuttings descriptions provides information about lithological variations throughout the Gassum Formation and the Karlebo Member. The interpretation of the expected lithology outside well control incorporates existing well data, including geological and wireline log data from the Margrethholm and Stenlille wells along with data from the Karlebo-1A and Lavø-1 wells. Detailed descriptions of the drilled sections, which are available in final well reports etc., support and validate the log-based interpretations.

### Estimation of clay content and porosity

The clay content (shale volume) is estimated from the gamma-ray (GR) log, if present. The calculation of the clay content is based on two well-specific shale parameters: background radiation (GR\_min) and the GR response for the clay-rich matrix (GR\_max). Table 6.7 lists the parameter values used for interpreting the clay content in the Gassum Formation and Karlebo Member in the selected wells.

The clay content ( $V_{clay}$ ) is calculated as follows:

$$V_{clay} = (GR - GR_{min}) / (GR_{max} - GR_{min})$$

As no GR log is available from the Lavø-1 well, the clay content is instead calculated from the SP log using a similar methodology.

Subsequent to calculating clay content, the porosity of the sandstone layers in the Margrethholm-1, Karlebo-1A and Stenlille-1 wells was determined using a standard petrophysical approach. The porosity is determined from the density log (RHOB) combined with information about the clay content ( $V_{clay}$ ). The equations used for calculating the effective porosity (PHIE) from the density log readings and the clay content are listed below:

$$PHIE = \frac{RHO_{ma} - RHOB}{RHO_{ma} - RHO_{fluid}} \quad (1)$$

where,

$RHOB$  is the density log readings.

$RHO_{fluid}$  is the fluid density (approximately 1.05 g/cc).

$RHO_{ma}$  is the density of the matrix material consisting of sandstone and varying amounts of clay. By using a sandstone density of 2.65 g/cc and a clay density of 2.4 g/cc, the matrix density is calculated as follows:

$$RHO_{ma} = 2.65g/cc \cdot (1 - V_{clay}) + 2.4g/cc \cdot V_{clay} \quad (2)$$

The amount of Potential reservoir sand is then determined by applying cut-offs to the interpreted log curves, i.e. PHIE and  $V_{clay}$ . Potential reservoir sand presumes a minimum porosity of 15% and a clay content less than 30%. Furthermore, the log-derived porosity values are averaged across the Gassum Formation–Karlebo Member interval after applying cut-offs.

**Table 6.7.** Parameter values used for interpreting the clay content from the gamma-ray (GR) and SP logs.

Well	Formation/member	Log	GR_min (API) SP_min (mV)	GR_max (API) SP_max (mV)
Margretheholm-1	Gassum Fm and Karlebo Mb	GR	90	160
Karlebo-1A	Gassum Fm and Karlebo Mb	GR	75	163
Lavø-1	Gassum Fm and Karlebo Mb	SP	37	180
Stenlille-1	Gassum Fm and Karlebo Mb	GR	15	125

### Estimation of permeability

Permeability logs are not acquired in any of the wells, meaning the permeability assessment must be based on porosity-permeability relationships (models) and core permeability data when available. In relation to Zealand, core analysis data from the Gassum Formation are available from ten of the Stenlille wells and permeability has additionally been measured on sidewall cores from the Gassum Formation in the Margretheholm-2 well.

Figure 6.14 illustrates a local Stenlille porosity-permeability model. Averaged values of core porosity and core permeability data form the basis for establishing the model, leading to a well-defined porosity-permeability relationship. The permeability is modelled using the log-derived porosities as input data, leading to a synthetic permeability curve. Such a permeability assessment, i.e. an indirect measure of the permeability, is of course associated with uncertainty as illustrated by the uncertainty band in the figure.

The Stenlille model relates the permeability (PERM\_log) to the log porosity (PHIE) through a power function:

$$\text{PERM\_log} = 0.000222 \cdot (\text{PHIE})^{4.3622}$$

Similarly, the Copenhagen model that is based primarily on data from the Margretheholm-2 well, relates the permeability (PERM\_log) to the log porosity (PHIE) in the following way:

$$\text{PERM\_log} = 0.000377 \cdot (\text{PHIE})^{4.3622}$$

In both models, the porosity (PHIE) is expressed in percent (%) and the log-derived gas permeability (PERM\_log) is expressed in millidarcies (mD). The two models differ to a certain degree, most likely reflecting differences in grain size distribution or different sediment source areas.

For quick-look analyses, GEUS suggests to use just one porosity-permeability model based on an average of the two models described above, i.e.:

$$\text{PERM\_log} = 0.0003 \cdot (\text{PHIE})^{4.3622}$$

The production capacity calculations utilize the latter relationship for assessing permeability in the simulation model (see Chapter 7).

The log-derived permeability (PERM\_log) is a gas permeability reflecting core permeability measurements in the laboratory. The laboratory permeability is up-scaled to reservoir con-

ditions using a scaling factor of 1.25. This scaling factor originates from an in-house GEUS study in which permeabilities measured on core material in the laboratory was compared with reservoir permeabilities interpreted from well-test data covering the cored interval.

### **Estimation of transmissivity**

The reservoir permeability multiplied by accumulated thickness of the potential reservoir sandstones provides the transmissivity. The transmissivity forms the basis for addressing the geothermal potential in a particular sandstone reservoir.

### **Estimation of temperature**

The temperature in the middle of the Gassum Formation and the Karlebo Member is estimated based on a general depth-temperature given by:  $\text{Temperature} = 0.027 \times \text{depth} + 8$  °C. The relation is constructed on the basis of temperature measurements in deep wells in the Danish Basin.

### **Uncertainty ranges of estimated reservoir parameters**

Each reservoir parameter is associated with an uncertain range of which an estimate is given in Table 6.8. The quantification of these uncertainty ranges is based on GEUS' experience, general geological knowledge and overall understanding of the Danish geothermal reservoirs. The derivation of the uncertainty range for permeability and transmissivity is described in detail in Kristensen et al. (2016).

**Table 6.8.** *Estimated uncertainty ranges of the reservoir parameters.*

<b>Reservoir parameter</b>	<b>Estimated uncertainty range</b>
Depth to top	+/- 5% (relative %)
Thickness of unit or formation	+/- 10% (relative %)
Temperature in middle	+/- 5% (relative %)
Gross sand/formation	+/- 5% (relative %)
Gross sand	+/- 5% (relative %)
Potential reservoir sand/formation	+/- 5% (relative %)
Potential reservoir sand	+/- 10% (relative %)
Porosity	+/- 5% (relative %)
Gas permeability	Multiplication/division by 2
Reservoir permeability	Multiplication/division by 2
Reservoir transmissivity	Multiplication/division by 2

# Margretheholm-1

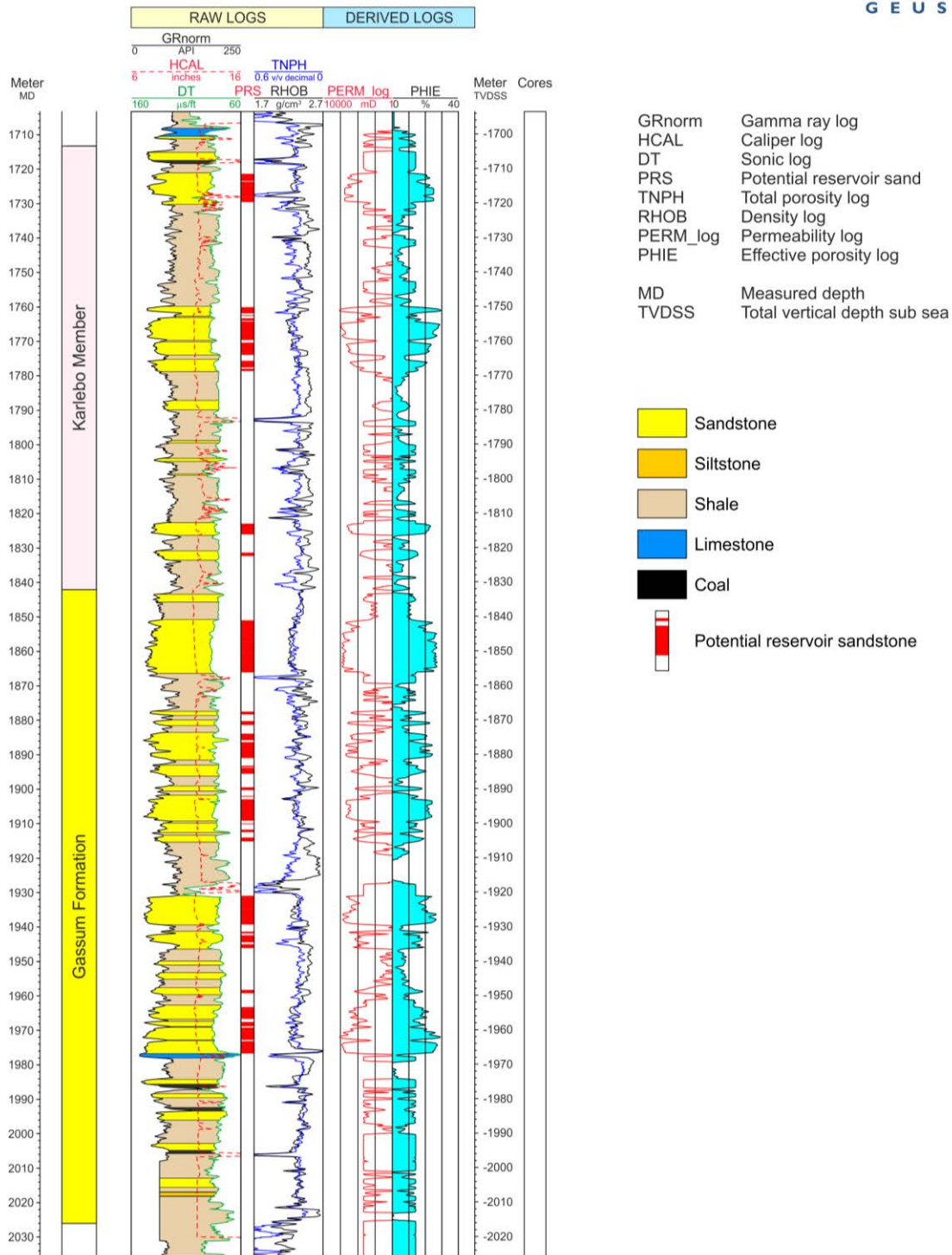


**Figure 6.10.** Lithological interpretation and petrophysical evaluation of the Margretheholm-1A well. Potential reservoir sandstones highlighted (red bars). Porosity in light blue, permeability illustrated by a red curve.

# Karlebo-1A

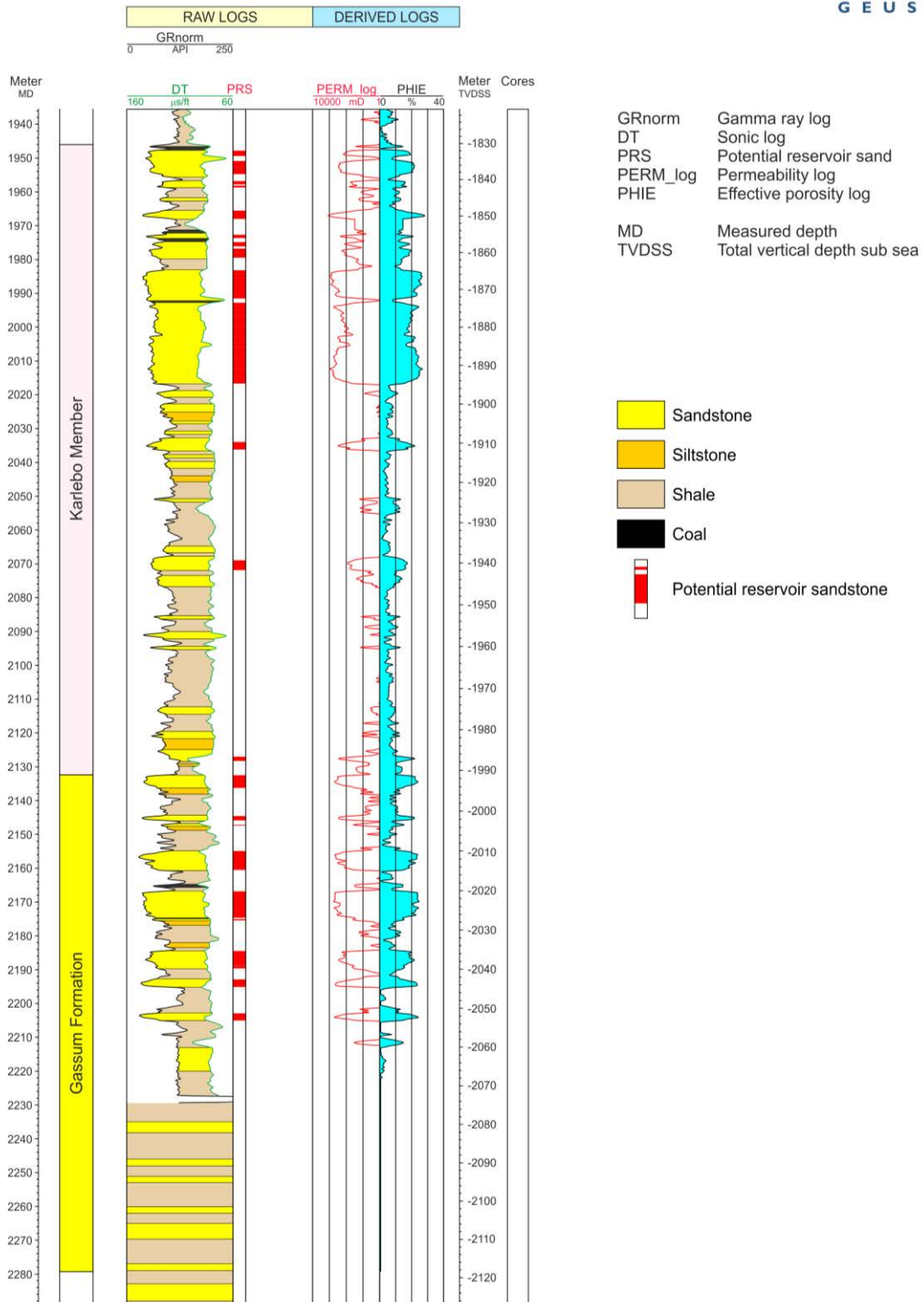


**Figure 6.11.** Lithological interpretation and petrophysical evaluation of the Karlebo-1A well. Potential reservoir sandstones highlighted (red bars). Porosity in light blue, permeability illustrated by a red curve.

# Lavø-1

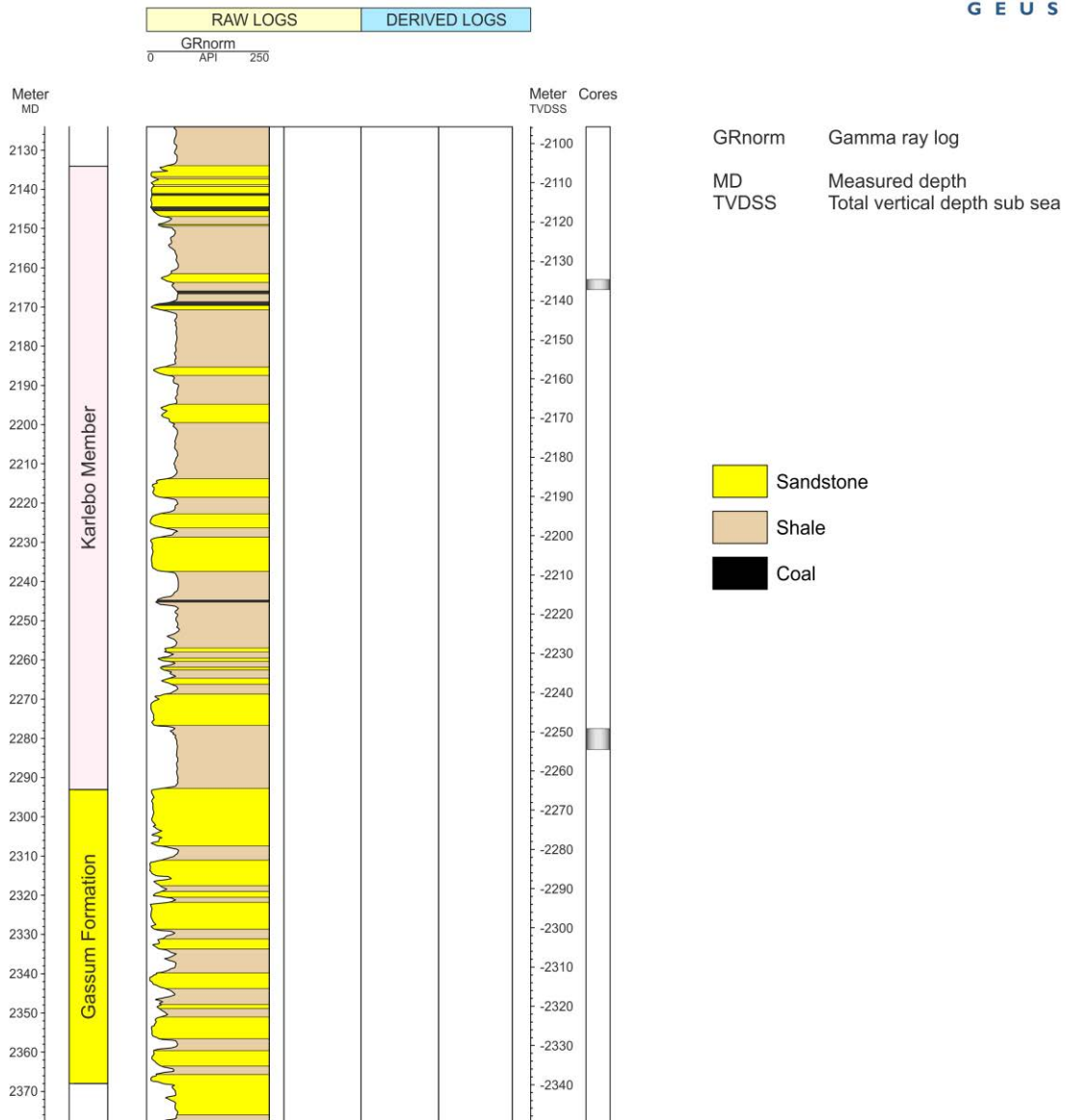


**Figure 6.12.** Lithological interpretation of the Lavø-1 well. A petrophysical evaluation is not possible due to an incomplete log suite. GRnorm corresponds to a re-scaled SP log.

# Stenlille-1

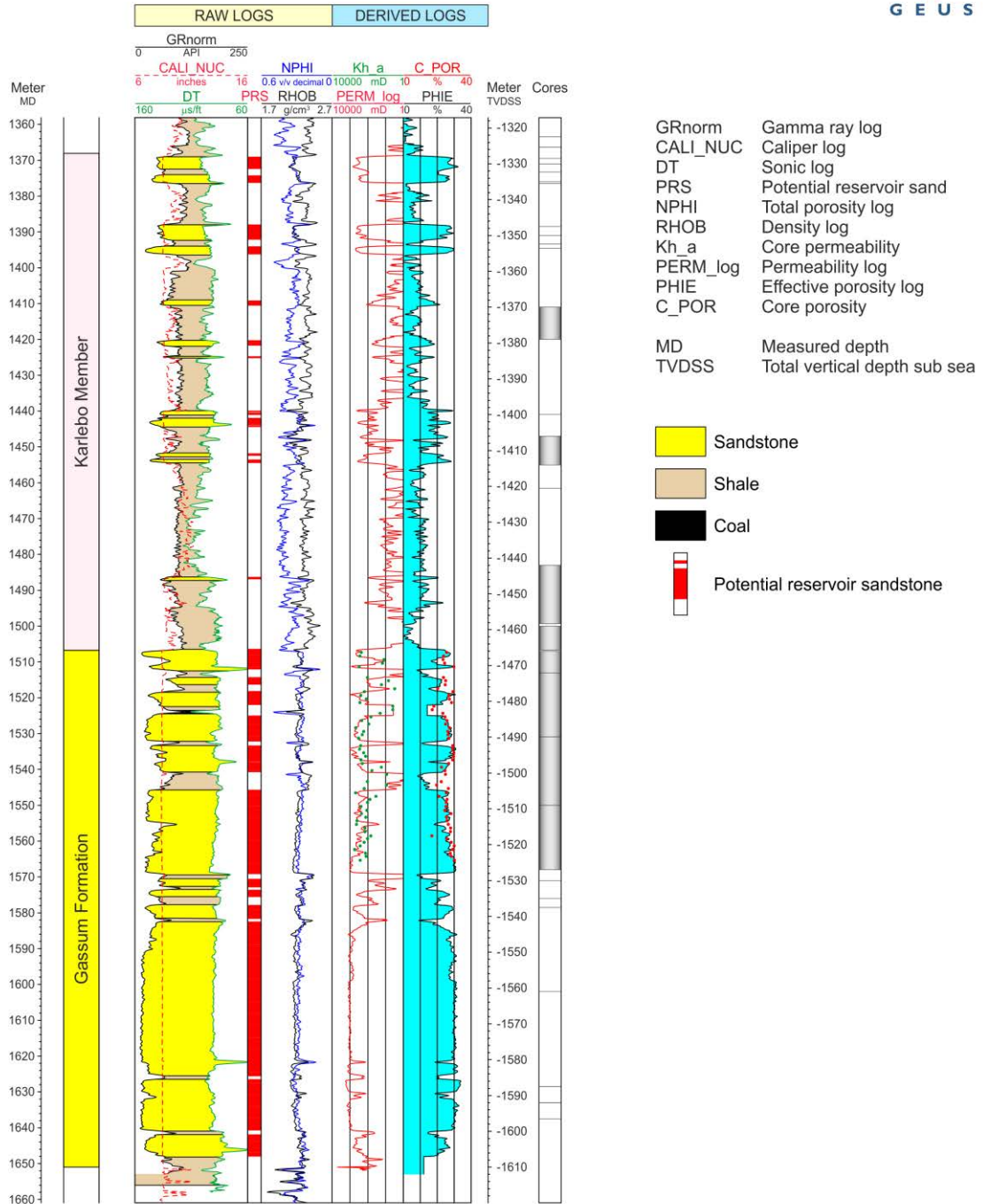


**Figure 6.13.** Lithological interpretation and petrophysical evaluation of the Stenlille-1 well. Potential reservoir sandstones highlighted (red bars). Porosity in light blue, permeability illustrated by a red curve.

## Local poro-perm model for the Stenlille area

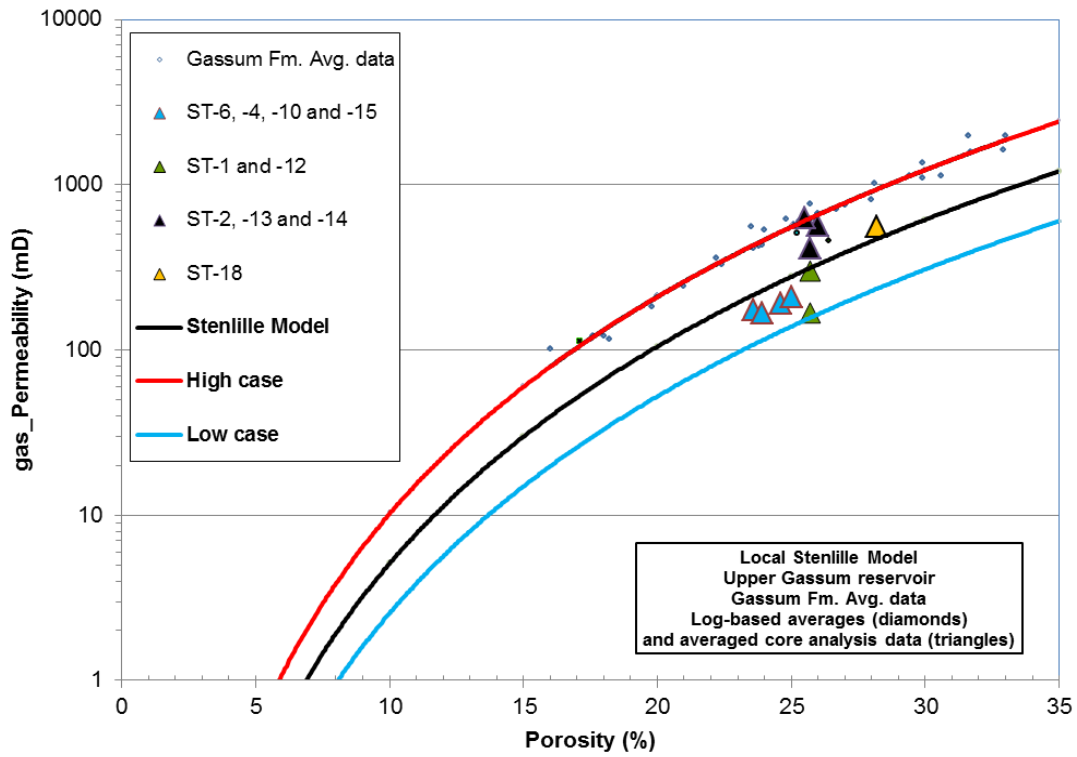


**Figure 6.14.** Local Stenlille porosity-permeability model. Triangles refer to averaged core analysis data from more Stenlille wells. Small diamonds refer to data from outside the Stenlille area (general model).

## 7. Production capacity

The productivity and injectivity capacities for a location within each of the areas of interest were assessed by use of reservoir simulation methodology. Coordinates for the two locations were provided by HOFOR (Fig. 7.1). The methodology is well proven from the oil and gas industry and can help quantify the potential of a given geothermal reservoir on basis on the available geological, geophysical and petrophysical data, *i.e.* before a dedicated well is drilled and tested.

A geological (or static model) is constructed based on the data presented in the preceding chapters. Several commercial software packages exist in the market, which can help construct a 3D model of the subsurface. In the present project, the Petrel (2015) software of Schlumberger was used. The static model is gridded in a 3D grid and exported together with reservoir properties (porosity and permeability) to a reservoir simulation software. Here the Eclipse 100 (2016) software of Schlumberger is used. The software can solve the governing equations for flow and temperature, where the differential equations are solved by use of the model grid and finite difference methodology. Both the used software's are state-of-the-art and widely used in the oil and gas industry.

The present chapter describes the construction of the static and dynamic (reservoir simulation) models together with the applied constraints and uncertainties that are discussed in the previous chapters. Results from a number of simulation scenarios are presented and discussed, in order to evaluate the productivity capacity of the two locations.

### 7.1 Static and dynamic modelling

For the model construction an area of interest (AOI) of 15 km x 20 km was used to encompass both the western and eastern locations (Fig. 7.1).

#### 7.1.1 Input data

##### Horizons

From the seismic interpretation work (Chapter 5) five key horizons were imported to Petrel; Top Vinding, Top Gassum, Top Karlebo, Top Fjerritslev and Top Lower Cretaceous (*cf.* Fig. 5.3). The individual horizons were depth adjusted to match the individual picks in the Margrethholm-1 well; the depth shifts were in the order of 30 – 35 meters.

Some “bulls-eyes” were smoothed around the Amager Fault zone and at the eastern edge of the horizons. This was done primarily for the Top Karlebo, Top Gassum and Top Vinding horizons with the use of the Petrel option “peak remover” (*cf.* Fig. 7.2).

##### Well data

The interpreted porosity log as a function of depth (TVD) from the Margrethholm-1 well was imported to Petrel. The log data were used to populate the 3D static model with porosi-

ty values for the individual grid cells, *i.e.* the Margrethholm-1 data were used on both side of the Amager Fault.

### **Temperature and formation water**

A constant temperature gradient of 27 °C/km and a constant surface temperature of 8 °C was used. Formation water density and viscosity values were taken from the Margrethholm-1 well data and adjusted to the shallower depths of the Karlebo and Gassum reservoirs at the two locations of interest.

## **7.1.2 Static modelling procedure**

This section describes the construction of the 3D static model together with the set-up of the dynamic reservoir simulation model.

### **Grid**

A 3D corner point grid was constructed from the adjusted and smoothed horizons. The grid was aligned with the Amager Fault orientation (deviated 23deg from North) in order to model the fault zone more easily in the grid, *i.e.* no fault plane was constructed but a number of grid cells were assigned to the fault zone.

A total of 54 layers was used in the z direction; 20 layers for each of the two main reservoir intervals, Karlebo Member and Gassum Formation, 4 layers for the underlying Vinding Formation and 10 layers for the overburden. The lateral grid resolution was 100 m x 100 m resulting in a total grid size of the AOI of 200 x 149 x 54 grid cells.

For the dynamic simulations the local grid refinement (LGR) option in Petrel and Eclipse was applied to avoid any numerical dispersion in the pressure and temperature calculations. The LGR option increases the grid resolution in the area around the wells, *i.e.* the size of the individual grid cells decreases (Fig. 7.3). LGR was only used in the x-y plan.

### **Grid properties (reservoir properties)**

As stated above, porosity values are distributed in the grid honouring the vertical variation in the Margrethholm-1 well. It was decided to first model the AOI as a “layer-cake” model, *i.e.* no lateral variation in reservoir properties, only vertical variation. The reason for this is that the seismic resolution is too low to govern a more detailed lateral variation in reservoir parameters for the relative narrow AOI.

The porosity log from the Margrethholm-1/1A well was up-scaled to assign a single averaged value for each of the individual layers that the well penetrates. The up-scaled porosity values are assigned to the respective layers in the 3D grid.

The only lateral variation for the porosity is a general porosity depth trend, with a porosity reduction of 0.065 (porosity in fraction) per 100 m. This trend was superimposed on the porosity distribution.

Chapter 6 describes how the reservoir permeability can be calculated as a function of the porosity (cf. Figs. 6.3 and 6.8). To populate the grid with permeability values the “Stenlille poro-perm” model was applied for the individual grid cells in the AOI west of the Amager Fault zone and the “Copenhagen poro-perm” model applied east of the fault zone. This was done for the reservoir intervals (Karlebo Member and Gassum Formation), whereas the over- and underburden layers was assigned a constant value in the range 1 – 10mD.

As described in the previous chapter a factor of 1.25 is multiplied on the permeability values to convert core analysis data, measured in the laboratory, to field scale and to convert from gas permeability to water permeability. Also based on core analysis data a ratio between the vertical and horizontal permeability of 0.3 was applied.

To accommodate for uncertainties in reservoir parameters uncertainty bands were applied for the porosity-permeability relation; the “Stenlille uncertainty-model” with uncertainty bands of 2 times higher and 2 times lower than the regression line in the porosity-permeability relationship were used for both the western and eastern part of the model (cf. Fig. 6.8). For the porosity a band of +/- 0.02 (porosity fraction) was applied. The introduction of uncertainty bands resulted in 9 discrete porosity-permeability sets that were used for the flow simulation with the reservoir model, cf. Figure 7.4.

Grid and grid properties as described above were exported from the Petrel software to the Eclipse 100 (2016) software for dynamic modelling of flow, pressure and temperature. The 3D permeability distribution is shown in Figure 7.5.

### 7.1.3 Dynamic modelling procedure

Eclipse 100 is a black-oil simulator widely used in the oil industry for reservoir simulation. It is a robust and well proven numerical code based on finite differentiation of the relevant equations; *i.e.* it solves Darcy’s law (flow) together with a generalised conservation equation (material balance).

#### Temperature modelling

Eclipse 100 is inherently an isothermal reservoir simulator, but it has an in-built temperature option that can be used to simulate temperature distribution. The option can keep track of the injected cold water and the temperature changes when the formation water and injected water mixes. Furthermore, heat conduction for the geological layers is built in the option.

Heat conduction for the geological layers is assumed to be 2.5 W/m/°C together with specific heat capacity of 2.5 MJ/m<sup>3</sup>/°C and 4.0 MJ/m<sup>3</sup>/°C for the geological layers and the formation water, respectively (Bording 2010).

A temperature prognosis for the AOI states a temperature gradient of 27 °C/km with an average surface temperature of 8 °C.

## **Boundary conditions**

Proper boundary conditions must be applied for the simulation model. Even though the simulation of a geothermal plant operation involves production and injection of equal volumes of water it must be secured that the simulated pressure development is not influenced by the model boundary. Pore volume multiplication is used as a pressure boundary condition; *i.e.* the pore volumes of the outermost grid cells of the model were multiplied by a high number (1000) to mimic that the model area is situated in an infinite aquifer. This is standard procedure in reservoir modelling to ensure that the reservoir boundaries does not influence the modelling results.

Further, as described above, the over- and underburden is included to secure correct handling of the temperature boundary conditions.

The build-in Eclipse well option (Eclipse 100 2016) is used to describe the production and injection wells in the simulator. The wells are controlled by volume rate at surface conditions, *i.e.* specific desired production and injection rates. The Eclipse well option balances the total production and injection values between the wells and the reservoir for the individual grid cells by the “connection transmissibility factor”.

All wells are modelled to be open in the entire reservoir interval, *i.e.* the wells have access to the entire thickness of the individual reservoirs (Karelbo Member, Gassum Formation) as well as the total reservoir interval in some simulation scenarios. The well diameter is arbitrarily set to 0.18 m with a skin factor of 0. Furthermore the wells are modelled as if the tubing head pressure (well pressure at ground level) is at 1 bar, *i.e.* the operation pressure for the plant is not included.

## **Initialisation of the dynamic model**

In the reservoir model the water phase is given properties to simulate the formation water in the area, *i.e.* a density of 1050 kg/m<sup>3</sup>. The initial pressure of the formation water is calculated as hydrostatic (hydrostatic equilibrium) for each grid cell from the density and the depth of the respective grid cell. Density is assumed to vary linearly with depth.

The temperature is calculated for each grid cell from the temperature-depth relation given above (27 °C/km and a surface temperature of 8 °C). It is assumed that the entire reservoir model is in thermal equilibrium.

### **7.1.4 Simulations cases**

A sequence of simulation cases was run, with the objective to evaluate the geothermal productivity potential of the western and eastern localities of the AOI. A well configuration of 2 production wells and 3 injection wells was used (Fig. 7.6).

The well configuration was defined to have a vertical “spud” well in the centre with additional four wells equally spaced around the centre. A well spacing of 1500 m was used for the

productivity evaluation, but simulations with different well spacing and configuration were run in Work Package 3. All 5 wells in a “geothermal unit” are planned to be drilled from the same spud location resulting in a well inclination for the four wells of 40 deg. in order to obtain 1500 m spacing at reservoir level.

A constant production rate of 100 m<sup>3</sup>/h pr. production well and 66.66 m<sup>3</sup>/h pr. injection well was simulated, in order to give a total production/injection of 4800 m<sup>3</sup>/day for the two production wells and the three injection wells. Each location was simulated separately and simulations were run for 25 years with constant production/injection ratios.

For each location the two reservoirs were tested separately (Karlebo Member and Gassum Formation) and added together as a single reservoir.

A simulation was run to check the influence of the Amager Fault zone. The fault zone was simulated to be fully closed, *i.e.* a permeability of 0, or fully open to flow.

A simulation suite with different well spacing and inclination, configuration and operation mode is presented in WP 3 of the present project.

### **7.1.5 Results**

To compare the productivity and injectivity for the two locations the production-/injection-index (WPI) was calculated. The WPI is the ratio between fluid rate and the effective draw-down in the well, and is a measure of the fluid output/input to the reservoir pr. bar applied overpressure to the well. The WPI is a normalized number, which makes it easy to compare the productivity/injectivity for wells operated at different rates

The simulation results for the assessment of the two locations are presented in Figure 7.7 and Tables 7.1, 7.2 and 7.3. Results for the individual reservoir intervals are shown together with results for simulations run for the two intervals added together.

The simulations showed suitable production capacities for both locations with the eastern location being most favorable with higher simulated WPI's. The eastern location has thicker reservoir intervals, which supports a higher WPI. Further, the eastern area in the model was populated with the “Copenhagen” poro-perm model, which is somewhat more optimistic with respect to the permeability.

The relative lower WPI's for the injection wells (approx. half the WPI for the production wells) reflects the influence of viscosity dependency of temperature; in the present setup with an injection temperature of 20 °C and an average production temperature of approx. 55 °C and a viscosity ratio of 0.5.

The temperature profiles for the two locations are similar and no cold-water breakthrough is observed after 25 years of constant production (Fig. 7.8). The eastern location has a higher production temperature due to the larger reservoir depth. The thicker reservoir interval at

the eastern location will be relative more favorable with respect to postponed cold-water breakthrough as the cold-water front is divided over a thicker reservoir interval.

Simulations run with the Amager Fault zone fully closed showed no significant differences relative to simulations with the fault zone open. This was the case for both the western and eastern locations.

The setup of 9 discrete cases to reflect the uncertainty in reservoir properties results in relative widespread simulated WPI values. A box-plot of WPI results for the eastern location is shown in Figure 7.9. It must be stressed that the extreme values are unlikely to be realistic cases, *e.g.* it is unlikely that the entire reservoir will consist of only sandstone in the low porosity and low permeability end or in the high-high end (*cf.* Fig. 7.4).

## 7.2 Productivity evaluation

An evaluation of productivity must be assessed with the constraints and assumptions described in the previous and present chapters. However, reservoir simulation results can help qualify the selection criteria for the two locations. Outcomes of the present simulations include:

- The reservoirs at the eastern location are thicker relative to those at the western location, and with the porosity distribution modelled from the Margrethholm-1 well for both locations, the reservoir net/gross ratio is higher at the eastern location.
- Simulated WPI's are higher at the eastern location. The reservoir thickness and more optimistic poro-perm model (Copenhagen model) compensates for the lower, probably depth related, reservoir porosity and permeability values for the eastern location compared to the western location.
- The reservoirs at the eastern location are situated deeper than at the western location implying that reservoir temperature, and subsequent production temperature, are higher at the eastern location. No cold-water breakthrough was observed for the two locations after the simulated 25 years production/injection period.
- The Amager Fault zone did not influence the simulation results for both locations.
- Overall, the reservoir simulation study shows that the eastern location has the most favorable production and temperature potential.

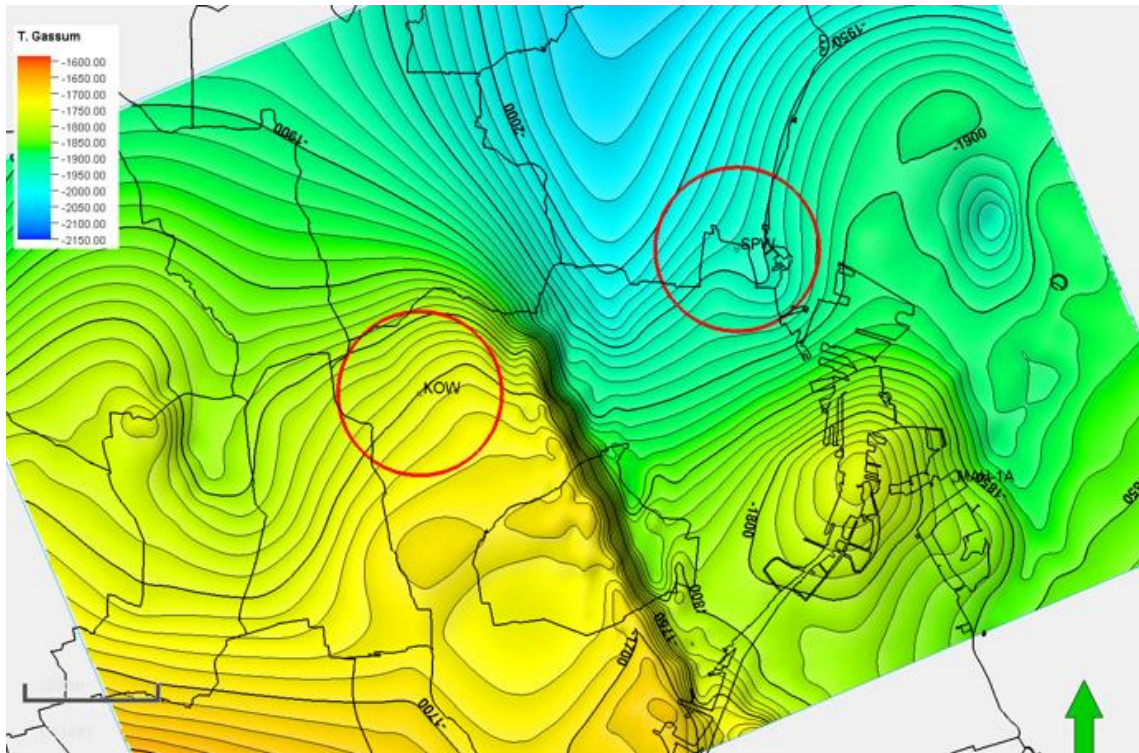


**Figure 7.1.** Model area (AOI) on Top Gassum depth map. An area of 15 km x 20 km was used for the model construction. Red circles enclosing the western (KOW) and eastern (SPW) areas on each side of the Amager Fault zone.

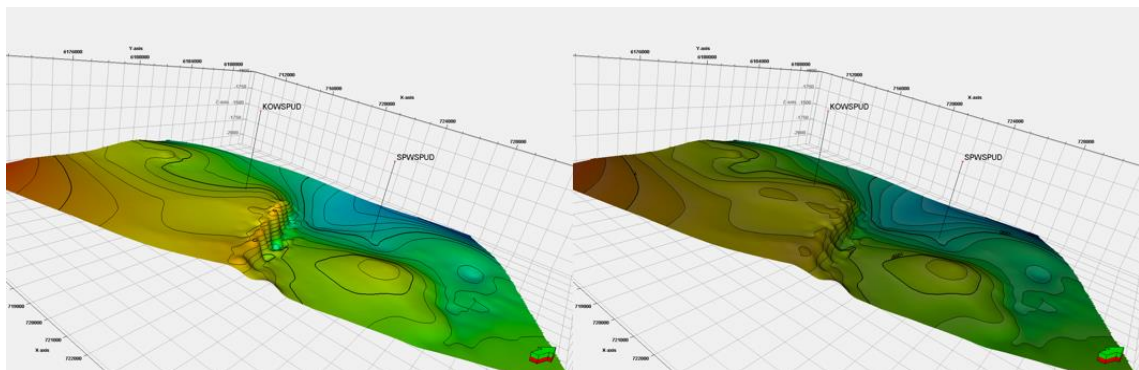


**Figure 7.2.** Top Gassum depth map in 3D view. Left: un-smoothed, Right: smoothed around fault zone.

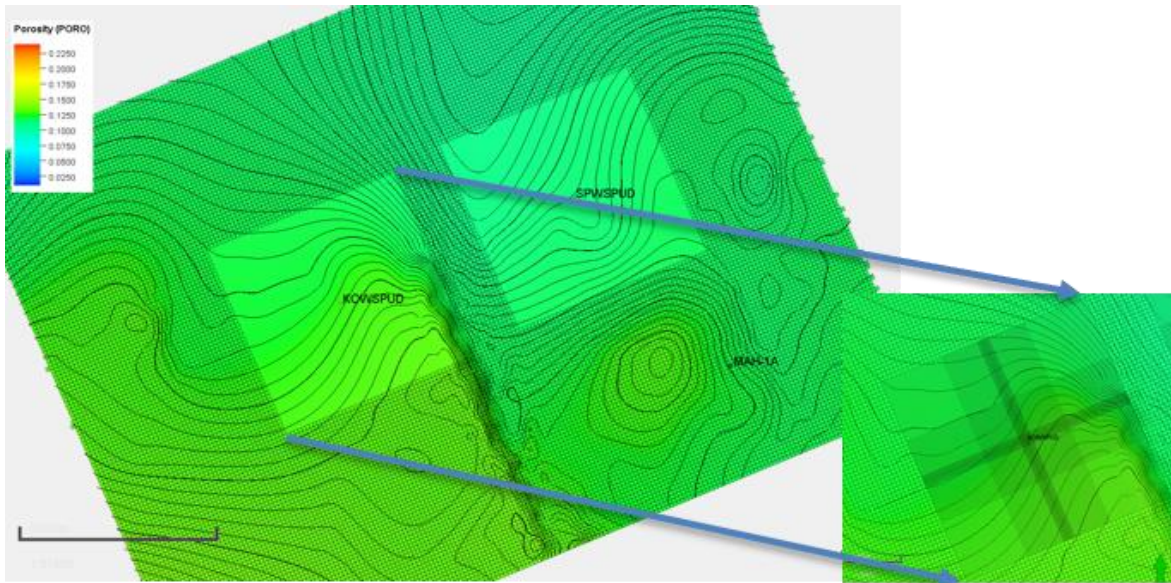


**Figure 7.3.** Grid orientation and local grid refinement (LGR) illustrated for the porosity distribution on the Top Karlebo horizon.

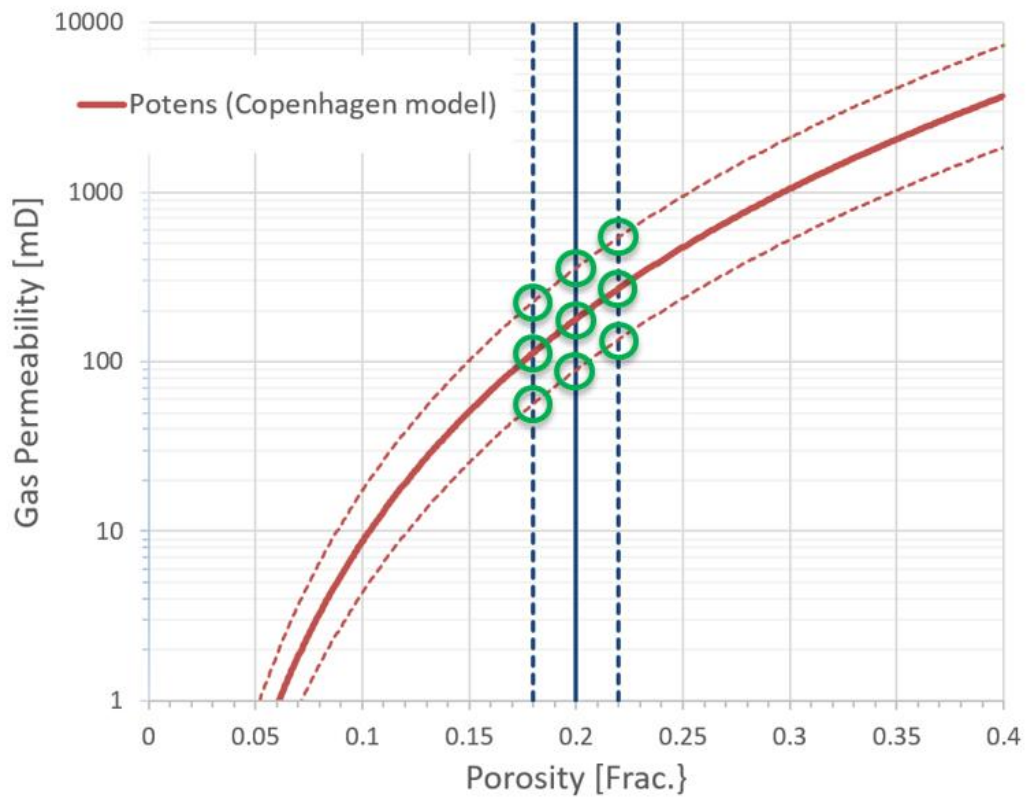


**Figure 7.4.** Uncertainty bands on reservoir parameters. 9 discrete values span the parameters to populate the reservoir model.

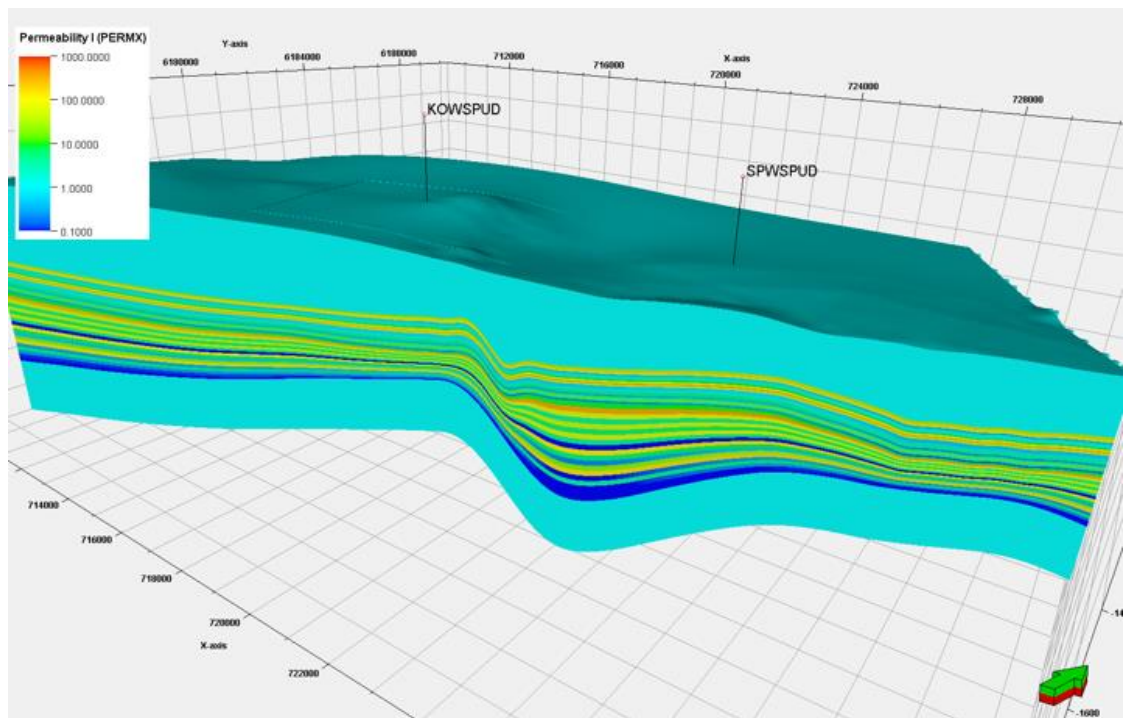


**Figure 7.5.** 3D geological model for the AOI showing the permeability distribution. KOWSPUD and SPWSPUD are the western and eastern spud locations, respectively.

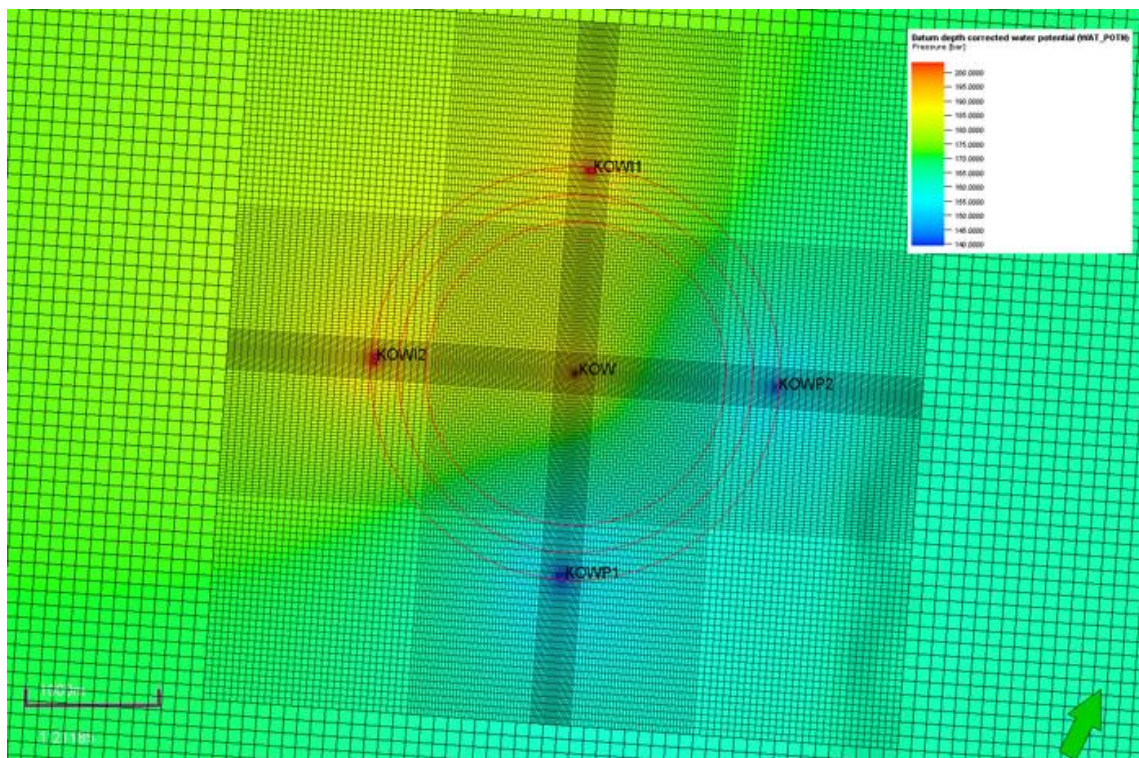


**Figure 7.6.** Well configuration for the western location. Two production wells (KOWP1, KOWP2) and three injection wells (KOW, KOWI1, KOWI2) with a well distance of 1500 m. The map displays the water potential (datum corrected pressure) after 25 years of production and injection.

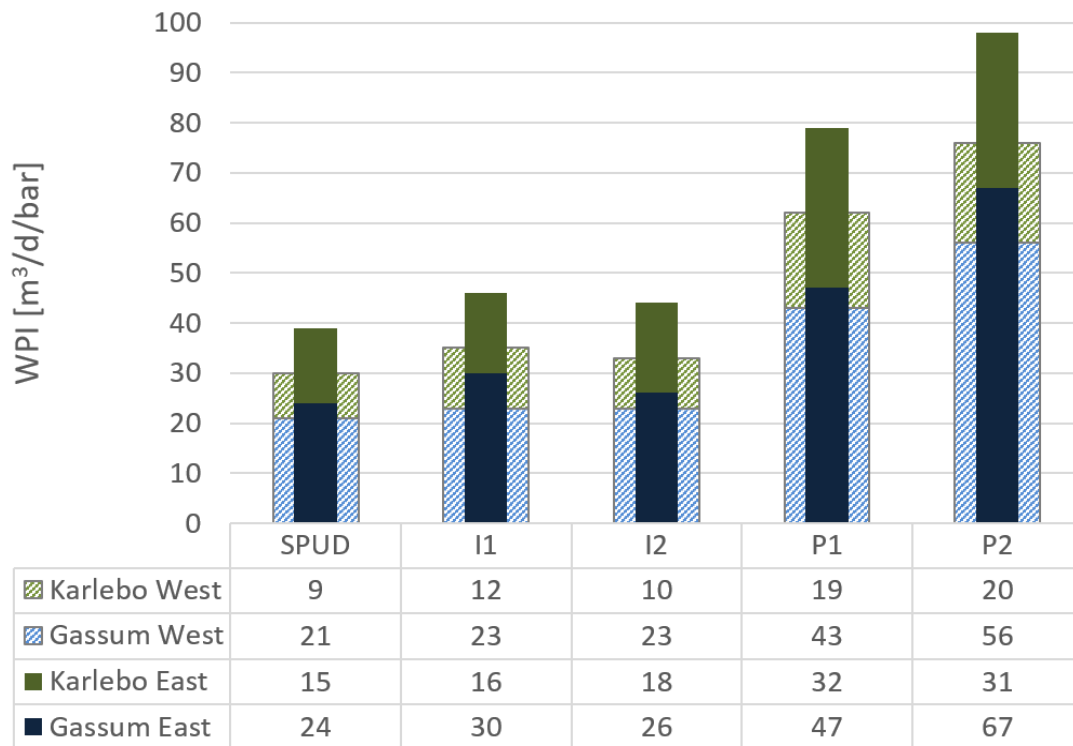


**Figure 7.7.** Simulated WPI's for the two locations. The eastern location has relative higher WPI's, both for the Karlebo Member and the Gassum Formation.

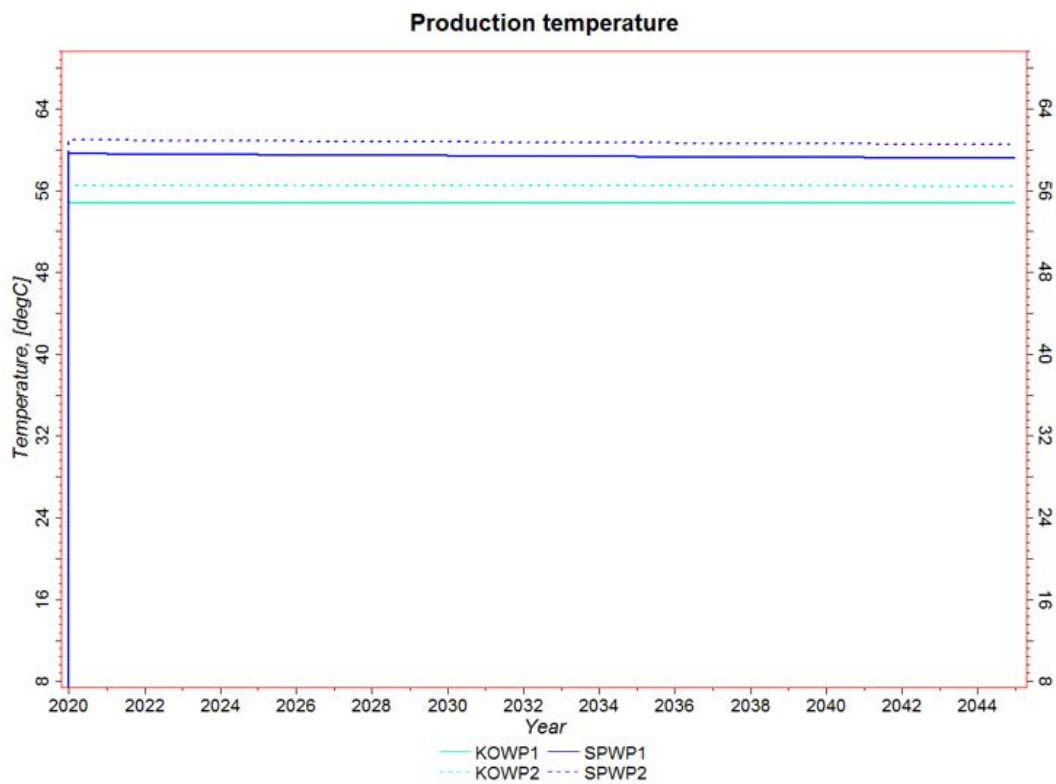


**Figure 7.8.** Production profile for the two locations. No cold-water breakthrough is observed after 25 years of constant production.

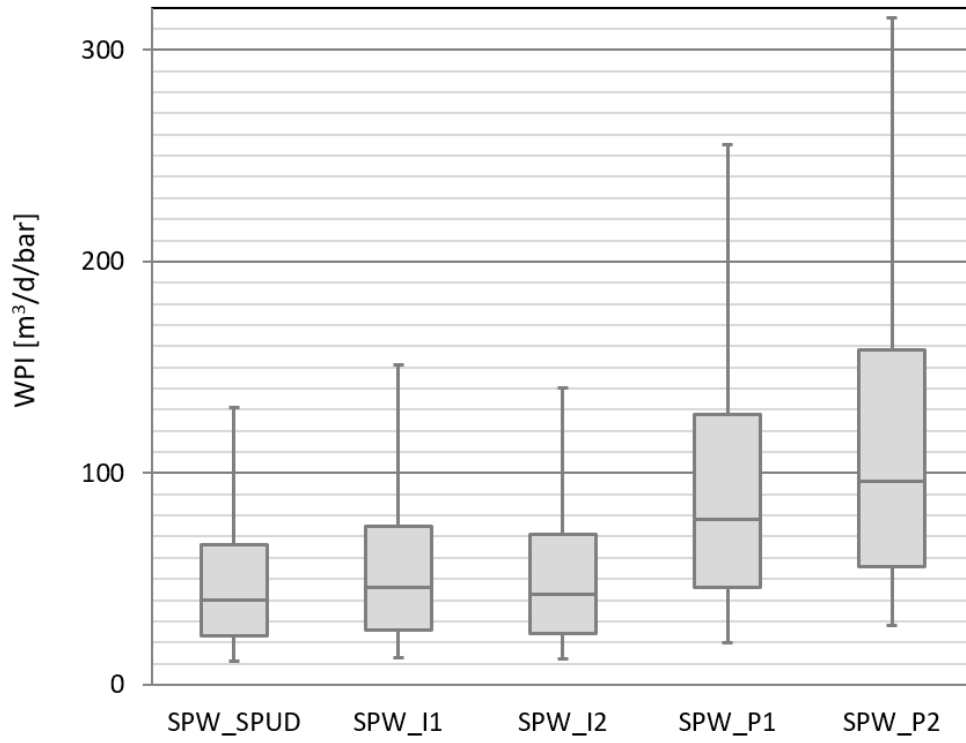


**Figure 7.9.** Box plot for the simulated WPI for the 5 wells at the eastern location.

**Table 7.1.** Simulated production and injection index for the western and eastern locations for the Karlebo Member and Gassum Formation in total. Well spacing is 1500 m. Simulations run with a constant production rate of 100 m<sup>3</sup>/h/well and an injection rate of 66.66 m<sup>3</sup>/h/well, i.e. a total production/injection of 4800 m<sup>3</sup>/d for the 5-spot well pattern.

<b>Location Wells</b>	<b>West (KOW) WPI [Sm<sup>3</sup>/d/bar]</b>	<b>East (SPW) WPI [Sm<sup>3</sup>/d/bar]</b>
Spud well (vertical)	30	40
Injection well 1 (40 deg. dev.)	34	46
Injection well 2 (40 deg. dev.)	32	43
Production well 1 (40 deg. dev.)	62	78
Production well 2 (40 deg. dev.)	76	97

**Table 7.2.** Simulated production and injection index for the western and eastern locations for the Gassum Formation. Well spacing is 1500 m. Simulations were run with a constant production rate of 100 m<sup>3</sup>/h/well and an injection rate of 66.66 m<sup>3</sup>/h/well, i.e. a total production/injection of 4800 m<sup>3</sup>/d for the 5-spot well pattern.

<b>Location Wells</b>	<b>West (KOW) WPI [Sm<sup>3</sup>/d/bar]</b>	<b>East (SPW) WPI [Sm<sup>3</sup>/d/bar]</b>
Spud well (vertical)	21	24
Injection well 1 (40 deg. dev.)	23	30
Injection well 2 (40 deg. dev.)	23	26
Production well 1 (40 deg. dev.)	43	47
Production well 2 (40 deg. dev.)	56	67

**Table 7.3.** Simulated production and injection index for the western and eastern locations for the Karlebo Member. Well spacing is 1500 m. Simulations were run with a constant production rate of 100 m<sup>3</sup>/h/well and an injection rate of 66.66 m<sup>3</sup>/h/well, i.e. a total production/injection of 4800 m<sup>3</sup>/d for the 5-spot well pattern.

<b>Location Wells</b>	<b>West (KOW) WPI [Sm<sup>3</sup>/d/bar]</b>	<b>East (SPW) WPI [Sm<sup>3</sup>/d/bar]</b>
Spud well (vertical)	9	15
Injection well 1 (40 deg. dev.)	12	16
Injection well 2 (40 deg. dev.)	10	18
Production well 1 (40 deg. dev.)	19	32
Production well 2 (40 deg. dev.)	20	31

## 8. Mineral composition of mudstones

### 8.1 Introduction

Certain minerals, especially clay mineral of the smectite group may cause problems during drilling, e.g. due to swelling of clay particles (see Chapter 9). The purpose of the investigation was to examine whether certain mudstone levels within the Gassum Formation, the Karlebo Member and the overlying parts of the Fjerritslev Formation contain smectite, and also to estimate how much the mineralogical composition of the mudstones varies within and between the lithostratigraphic units. Furthermore, it has been an object to examine whether the mudstone lithologies changes systematically from the marginal parts to the central parts of the Danish Basin. The investigation is based on X-ray diffraction only.

The mineralogical composition of the mudstones has been examined in two sets of analyses: bulk-mineralogy (95 analyses) and clay mineralogy (31 samples). Most of the samples are cuttings, but a few core samples from the Stenlille wells have been included. The samples are located relative to the lithological logs of the Margretheholm-1, Karlebo-1A, Kvoles-2A, Stenlille-1 and Stenlille-2 wells (Figs. 8.1–8.4 and Enclosure 2). The samples for bulk mineralogy are either bulk samples or samples of picked mudstone cuttings. The bulk mineralogy has been determined from powdered, but otherwise untreated samples. The method is quick, qualitative and, at best, semi-quantitative. It has been used as a screening, in order to choose the most suitable samples for the clay mineral analysis. In contrast, the identification of clay minerals requires a careful and time-consuming treatment of the samples. Consequently, a much lower number of samples was analysed for their clay mineralogical composition. In a few cases, samples were analyzed for their clay mineralogy without a preceding analysis of their bulk mineralogy.

The graphic presentation of the analyses shows that the mineralogical composition is fairly uniform from the Gassum Formation, through the Karlebo Member and up into the overlying parts of the Fjerritslev Formation (Figs. 8.1–8.4).

### 8.2 Methods

#### 8.2.1 Bulk mineralogy

The bulk mineralogy was determined on samples (mostly cuttings) that were crushed to a powder <0.125 mm and analysed. It is assumed that the grains are randomly oriented when measured. Minerals, which are present in small amounts (less than c. 5%) may not be detected in the powdered samples, because their peaks cannot be distinguished from the background.

The minerals identified in the powdered samples include quartz, feldspars (microcline and albite), phyllosilicates with basal reflections at 7Å, 10Å and 10–14Å, pyrite, gypsum, and carbonate minerals such as calcite, siderite, and ankerite. Some samples contained ‘exotic’ minerals such as barite and sylvite, which are probably additives to the drilling mud.

The samples analysed for bulk-mineralogy are listed in a table in Appendix 6. The table shows that the samples are mostly of two types: either bulk-samples (a fraction of the entire amount of cuttings from a certain depth) or a sample of picked mudstone cuttings. The latter provide better data on the mudstones, especially in samples with high contents of quartz sand or caving. The mudstones themselves contain large amounts of quartz, most of which is probably silt-sized. At certain depths two or more subsamples were analyzed.

## 8.2.2 Clay mineralogy

Identification of the clay minerals involves removal of organic matter, Fe- and Al-oxides and hydroxides, separation of the clay-sized minerals from the coarser particles, and saturation of the clay minerals with ions of known size (Mg and K). Following the last step the clay minerals are suspended in distilled water. One to two drops of the suspension are placed on a glass slide and are left to dry at room temperature. The clay minerals settle parallel to the glass. One of the Mg-saturated subsamples is treated with glycerol, which expands the lattice of smectite, if present. Two of the K-saturated subsamples are heated to 300 °C (which causes smectite and vermiculite to collapse) and to 550 °C, which destroys kaolinite. The sum of informations from these, variously treated subsamples allow identification of the clay minerals (Table 8.1). Thirty samples were analyzed for their clay mineral content (Figs. 8.1–8.4).

**Table 8.1.** Basal reflections of various clay minerals.

	Smectite	Vermiculite	Mixed layer minerals	Illite, mica	Chlorite	Kaolinite
Subsample	Basal reflection, Å					
Mg-saturated, glycerol	18	14	10-14	10	7	7
Mg-saturated, air dried	14	14	10-14	10	7	7
K-saturated, air dried	14	14	10-14	10	7	7
K-saturated, 300°C	10	10	10	10	7	7
K-saturated, 550°C				10	7	

## **8.3 Results**

### **8.3.1 TOC content**

The mudstone samples contain varying amounts of organic matter. This is removed, along with Fe- and Al-oxides and hydroxides prior to isolation of the clay minerals. Data on the TOC content in the Kvols-1 well are shown in Fig. 8.5. The TOC-values are very uniform, 1 wt. %, except for a narrow interval in the top of the F-III Member (Michelsen 1989).

### **8.3.2 Silt content**

In the samples analyzed for clay minerals the amounts of particles larger than clay (>0.002 mm) were determined (Table 8.2). As the samples had been crushed to <0.125 mm, it may be concluded that the coarser particles represent silt and very fine-grained sand.

**Table 8.2.** *The clay content is less than 50 wt. % in most samples analysed for clay minerals. This indicates silt and very fine-grained sand constitutes approximately 50 wt. % of the mudstones.*

	Lithostratigraphy	Depth m	Clay content, after removal of TOC and oxides wt. %
Margretheholm-1			
	Fjerritslev Fm	1655	40
	Fjerritslev Fm	1680	50
	Fjerritslev Fm	1700	63
	Karlebo Mb	1747.5	28
	Karlebo Mb	1792.5	23
	Karlebo Mb	1817.5	49
	Karlebo Mb	1837.5	28
	Gassum Fm	1870	33
	Gassum Fm	1920	42
	Gassum Fm	1980	46
	Gassum Fm	2055	42
Karlebo-1A			
	Fjerritslev Fm	1875	51
	Fjerritslev Fm	1895	57
	Fjerritslev Fm	1920	56
	Fjerritslev Fm	1945	50
	Karlebo Mb	196.5	45
	Karlebo Mb	2047.5	38
	Gassum Fm	2107.5	
	Gassum Fm	2142.5	55
	Gassum Fm	2195.5	52
	Skagerrak Fm	2250	49
Kvols- 2A			
	Fjerritslev Fm	2160	43
	Fjerritslev Fm	2240	46
	Fjerritslev Fm	2360	44
	Fjerritslev Fm	2440	26
	Fjerritslev Fm	2480	43
	Fjerritslev Fm	2520	42
	Fjerritslev Fm	2550	45
Kvols-1			
	Fjerritslev Fm	2323	43
	Fjerritslev Fm	3271	44
	Fjerritslev Fm	2420	45

### 8.3.3 Bulk mineralogy

The bulk mineralogy is dominated by detrital minerals, but includes also minerals formed during diagenesis.

**Quartz**, the dominant mineral in all samples.

**Feldspars**, varying, but generally small amounts of feldspars (microcline and albite) are present in most samples. The feldspar content is highest in Margretheholm-1 (Fig. 8.1 compared to Figs. 8.2–8.4) This may suggest a different provenance, or that Margretheholm-1 represent a position closer to the coastline.

**Kaolinite** is present in most samples. Kaolinite is probably both detrital and diagenetic. In the bulk-mineral analyses the peak at 7Å may represent both kaolinite and chlorite. However, chlorite has not been identified in the clay mineral analyses.

**Mica and/or illite:** Muscovite is seen in some of the mudstone cuttings, and is probably detrital. Illite may be present as well (both minerals have a basal reflection of 10Å).

**Pyrite** is present in some mudstone samples in small amounts. It may be present, but below detection level, in additional samples.

**Gypsum** is seen as tiny aggregates on cuttings, especially from Kvals–1. Gypsum often forms from oxidation of pyrite.

**Calcite** is present in some samples in small amounts. Some cuttings contain fragments of fossils.

**Siderite** is common as a diagenetic mineral in the mudstones, possibly precipitated as concretions. Its presence is established in subsamples of red-brown cuttings. Siderite is recorded in most samples from Margretheholm-1, but is generally below detection level in the samples from Kvals-1, -2A (Figs. 8.1, 8.3).

**Ankerite** is present in small amounts in few samples, and is also interpreted as formed during diagenesis.

The bulk-mineralogy has not been quantified, but the relative amounts of the minerals are indicated in Figures 8.1–8.4. Comparison of the samples show that they all have high contents of quartz and kaolinite, smaller amounts of mica/illite, and varying, but small amounts close to the detection limit, of feldspars, pyrite and carbonates.



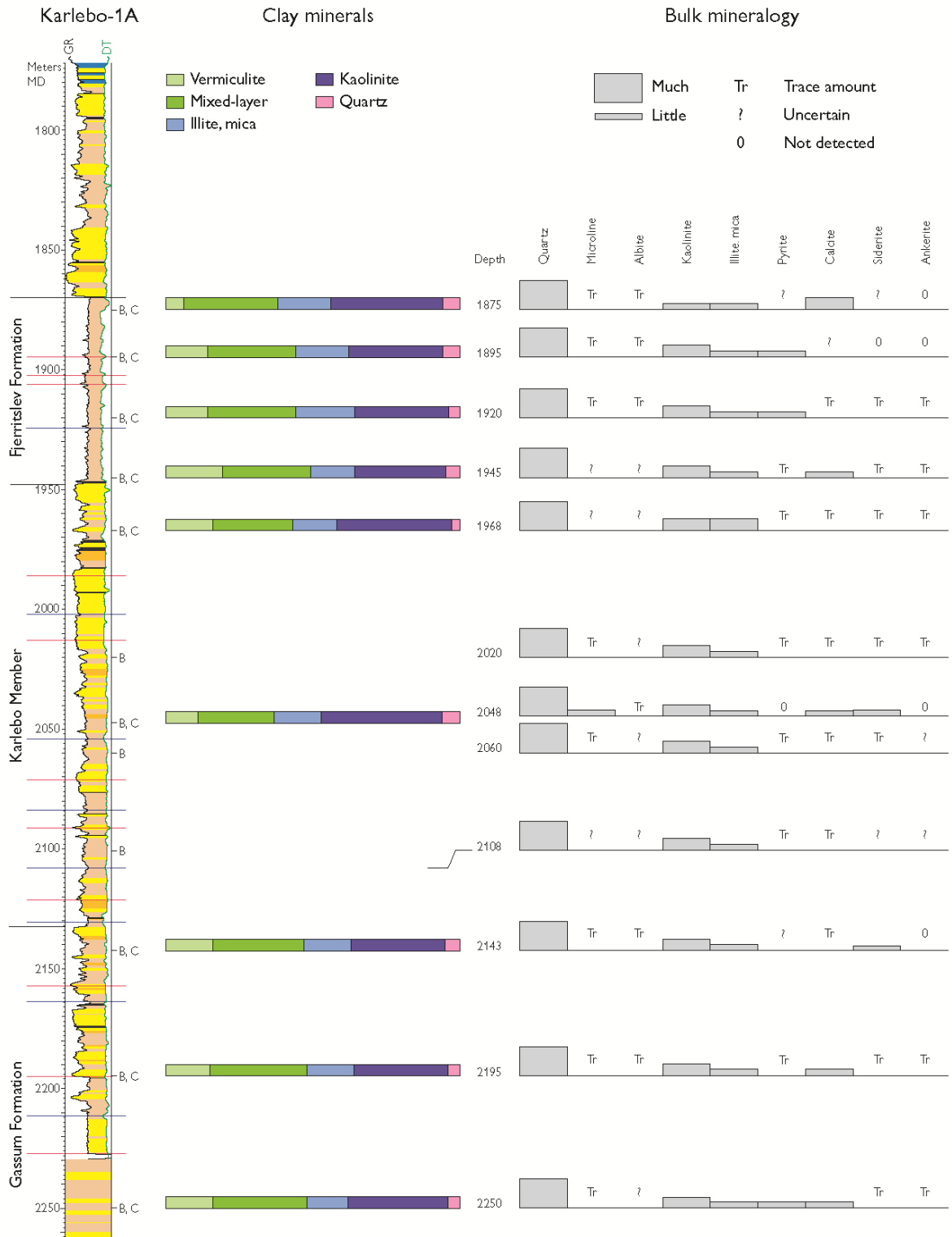


Figure 8.2. Bulk mineralogy, and clay minerals from Karlebo-1A.

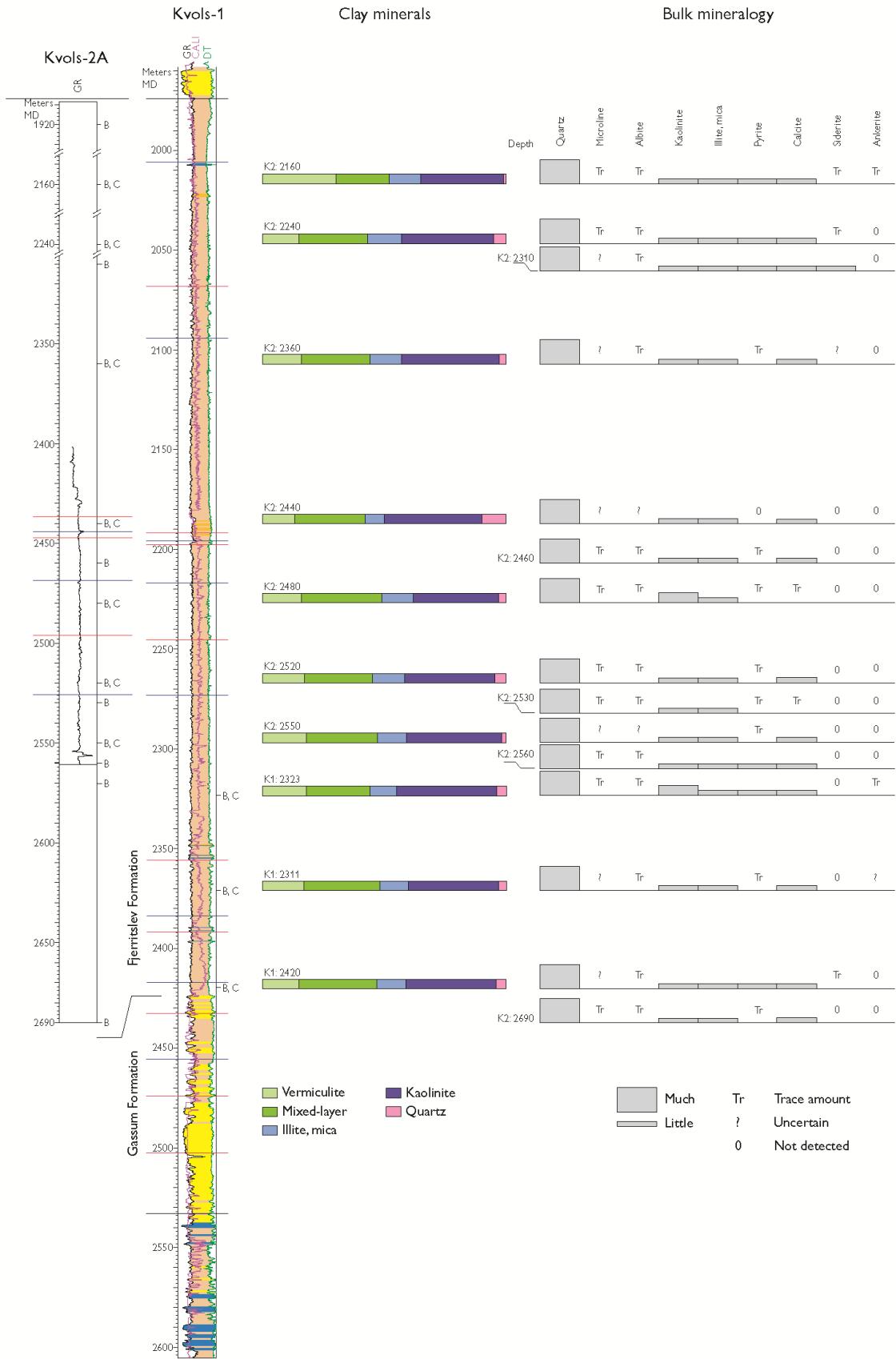


Figure 8.3. Bulk mineralogy, and clay minerals from Kvals-1, -2A.

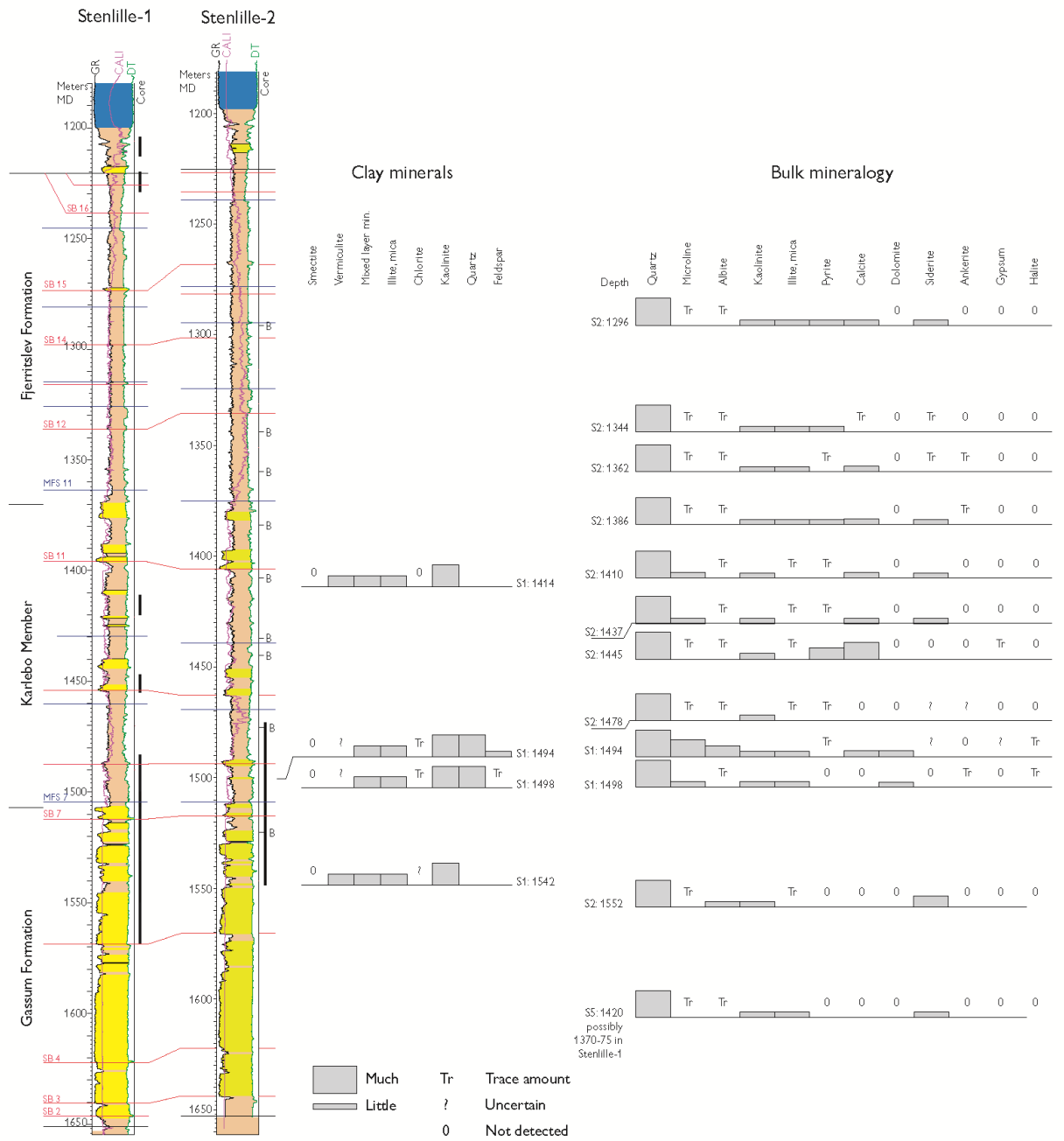


Figure 8.4. Bulk mineralogy, and clay minerals from Stenlille-1, -2.

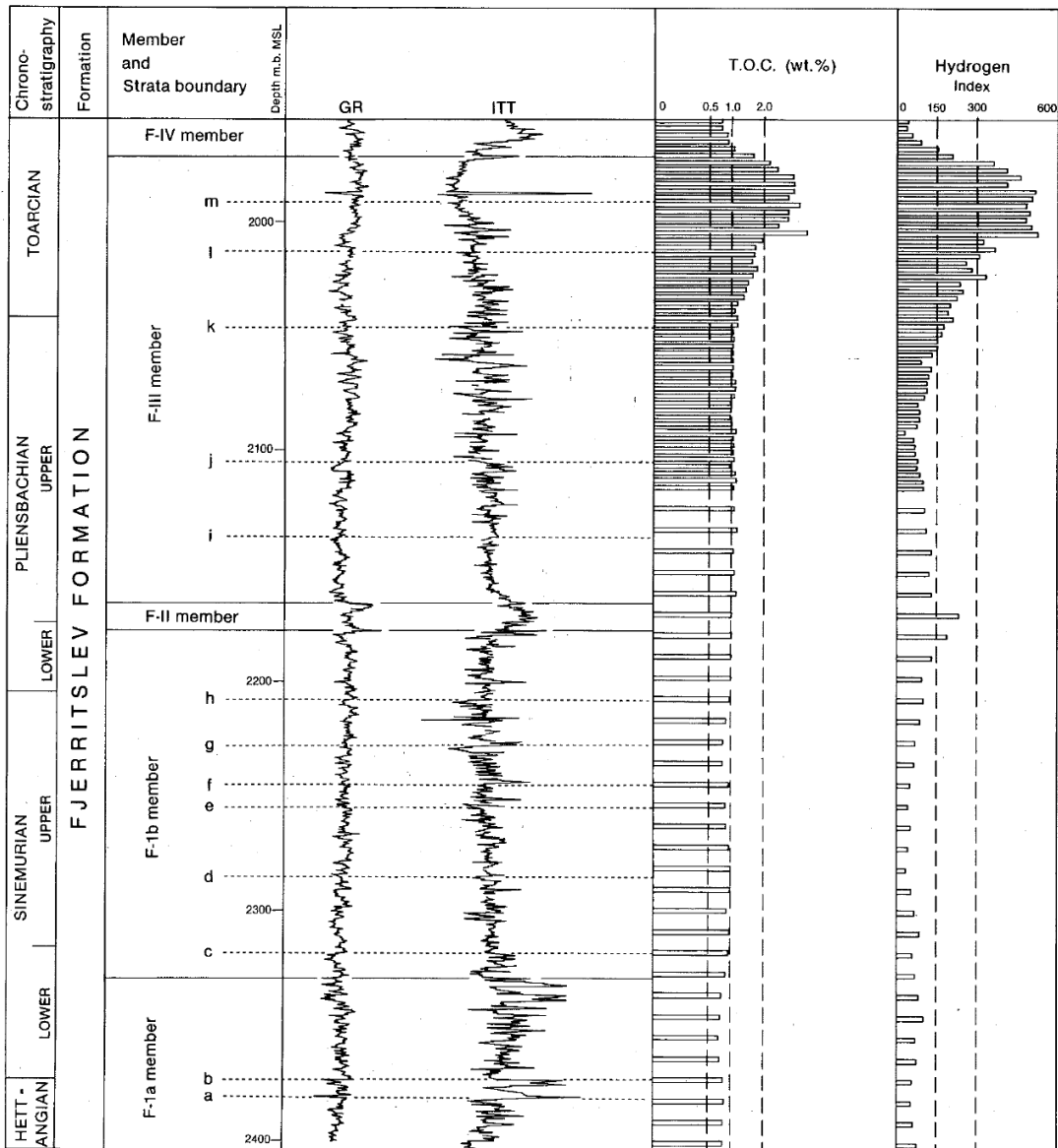


Figure 8.5. TOC-contents and Hydrogen index (HI) for samples from Kvoles-1 (Michelsen 1989).

### 8.3.4 Clay mineralogy

The clay mineral assemblages are very uniform in the Gassum and Fjerritslev formations (Figs. 8.1–8.4).

**Smectite** is not detected in any of the samples

**Vermiculite** is present in small to moderate amounts in all samples.

**Mixed-layer minerals** are present in large amounts in all samples. The terms interlayering, mixed-layering, or interstratification describe phyllosilicate structures in which two or

more kinds of layers occur in a vertical stacking sequence along the C-axis. Phyllosilicate layers are strongly bonded internally but rather weakly bonded to each other. Consequently, layers with different internal arrangements can stack together. Interstratification can be random, ordered or partially ordered (Reynolds 1980). The mixed-layer minerals in the Gassum and Fjerritslev formations have basal reflections of 10–14Å, and collapse to 10Å after heating to 300 °C. This indicates that the 14Å component is either smectite or vermiculite (not chlorite). As they are also unaffected by the treatment with glycerol, it is most likely that they may be described as an interstratification of vermiculite and illite/muscovite. Such mixed-layer minerals are known from the literature.

**Kaolinite** is the dominant clay mineral in all the samples. Kaolinite may be both detrital and diagenetic. Beautiful examples of diagenetic kaolinite are known from sandstones in the Gassum Formation, especially at great burial depths, and has also been identified in minor amounts in thin section analysis of sandstones in the present study (see section 6.1).

**Quartz** is present in very small amounts in nearly all samples.

Figures 8.1–8.3 show that the variation in clay mineralogy within each well is small. Margrethholm-1 has low contents of vermiculite and high contents of kaolinite and mica/illite, and the difference between the Gassum and the Fjerritslev formations is negligible. In Karlebo-1A the Fjerritslev Formation above the Karlebo Member has slightly more vermiculite, and less kaolinite than the underlying samples. In Kvols-1, -2A the clay mineral assemblage is remarkably uniform. Generally the content of vermiculite is relatively large, whereas the amounts of kaolinite and mica/illite are relatively small. The uppermost sample deviates from this pattern by its high content of vermiculite, lower contents of mixed-layer minerals and kaolinite, and its negligible amount of quartz.

Kaolinite and mica may form coarser particles than vermiculite. The relatively higher contents of kaolinite and mica/illite in the samples from Margrethholm-1, may reflect the palaeogeographical position closer to the margin of the Danish Basin. The higher content of vermiculite in the samples from Kvols-1, and -2 may reflect a longer transport to the central parts of the basin. Karlebo-1A appears to be intermediary between Margrethholm-1 and Kvols-1, -2A.

## 8.4 Discussion

### **Problems encountered during drilling**

Problems during the drilling of wells through the Lower Cretaceous, Jurassic and Upper Triassic successions, as reported in completion reports, are summarized for selected well in Appendix 7. The completion reports describe problems caused by 'water-washable claystone', 'sticky parts' and 'tight spots' in the Fjerritslev and Gassum formations. It is not clear, however, if these problems are caused solely by the lithologies (especially the clay minerals) or other factors. For instance, high angles of deviation of the borehole may cre-

ate difficulties as may the use of unsuitable drilling mud which may cause caving or collapse of the borehole.

Inspection of cuttings in the present investigation showed the presence of friable sandstones as well as large amounts of loose sand grains, which suggests that the sandstones may also present difficulties during drilling.

#### **The significance of the quartz content in the mudstones**

Many of the samples of picked mudstone cuttings have quartz and kaolinite as the most common minerals. Neither of these minerals contains radioactive elements, such as K, Th and U, and is therefore 'invisible' on the gamma log, and may be interpreted as 'sand' if the interpretation is based on the gamma ray log only. In the present study, other log data has been added to the gamma ray log in the interpretation of the penetrated lithology (see section 6.3).

### **8.5 Main results**

The bulk-mineralogy of the mudstones changes little through the Gassum and Fjerritslev formations, and the variations are most obvious for minerals occurring in small amounts or trace amounts (feldspar, pyrite and various carbonates).

The clay mineralogy has been determined qualitatively and semi-quantitatively for 30 samples. The following clay minerals are present (in decreasing amounts) in all samples: Kaolinite, mixed-layer minerals, vermiculite and illite/mica. Smectite and chlorite has not been detected in any of the samples.

The clay mineral assemblage varies surprisingly little through the Gassum and Fjerritslev formations.

## **9. Formation damage control**

### **9.1 Introduction**

Formation damage is a well-known and unwanted phenomenon in geothermal as well as oil bearing reservoirs. Formation damage reduces the productivity of the reservoir leaving the exploitation of the reservoir unfeasible. Therefore, formation damage assessment, control and remediation are among the most important issues to be resolved for efficient exploitation of geothermal as well as oil bearing reservoirs (Civan 2007).

The aim of this literature study is to give a short introduction to formation damage and an overview of the possible measures to formation damage control. The focus will be on geological related formation damage and –control in geothermal reservoirs.

### **9.2 Formation damage**

Formation damage can be defined as any reduction in near wellbore permeability which is the result of any well intervention such as drilling, completion, production, injection and attempted stimulation (Byrne 2010, Civan 2007). It is typically caused by invasion of foreign-fluids, e.g. fluids used during drilling or completion of the well and workover operations (Civan 2007). These fluids may interact with primarily the diagenetic clay minerals present in the reservoir leading to permeability reduction. There are principally two different processes by which the interaction between the fluids and the clay minerals may lead to formation damage in clayey sedimentary formations:

#### **9.2.1 Clay swelling**

In swelling clays, such as smectites and mixed-layer clays, the negative charged clay platelets are held together by the presence of cations in the interlayer (de Siqueira et al. 1999, Xu et al. 2006). When exposed to low ionic strength aqueous solutions, the interlayer cations adsorb water molecules from the aqueous solution and form thick envelopes of water films over the clay platelets (Chilingarian & Vorabutr, 1981, Xu et al. 2006) thereby increasing the volume of the clay minerals significantly. The swelling clays may reduce formation permeability not only by reducing the porosity but also by disintegration, migration and plugging of pore throats (Civan 2007). The swelling of clay particles occurs when the clay is exposed to aqueous solutions having a brine concentration below a critical salt concentration (Khilar & Fogler 1983). Thus, clay swelling is controlled primarily by the composition of the aqueous solutions with which the clay comes into contact (Zhou 1995).

### 9.2.2 Fines migration

Migration of fine grained minerals, primarily kaolinite, and subsequently plugging of the pore throats may reduce the formation permeability (Khilar & Fogler 1984, Rosenbrand et al. 2005, Bedrikovetsky & Caruso 2014). The fines are not restrained by the confining pressure and are under certain conditions mobile to move with the fluid phase. The mobility of the fines is controlled by the forces acting on the particles, primarily the attractive van der Waals forces and the repulsive electrostatic forces. At "high" salt concentrations, the van der Waals forces are sufficiently large to keep the fines attached to the pore surfaces. However, at decreasing salinity fewer ions are present in the brine to shield the negative charge on the surface of the pores and fines, and the repulsive electrostatic forces increase. At a critical salt concentration the repulsive electrostatic forces exceed the attractive van der Waals forces and the fines are released from the pore surfaces (Khilar & Fogler 1984). Thus, if a water-sensitive sandstone is exposed to brine with a salinity below the critical salt concentration, fines are released, and significant reductions in permeability are observed. Fines migration can also be induced when the fluid velocity is above a critical velocity (Gruesbeck & Collins 1982, Sharma & Yortsos 1987, Sharma et al. 1992, Das et al. 1995, Freitas & Sharma 1997). Furthermore, at high pH values fines may be generated in the presence of alkali hydroxide by the alteration of kaolinite to dickite, nacrite and halloysite through chemical oxidation (Hayatdavoudi 1998).

Previously it was believed that clay swelling was the primary cause of formation damage (Civan 2007). However, now it is well accepted that formation damage in sandstones is more commonly the result of fines migration and only rarely of swelling clays (Jones 1964, Mungan 1965, Khilar & Fogler 1984, Rosenbrand et al. 2015, Bedrikovetsky & Caruso, 2014).

Geological related formation damage, i.e. clay swelling and fines migration, may thus be induced by any operation that introduces "low" salinity fluids into the reservoir, fluids with "high" (>9) pH or by "high" flow rates in the near wellbore region. Examples of operations at geothermal plants that may cause formation damage include loss of freshwater-mud filtrate or completion fluid to the formation during drilling and completion of the wells, and high well production rates (rates above the critical velocity).

Injection of the clear, cooled brine during production will typically not cause formation damage due to clay swelling or fines migration (Schembre & Kovscek 2005, Holmslykke et al. 2016). However, injection of the brine may still cause formation damage, mainly due to the introduction of particles formed by processes in the geothermal surface loop, e.g. scaling due to degassing, corrosion, oxygen contamination, or addition of incompatible chemical additives and inhibitors (Seibt & Kellner 2003, Ungemach 2003). The generated particles may form filter cakes or plug the pores in the reservoir. This is considered the greatest threat of formation damage in geothermal wells (Seibt & Kellner 2003, Ungemach 2003).

### 9.3 Formation damage control

Formation damage is not necessarily reversible (Porter 1989, Civan 2007) and therefore it is better to prevent formation damage than to try to restore it. Also, there is a risk that remedial treatments may cause other types of damages. When the formation damage is limited to the region very close to the wellbore, the damage may to some extent be circumvented e.g. by acid treatment or hydraulic fracturing. However, the near wellbore damage is more challenging to restore (Bennion 1999).

Clay swelling and fines migration may be prevented by the presence of clay stabilisers in the injection fluids, as described below (Civan 2007):

**Inorganic cations:** As mentioned above, clay stabilisation may be accomplished by maintaining the aqueous solution salinity above the critical salt concentration. This may be achieved either by applying the reservoir brine or by addition of certain ions in the injection fluids (Keelan & Koepf 1977).

**Cationic Inorganic Polymers:** Reduces the cation exchange and are applicable in non-carbonate-containing sandstones. The formation should be retreated after acidizing (Himes et al. 1991). Examples of cationic inorganic polymers are hydroxyl aluminium and zirconium oxychloride.

**Cationic Organic Polymers:** May permanently stabilise clay (especially smectite clays) and control fines and sand in sandstone as well as carbonate formations. The organic polymers may be applied in acidizing and fracturing treatments. The polymers are, however, high molecular weight and long chain polymers with molecular sizes comparable with some pore size fractions in porous rock. Therefore there is a risk that they will plug the pore throats and thereby cause permeability damage. Their applicability in tight formations is therefore limited to low concentrations (Himes et al. 1991).

**Oligomers:** Oligomers are low-molecular weight, cationic, organic molecules having an average of 0.017  $\mu\text{m}$  length (Himes et al. 1991). The polymers prevent fines migration by coating over the pore surface and blocking the clay particles. The low-molecular-weight polymers have comparable stabilizing capability to high-molecular-weight polymers and are more advantageous because they cause less treatment-induced permeability damage (Zaitoun & Berton 1996).

**pH-Buffer-Solutions:** The alteration of kaolinite to dickite, nacrite and halloysite may be prevented by buffering the pH of brines to 8 or below and avoiding aeration of injected (Hayatdavoudi 1998).

**Chemical alteration of clay with KOH:** The chemical structure of the clay minerals can be permanently transformed to non-damaging types by reaction with KOH. KOH causes the divalent ions in the reservoir brine to form damaging precipitates and these ions should therefore be removed from the region in the reservoir that is to be treated before the treatment with KOH. KOH is very corrosive and damaging and therefore treatment with KOH should only be performed when the well material and conditions are suitable (Civan 2007).

Despite exhaustive research and development efforts, particularly within the oil and gas industry, the cost-effective mitigation of formation damage is still not straightforward. This is mainly due to the fact that the damaging potential of a particular fluid depends on the particular site-specific application and the formation in which the well is completed. Thus, a universal nondamaging fluid does not exist (Civan 2007).

Most formation damage can be minimised through the understanding of the formation damaging mechanisms and the response of the reservoir to various well interventions (Byrne 2010, Civan 2007). To minimise formation damage it is therefore recommended to make a thorough investigation of the geological, geohydraulic and geochemical parameters of the reservoir as well as the procedures for drilling and completion of the wells and the design of the surface loop. An important task in the investigation is conduction of laboratory and field tests e.g. to test how the reservoir responds to different drilling and completion fluids (Ungemach 2003, Civan 2007). The overall aim of the investigation is to gain knowledge of the geological and geochemical conditions in the reservoir to identify potential formation damaging processes at any step in the construction and operation of the geothermal plant. This will enable the selection of the optimal planning, construction and operation of the geothermal plant (Seibt & Kellner 2003, Civan 2007).

Tague (2000a,b,c,d) have proposed a systematic and comprehensive approach for the investigations required to ensure the mitigation of formation damage in petroleum reservoirs. This methodology may also be applicable for geothermal plants and includes:

### **9.3.1 Identification of formation damage**

Includes investigation and identification of the potential sources and mechanisms affecting formation damage and is the most important task since the findings may critically affect the actions to be taken in the remaining tasks. Tague (2000a,b,c,d) recommends a life-cycle investigation and monitoring approach for determination of the potential damage mechanisms that are effective during the course of the various phases of the wells. These phases involve:

*Characterisation of the reservoir depositional environment:* E.g. information about the reservoir formation (mineralogy, grain size and sorting, and cementation) and properties of the brine and the externally introduced fluids used for various purposes such as drilling fluids.

*Damage caused by well-drilling practices:* The various drilling procedures are reviewed and the prevailing damage mechanisms due to drilling of the wells are identified.

*Damage caused by well-completion methods:* Well-completion practices may frequently lead to significant formation damage problems due to the use of completion fluids that are incompatible with the formation leading to clay swelling and migration problems and the insufficient removal of filter cakes from wells completed with tight liners.

*Damage caused by reservoir-production schemes:* It may be difficult to identify and control the production-related damage mechanisms such as those induced by fines migration and scaling since this requires the accurate description and understanding of the rock-fluid-particle interactions by various processes coupled with the transport of the fine particles and fluids through the reservoir.

*Damage caused by well-intervention practices:* Improperly conducted well-intervention practices may lead to various formation damage problems such as corrosion products, mineral dissolution and subsequent re-precipitation.

### **9.3.2 Quantification of reservoir formation damage**

Refers to the assessment of the formation damage effects on injectivity of wells in terms of type, degree, and location. This may be accomplished by means of one of the following methods or a combination of them:

*Production data comparison:* May help determine a damaged well.

*Well-testing and pressure transient data analysis:* Analysis and interpretation of the pressure transient data measured by well testing may provide critical information required for formation damage quantification. However, pressure transient analysis cannot distinguish among the multiple mechanisms involved in formation damage. Therefore, resolution is only possible through supplementing the pressure transient analysis with other approaches, including model-assisted (Civan 2007) and laboratory testing of core samples with fluids involved in reservoir exploitation (Tague 2000a,b,c,d).

*Laboratory testing:* Examples of laboratory tests may include flooding reservoir cores samples with damaging fluids under in situ pressure, temperature and stress condition. The outcome of the laboratory testing may provide the critical information and insights essential for accomplishing the task of identifying the governing formation damage mechanisms.

*Wellbore examination:* The information obtained from downhole video images and production logs may be utilised to infer about the effect of formation damage on the productivity or injectivity of wells. Downhole video images may help determine the type and nature of damage, such as caused by fine particle and precipitation.

### **9.3.3 Remediation of formation damage**

Remediation refers to all measures taken or treatment of damaged wells for restoring an optimal performance. Successful implementation and realization of effective treatment strategies for removal of various types of damages require a three-step approach:

*Treatment selection and design:* Treatment selection and design suitable to remove formation damage is a difficult task and any mistakes made at this attempt may not be readily correctable in the field. There are several treatment methods available, including mechanical, solvent, acid, and thermal treatments (Tague 2000a,b,c,d, Dusseault et al. 2002) and each should be reviewed carefully to address the damage mechanisms identified and quantified in the previous tasks.

*Treatment field testing:* Field testing of remediation treatments prior to routine field-wide applications in other wells in a given field is recommended. Such test should include: 1) a multivariate statistical analysis of the experimental data obtained from field testing 2) determination of the variables most affecting the remediation treatments 3) examination of the downhole video images of the well before and after the treatment 4) refinement and optimisation of an effective treatment type and its application procedure.

*Routine field-wide treatment applications:* Routine field-wide treatment applications: A damage remediation protocol and program for routine applications in a given field should be developed.

### **9.3.4 Prevention of formation damage**

It may be possible to minimise the formation damage in the reservoirs by taking proper measures based on the understanding of the behaviour of the rock-fluid-particle system during flow through the reservoir formation under varying in situ conditions (Civan 2007).

Minimising formation damage requires application of the least-intrusive well drilling and completion procedures combined with the optimisation of the design and operation of the geothermal plant. This can be accomplished by a combination of understanding the behaviour and response of the reservoir formation, fluid and particles under varying conditions with model-assisted analysis and interpretation of properly designed laboratory and field tests.

Tague (2000a,b,c,d) recommends that all personnel involved in field operations is trained in formation damage. The benefits of the training is that the personnel will 1) gain general knowledge about reservoir formation damage 2) understand and become familiar with the procedures applied to prevent and mitigate formation damage 3) recognise the signs of formation damage and 4) facilitate early warnings to the management that formation damage remediation should be implemented.

## **9.4 Concluding remarks**

When clays are exposed to low salinity solutions, two mechanisms may cause formation damage 1) swelling clays imbibe water into their crystalline structure and enlarge in size and plug the pore space and 2) mobilization, migration and re-deposition of clays can plug

the pore space. These processes may be prevented by the presence of various clay stabilisers in the injection fluid.

Formation damage may occur by several different processes during drilling and completion of the wells, the operation of the plant etc. and there are no universally proven technologies that are panacea for all problems. The recommendations are to use clear brines that are compatible with the reservoir rock. However, the best solutions are achieved by individual considerations in each case.

Therefore, a thorough investigation to identify the potential formation damaging mechanisms during the lifetime of the geothermal plant is recommended. This investigation ensures that minimisation of formation damage is considered in every step of the construction and operation of the plant. The investigation may among other tasks include a characterisation of the reservoir depositional environment to identify the conditions in the reservoir, and laboratory tests to provide scientific guidance to the development of strategies to avoid or minimise formation damage. To ensure that the formation damaging strategies are implemented it is recommended that all personnel involved with the well drilling and field operation of the plant is thoroughly trained in formation damage.

## References

- Ahlberg, A. 1994: Deposition and diagenesis of the Rhaetian-Hettangian succession (Triassic-Jurassic) in southern Sweden. *Lund Publications in Geology* 123, 1–56.
- American Petroleum Institute 1998: API RP 40: Recommended practices for core analysis. Second edition. American Petroleum Institute, Washington DC.
- Batten, D.J. & Koppelhus, E.B. 1996: Biostratigraphic significance of uppermost Triassic and Jurassic miospores in Northwest Europe. In: Jansonius, J., McGregor, D.C. (eds): *Palynology: principles and applications*, American Association of stratigraphical palynologists Foundation 2, 795–806.
- Bedrikovetsky, P. & Caruso, N. 2014: Analytical model for fines migration during water injection. *Transport in porous media*, 101, 161–189.
- Bennion, B. 1999: Formation damage – The impairment of the invisible, by the inevitable and uncontrollable, resulting in an indeterminate reduction of the unquantifiable. *Journal of Canadian petroleum technology*, 38 (2), 11–17.
- Bertelsen, F. 1978: The Upper Triassic – Lower Jurassic Vinding and Gassum Formations of the Norwegian–Danish Basin. *Danmarks Geologiske Undersøgelse Serie B*, Nr. 3, 26 pp.
- Bingen, B. & Solli, A. 2009: Geochronology of magmatism in the Caledonian and Sveconorwegian belts of Baltica: synopsis for detrital zircon provenance studies. *Norwegian Journal of Geology* 89, 267–290.
- Bjærke, T. 1980: Mesozoic palynology of Svalbard IV. Toarcian dinoglagellates from Spitsbergen. *Palynology* 4, 57–77.
- Bording, T. 2010: En procedure til modellering af temperature for geotermiske reservoirer med anvendelse i det nordlige Jylland, Geologisk Institut, Århus Universitet. 1–34.
- Butler, N. 1995: *Mendicodinium morgenrothum*, a new species of dinocyst from the Middle Jurassic, Aalenian to lowermost Bajocian Ness Formation (Brent group), northern North Sea. *Journal of Micropalaeontology* 14, 25–28.
- Byrne, M. 2010: Formation damage – any time, any place, any where. Society of Petroleum Engineers Distinguished Lecturer Program. <http://www.spe.org/dl/docs/2010/MichaelByrne.pdf>
- Chilingarian, G.V. & Vorabutr, P. 1981: *Drilling and Drilling Fluids*, Developments in Petroleum Science, Elsevier Scientific Publishing Co., New York.
- Civan, F. 2007: *Reservoir formation damage. Fundamentals, modelling, assessment and mitigation*. 2nd Edition. Elsevier Scientific Publishing Co.
- Coppel, C.P., Jennings Jr., H.Y. & Reed, M.G. 1973: Field results from wells treated with hydroxy-aluminum. SPE-3998-PA. *Journal of Petroleum Engineers* 25 (9): 1108–1112.
- CREWES Fluid Property Calculator. 2007. University of Calgary 2007: (<http://www.crewes.org/ResearchLinks/ExplorerPrograms/FIPProp/FluidProp.htm>).
- Das, S.K., Sharma, M.M. & Schechter, R.S. 1995: Adhesion and hydrodynamic removal of colloidal particles from surfaces. *Particle Science and Technology* 13: 227–247.
- De Siqueira, A.V., Lobban, C., Skipper, N.T., Williams, G.D., Soper, A.K., Done, R., Dreyer, J.W., Humphreys, R.J. & Bones, J.A.R. 1999: The structure of pore fluids in swelling

- clays at elevated pressures and temperatures. *Journal of Physic-condensed Matter*, 11(47), 9179–9188.
- Dusseault, M.B., Shand, D. & Davidson, B. 2002: Pressure pulse workovers in heavy oil. Paper SPE 79033, SPE/PS-CIM/CHOA international thermal operations and heavy oil symposium and international horizontal well technology conference, Calgary, Alberta, Canada, November 4-7 2002.
- Dybkjær, K. 1991: Palynological zonation and palynofacies investigation of the Fjerritslev Formation (Lower Jurassic–basal Middle Jurassic) in the Danish Subbasin. DGU ser. A 30, 1–150.
- Dybkjær, K., Nøhr-Hansen, H., Rasmussen, J.A. & Sheldon, E. 2002: Biostratigraphical analysis of 12 ditch cuttings samples from the Margretheholm-1 (MAH-1) well, Copenhagen, Denmark. Geological Survey of Denmark and Greenland report 2002/85, 1–13.
- ECLIPSE 100 2016: Schlumberger Information Solutions, version 2016.1.
- Erlström, M., Bidstrup, T., Lindström, S., Nielsen L.H., Kristensen, L. & Mathiesen, A. 2013: Structural outline, depositional setting and assessment of Mesozoic low enthalpy geothermal aquifers in the marginal eastern parts of the Danish Basin. European Geothermal Congress 2013, Pisa, 3–7 June 2013.
- Feist-Burkhardt, S. & Pross, J. 2010: Dinoflagellate cyst biostratigraphy of the Opalinuston Formation (Middle Jurassic) in the Aalenian type area in southwest Germany and north Switzerland. *Lethaia* 43, 10–31.
- Folk, R.L. 1966: A review of grain-size parameters. *Sedimentology* 6, 73–93.
- Frei, D. & Gerdes, A. 2009: Precise and accurate in situ U-Pb dating of zircon with high sample throughput by automated LA-SF-ICP-MS. *Chemical Geology* 261, 261–270.
- Freitas, A.M. & Sharma, M.M. 1997: Effect of surface hydrophobicity on the hydrodynamic detachment of particles from surfaces. *Langmuir* 15, 2466–2476.
- Gruesbeck, C. & Collins, E. 1982: Entrainment and deposition of fine particles in porous media. SPE-8430-PA. *Society of Petroleum Engineering Journal* 22 (6): 847–856.
- Hamberg, L. & Nielsen, L.H. 2000: Shingled, sharp-based shoreface sandstones: depositional response to stepwise forced regression in a shallow basin, Upper Triassic Gasum Formation, Denmark. In: Hunt, D. & Gawthorpe, R.L. (eds): *Sedimentary responses to forced regressions*. Geological Society Special Publication (London) 172, 69–89.
- Hayatdavoudi, A. 1998: Controlling formation damage caused by kaolinite clay minerals: Part II. SPE39464 paper, SPE International Symposium on formation damage control, Lafayette, Louisiana, February 18-19, 1998, 421–429.
- Herngreen, G.F.W., Kouwe, W.F.P. & Wong, T.E. 2003: The Jurassic of the Netherlands. Geological Survey of Denmark and Greenland Bulletin 1, 217–229.
- Himes, R.E, Vinson, E.F. & Simon, D.E. 1991: Clay stabilization in low-permeability formations. *SPE Production Engineering*, August 1991, 252–258.
- Hjuler, M.L., Erlström, M., Lindström, S., Nielsen, L.H., Kristensen, L., Mathiesen, A. & Bidstrup, T. 2014: Extended evaluation of possible geothermal reservoirs in the Helsingør area including geological data from Helsingør and Øresund. Contribution to an evaluation of the geothermal potential. Danmarks og Grønlands Geologiske Undersøgelse Rapport 2014/29.
- Holmslykke, H.D., Kjøller, C., Azaroual, M., Durst, P. & Fabricius, I.L., in prep: Geochemical and reactive transport modelling of injection of heated formation water into the Gasum Formation.

- Holmslykke, H. D., Kjøller C. & Fabricius I. L. 2016: The effect of heating and flow velocity on the permeability in the Gassum and Bunter sandstone formations. *In prep.*
- Japsen, P. & Bidstrup, T. 1999: Quantification of late Cenozoic erosion in Denmark based on sonic data and basin modelling. *Bulletin of the Geological Society of Denmark* 46, 79–99.
- Japsen, P., Green, P.F., Bonow, J.M. & Erlström, M. 2016: Episodic burial and exhumation of the southern Baltic Shield: Epeirogenic uplifts during and after break-up of Pangaea. *Gondwana Research* 35, 357–377.
- Japsen, P., Green, P.F., Nielsen, L.H., Rasmussen, E.S. & Bidstrup, T. 2007: Mesozoic-Cenozoic exhumation events in the eastern North Sea Basin: a multi-disciplinary study based on palaeothermal, palaeoburial, stratigraphic and seismic data. *Basin Research* 19, 451–490.
- Johnsen, M.R. 1994: Thin section grain size analysis revisited. *Sedimentology* 41, 985–999.
- Jones Jr., F.O. 1964: Influence of chemical composition of water on clay blocking of permeability. *Journal of Petroleum Technology* 16 (4), 441–446.
- Keelan, D.K. & Koepf, E.H. 1977: The role of cores and core analysis in evaluation of formation damage. SPE-5696-PA. *Journal of petroleum technology*, 29, 482–490.
- Khilar, K.C. & Fogler, H.S. 1983: Water sensitivity of sandstones, SPE-10103-PA. *Society of Petroleum Engineers Journal*, 23, 55–64.
- Khilar, K.C. & Fogler, H.S. 1984: The existence of a critical salt concentration for particle release. *Journal of colloid and interface science*, 101, 214–224.
- Koppelhus, E.B. 1991: Palynology of the Lower Jurassic Rønne Formation on Bornholm, eastern Denmark. *Bulletin of the Geological Society of Denmark* 39, 91–110.
- Koppelhus, E.B. & Dam, G. 2003: Palynostratigraphy and palaeoenvironments of the Rævekløft, Gule Horn and Ostreaelv Formations (Lower–Middle Jurassic), Neill Klint Group, Jameson Land, East Greenland. In: Ineson, J.R. & Surlyk, F. (eds): *The Jurassic of Denmark and Greenland*. Geological Survey of Denmark and Greenland Bulletin 1, 723–775.
- Koppelhus, E.B. & Nielsen, L.H. 1994: Palynostratigraphy and palaeoenvironments of the Lower to Middle Jurassic Bagå Formation of Bornholm, Denmark. *Palynology* 18, 139–194.
- Kristensen, L., Hjuler, M.L., Frykman, P., Olivarius, M., Weibel, R., Nielsen, L.H. & Mathiesen, A. 2016: Pre-drilling assessments of average porosity and permeability in the geothermal reservoirs of the Danish area. *Geotherm Energy* 4:6, 2–27, <http://dx.doi.org/10.1186/s40517-016-0048-6>
- Kürschner, W.M. & Hengreen, G.F.W. 2010: Triassic palynology of central and northwestern Europe: a review of palynofloral diversity patterns and biostratigraphic subdivisions. *Geol. Soc. London, Spec. Publ.* 334, 263–283.
- Larsson, L.M. 2009: Palynostratigraphy of the Triassic-Jurassic transition in southern Sweden. *GFF* 131, 147–163.
- Lindström, S. 2002: *Lunnomidinium scaniense* Lindström, gen. et sp. nov., a new suessiacan dinoflagellate cyst from the Rhaetian of Scania, southern Sweden. *Review of Palaeobotany and Palynology*, 120(3-4), 247–261.
- Lindström, S. 2016: Palynofloral patterns of terrestrial ecosystem change during the end-Triassic event – a review. *Geological Magazine* 153, 223–251.

- Lindström, S. & Erlström, M. 2006: The Late Rhaetian transgression in southern Sweden: regional (and global) recognition and relation to the Triassic–Jurassic boundary. *Palaeogeography, Palaeoclimatology, Palaeoecology* 241, 339–372.
- Lindström, S. & Erlström, M. 2007: Erratum to "The Late Rhaetian transgression in southern Sweden: regional (and global) recognition and relation to the Triassic–Jurassic boundary". (*Palaeogeography, Palaeoclimatology, Palaeoecology* 241, 339–372), *Palaeogeography, Palaeoclimatology, Palaeoecology* 249, 229–231.
- Lindström, S. & Erlström, M. 2011: Basin analysis of the uppermost Triassic to Lower Cretaceous, Danish Basin. *Biostratigraphy and log correlation. Geological Survey of Denmark and Greenland Report 2011/82*, 1–55.
- Lindström, S., Erlström, M., Piasecki, S., Nielsen, L.H. & Mathiesen, A. in press: Palynology of the Middle Triassic to lowermost Jurassic succession of the eastern Danish Basin: implications for terrestrial ecosystem change. *Review of Palaeobotany and Palynology*.
- Lindström, S., van de Schootbrugge, B., Dybkjær, K., Pedersen, G.K., Fiebig, J., Nielsen, L.H. & Richoz, S. 2012: No causal link between terrestrial ecosystem change and methane release during the end-Triassic mass extinction. *Geology* 40, 531–534.
- Lund, J.J. 1977: Rhaetic to Lower Liassic palynology of the onshore south-eastern North Sea Basin. *Danmarks Geologiske Undersøgelse II. Række* 109, 129 pp.
- Lund, J.J. 2003: Rhaetian to Pliensbachian palynostratigraphy of the central part of the NW German Basin exemplified by the Eitzendorf 8 well. *Courier Forschungsinstitut Senckenberg* 241, 69–83.
- Mathiesen, A., Nielsen, L.H., Bidstrup, T. & Lindström, S. 2007: Vurdering af de geotermiske ressourcer i hovedstadsområdet. *Danmarks og Grønlands Geologiske Undersøgelse rapport 2007/82*, 1–20 + appendix.
- Mathiesen, A., Kristensen, L., Nielsen, C.M., Weibel, R., Hjuler, M.L., Røgen, B., Mahler, A. & Nielsen, L.H. 2013: Assessment of sedimentary geothermal aquifer parameters in Denmark with focus on transmissivity. *European Geothermal Congress 2013, Pisa*, 3–7 June 2013.
- Michelsen, O. 1989: Log-sequence analysis and environmental aspects of the Lower Jurassic Fjerritslev Formation in the Danish Subbasin. *Geological Survey of Denmark Series A*, 25, 22 pp.
- Michelsen, O. & Bertelsen, F. 1979: Geotermiske reservoirformationer i den danske lagserie. *Danmarks Geologiske Undersøgelse, Årbog 1978*, 151–164.
- Michelsen, O., Nielsen, L.H., Johannessen, P.N., Andsbjerg, J. & Surlyk, F. 2003: Jurassic lithostratigraphy and stratigraphic development onshore and offshore Denmark. In: Ineson, J.R. & Surlyk, F. (eds): *The Jurassic of Denmark and Greenland. Geological Survey of Denmark and Greenland Bulletin* 1, 147–216.
- Milliken, K.L., McBride, E.F. & Land, L.S. 1989: Numerical assessment of dissolution versus replacement in the subsurface destruction of detrital feldspars, Oligocene Frio Formation, South Texas. *Journal of Sedimentary Petrology* 59, 740–757.
- Mungan, N. 1965: Permeability reduction through changes in pH and salinity. SPE-1283-PA. *Journal of Petroleum Technology* 17 (12), 1449–1453.
- Nielsen, L.H. 2003: Late Triassic – Jurassic development of the Danish Basin and the Fennoscandian Border Zone, southern Scandinavia. In: Ineson, J.R. & Surlyk, F. (eds): *The Jurassic of Denmark and Greenland. Geological Survey of Denmark and Greenland Bulletin* 1, 459–526.

- Nielsen, L. H., Larsen, F. & Frandsen, N. 1989: Upper Triassic-Lower Jurassic tidal deposits of the Gassum Formation on Sjælland, Denmark. *Danmarks Geologiske Undersøgelse Series A*, 23, 30 pp.
- Nielsen, O.B., Seidenkrantz, M.-S., Abrahamsen, N., Schmidt, B.J., Koppelhus, E.B., Ravn-Sørensen, H., Korsbech, U. & Nielsen, K.G. 2003: The Lower–Middle Jurassic of the Anholt borehole: implications for the geological evolution of the eastern margin of the Danish Basin. *Geological Survey of Denmark and Greenland Bulletin* 1, 585–609.
- Olivarius, M. 2015: Diagenesis and provenance of Mesozoic sandstone reservoirs onshore Denmark (PhD thesis). Geological Survey of Denmark and Greenland. Report 2015/19, 146 pp.
- Olivarius, M. & Nielsen, L.H. 2016: Triassic paleogeography of the greater eastern Norwegian-Danish Basin: constraints from provenance analysis of the Skagerrak Formation. *Marine and Petroleum Geology* 69, 168–182.
- Olivarius, M., Nielsen, L.H., Weibel, R., Kristensen, L. & Thomsen, T.B. in prep: Sequence stratigraphic evidence for Late Triassic uplift of southern Norway using detrital zircons.
- Olivarius, M., Weibel, R., Friis, H., Boldreel, L.O., Keulen, N. & Thomsen, T.B. in press: Provenance of the Lower Triassic Bunter Sandstone Formation: implications for distribution and architecture of aeolian vs. fluvial reservoirs in the North German Basin. *Basin Research*, doi: 10.1111/bre.12140.
- Paton, C., Hellstrom, J.C., Paul, P., Woodhead, J.D. & Hergt, J.M. 2011: Lolite: Freeware for the visualisation and processing of mass spectrometric data. *Journal of Analytical Atomic Spectrometry* 26, 2508–2518.
- Peters, F.W. & Stout, C.M. 1977: Clay stabilization during fracturing treatments with hydrolyzable zirconium salts. SPE-5687-PA. *Journal of Petroleum Technology* 29 (2), 187–194.
- Petrel 2015: Schlumberger Information Solutions, version 2015.2.
- Porter, K. E. 1989: An overview of formation damage. *Journal of petroleum Technology*, 41 (8), 780–786.
- Poulsen, N.E. 1996: Dinoflagellate cysts from marine Jurassic deposits of Denmark and Poland. *AASP contribution series* 31, 1–227.
- Poulsen, N.E. & Riding, J.B. 2003: The Jurassic dinoflagellate cyst zonation of Subboreal Northwest Europe. *Geological Survey of Denmark and Greenland Bulletin* 1, 115–144.
- Poulsen, N.E., Gudmundsson, L., Hansen, J.M. & Husfeldt, Y. 1990: Palynological preparation techniques, a new Maceration tank-method and other modifications. *DGU series C10*, 23 pp.
- Reynolds, R.C. 1980: Interstratified clay minerals. In: Brindley, G.W. & Brown, G. (eds): *Crystal structure of clay minerals and their X-ray identification*. Mineralogical Society, 495 pp.
- Riding, J.B. & Thomas, J.E. 1992: Dinoflagellate cysts of the Jurassic system. In: Powell, A.J. (Ed.) *A stratigraphic index of dinoflagellate cysts*, British Micropalaeontological Society Publication Series, Chapman & Hall, London, 7–98.
- Riding, J.B., Mantle, D.J. & Backhouse, J. 2010: A review of the chronostratigraphical ages of Middle Triassic to Late Jurassic dinoflagellate cyst biozones of the North West Shelf of Australia. *Review of Palaeobotany and Palynology* 162, 543–575.
- Rosenbrand, E., Kjøller, C., Riis, J.F., Kets, F. & Fabricius, I.L. 2015: Different effects of temperature and salinity on permeability reduction by fines migration in Berea sandstone. *Geothermics* 53, 225–235.

- Schembre, J.M. & Kovscek, A.R. 2005: Mechanism of formation damage at elevated temperature. *Journal of Energy Resources Technology-Transactions of the Asme* 127(3), 171–180.
- Schulz, E. & Heunisch, C. 2005: Palynostratigraphische Gliederungsmöglichkeiten des deutschen Keupers. *Courier Forschungsintitut Senckenberg* 253, 43–49.
- Seibt P. & Kellner T. 2003: Practical experience in the reinjection of cooled thermal waters back into sandstone reservoirs. *Geothermics* 32, 733–741.
- Seidenkrantz, M.-S., Koppelhus, E.B. & Ravn-Sørensen, H. 1993: Biostratigraphy and palaeoenvironmental analysis of a Lower to Middle Jurassic succession on Anholt, Denmark. *Journal of Micropalaeontology* 12, 201–218.
- Sharma, M.M. & Yortsos, Y.C. 1987. Fines migration in porous media. *AIChE Journal* 33 (10), 1654-1662.
- Sharma, M.M., Chamoun H., Sarma, D.S.H. S.R. & Schecter, R.S. 1992: Factors controlling the hydrodynamic detachment of particles from surfaces. *Journal of Colloid and Interface Science*, 149, 121-134.
- Springer, N. 2003: Margrethholm-2 (MAH-2). Sidewall core analysis data. GEUS report file no. 27980, 2 pp.
- Tague, J.R. 2000a: Optimizing production in fields with multiple formation damage mechanisms. Paper SPE 58745, the 2000 SPE International symposium on formation damage held in Lafayette, Louisiana, February 23-24 2000.
- Tague, J.R. 2000b: Clay stabilization improves sand control. SPE paper 62524, the 2000 SPE/AAPG Western regional meeting held in Long Beach, California, June 19-23 2000.
- Tague, J.R. 2000c: Overcoming formation damage in heavy oil fields: A comprehensive approach. Paper SPE 62546, the 2000 SPE/AAPG Western regional meeting held in Long Beach, California, June 19-23 2000.
- Tague, J.R. 2000d: Multivariate statistical analysis improves formation damage remediation, Paper SPE 63004, the 2000 SPE annual technical conference and exhibition held in Dallas, Texas, October 1-4 2000.
- Ungemach, P. 2003: Reinjection of cooled geothermal brines into sandstone reservoirs. *Geothermics* 32, 743–761.
- Vajda, V. 2001: Aalenian to Cenomanian terrestrial palynofloras of SW Scania, Sweden. - *Acta Palaeontologica Polonica* 46, 3, 403--426.
- Weibel, R., Olivarius, M., Kristensen, L., Friis, H., Hjuler, M.L., Kjøller, C., Mathiesen, A. & Nielsen, L.H. 2017: Predicting permeability of low enthalpy geothermal reservoirs: A case study from the Upper Triassic–Lower Jurassic Gassum Formation, Norwegian–Danish Basin. *Geothermics* 65, 135–157.
- Wentworth, C.K. 1922: A scale of grade and class terms for clastic sediments. *Journal of Geology* 30, 377–392.
- Woollam, R. & Riding, J.B. 1983: Dinoflagellate cyst zonation of the English Jurassic. *Rep. Inst. Geol. Sci.* 83/2, 41 pp.
- Xu, T., Sonnenthal, E., Spycher, N. & Pruess, K. 2006: TOUGHREACT – A simulation program for nonisothermal multiphase reactive geochemical transport in variably saturated geologic media: Applications to geothermal injectivity and CO<sub>2</sub> geological sequestration. *Computers & Geosciences*, 32(2), 145–165.
- Zaiton, A. & Berton, N. 1996: Stabilisation of montmorillonite clay in porous media by polyacrylamides. SPE 31109 paper, SPE Formation damage control symposium, Lafayette, Louisiana, February 14-15 1996, 423–428.

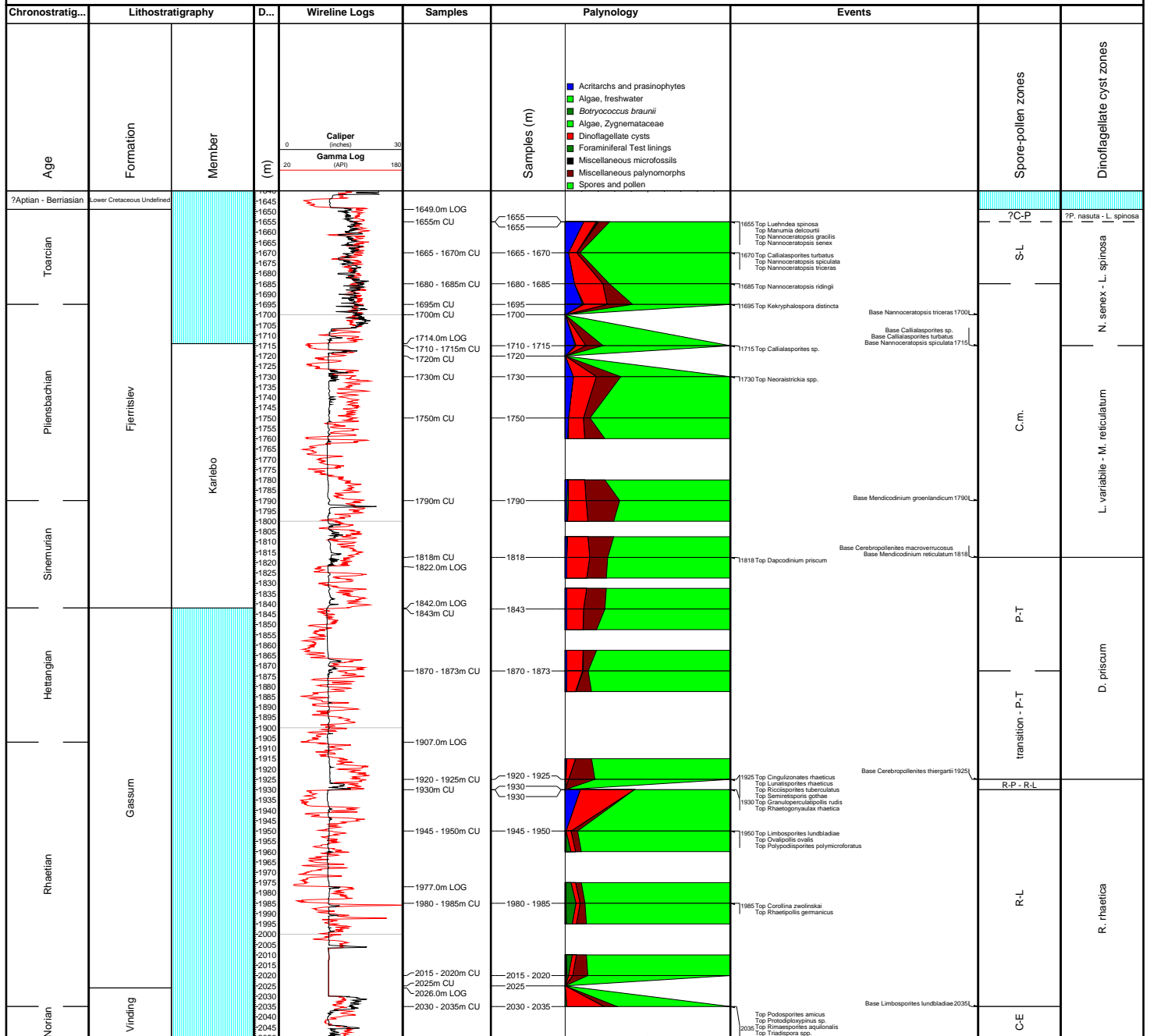
Zhou, Z. 1995: Construction and application of clay-swelling diagrams by use of XRD methods. *Journal of Petroleum Technology* 47, 306–306.

## **Appendices 1 – 5:**

**Stratigraphic summary charts of wells.**

**(Margretheholm-1, Karlebo-1A, Höllviken-2, Lavø-1, Stenlille-1).**

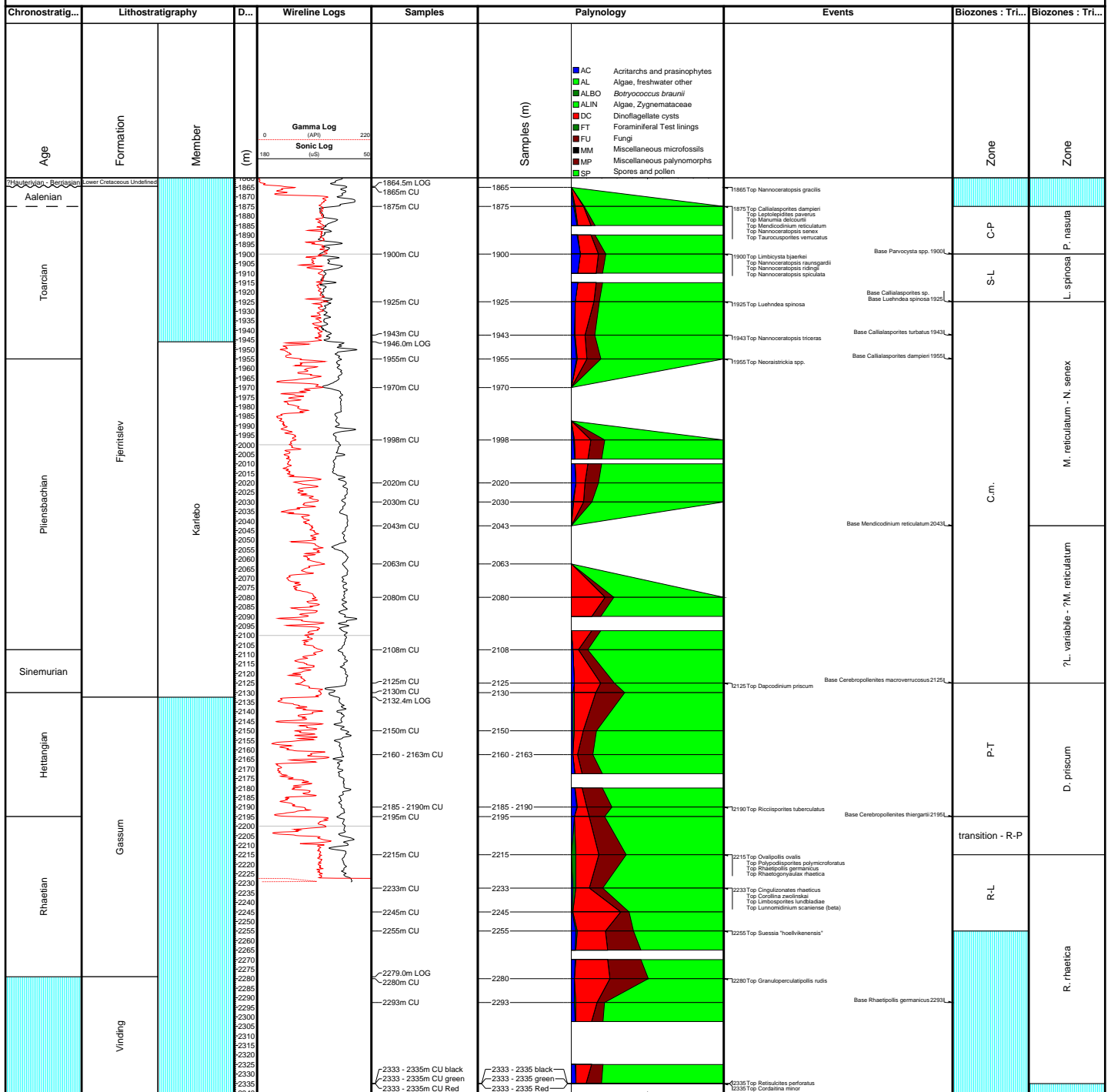
# Margrethholm-1



# Karlebo-1A

## Appendix 2

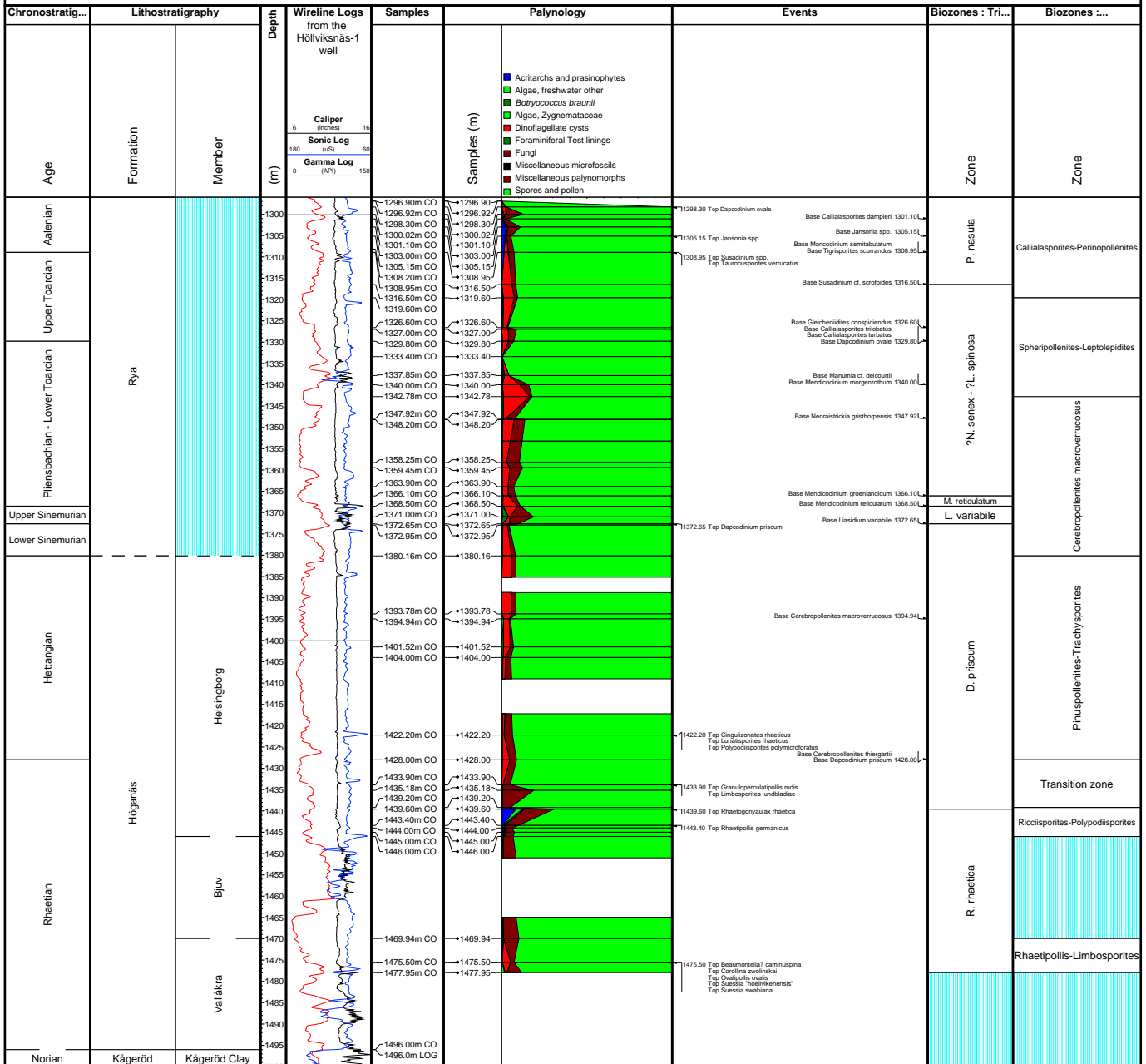
Stratigraphic summary chart



Scale : 1:500

# Höllviken-2

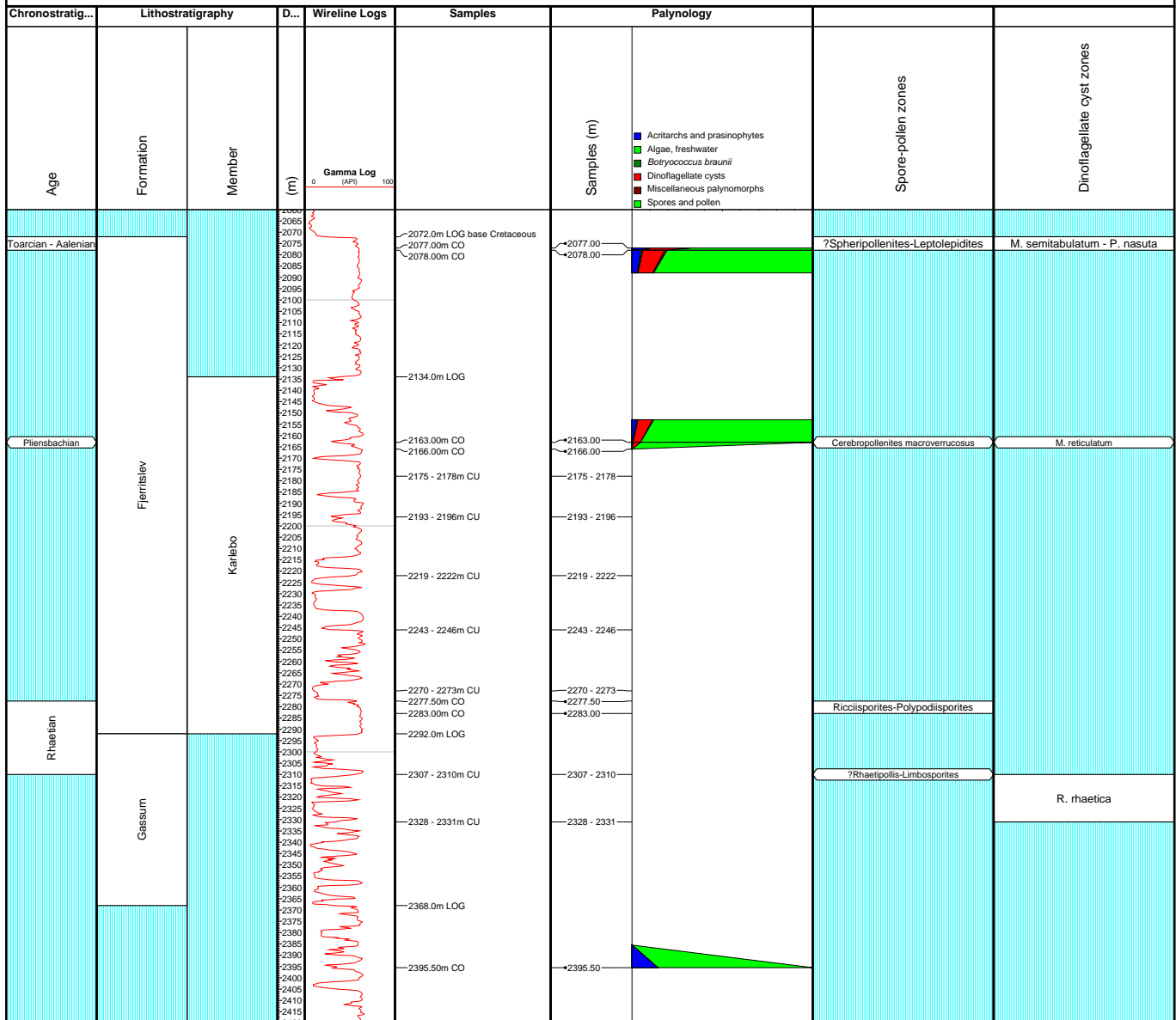
## Appendix 3 Stratigraphic summary chart



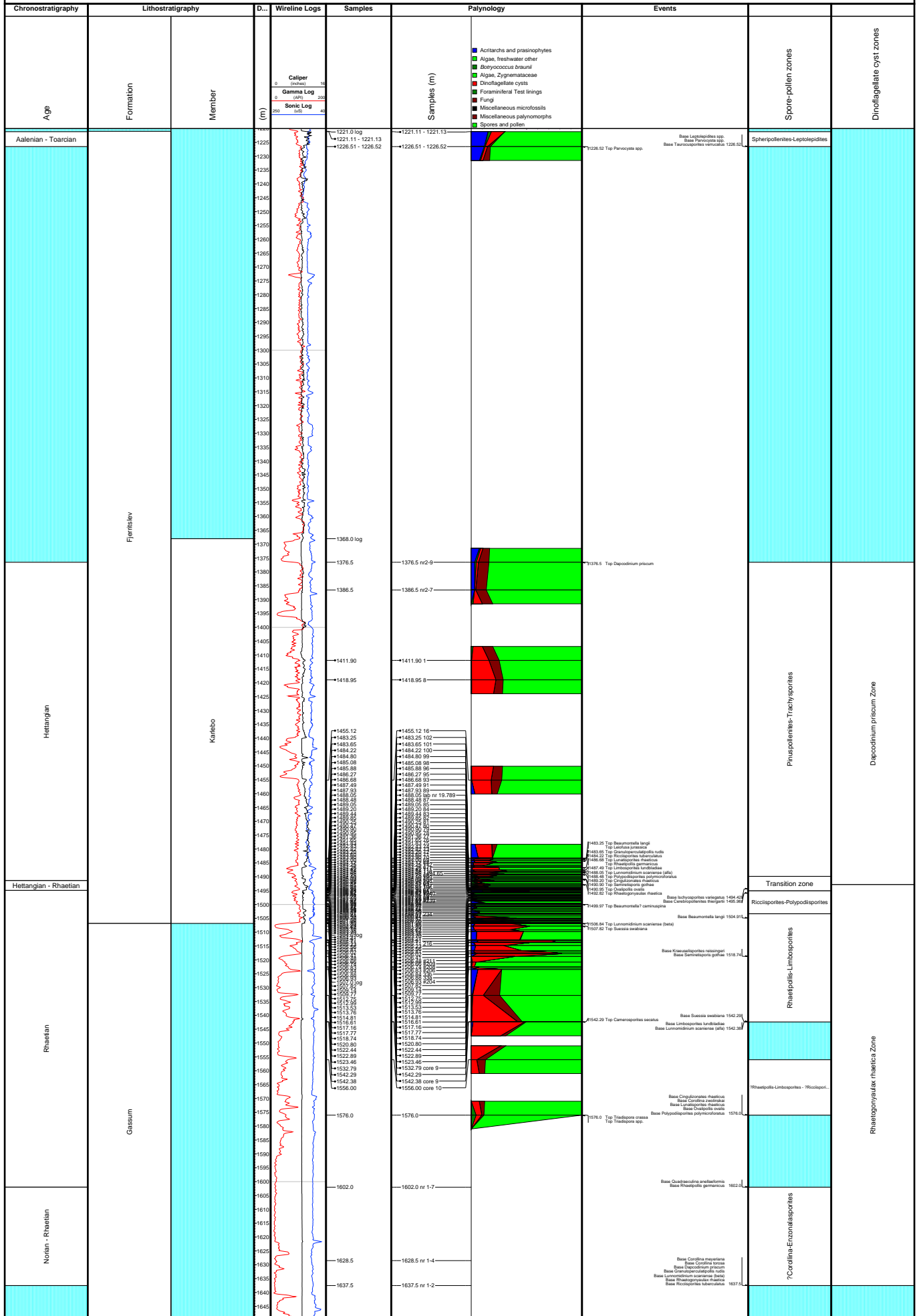
# Lavø-1

## Appendix 4

Stratigraphic summary chart



# Stenlille-1



## Appendix 6:

### Description of cuttings from the Gassum and Fjerritslev formations selected for analyses of their bulk mineralogy

Samples from Kvols-1a, Kvols-2, Sønderborg-1, Thisted-3, Stenlille-1, -2, -5, Margretheholm-1 and Karlebo-1 were selected for examination. Washed cuttings from a certain depth (bulk samples, or picked cuttings of distinctive lithologies) were crushed and the powders were analysed by X-ray diffraction.

The mudstone cuttings are dominantly:

- Grey, fissile mudstones. These cuttings are thin and often very large.
- Grey, homogeneous mudstones, in places greenish grey. The mudstones appear silty and form more equidimensional cuttings.
- Brown cuttings of mudstone cemented by siderite

The sandstone cuttings are dominantly:

- Clean, white, well-sorted sandstone, grain-size around 125  $\mu\text{m}$ , sometimes slightly coarser. This lithology is often friable, and forms spherical cuttings, systematically smaller than the mudstone cuttings from the same sample. This lithology is probably the main source of all the loose sand grains in the samples.
- Heterolithic sandstone, which is finer-grained and less well-sorted than the clean sandstones, is also less friable and forms larger cuttings. They show mudstone drapes, locally coalified plant debris, or interbedded sandy siltstone.

In addition cuttings of chalk occur in various amounts.

**Methods.** In some samples cuttings of mudstone and sandstone were picked from the washed and dried samples, in other samples the washed cuttings were gently sieved before the mudstone cuttings were picked from the coarse fraction. It saves time to sieve the samples, but some information is lost because only a fraction of the bulk sample of cuttings is inspected in the microscope, and it is thus possible that the silty mudstones become over-represented in the analysis.

The sieving showed that nearly all of the sand-sized quartz grains passed the 250 $\mu\text{m}$  sieve, and that a large proportion of the sand passed the 125 $\mu\text{m}$  sieve. This indicates that most of the sand is very fine-grained or fine-grained, which is in agreement with measured logs from Stenlille-1 (Nielsen et al. 1989, Nielsen 2003).

In the table below the lithology at a certain depth, interpreted from petrophysical logs, is listed. The dominant lithology of cuttings is listed as well. Generally the agreement between petrophysical interpretation and cutting lithologies is good. The column headed "comments" provide information on the type of material analysed by XRD. The following abbreviations have been used:

bulk	A subsample of the washed cuttings
bulk >2mm	The washed cuttings were sieved, and the crushed sample was a subsample of the cuttings > 2 mm
picked mudst	Mudstone cuttings were picked from the bulk sample
picked mudst >2mm	The cuttings were sieved, and mudstone cuttings were picked from the fraction > 2mm. This is the quickest way to pick a sufficiently large sample
bulk + picked mudst (+ others)	The original sample is represented by a bulk sample as well as one or two subsamples of picked cuttings (see Margretheholm 1-1A, Sønderborg-1 and Thisted-3). Some, or all, subsamples were analysed in order to test whether for instance white cuttings are chalk or whether brown cuttings are cemented by siderite. Subsamples of mudstone have been picked (and analysed) to test how much they differ from the bulk sample. In some samples 1–2 subsamples were not analysed but stored for future use.

In some samples the analysed bulk sample consists of particles >2mm, and the finer fractions were stored. Typically, this will result in an over-representation of mudstone in the bulk sample.

## List of samples

Well Depth (m)	Lithostratigraphy	Lithology		Comments Analyzed samples
		Log interpretation	Cuttings	
<b>Karlebo-1A</b>				
1875	Fjer. Fm >SB17	mudst	Low quality cuttings	bulk >1mm
1895	Fjer. Fm>SB16	mudst	Dominantly mudst	picked mudst >2mm
1920	Fjer. Fm>MFS15	mudst	Fissile mudst	picked mudst >2mm
1945	Fjer. Fm>SB15	mudst	Fissile mudst	picked mudst
1920, 1945	Fjer. Fm>SB15		Green particles, mud-add?	Not analyzed
1967.5	Karlebo Mb>SB14	sst	Fissile mudst	picked mudst
2020	Karlebo Mb>SB13	sst	Sandst, qz<250µm	picked mudst >2mm
2047.5	Karlebo Mb>MFS12	mudst	Dominantly sst	bulk >2mm
2060	Karlebo Mb >MFS12	mdst	Fissile mudst	picked mudst >2mm
2107.5	Karlebo Mb >MFS11	mudst	Silty mudst	picked mudst >2mm
2142.5	Gassum Fm>SB10	mudst	Fissile mudst	picked mudst >2mm
2160-2162.5	Gassum Fm > MFS9	mudst	Mudst	Not analyzed
2185-2190	Gassum Fm >SB9	sst	Fissile mudst	
2195	Gassum Fm, MFS7	mudst	Mudst	picked mudst >2mm
2250	Gassum Fm>SB5	mudst	Mudst + mud-additive	picked mudst >2mm
2332-2335	Skagerrak Fm	Sst, mudst	Variogated mudst	Not analyzed
<b>Kvols-1</b>				
2323 m (7620')	F-Ib, >SB-11	mudst	Fissile mudst, gypsum	bulk
2371 m (7780')	F-Ia, >MFS-10	mudst	Fissile mudst	bulk
2420 m (7940')	Base F-Ia, > SB-9	mudst	Fissile mudst, gypsum	bulk
<b>Kvols-2A</b>				
1920	Vedsted Fm		Mudst, chalk, small cutt	bulk + picked mdst +chalk
2160	F-IV	mudst	Fissile mudst	bulk
2240	F-III	mudst	Mudst, small cuttings	bulk
2310	F-III	mudst	Mdst many small cuttings	bulk
2360	F-III	mudst	Silty mudst	bulk
2440	F-II, > MFS-13	mudst	Silty mudst	bulk
2460	F-Ib, >MFS-12	mudst	Silty mudst	bulk
2480	F-Ib, >SB-12	mudst	Siltst? Very small cuttings	bulk
2520	F-Ib, >MFS-11	mudst	Muddy siltst	bulk
2530	F-Ib	mudst	Silty mudst	bulk
2550	F-Ib	mudst	Silty mudst, fissile	bulk
2560	F-Ib	mudst	Silty udst, fissile	bulk
2570	F-Ib	mudst	Silty mudst, fissile	bulk
2690	F-Ia, >MFS-7	mudst	Mudst, large cuttings	bulk
<b>Margretheholm-1</b>				
1655-1660	Fjer. Fm, >SB-17	mudst	Mudst , sandst	bulk + mudst + sst
1665-1670	Fjer. Fm, >SB-16	mudst	Mudst	Not analyzed
1680-1685	Fjer. Fm, >MFS-15	mudst	Mudst, red lithology	2 subsampl: mudst + other
1700-1705	Fjer. Fm, >SB-15	mudst	Silty mudst	bulk
1710-1715	Base Fjer. Fm, >SB-15	mudst	Fissile mudst	Not analyzed
1732.5-1735	Karlebo Mb, >MFS-13	mudst	Siltst to very fine sst	Bulk + picked mudst
1747.5-1750	Karlebo Mb, >SB-1	mudst	Very fine-grained sst	bulk + picked mudst
1782.5-1785	Karlebo Mb, at MFS-12	mudst	White sst, as 1810 m	bulk
1792.5-1795	Karlebo Mb, >MFS-11	mudst	Very fine- to fine-gr sst	Bulk + picked mudst
1810-1812,5	Karlebo Mb, >MFS-11	mudst	White sst	bulk
1817.5-1820	Karlebo Mb, >MFS-7	mudst	Mostly friable sandstone	picked mudst
1837.5-1840	Karlebo Mb, >MFS-10	mudst	Mostly sandstone	bulk
1850-1852.5	Gassum Fm, > SB-10	one thick sandstone unit	Mostly friable sandstone	picked mudst
1855-1857.5	Gassum Fm, >SB-10		Mostly friable sandstone	picked mudst
1857.5-1860	Gassum Fm, >SB-10		Mostly friable sandstone	picked mudst
1860-1862.5	Gassum Fm, >SB-10		Mudst and friable sst	Picked mudst >2mm

1862.5-1865		Gassum Fm, at SB-10		Mudst and friable sst	Picked mudst >2mm
1870-1872.5		Gassum Fm at MFS-9	mudst	Mostly sandstone	Bulk
1895-1900		Gassum Fm, >SB-9	mudst, sst	Mudst, sst, and coal	Picked mudst >2mm
1920-1925		Gassum Fm, at MFS-7	mudst	Large lithologic variation	Bulk+subsamples: mudst+red
1945-1950		Gassum Fm, >SB-5	sst, mudst	Mudst and sandstone	Not analyzed
1980-1985		Gassum Fm, <SB-5	mudst, sst	Mostly sandstone	Picked mudst >2mm
2000		Gassum Fm	mudst	Mostly sandstone	Picked mudst >2mm
2015-2020		Gassum Fm	mudst, sst	Friable sst and mudst	Not analyzed
2030-2035		Kågeröd Fm?	mudst	Variiegated mudst and sst	
2055		Kågeröd Fm?	mudst	Dark red mudst + others	
<b>Stenlille-1</b>					
1226.52	#2	Fjer. Fm at SB-17	mudst	Mudst, pale green	Clay mineralogy only (unpublished data from other projects)
1414	#3	F-la, >SB-10	mudst	Mudst	
1494.44	#5	F-la, >MFS-7	mudst	Mudst	
1498.57	#5	F-la, >MFS-7	mudst	Siltstone	
1505	#6	F-la, at MFS-7	mudst	Mudst	
1542.29	#9	Gassum Fm, at MFS-5	mudst	Mudst, heterolithic	Not analyzed
<b>Stenlille-2</b>					
1296-1299		Fjer. Fm, at SB-13	mudst	Heterolithic mudst	bulk
1344-1347		Fjer. Fm, > MFS-11	mudst	Mudst	bulk
1362-1365		Fjer. Fm, >MFS-11	mudst	Mudst	bulk
1386-1389		Karlebo Mb	mudst	Mudst	bulk
1410-1413		Karlebo Mb, >MFS-10	mudst	Mudst+sst, very small cuttings	bulk
1437-1440		Karlebo Mb, >MFS-10	mudst		bulk
1445-1448		Karlebo Mb, >SB-10	mudst	Very few, small cuttings	bulk
1447.7		Karlebo Mb, >SB-10	mudst	Sandstone?	bulk
1552.52		Gassum Fm, >SB-5	sst	Sandstone	bulk
<b>Stenlille-5</b>					
1420,15	#2			Silt-streaked mudst	bulk
<b>Sønderborg-1</b>					
876		F-III, >MFS-13	mudst	Different lithologies	Bulk +picked mudst +others
918		F-II at MFS-13	mudst	Different lithol., small cutt.	Bulk + picked mudst
990		F-Ib, >MFS-11	mudst	Siltstone, fossil fragments	Bulk + picked mudst
1050		F-Ib, >SB-11	mudst	Silty mudst	Bulk + picked mudst
1110		F-la, at TS-10	mudst	Siltst	Bulk + picked mudst
1140		Gassum Fm at MFS-9	mudst	Mudst, silt-streaked	Bulk + picked mudst+ other
<b>Thisted-3</b>					
1035-40		Fjer. Fm, >SB-11	mudst	Different lithologies	Bulk + picked mudst
1085-90		Fjer. Fm, >MFS-10	mudst	Clayey siltst	Bulk + picked mudst
1135-40		Gassum Fm, >SB-9	mudst	Variiegated siltst + sst	Bulk + picked mudst +others

The majority of the 95 samples analysed for bulk mineralogy represent the Fjerritslev Formation (grey) above the Karlebo Member (green). The samples from the Gassum Formation are shown in dark yellow, and older Triassic formations are shown in brown.

Thirty samples were also analysed for clay minerals (bright yellow).

## **Appendix 7:**

**Drilling problems reported in completion reports of selected wells.**

**(Karlebo-1/1A, Kvovls-1, Lavø-1, Margretheholm-1/1A and -2, Stenlille-1, Stenlille-19).**

# Karlebo-1/1A

Year: 2006  
Orientation: Deviated  
TD: 2489 m MD RT  
2301.5 m TVDSS  
Status: Plugged and abandoned

## Encountered problems during drilling

Information on drilling problems in the Karlebo-1A well is based on information from the final well report:

Tethys Oil AB: Karlebo-1, Karlebo-1A Final well report, January 2007. Report file no. 26960.

### Overview scheme (Fig. 1)

Drilling problems are presented in an overview scheme (Fig. 1) with relation to depth (MD) and lithostratigraphic units.

To the far right page numbers refer to sections in the final well report where the particular drilling problem is explained. The relevant sections are extracted from the final well report and presented subsequently. The extracts from the final well report concentrate on geology-induced drilling problems and how they were solved. Technical problems with no connection to geological conditions are not included. Sections with geological information that may turn out helpful during the drilling process may be included.

# Karlebo-1/1A

Depth m MD	Period	Litho-stratigraphic unit	Drilling problem	Solution to drilling problem	Completion report
0		Post Chalk Group			
100	Cretaceous	Chalk Group	150-175 Mud loss	Continued drilling with water	p. 29
200					
300					
400					
500					
600					
700					
800					
900					
1000					
1100					
1200					
1300					
1400			1375-1400 Mud loss	Diluting mud system with water and mixing an LCM pill. Hole circulated clean w. hi vis pill. LCM pill pumped and replaced w. water	p. 30
1500					
1600					
1700			1742 Bit stood up	Hole reamed to bottom	p. 31
1800	Lower Cretaceous		1813 ROP drop, bit balled w. clay		
1900					
1920	Jurassic	Fjerritslev Fm	1920 String w. bit stuck	10 right hand turns of rotary table and pulling up	p. 32
1916			1916 Drill string stuck due to swelling shales in L. Cret. and Fjerritslev Fm		
2000					
2100					
2200	Triassic	Gassum Fm			
2288			2288 Bit stuck	Bit worked free	p. 33
2300			2289 Bit stuck	Bit jarred free	p. 34
2400					

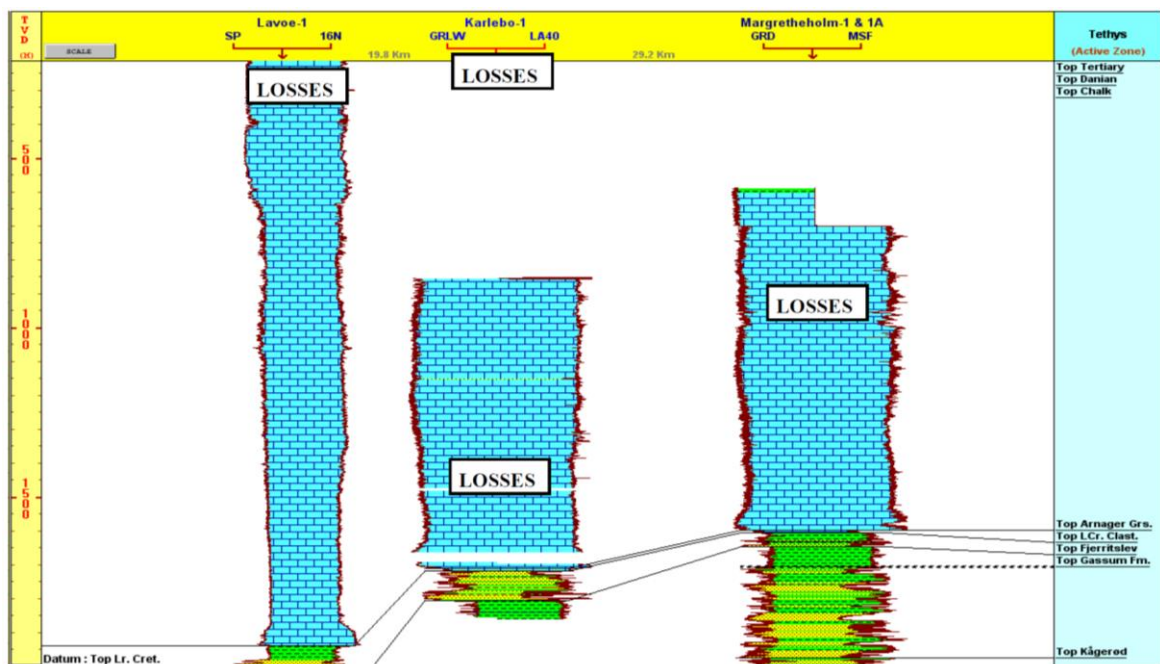
Figure 1. Overview of drilling problems related to depth and lithostratigraphic units in the Karlebo-1A well.

## Extracts from the final well report (Report file no. 26960)

p. 5 SUMMARY

The Karlebo-1 well was deviated in order to encounter the off-set Early Cretaceous/Jurassic and Triassic objectives in optimal positions. **Problems with swelling shales in the Early Cretaceous and Early Jurassic (Fjerritslev Fm.) sections caused drilling problems and led to the drill string becoming stuck at 1,957 m.** The Karlebo-1A sidetrack was kicked off in the basal part of the Chalk and penetrated the problematic shale section with less deviation than the original well (20 degrees vs. 40 degrees). Intermediate logs were run at a depth of 2,489 m in order to evaluate the objectives, which had all been penetrated at that time, before drilling on towards the Bunter Fm. However, **the logging tool became stuck before reaching bottom** and could not be recovered. It was then decided to abandon the well.

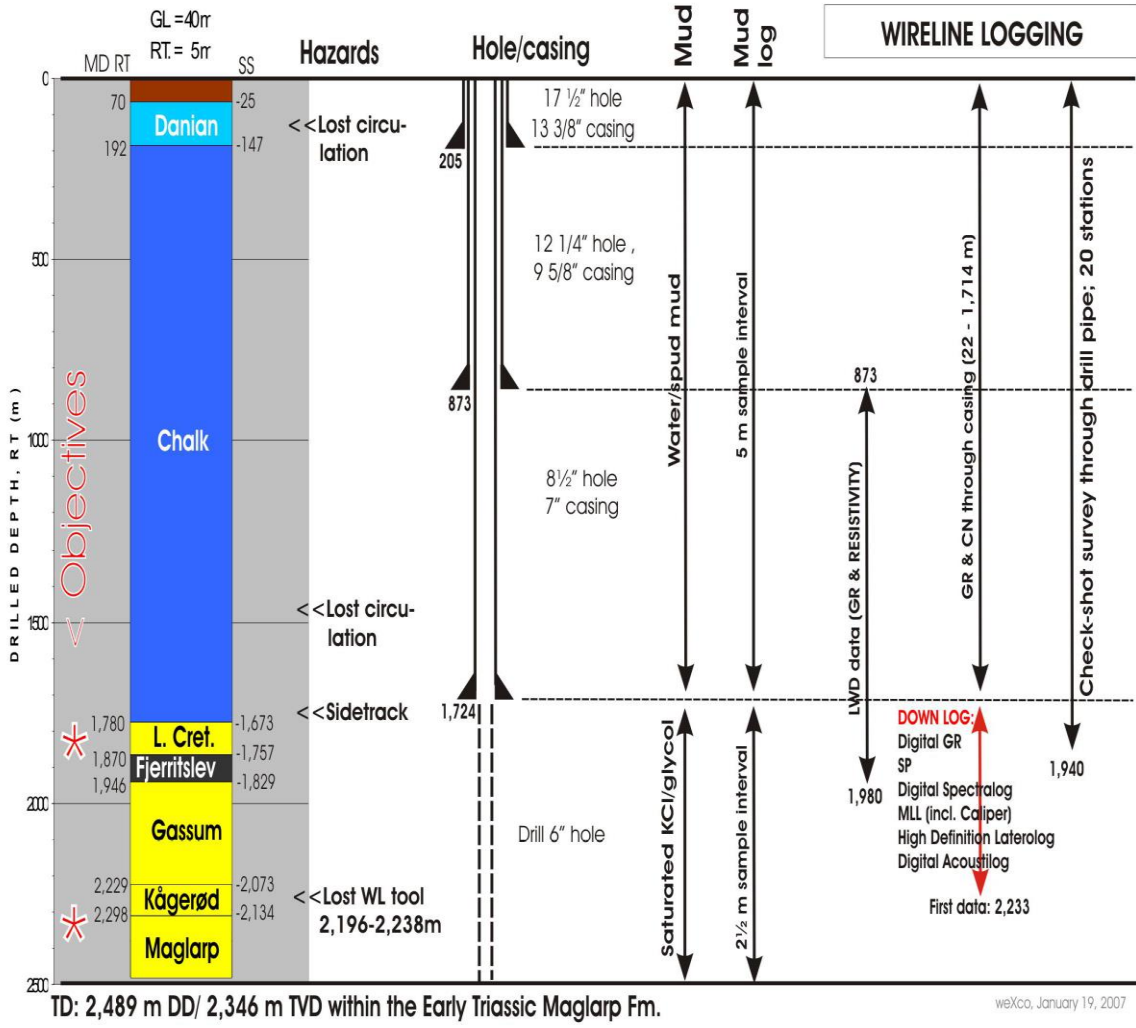
p. 11 **Mud losses of up to 180 bbsl/hr were experienced while drilling the section from ca. 1,375 to 1,400 m.** Losses coincided with the presence of crystalline calcite with rhombic cleavage, presumably indicating fractures partly filled with calcite.



*TVD section comparing the Danian and Chalk section of the Lavø-1, Karlebo-1 and Margretheholm- 1/1A wells. The figure also indicates levels in these wells where mud losses were*

p. 14 The Fjerritslev Fm. consists of varicolored (green, grey and olive) claystone with traces of organic material and dolomitic limestone stringers. The Fjerritslev Fm. is known to cause drilling problems, and this was also the case in the Karlebo wells. **The drill string became stuck twice while drilling the Fjerritslev Fm. with a deviation of ca. 40 degrees in Karlebo-1;** first time it was apparently differentially stuck to Early Cretaceous sands (had circulation) and it was possible to work loose; the second time the formation apparently collapsed as there was no circulation, and it was necessary to shoot off the bottom-hole-assembly. The Karlebo-1A well penetrated the Fjerritslev Fm. with a deviation of 20 degrees with few problems, so **hole angle may be related to drilling problems** in this formation.

# KARLEBO-1 & 1A ACTUAL DRILLING & EVALUATION PROGRAM



used until the stabilisers were past the conductor pipe. After this the RPM was increased to 100 and the flow to 600gpm. Due to the clay content of the formation washing out the mud weight increased rapidly. At approx 150m mud losses began of 20bbl/hr (dynamic). The loss rate gradually increased to 60bbl/hr dynamic and 20bbl/hr static. At 175m a 75bbl LCM pill was spotted and allowed to soak, Static losses slowed to 5bbl/hr, but quickly returned to the previous level on resuming drilling. Drilling continued with water, while sweeping the hole at each connection. Once the well was displaced to water the losses reduced to zero.

Hole was drilled to 206.5m, the hole was circulated clean with a high vis sweep, displaced to hi vis mud and the assembly pulled out after dropping the survey tool (miss-run). The stovepipe was cut off at the base of the cellar. 13 3/8" casing was run to 205m. A cement stinger was run in on 5"

p. 30	<p>DP to surface. The bit was run to bottom and drilling resumed. At 1367m approx mud losses of 180bbl/hr occurred. The hole was flow checked and static losses of 150bbl/hr observed. Hole was drilled to 1400m while diluting the mud system with water and mixing a LCM pill. The hole was circulated clean with a hi vis pill. The kelly was broken off and the bit pulled back to 1350m. A 90bbl LCM pill was pumped and displaced with 104 bbl of water and allowed to soak. The well was monitored on the trip tank and the losses were seen to reduce from 75bbl/hr to 20bbl/hr. The bit</p>
p. 31	<p>HWDP, 3 ½" DP to surface. The bit was run in to 1742m where it stood up. The hole was reamed to bottom and the bottom section logged with the LWD. Hole was drilled to 1813m where the ROP dropped dramatically. The bit was pulled out and found to be balled up with clay. RRB#7 DDS MDL643 6" (s/n S1H0367) was run in on the following BHA- Mud Motor, Float sub, X/O MWD, NM String Stab, 2 x 4 ¾" NMDC, 7 x 4 ¾" DC, Jar, 3 x 4 ¾" DC, Accelerator, 1 x 4 ¾" DC, 3 ½" HWDP, 3 ½" DP to surface. 6" hole was drilled to 1834m where the kelly was broken off and the hole wiped back to 1804m. Drilling continued to</p>
p. 31	<p>was broken off and the hole wiped back to 1804m. Drilling continued to 1839m where a drill break occurred. Bottoms up was circulated and the hole wiped back to 1800m to check for swabbing. Hole was drilled to 1845m where the ROP dropped to 1.2m/hr. The hole was flow checked and the bit pulled.</p>
p. 32	<p>ledges. At 1920m a vis pill was pumped and circulated to clean the hole. The bit was washed down to 1928m. As the bit was being washed down after making a connection the string became stuck with the bit at 1924m. Circulation was possible but the string could not be moved up or down. A KCL citric acid pill was spotted to break up the wall cake and the string worked and jarred but with no success. The hole was displaced to 9.4ppg mud and the string jarred. After applying 10 right hand turns of the rotary table and pulling up the string came free. Singles were pumped out to the base of the chalk and the string was pulled out. The directional tools and LWD were laid out and a rotary assembly was made up.</p>
p. 32	<p>x 3 ½" HWDP, 3 ½" DP to surface. The assembly was run in and the hole reamed to 1927m. While pulling up to make a connection the hole packed off and the pipe became stuck at 1916m. Circulation could not be established and the pipe could not be moved up or down. Jarring proved unsuccessful and it was decided to sever the string and sidetrack. Baker Atlas were mobilised and on arrival rigged up and ran in with a charge. The first charge was fired at 1898m but failed to sever the string. A second charge was run and fired at the bottom of the jars at 1843m. This succeeded in severing the string. The freed string was pulled out and the retrieved portion of the BHA was laid out.</p>

p. 33 HWDP, 3 ½” DP to surface. The bit was run in and washed down from 2250m to bottom. Hole was drilled without incident to 2372m where the hole was circulated and the bit pulled. At 2288m the bit became stuck but was worked free. The hole was circulated and the mud weight stabilised. Singles were pumped out to 1790m where stands were pulled.

p. 34 drilled to 2489m where it was decided to run intermediate logs. The hole was circulated and a wiper trip carried out to 1705m. The bit became stuck at 2289m but was successfully jarred free. After slipping line at the shoe the bit was run back to bottom and the hole circulated clean. A short trip was then carried out back to 2252m without incident. The hole was again circulated before pulling out to run logs.

p. 34 tools were function tested. The tools were then run in logging down. At 2236m the tools were picked up to test the wireline pick up weight. This was recorded at 5500lb and was found to match the predicted model. The tools were run in to 2240m where they stood up. Attempting to pull back was unsuccessful. There was no tension shown on the tension indicator below the rope socket of the tools, suggesting that the wireline was stuck somewhere above the tools. The wireline was pulled up in increments and the results plotted, indicating sticking between the shoe and the rope socket. Working the wireline failed to free it. A 4 3/8” overshot dressed with a 2 3/8” grapple was made up on 3 ½” DP and stripped over the wireline. The grapple was stripped in to the top of the fish and engaged on the logging tool. However the logging tools would not move with overpull of up to 45tonnes. It was not possible to unlatch from the fish as the drillpipe was rotating on the logging tool swivel. As the wireline snap connector was now inside the drillpipe and not accessible it was not possible to sever the wireline at the weak point on the rope socket. Therefore the bell nipple was rigged down and the annular lifted off in an attempt to access the drillpipe below the rotary table. However there was not enough clearance to install a set of elevators. The annular and bell nipple were reinstalled. The drillpipe was set in the slips in neutral weight and a tube clamp installed on the tube of the DP. The drillpipe was cut off approx 1.3m above the rotary table. The wireline snap connector was now accessible and this was disconnected. The wireline was connected to the hook and successfully pulled out of the rope socket and retrieved. The cut drillpipe was rigged up to allow circulating. The drillpipe was found to be capable of rotation as the swivel on the logging array could turn. While waiting on the arrival of cutting tools to sever the string down hole, the pipe was rotated and circulated slowly. A sharp increase in torque was seen and then a decrease to less than the previous level, indicating that either the drillpipe had parted from the fish or the fish had come free. The string was pulled out to investigate and the cable head and half of the swivel were recovered.

p. 35

The well was abandoned as per the abandonment programme.

# Kvols-1

Year: 1976  
Orientation: Vertical  
TD: 2641 m MD RT  
2622 m TVDSS  
Status: Plugged and abandoned

## Encountered problems during drilling

Information on drilling problems in the Kvols-1 well is based on information from the completion report:

Dansk Boresekskab A/S: Kvols-1, Completion report. December 1976. Report file no. 3474.

Furthermore, lithological information regarding the Fjerritslev Fm is extracted from the Geological End of Well Report for Kvols-2:

Petrolog: Geological End of Well Report for Kvols-2. Geothermal Exploration Well, Kvols-2, Kvols-2A. Report file no. 29342.

## Overview scheme (Figs. 1 and 2)

Drilling problems are presented in an overview scheme (Fig. 1) with relation to depth (MD) and lithostratigraphic units.

To the far right page numbers refer to sections in the completion report/End of Well Report where the particular drilling problem is explained. The relevant sections are extracted from the end of well report and presented subsequently. The extracts from the Kvols-1 completion report concentrate on geology-induced drilling problems and how they were solved. Technical problems with no connection to geological conditions are not included. Sections with geological information that may turn out helpful during the drilling process may be included.

# Kvols-1

Depth m MD	Period	Litho-stratigraphic unit	Drilling problem	Solution to drilling problem	Completion report
0					
100		Post Chalk Group			
200					
300	Upper Cretaceous	Chalk Group			
400					
500					
600					
700					
800					
900					
1000					
1100					
1200					
1300					
1400					
1500					
1600					
1700					
1800	Lower Cretac.	Vedsted Fm			
1900		Frederikshavn Fm			
		Borglum Fm			
		Haldager Sand Fm			
2000	Jurassic	Fjerritslev Fm			
2100			F-III		
2200			F-IIIb		
2300			F-Ib		
2400					
2500	Triassic	Gassum Fm	2500 Heaving shales	Mudweight increased	p. 38
		Vinding Fm			
2600		Oddesund Fm			

Figure 1. Overview of drilling problems related to depth and lithostratigraphic units in the Kvols-1 well.

## Comments

No drilling problems are mentioned in the Kvols-1 completion report with respect to the Fjerritslev Fm. Heaving shales are noted in the Gassum Fm.

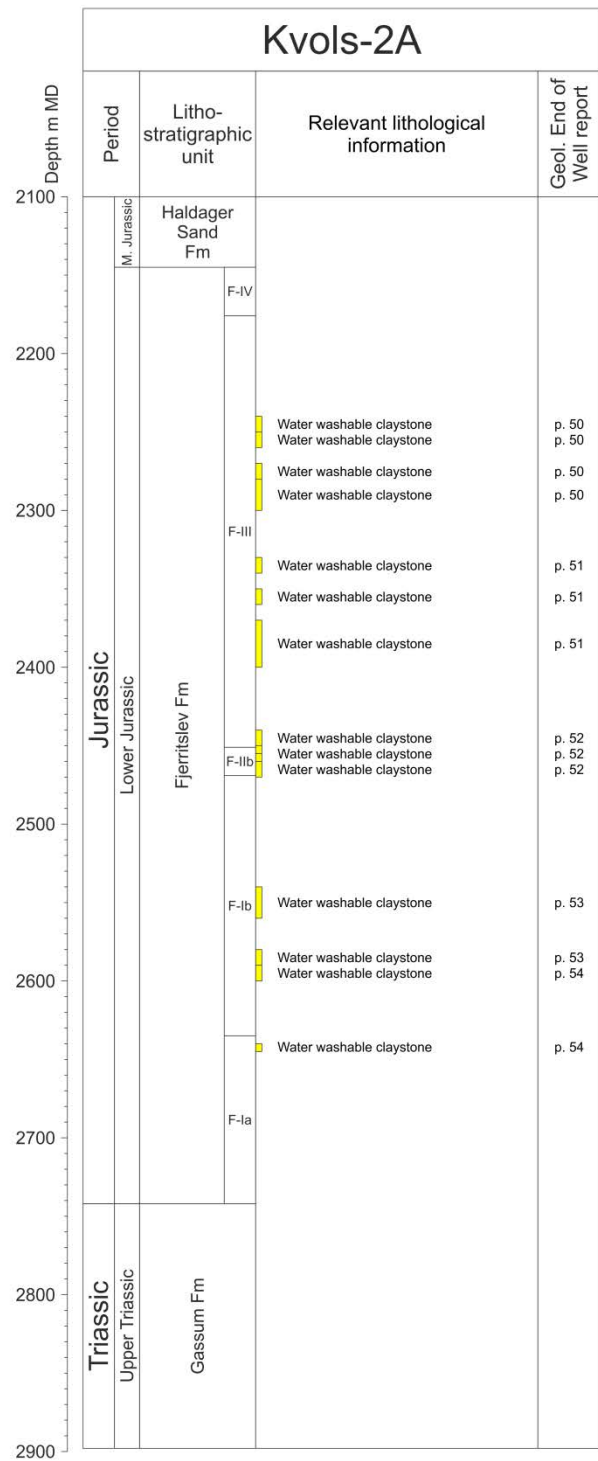
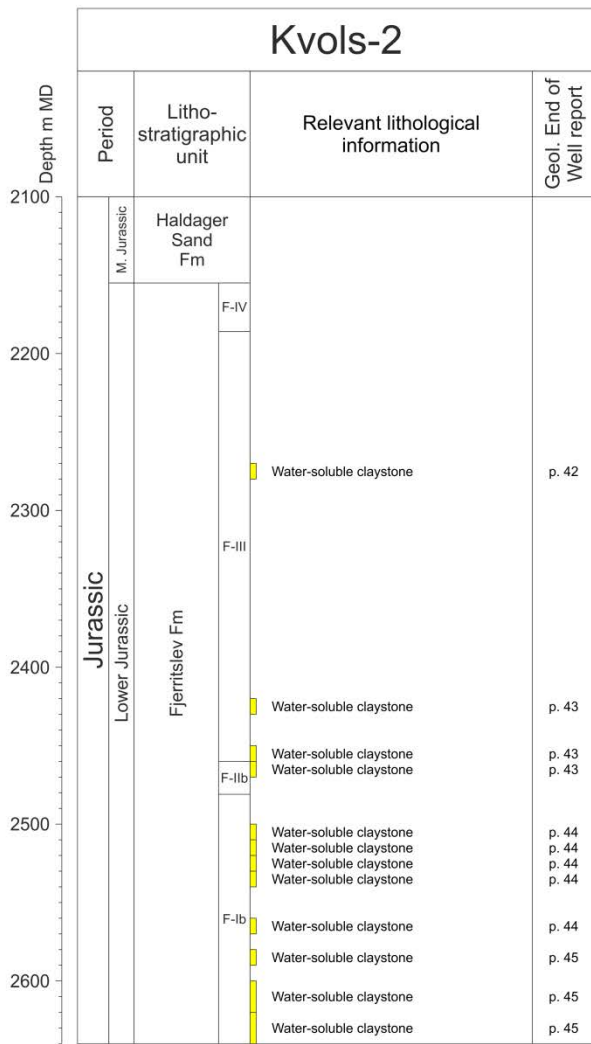


Figure 2. Overview of relevant lithological information related to depth and lithostratigraphic units in the Kvols-2 and -2A wells.

### Comments

With respect to the Fjerritslev Fm in the Kvols-2 and -2A wells soluble claystones are present in several sections and may cause problems. Sticky and plastic clays are present in the Frederikshavn Fm, but are not mentioned in the Fjerritslev Fm.

## Extracts from the completion report (Report file no. 3474)

### Drilling Summary

p. 45      The section of 8 1/2" hole from 3460' to 8664' was drilled with no problems until heaving shales and a resultant slow ROP were noted at a depth of approximately 8200'. Mud weight was increased to 10 lb/gal and there were no further difficulties. A logging program was run

# Lavø-1

Year: 1959  
 Orientation: Vertical  
 TD: 2441 m MD RT  
 2413 m TVDSS  
 Status: Plugged and abandoned

## Encountered problems during drilling

Information on drilling problems in the Lavø-1 well is based on information from the completion report:

DAPCO: Completion report. Well: LAVØ-1, April 1959. Report file no. 8623.

## Overview scheme (Fig. 1)

Drilling problems are presented in an overview scheme (Fig. 1) with relation to depth (MD) and lithostratigraphic units.

To the far right page numbers refer to sections in the completion report where the particular drilling problem is explained. The relevant sections are extracted from the final well report and presented subsequently. The extracts from the completion report concentrate on geology-induced drilling problems and how they were solved. Technical problems with no connection to geological conditions are not included. Sections with geological information that may turn out helpful during the drilling process may be included.

### Lavø-1

Depth m MD	Period	Litho-stratigraphic unit	Drilling problem	Solution to drilling problem	Completion report
0					
20		Post Chalk Group	Circulation broke out	Conductor pulled, 12 1/2" hole opened to 22"	p. 26, 37
89			Mud loss	Dropping mud weight, pumping in peat moss	p. 26, 37
100					
200					
300					
400					
500					
600					
700					
800					
900					
1000	Cretaceous	Chalk Group			
1100					
1200					
1300					
1400					
1500					
1600					
1700					
1800					
1900					
2000					
2100	Lower Cretaceous				
2200		Flemislev Fm	Karlebo Member		
2300			Gassum Fm		
2400		Vinding Fm			
2500	Triassic				

Figure 1. Overview of drilling problems related to depth and lithostratigraphic units in the Lavø-1 well.

Extracts from the completion report (Report file no. 8623)

p. 26	20/1/59	16	0	20	HO 22"	Circulation broke out around conductor pulled
						conductor, opened 12 1/2" hole to 22" from 0-16 m,
						ran 12 m of 18" pipe & cemented with 40 sacks
						of rapid construction cement about 16 meters, cement in place at 1830, waiting on cement.

p. 26	21/1/59	212.5	196.5	21	2	H&F1 17 1/2" 088-3J 12 1/2"	Drilled out conductor, drilled to 212.5 m with
							12 1/2" bit, opened hole 16-89 m with 17 1/2" H10,
							lost returns, mixing mud & peat moss, mud wt.
							10.2, visc. 67, W.L. 12, sand 3%, survey 0° 15'

p. 27	29/1/59	1089	88	29	10	IT5 8-5/8"	Survey, trip & check bop., survey 0° 30' at 1055
							m, mud wt. 10.5, visc. 58, w.l. 4.2, sand 1%,
							pH 9.5, sal. 1200 ppm.
	30/1/59	1151	62	30	11 12 13	8-5/8" 8-5/8" 8-5/8"	Trips, survey, bop drill, now drilling on
						cone junk with bit # 13, survey 0° 15' at 1092 m	
						0° 30' at 1130 m, mud wt. 10.4, visc. 45, w.l.	
						3.9, sand 1%, pH 10.2, sal. 1300 ppm.	
31/1/59	1210	59 m	31	14 15	8-5/8" 8-5/8"	Trips, survey & check bop, serviced junk sub &	
						recovered large percentage of cone, survey	

p. 32	1/3/59	-	-	60	-	-	Hung drill pipe at 215 m & plugged with 90
							sacks rapid construction cement, in place at
							1000 hours. Felt for plug at 2100 hours & found
							top at 197 m. Tearing out. Placed 10 sack ce-
						ment plug in top of 13-5/8" casing & welded	
						1/2" steel plate on top. Laid mast down at	
						1330 hours. Tearing out. Well plugged and	
						abandoned 2400 hours 1/3/59.	

p.  
37

The well was spudded on January 19, 1959. At 16 meters circulation broke out around the hand set conductor which was pulled. The hole was opened to 22 inches and 18-1/2 inch conductor pipe was run to 16 meters and cemented with 40 sacks cement. A 12-1/4 inch hole was drilled to 212.5 meters and opened up to 17-1/2 inches. At 89 meters, while opening up the hole, circulation was lost but was regained after dropping the mud weight and pumping in some peat moss. The hole was opened up to 210.54 meters and was cemented with 520 sacks. After standing cemented for 24 hours, the casing shoe was drilled out with a 12-1/4 inch bit. This bit was pulled and an 8-5/8 inch bit substituted.

At a depth of 1150 meters, a cone was lost off a Reed bit. A Hughes W7R bit was run in conjunction with a junk sub and the cone was milled up and most of it was recovered in the junk sub.

No further drilling difficulties developed while drilling to total depth.

p.  
38

A cement plug was placed at 1903 meters with 80 sacks of rapid construction cement. However, when feeling for the plug, no cement could be found to a depth of 1953 meters. When pulling up after feeling for the plug, the pipe hung up in several spots and it was decided not to attempt to put another plug at this depth. A second plug was placed at 215 meters around the casing shoe with 90 sacks of rapid construction cement. When feeling for this plug nine hours later, the cement had not set up and was circulated out of the hole. A third plug was placed again at 215 meters with 70 sacks of rapid construction cement. Top of this plug was found at 197 meters. A ten sack cement plug was placed from the cellar floor to a depth of four meters. A one-half inch steel plate was welded across the top of the 13-3/8 inch casing.

The well was abandoned at 2400 hours, March 1, 1959.

# Margretheholm-1/1A

Year: 2002  
Orientation: Deviated  
TD: 2686 m MD RT  
2685.4 m TVDSS  
Status: Completed for production

## Encountered problems during drilling

Information on drilling problems in the Margretheholm-1/1A well is based on information from the final well report:

Dong Efterforskning og Produktion A/S: Final well report. MAH-1, MAH-1A (Margretheholm), February 2003. Report file no. 19622.

## Overview scheme (Fig. 1)

Drilling problems are presented in an overview scheme (Fig. 1) with relation to depth (MD) and lithostratigraphic units.

To the far right page numbers refer to sections in the final well report where the particular drilling problem is explained. The relevant sections are extracted from the final well report and presented subsequently. The extracts from the final well report concentrate on geology-induced drilling problems and how they were solved. Technical problems with no connection to geological conditions are not included. Sections with geological information that may turn out helpful during the drilling process may be included.

# Margretheholm-1/1A

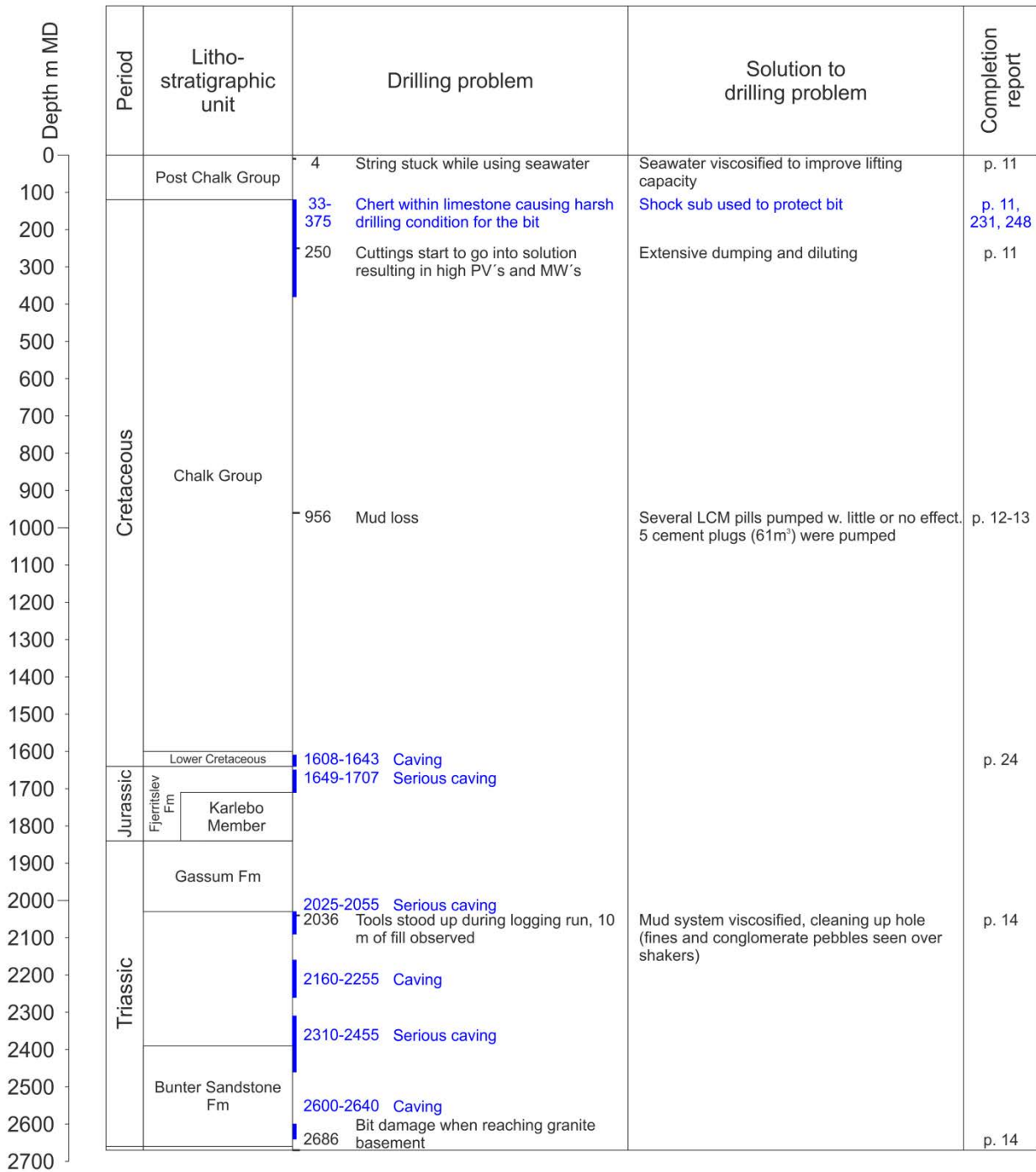


Figure 1. Overview of drilling problems related to depth and lithostratigraphic units in the Margretheholm-1/1A well.

## Extracts from the final well report (Report file no. 19622)

### Operations summary

p. 11	<b>3</b>	<b>17-1/2" Section</b>	33 – 705 metres.  The 30" shoetrack and rathole were drilled out using seawater. The construction cement proved difficult to drill, after 4 m of drilling the string became temporarily stuck. At first junk was suspected. When investigating it was found that the seawater was unable to carry out the small pebbles from the construction cement. The seawater was then viscosified to improve the lifting capacity.
p. 11			The drilling was very rough throughout the section and severe vibration and bouncing of the drill string was experienced. Chert was encountered from beneath the 30" shoe at 33 metres, within the limestone, to 115 metres and to a much lesser degree within the chalk to 575 metres. A 9 1/2" shock sub is invaluable to protect the bit and the top drive when drilling under such conditions.
p. 11			From approx. 250m the cuttings started to go into solution. Resulting in high PV's and MW's. Extensive dumping and diluting was required. This created a logistical problem with approx. 30 tank trucks hauling 1000 m <sup>3</sup> of "dumped" mud off location during the following 4 days.
p. 12	<b>4</b>	<b>12-1/4" Section</b>	705 – 2686 metres.  At 956 m a short drilling break was followed by total losses. Several LCM pills were pumped to cure the losses, with little or no success. Continued drilling with 20 to 30 m <sup>3</sup> /h dynamic losses.  When making a connection at 973 m the well started flowing. The well was shut in and circulated over the choke. The flow was concluded to be supercharging of the formation and drilling resumed with dynamic losses of 20-35 m <sup>3</sup> /h. The back flow rate when making connections was 40-60 m <sup>3</sup> /h.
p. 13			At surface approx. 3m of LCM was found above the Teledrift tool. It is suspected that the LCM pill was slightly underdisplaced. The bit was dull graded 1-1-WT-A-E-IN-LN-PP.  The Teledrift tool was laid out and the assembly run back to bottom to make a last attempt of curing the losses with LCM. The attempt was unsuccessful and it was decided to pump thixotropic cement.  A total of 5 plugs had to be pumped and bull headed to cure the losses, a total of 61 m <sup>3</sup> cement was pumped.

p. 13	<p>At 1919m the Top drive lube oil system failed, and the assembly was pulled out of hole for a bit change while waiting for spare parts for the TDS.</p> <p>At 313 m a repair of the Top Drive was achieved and it was decided to run the bit back to bottom and resume drilling.</p> <p>The assembly continued to drill ahead from 1919 m but, when reaming a stand prior to connection at 2219m, the assembly was unable to get back to bottom and the string kept stalling out 1 m off bottom. The assembly was pulled out of hole and it was found that the bit had lost one cone downhole.</p> <p>A junk run was performed with a 12 ¼” MGGH+ junk bit. When reaming back to bottom the string stalled out 1 m off bottom. The string was worked to bottom but no evidence of junk on bottom. It was concluded that the cone was sitting 1 m above bottom. Worked past the spot several times until the torque disappeared. When back at bottom it was evident that the cone was now located at the bottom of the hole. Unsuccessfully attempted to drill the junk.</p> <p>A reverse circulating junk basket was run, but failed to catch the junk.</p>
p. 14	<p>An 8 m<sup>3</sup> kick-off plug was then set from 2219m to 2135m.</p> <p>A 12 ¼” kick-off assembly, FGXi milled tooth bit, Motor with 1.15 deg bend and MWD was run. The well was successfully sidetracked at 2147m. Continued drilling to 2252m.</p> <p>A 12 ¼” MA89BHPXER PDC bit was run and drilled with an average ROP of 12.5 m/h to TD of 2686m. The bit suffered severe damage – probably when reaching/drilling the granite basement. Drilling operations continued at low ROPs in order to verify that the granite basement had indeed been penetrated thus avoiding another bit run.</p>
p. 14	<p>On the first logging run the tools stood up at 2036m. A check trip was performed and the entire mud system viscosified. 10m of fill was observed and while cleaning up the hole large volumes of both fines and conglomerate pebbles were seen over the shakers.</p> <p>The check trip assembly was pulled out of hole with no washing or reaming required.</p>
p. 14	<p><b>5 Clean out and Completion</b></p> <p>A clean out assembly incorporating a scraper and a brush was run and the hole displaced to clean water over 325 mesh shaker screens.</p> <p>A 9 5/8” test completion string with gas lift check valves was run to 599m. The tubing hanger landed off and pressure tested to 100bar.</p> <p>Rig release 00:00 15/07/02</p> <p>Well Handed over to Well services:</p> <p>Planned time (BCTP): 71.0 hrs.</p> <p>Actual time: 59.5 hrs.</p>

## Geological and geophysical data

p. 24

### EARLY CRETACEOUS (LATE ALBIAN-LATE BARREMIAN)

**Lower Cretaceous undifferentiated:** 1607.6-1643.8 m (1597.9-1634.0 m TVDMSL)

The top of this sequence of siltstone and claystone with local sandstone occurrences, claystone gradually increasing downwards, is picked at the base of the Arnager Greensand sandstone bed. Fairly distinct log changes are observed at this depth, particularly one that is typical for the rest of the hole: The caliper log shows that claystone dominated intervals are caved, sometimes severely, whereas the hole is in gauge or has mudcake in sandstone dominated intervals.

p. 25

### EARLY JURASSIC (TOARCIAN-PLIENSBAKIAN)

**Fjerritslev Formation:** 1648.4-1706.7 m (1638.6-1696.9 m TVDMSL)

The Fjerritslev Fm. is characterised as a sequence of almost pure claystone marked by serious caving, high GR values and high resistivities.

p.28

### LATE-EARLY TRIASSIC

**Maglarp Formation:** 2025.5-2367.7 m (2015.7-2357.7 m TVDMSL)

The Maglarp Fm. is also an intense interbedding of claystones, siltstones and thin sandstones. Claystone caving in the formation is worse than in the Kågeröd Fm. but less severe than in the Fjerritslev Fm. The top of the formation was picked at the top of a fairly thick, badly caved claystone unit.

p.29

### EARLY TRIASSIC

**Bunter Sandstone Formation:** 2367.7-2640.0 m (2357.7-2629.8 m TVDMSL)

The Bunter Sandstone Fm. is a sequence of claystones, siltstones and sandstones characterised by being dominated by claystone in the upper  $\frac{1}{3}$  and the lower  $\frac{1}{4}$  whereas the rest is sandstone dominated. GR values and sonic velocities are generally at a slightly higher level than in the Maglarp Fm. and increase slightly down through the formation. Claystone caving is fairly bad. The top of the formation was picked at the top of the claystone-dominated part, marked by a GR increase and drops in sonic velocity and resistivities.

p. 30

PRECAMBRIAN

**Basement:** 2684.4-2686.0 m (2674.2-2675.8 m TVDMSL)

The basement brought drilling of the well to a stop after 2 m as the bit got worn out completely. Therefore, the main indicator of the top of the unit is the ROP curve combined with a change in the character of the cuttings samples.

The basement consists of weathered and fresh *granite/gneiss*: Pink to orange brown, light grey, very hard, with angular fracture, crystalline quartz and feldspar with some mica.

p. 31

The basement consists of weathered and fresh *granite/gneiss*: Pink to orange brown, light grey, very hard, with angular fracture, crystalline quartz and feldspar with some mica.

**9 Pore Pressure and Total Gas**

Pore Pressure

The composite pressure plot for the well is shown in Figure 3.9.1.

The pore pressure gradient was close to normal hydrostatic, equivalent to 1.03 s.g. mud weight, throughout the well.

# Actions and Lessons Learned Tracking System

p. 230

Det@il - Action and Lessons Learned Tracking System

Page 1 of 1

Close

## 10 Cleanout of 30" conductor on MAH-1

<b>Originator:</b>	Ewan Anderson	<b>Project:</b>	Geothermal - Operations	
<b>Suggestor:</b>	MAH-1 Drilling Supervisor	<b>Work Site:</b>	Deutag T61	
<b>Event Date:</b>	31/05/2002	<b>Well:</b>	MAH-1	
<b>Work Operation:</b>	Drilling Operations	<b>Action Party:</b>	Cliff Law	
<b>Work Type:</b>	Make Selection	<b>Service Company:</b>	Make Selection	
<b>Applicability</b>	<b>Rig Type:</b>	Make Selection	<b>Project Stage:</b>	Not Assigned Phase
	<b>Area &amp; Field:</b>	This Well Only	<b>Activity &amp; Phase:</b>	Not Assigned

### Description:

The 30" conductor had been pre-set in place by a construction firm. It had been cemented using an industrial concrete which contained gravel and pebbles. This proved problematic to drill, and especially to cleanout, as it was difficult to lift out the large "cuttings" inside the 30".

### Suggestion:

Do not use this type of concrete for the conductor on future wells. A simple oilfield cement will be much easier to drill out.

### Immediate Action Taken:

Took time to free stuck string. Cleaned hole using bentonite Hi-Vis sweeps. Pulled out to check condition of bit (no damage). Viscosified seawater system to mud to ensure best hole cleaning.

### Conclusions:

Stuck pipe due to gravel used in cementation of conductor by 3rd party contractor. The 3rd party contractor had been requested to use smooth cement prior to the job.

### Recommendations:

Never use gravel in this process in future. Better control from Dong and E2 when cementing any future conductors.

### Learning Points Implemented:

There were no problems of this nature on FFC-1 as the cement used for the conductor was homogeneous.

### Comments:

### Files Attachments:

There are no file attachments

p.231

Det@il - Action and Lessons Learned Tracking System

Page 1 of 1

Close

## 11 Top hole drilling on MAH-1

<b>Originator:</b>	Ewan Anderson	<b>Project:</b>	Geothermal - Operations	
<b>Suggestor:</b>	MAH-1 Drilling Supervisor	<b>Work Site:</b>	Deutag T61	
<b>Event Date:</b>	31/05/2002	<b>Well:</b>	MAH-1	
<b>Work Operation:</b>	Construction/Installation	<b>Action Party:</b>	Not Required	
<b>Work Type:</b>	Make Selection	<b>Service Company:</b>	Make Selection	
<b>Applicability</b>	<b>Rig Type:</b>	Make Selection	<b>Project Stage:</b>	Not Assigned Phase
	<b>Area &amp; Field:</b>	This Well Only	<b>Activity &amp; Phase:</b>	Not Assigned

### Description:

The top hole drilling on MAH-1 was problematic. The hard formation below the shoe (32.5m) caused the string to bounce a lot and ROP was very slow. The hole was not yet deep enough to get optimal weight to the bit.

### Suggestion:

For future wells, consider setting conductor deeper (100m). Also ensure conductor is drilled out before rig reaches location.

### Immediate Action Taken:

Took time to deepend hole and allow BHA weight to permit more aggressive drilling.

### Conclusions:

A deeper start would reduce drill string bouncing

### Recommendations:

As suggestion

### Learning Points Implemented:

Not yet

### Comments:

### Files Attachments:

There are no file attachments

**Close**

**13 Vibration in string and rig due to top hole drilling.**



<b>Originator:</b>	Ewan Anderson	<b>Project:</b>	Geothermal - Operations
<b>Suggestor:</b>	MAH-1 Drilling Supervisor	<b>Work Site:</b>	Deutag T61
<b>Event Date:</b>	01/06/2002	<b>Well:</b>	MAH-1
<b>Work Operation:</b>	Drilling Operations	<b>Action Party:</b>	Cliff Law
<b>Work Type:</b>	Maße Selection	<b>Service Company:</b>	Deutag

<b>Applicability</b>	<b>Rig Type:</b>	Make Selection	<b>Project Stage:</b>	Not Assigned Phase
	<b>Area &amp; Field:</b>	This Well Only	<b>Activity &amp; Phase:</b>	Not Assigned

**Description:**

The hard top hole drilling in MAH-1 caused a lot of vibration in the string and top drive. At connections the vibration caused the top drive components to excessively M/U. This caused problems breaking out the saver sub. Also time was required to check the top drive and derrick bolts and fastenings in case any had worked loose.

**Suggestion:**

Consider using 2 x shock subs on FFC-1 well in Sweden to reduce vibration.

**Immediate Action Taken:**

Used rig tongs to break out top drive, (extra time).  
Checked derrick and top drive for loose bolts.

**Conclusions:**

One shock sub was run on FFC-1. There was far less vibration during top hole drilling of this well. The formation was quite similar to MAH-1. It is possible that the shock sub used on MAH-1 was not functioning correctly

**Recommendations:**

The use of 2 shock subs may cause detrimental string harmonics. If vibrations are serious in future wells, POOH & change shock sub.

**Learning Points Implemented:**

For future

**Comments:**

**Files Attachments:**

There are no file attachments

**Close**

**77 Bit choice**



<b>Originator:</b>	Geothermal Drilling Supervisor	<b>Project:</b>	Geothermal - Operations
<b>Suggestor:</b>	Kåre Pedersen	<b>Work Site:</b>	Deutag T61
<b>Event Date:</b>	11/07/2002	<b>Well:</b>	MAH-1
<b>Work Operation:</b>	Drilling Operations	<b>Action Party:</b>	Smith International Norway AS
<b>Work Type:</b>	Normal	<b>Service Company:</b>	

<b>Applicability</b>	<b>Rig Type:</b>	Same type of Rig	<b>Project Stage:</b>	Not Assigned Phase
	<b>Area &amp; Field:</b>	This Well Only	<b>Activity &amp; Phase:</b>	Not Assigned

**Description:**

ROPs through the jurassic and triassic sequences were rather disappointing.

**Suggestion:**

Once below the chalk a PDC bit should be run to improve drilling performance

**Immediate Action Taken:**

PDC run in lower triassic with a marked improvement.

**Conclusions:**

The PDC was run on FFC-1 successfully

**Recommendations:**

As suggestion

**Learning Points Implemented:**

Yes

**Comments:**

**Files Attachments:**

There are no file attachments

Close

79 Mud selection

Originator:	Geothermal Drilling Supervisor	Project:	Geothermal - Operations
Suggestor:	Kåre Pedersen	Work Site:	Deutag T61
Event Date:	11/07/2002	Well:	MAH-1
Work Operation:	Drilling Operations	Action Party:	Not Required
Work Type:	Normal	Service Company:	MI Denmark A/S

Applicability	Rig Type:	Same type of Rig	Project Stage:	Not Assigned Phase
	Area & Field:	This Well Only	Activity & Phase:	Not Assigned

Description:

Due to losses of 2-4m<sup>3</sup> per hour while drilling with glydrill mud additional costs were incurred. It was originally thought that the disposal costs would be based on cuttings being classed as class 2 soil. In the end it turned out to be classified as class 4 with huge cost implications.

Suggestion:

It should be investigated for future wells if a polymer mud system would suffice. My personal opinion is that as long as it can be inhibitive with K+ and glycol and the fluid loss can be kept at 5 or below it would do the job. Alternatively a bentonite based system could be even better.

Immediate Action Taken:

Attempting at all times to limit losses and discharges by developing a small mud processing facility.

Conclusions:

Disposal costs were much higher than expected

Recommendations:

Account for the disposal costs in AFE or investigate using a cheaper mud system

Learning Points Implemented:

Not yet

Comments:

Files Attachments:

There are no file attachments

Back

94 BHA selection

Originator:	Geothermal Drilling Supervisor	Project:	Geothermal - Operations
Suggestor:	Kåre Pedersen	Work Site:	Deutag T61
Event Date:	18/07/2002	Well:	MAH-1
Work Operation:	Drilling Operations	Action Party:	Not Required
Work Type:	Make Selection	Service Company:	Deutag

Applicability	Rig Type:	Make Selection	Project Stage:	Not Assigned Phase
	Area & Field:	This Well Only	Activity & Phase:	Not Assigned

Description:

The chalk drills best with weight on bit as the main parameter. It is thought that more weight on bit would result in higher ROPs.

Suggestion:

For future wells it is recommended to run more drill collars.

Immediate Action Taken:

18 DCs has been ordered vis Deutag for FFC-1

Conclusions:

More weight could help

Recommendations:

Run more drill collars on the next well FFC-1

Learning Points Implemented:

Yes. Seemed to help with ROPs

Comments:

Files Attachments:

There are no file attachments

[Back](#)

**103 Conductor cement**



<b>Originator:</b>	Geothermal Drilling Supervisor	<b>Project:</b>	Geothermal - Operations	
<b>Suggestor:</b>	Kåre Pedersen	<b>Work Site:</b>	Deutag T61	
<b>Event Date:</b>	19/07/2002	<b>Well:</b>	MAH-1	
<b>Work Operation:</b>	Drilling Operations	<b>Action Party:</b>	Not Required	
<b>Work Type:</b>	Normal	<b>Service Company:</b>	Make Selection	
<b>Applicability</b>	<b>Rig Type:</b>	Same type of Rig	<b>Project Stage:</b>	Operations Phase
	<b>Area &amp; Field:</b>	This Well Only	<b>Activity &amp; Phase:</b>	Not Assigned

**Description:**

Drilling out the conductor proved difficult due to pebbles in the cement.

**Suggestion:**

Ensure neat cement without pebbles is used for future conductors. For MAH-2 it is important to drill out the conductor shoe with hivi mud to lift pebbles out.

**Immediate Action Taken:**

Pumped Hi vis pills and continued drilling.

**Conclusions:**

Pebbles from construction cement caused the drill string to become temporarily stuck.

**Recommendations:**

Do not use hardcore in conductor cement. If there is known to be hardcore in the cement, use adequate hi vis pills to keep the hole clean.

**Learning Points Implemented:**

**Comments:**

**Files Attachments:**

There are no file attachments

# Margretheholm-2

Year: 2003  
Orientation: Deviated  
TD: 3300 m MD RT  
2757.4 m TVDSS  
Status: Completed for production

## Encountered problems during drilling

Information on drilling problems in the Margretheholm-2 well is based on information from the end of well and final well reports:

Schlumberger: End of Well Report. Well: Margretheholm-2 (MAH-2). December 2003. Report file no. 27981.

GEO-data GmbH: Final Well Report. Geological Report Summary for the Well Margretheholm-2, MAH-2. August 2011. Report file no. 25430.

## Overview scheme (Fig. 1)

Drilling problems are presented in an overview scheme (Fig. 1) with relation to depth (MD) and lithostratigraphic units.

To the far right page numbers refer to sections in the end of well and final well reports where the particular drilling problem is explained. The relevant sections are extracted from the final well report and presented subsequently. The extracts from the end of well report (Report file no. 27981) concentrate on geology-induced drilling problems and how they were solved. Technical problems with no connection to geological conditions are not included. Sections with geological information that may turn out helpful during the drilling process may be included.

# Margretheholm-2

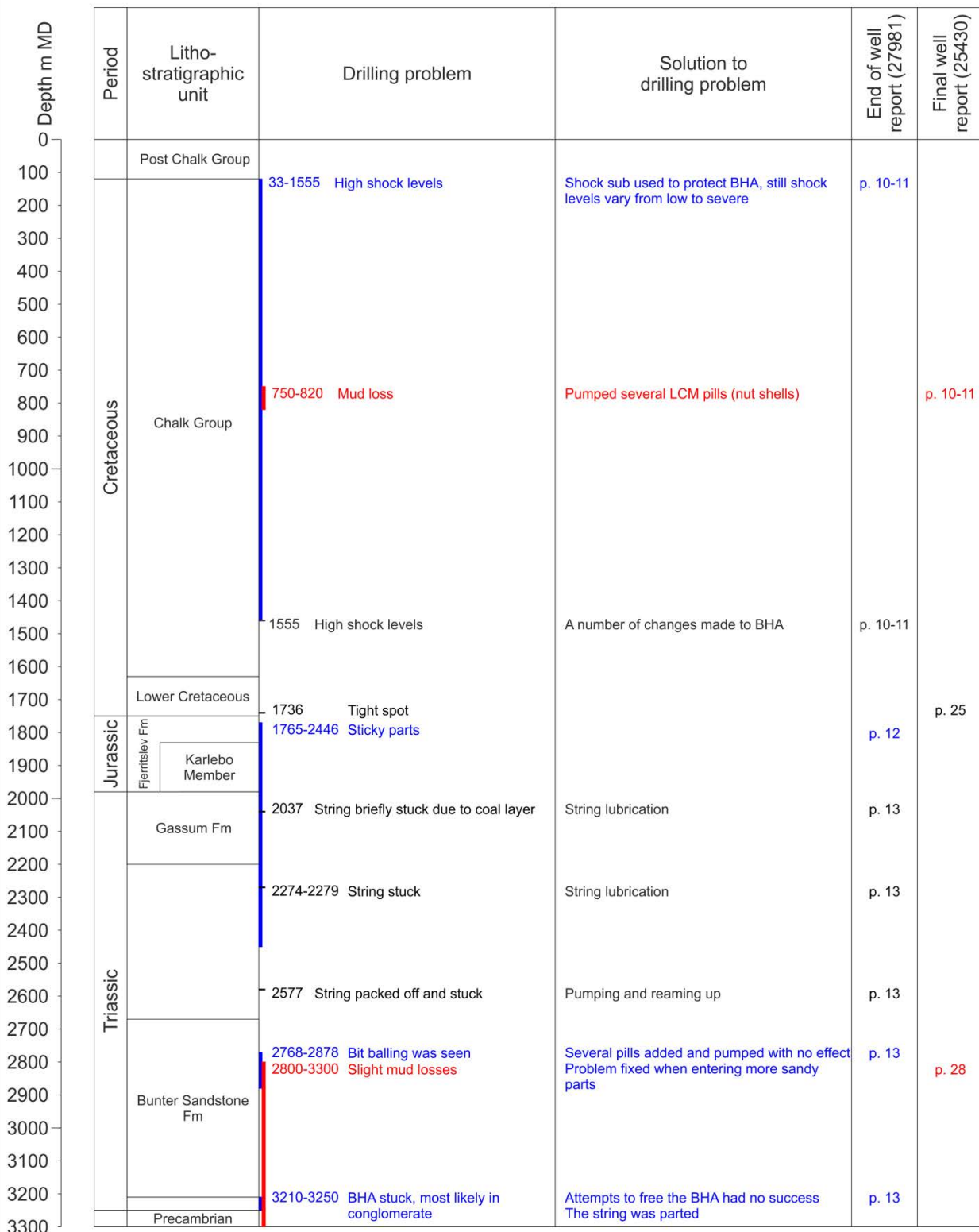


Figure 1. Overview of drilling problems related to depth and lithostratigraphic units in the Margretheholm-2 well.

## Extracts from the end of well report (Report file no. 27981)

### Directional Drilling Summary

#### 17.5" Hole Section

p. 10	<b>BHA 1 (33m – 975m)</b> The first BHA also included a shock sub to lower the high shocks expected in the upper part of the well, but even with this in the string, shocks were seen all the way through the run in a range from low to severe. While drilling the first 150m prior to kick off, the magnetic interference of the surveys was
p. 10	<b>BHA 3 (975m – 1177m)</b> Towards the end of the run when the formation became very hard there was an increase in the shocks and vibrations recorded from the BHA. At surface the bit was badly damaged with the entire second row of teeth broken off. It would appear from the wear characteristics that the bit was subjected to too much weight even though the recommended limits were never exceeded.
p. 10	<b>BHA 4 (1177m – 1555m)</b> Due to the high shock environment the motor, MWD and Jar were all replaced at the end of this run.
p. 10	<b>BHA 5 (1555m – 1765m)</b> Due to the high shock levels, which could not be controlled during the previous run a number of changes were made to the BHA. Firstly the bend was decreased to 0.78° as the amount of steering was minimal and secondly an 11 3/4" stabiliser was run on top of the MWD. There was a notable decrease in the shocks throughout the run.
p. 11	Directionally, 21% of the section was steered to control the drop in inclination of 0.6°/30m and the right hand walk of 0.8°/30m observed in the limestone. In the underlying sandstone and claystone the walk rate decreased slightly while the assembly built at a rate of 0.4°/30m.  Static and dynamic losses continued throughout this run and some LCM pills were spotted. Once through the hard Limestone the drilling rate increased to 20m/hr in the sand and 8 m/hr in the claystone. To maintain the stability of the claystone it was necessary to increase the mud weight to 1.22sg and increase the KCl concentration in the mud. Having done this it was not possible to control the losses therefore the section TD was set at 1765m. The hole condition was very good and no problems were observed while pulling out. The motor was in good condition as was the bit.
p. 11	<b>Lessons Learned / Recommendations</b>  High shocks were evident through the hard limestone drilled with BHA 3 and 4. It was not possible to eliminate these by manipulating the drilling parameters. In run 5 an 11 3/4" stabiliser was picked up above the MWD and the motor bend was decreased to 0.78°, which greatly reduced the shocks. This configuration should be run where possible but it is not recommended that a larger stabiliser be used above the MWD as this could significantly affect the steerability of the system.

## 12 1/4" Hole Section

p. 12

### **BHA 6 (1765m – 2446m)**

Since the well was in the tangent section the BHA was rotated with 60RPM and 8 to 14Tons on the bit. The BHA was designed to give some natural build when rotating in order to reduce the need for sliding. Some corrections on the Azimuth was attempted, this was made difficult, as the formation was very sticky. It was then attempted to force the build in rotary to minimise steering in the next part of the well. This was partly successful, it was seen that 0.6 ° /30m was achievable when 14 Tons WOB was used.

p. 13

### **BHA 9 (2768m –2878m)**

A PDC bit was picked that was the same as used in BHA 7 and a GT motor with a 0.77deg bend. The NM Pony above the motor was taken out to give less build in rotary as the inclination was already close to 58deg. With this assembly there were no problems rotating. Bit balling was seen and pills were added and pumped but this did not ease the problems. The Pump Rate was optimised to get as high HSI as possible. The problem was eventually fixed when the formation was getting into the more sandy parts. The Drilling parameters were constantly monitored and drill-off tests were performed several times.

Near to the end of the run sliding and reaming was attempted as the BHA was building too much, up to 1.5 degrees / 30m was seen. Sliding was not really an option but was still tried out but without any success, there was also a possibility of getting stuck. Rotating continued to see if it was possible by working the parameters to get a dropping tendency but this was difficult with any acceptable ROP. The decision was made to pull out of hole and modify the BHA before getting too far above 60 degrees in inclination. When out of hole the bit was found to be balled up.

p. 13

### **BHA 10 (2878m –2978m)**

A PDC bit was picked that was more aggressive and a rotary assembly was to be used to be able to drop down to the planned 60deg.

Running in was attempted the first time and at 2037m coal was hit and the string became briefly stuck. When free, maintenance was required on the top drive and block in the shoe. When running in hole the second time a different approach was used, to lubricate through the coal. This was effective and the string went through the coal layers with only 4tons weight through the problem area. At 2274-2279m in the Male formation the string had to be lubricated through again when it was partly stuck. At 2577m and down the string was packed off and stuck with no pipe movement either up or down possible. This was fixed in a gentle way and after a while pumping and reaming up was possible. Before running in again the well was circulated clean with high RPM up and sliding down. Washing to bottom was continued with on going problems.

The ROP on bottom was not good and different tactics were tried. It was noticed that the full gauge stabiliser was hanging up and this was holding back the ROP until we hit the top sand reservoir at 2897m. In the sand reasonable performance was seen from the bit and BHA, but as we exited the sand into a new claystone the ROP came down to 1 m/hr. The BHA was then pulled to change out the bit. This rotary assembly dropped more than planned with an average drop rate of 1.75deg/30m. Both bit and first stabiliser being underage upon retrieval out of hole can partly explain this.

p. 13

### **BHA 12 (3069m – 3300m)**

A rotary drop BHA was picked up as planned to drill the remainder of this section. The BHA performed well and the final TD was reached at 3300m. The final TD was below the reservoir as planned in order to provide a sump for the wireline logging tools. This placed the well in a conglomerate sequence. At TD the last stand was backreamed and a connection made. During the connection the pipe became mechanically stuck. It is likely that instability in the conglomerates caused the BHA to become stuck. The BHA subsequently became differentially stuck. Attempts were made to free the BHA but with no success and the string was parted.

## Extracts from the final well report (Report file no. 25430)

### Technical summary

p. 25 Losses/Gains:

At 750 m 42 m<sup>3</sup> dynamic losses, reducing to 8 m<sup>3</sup>/hr. At 820 m reducing to zero. Between 750 m and 820 m 167 m<sup>3</sup> losses. Ongoing dynamic losses to depth 1765 m appr. 8-14 m<sup>3</sup>/hrs. Static losses between 5-10 m<sup>3</sup>/hrs. Total volume lost in hole: 1091 m<sup>3</sup>

p. 25 Problem Zones:

Tight spot at 1736 m. Overpull up to 25t.

p. 28 Losses/Gains:

From 2800 m (Early Triassic) to 3300 m (TD) slight losses of about 250 l/hr.

p. 29 Reaming:

Date	Depth	Operation
20.05.03	2315 – 2446 m	Reamed in hole, due to previous under-gauge bit
22.05.03	2531 – 2634 m	Reamed in hole
25.05.03	2720 – 2768 m	Reamed to bottom
29.05.03	2038 m 1980 – 2878 m	Attempt to ream down – no go (top drive stalling out, POOH to Casing shoe for repairing TDS) Washed down to bottem on several tight spots
01.06.03	1878 – 2780 m 2826 m	Tight spots encountered correspond to sandstone formation (excessive filter cake), washed and reamed down
14.06.03	2730 – 2700 m 2488 – 2450 m	Reamed in hole

Sticking:

Date	Depth	Operation	Overpull (MT)
16.05.03	1872 – 1886 m	Attempted to orient. Drilling	10 – 15
19.05.03	2445 m	POOH with overpull, backreamed first stand	15
22.05.03	2653 - 2655 m 2660 – 2664 m	Picked up off bottom	35 – 40 45
24.05.03	2584 – 2564 m 2540 – 1761 m	POOH with overpull	15-30 up to 50
27.05.03	2825 m	Picked up off bottom	35
27.05.03	2878 – 2654 m	POOH. Max. Overpull at 2836m	up to 35
29.05.03	2038 m 2577 m	Picked up string	up to 27 up to 35
31.05.03	2579 – 2555 m 2110, 2065 m	POOH with overpull	max. 25
08.06.03	3272 m	BHA stuck with bit at +/- 3272 m while POOH	up to 50
14.06.03	2716 m 2485 – 2473 m	POOH with overpull	30 30

p. 29

Problem Zones:

16.05.03 Attempted to orientated drilling without success  
 18.05.03 Attempted to orientated drilling without success, unable to transfer weight to the bit  
 20.05.03 Attempted to orientated drilling without success, difficulty to transfer weight to the bit, difficulty controlling tool face orientation  
 21.05.03 Attempted to orientated drilling from 2633 to 2634 m without success  
 26.05.03 Strong build tendency in rotary mode. Orientated drilling from 2818-2825. Difficult to transfer weight to the bit.

**TROUBLE HORIZONS**

Sticking and tight hole :

Date	Depth	Operation	Overpull (MT)
16.05.03	1872 – 1886 m	Attempted to orient. Drilling	10 – 15
19.05.03	2445 m	POOH with overpull, backreamed first stand	15
22.05.03	2653 - 2655 m 2660 – 2664 m	Picked up off bottom	35 – 40 45
24.05.03	2584 – 2564 m 2540 – 1761 m	POOH with overpull	15-30 up to 50
27.05.03	2825 m	Picked up off bottom	35
27.05.03	2878 – 2654 m	POOH. Max. Overpull at 2836m	up to 35
29.05.03	2038 m 2577 m	Picked up string	up to 27 up to 35
31.05.03	2579 – 2555 m 2110, 2065 m	POOH with overpull	max. 25
08.06.03	3272 m	BHA stuck with bit at +/- 3272 m while POOH	up to 50

**Lost circulation horizons**

Between 750 m and 820 m (Late Cretaceous: Chalk Group) lost circulation. 167 m<sup>3</sup> accumulated mud losses. Pumped several LCM-Pills (nutshells).

# Stenlille -1

Year: 1980  
 Orientation: Vertical  
 TD: 1664 m MD RT  
 1622 m TVDSS  
 Status: Gas storage completion

## Encountered problems during drilling

Information on drilling problems in the Stenlille-1 well is based on information from the completion report:

DANSK NATURGAS/DANSK OLIE OG GASPRODUKTION : Completion report, Stenlille-1, June 1989. Report file no. 12417.

## Overview scheme (Fig. 1)

Drilling problems are presented in an overview scheme (Fig. 1) with relation to depth (MD) and lithostratigraphic units.

To the far right page numbers refer to sections in the completion report where the particular drilling problem is explained. The relevant sections are extracted from the final well report and presented subsequently. The extracts from the completion report concentrate on geology-induced drilling problems and how they were solved. Technical problems with no connection to geological conditions are not included. Sections with geological information that may turn out helpful during the drilling process may be included.

## Stenlille-1

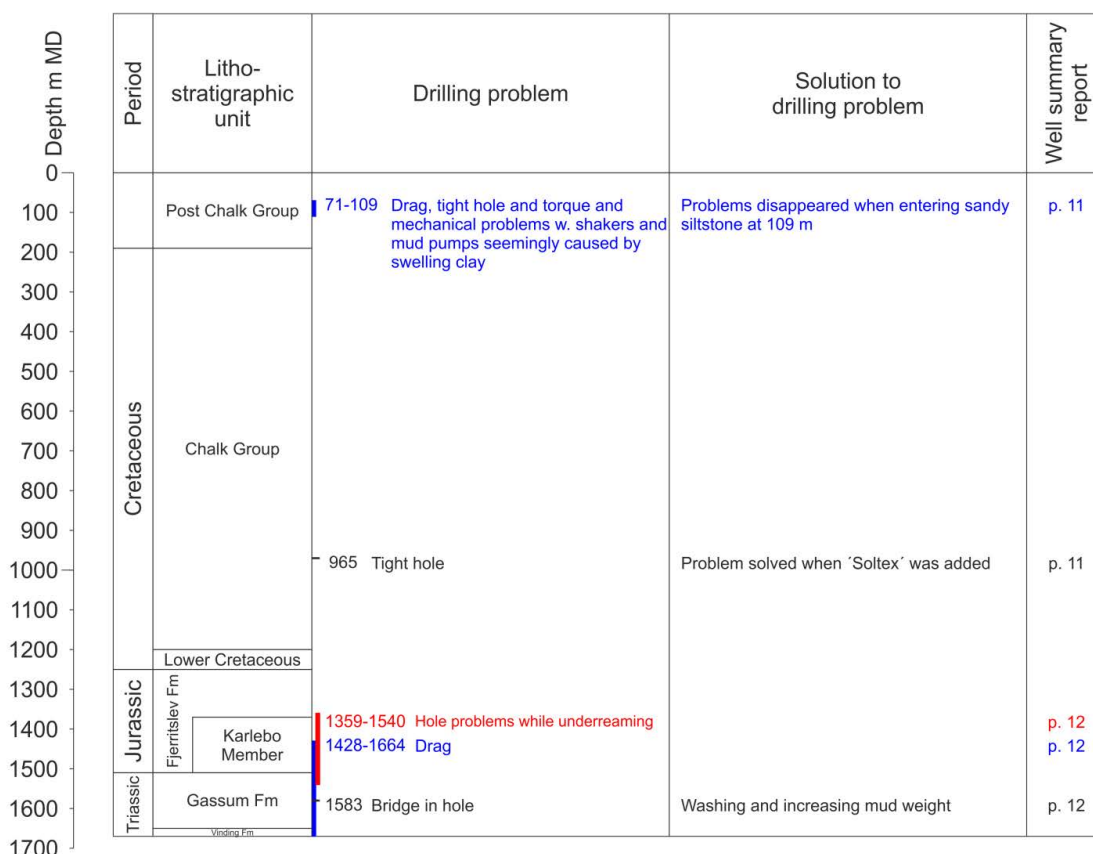


Figure 1. Overview of drilling problems related to depth and lithostratigraphic units in the Stenlille-1 well.

## Extracts from the completion report (Report file no. 12417)

### Introduction

p. 8 The Stenlille-1 well was spudded on 6th June, 1980, and TD (1664 m b.KB) was reached on 2nd July, 1980. No abnormal pressure, excessive gas or lost returns were encountered. The well was completed with 13 3/8" surface casing, 9 5/8" protective pipe and a 7" liner to TD. The maximum mud weight used was 10.3 ppq (1.24 s.g.).

### Drilling

p. 11 Stenlille-1 was spudded with a 17 1/2" bit through previously set 30" drive pipe on June 7, 1980. The surface hole was drilled to 337 m with a fresh water/bentonite mud. Some difficulties were experienced with drag, tight hole and torque in the interval from 71 - 109 m. A swelling clay seemed to be responsible and mechanical problems were experienced with the shakers and mud pumps. The formation problem disappeared going from the clay to sandy siltstone at 109 m. The well was logged and a conditioning trip was

p. 11 bly used below 368 m. At 965 m, the hole became tight and "Soltex" - an asphaltic fluid loss and encapsulating agent - was added to the mud in a concentration of 4-8 ppb. "Soltex" greatly reduces fluid loss and plasters the hole to plug weak matrix microfractures present in the shale which often cause sloughing problems. The

p. 12 The hole was logged and 9 5/8" casing set at 1048 m. A DV cement collar was placed at 565 m and the casing cemented in two stages due to potential lost returns problems. Full returns were maintained by slowing down the displacement after losing 30 bbl. The

p. 12 5/8" cement job. The 8 1/2" hole continued to a total well depth of 1664 m with minimal hole or mud problems. Drag was noted (5-15 tons) from 1428 m to TD which could have caused a problem had the hole been left open for a longer period of time. At TD, a full

p.12 As the cement job for the 7" liner was very important to isolate the zones to be tested from the caprock, the hole was underreamed to 11" from 1359 - 1540 m. The intent was to set the cement in plug flow to improve the chance of bond and decrease the probability of a channel. Hole problems were encountered while underreaming. When running in the hole after a trip, a bridge was encountered at 1583 m. The hole was washed and fresh shale cavings were observed at the shakers. Drag of up to 28 tons was noted. The mud weight was eventually increased to 10.3 ppq after about 1 1/2 days working on the hole and mud.

p.13 The mud system used in the Stenlille well with the use of "Soltex" was recommended to avoid possible problems due to a possibility of sloughing shales. It is difficult to judge the success of the mud system as problems did result after the hole had been open for 10 days while underreaming. In general, the "Soltex" was deemed successful although no comparison can be made with an offset well. The "Soltex" did provide an extremely low water loss, 1-3 cc API at a reasonable cost. Perhaps an explanation of the problem at the end of the well was that the concentration had decreased due to loss across the shakers and when underreaming, new hole was opened which required a high concentration of "Soltex" to plug the microfracture. A summary of mud parameters at various depths is listed in section 2.2 Mud Summary.

## Extracts from the end of well report (Report file no. 28567)

### Operations Summary

p. 29

17.5 " section                      123-587 m

The drilling was very rough from 123 to 158 m where an excessive bounce in the drillstring was experienced. Chert was encountered from 240 to 475 m.

Mud losses of 5 m<sup>3</sup>/hr were experienced from 465m to TD. LCM was pumped which minimised the losses to 2 m<sup>3</sup>/hr.

p. 30

12 1/4" section                      587-1551 m

Chert was encountered in the base of the Chalk Group. Before entering the Fjerritslev Formation the mudweight and KCl content were increased and 3% glycol added to reduce problems with hole instability in the reactive clays.

Adverse hole conditions, including hole sloughing and BHA packing off were encountered after drilling through the top of the Fjerritslev Formation.

Tight hole conditions were encountered while running in and out of the hole on the second BHA run. Overpulls up to a maximum of 33 MT were experienced between 1100 and 1550 m.

p. 31

8.5 " Hole section                      1551-2570 m

The mud weight was gradually increased from 1.20 to 1.26 sg to compensate for problems related to hole stability (tight hole, sloughing shales and hole fill).

## Daily Drilling Summary

p. 67	<p>Drilled 17 1/2" hole from 494m to 501m with reduced bit weight, and reduced pump rate. Slowed the pump rate to 2500 l/m and reduced the bit weight to 5 ton in an attempt to minimize mud losses. Sent a Hi Vis LCM pill around also. Losses did not immediately slow.</p> <p>Shut down and cleaned the LCM out of the screens in the pumps.</p> <p>Drilled 17 1/2" hole from 501m to 509m. The mud losses were steady at 5m<sup>3</sup>/hr. Drilling parameters were 2500 l/m, 5 ton wob, 74 bar, and 80 rpm. Continued to mix LCM into the active system. A visual check was made on the LCM content in and out. Going in the LCM content was approximately 4% by volume, and out was just a trace.</p> <p>Shut down and cleaned the LCM out of the pumps.</p> <p>Drilled 17 1/2" hole from 509m to 587m. The mud losses slowed to 2m<sup>3</sup>/hr. As stated above, the drilling parameters were reduced in order to minimize mud losses.</p>
p. 70	<p><b>Note:</b> There were traces of Chert in the samples from 1090m and increasing up to as much as 50% at 1100m. Reduced the rotary rpm to 20 after seeing the chert.</p>
p. 71	<p>Experienced some tight hole conditions at 1102m at which time, started washing and reaming in the hole at 500 m/h or less. Washed and reamed at this rate to a depth of 1180m.</p>
p. 72	<p>Worked tight hole from 1337m up to 1332m. Reamed this section 4 times then the tight hole and sloughing stopped. Made a connection.</p> <p>Directionally drilled and logged 12 1/4" hole from 1337m to 1349m.</p> <p>Worked tight hole from 1349m to 1345m. Again, after reaming 4 times, the sloughing and tight hole conditions stopped.</p> <p>Directionally drilled and logged 12 1/4" hole from 1349m to 1364m.</p> <p>Worked tight hole from 1364m to 1359m. After working through tight spots, hole conditions improved dramatically.</p> <p>Made a wiper trip from 1364m up to 1255m. Tight spots were encountered while pulling out from 1359m up to 1328m. Above 1328m the hole conditions were good. There were no bridges or tight spots going back in the hole. Maximum overpull was 22 ton.</p>

Washed and reamed tight hole from 1447m to 1420m. The bottom hole assembly would pack off causing an increase in pump pressure and would lift the drill string. Also saw sloughing causing excessive rotary torque. After reaming this section 4 times, hole conditions improved dramatically.

Normal rotary torque was 7000 to 11000 Nm. While reaming tight hole, the torque would increase to 11000 to 15000 Nm. Normal off bottom pump pressure at 200 spm was 185 bar. When the bottom hole assembly would pack off, the pump pressure would increase to as much as 210 bar.

Made a wiper trip from 1447m up to 1255m. The maximum overpull was 12 to 18 ton at 1376m, 1374m, and 1325m. Encountered tight hole when going back in hole at 1424m. Reamed back to bottom from 1424m.

## Drilling Fluids Summary

**17.5 " section**                      **123-587 m**

- p. 99        The 17-1/2" hole was drilled to 465 m, where losses were observed. A  
p. 100      10 m<sup>3</sup> LCM pill was pumped. The LCM pill was incorporated into the  
system to control losses to an acceptable level. Pumped high visc pill to  
clean the hole at TD.

This mud system turned out to work well and it is recommended for  
future wells in this area.

- p. 100      At 465 m, losses occurred. Losses were controlled by additions of  
Nutplug and Mica in different sizes.

**12 1/4" section**                      **587-1551 m**

- p. 101      Adverse hole conditions, including hole sloughing and BHA packing  
off, were encountered after drilling the top of the Fjerritslev Formation.

Tight hole conditions were encountered while running in and out of the  
hole on the second BHA run. Overpull at maximum 33 MT was  
experienced between 1100 and 1550 m.

The casing got stuck at TD after stopping reciprocation. The casing  
was freed again with 30 MT overpull.

**8.5 " Hole section**                      **1551-2570 m**

- p. 103      The mud weight was gradually increased from 1.20 s.g. to 1.26 s.g. to  
compensate for problems related to hole stability (tight hole, sloughing  
shale and hole fill). KCl was maintained at 140 kg/m<sup>3</sup> throughout the  
section.

# Stenlille-19

Year: 2000  
Orientation: Deviated  
TD: 2570 m MD RT  
2521 m TVDSS  
Status: Completed with Xmas tree

## Encountered problems during drilling

Information on drilling problems in the Stenlille-19 well is based on information from the end of well and final well reports:

DATALOG TECHNOLOGY LTD.: ST-19 (Stenlille-19). End of well report, August 2000. Report file no. 18092.

Schokker, H., DONG: ST-19 (Stenlille-19). Final well report, February 2001. Report file no. 28567.

## Overview scheme (Fig. 1)

Drilling problems are presented in an overview scheme (Fig. 1) with relation to depth (MD) and lithostratigraphic units.

To the far right page numbers refer to sections in the end of well and final well reports where the particular drilling problem is explained. The relevant sections are extracted from the final well report and presented subsequently. The extracts from the End of well report (Report file no. 18092) and the final well report (Report file no. 28567) concentrate on geology-induced drilling problems and how they were solved. Technical problems with no connection to geological conditions are not included. Sections with geological information that may turn out helpful during the drilling process may be included.

# Stenlille-19

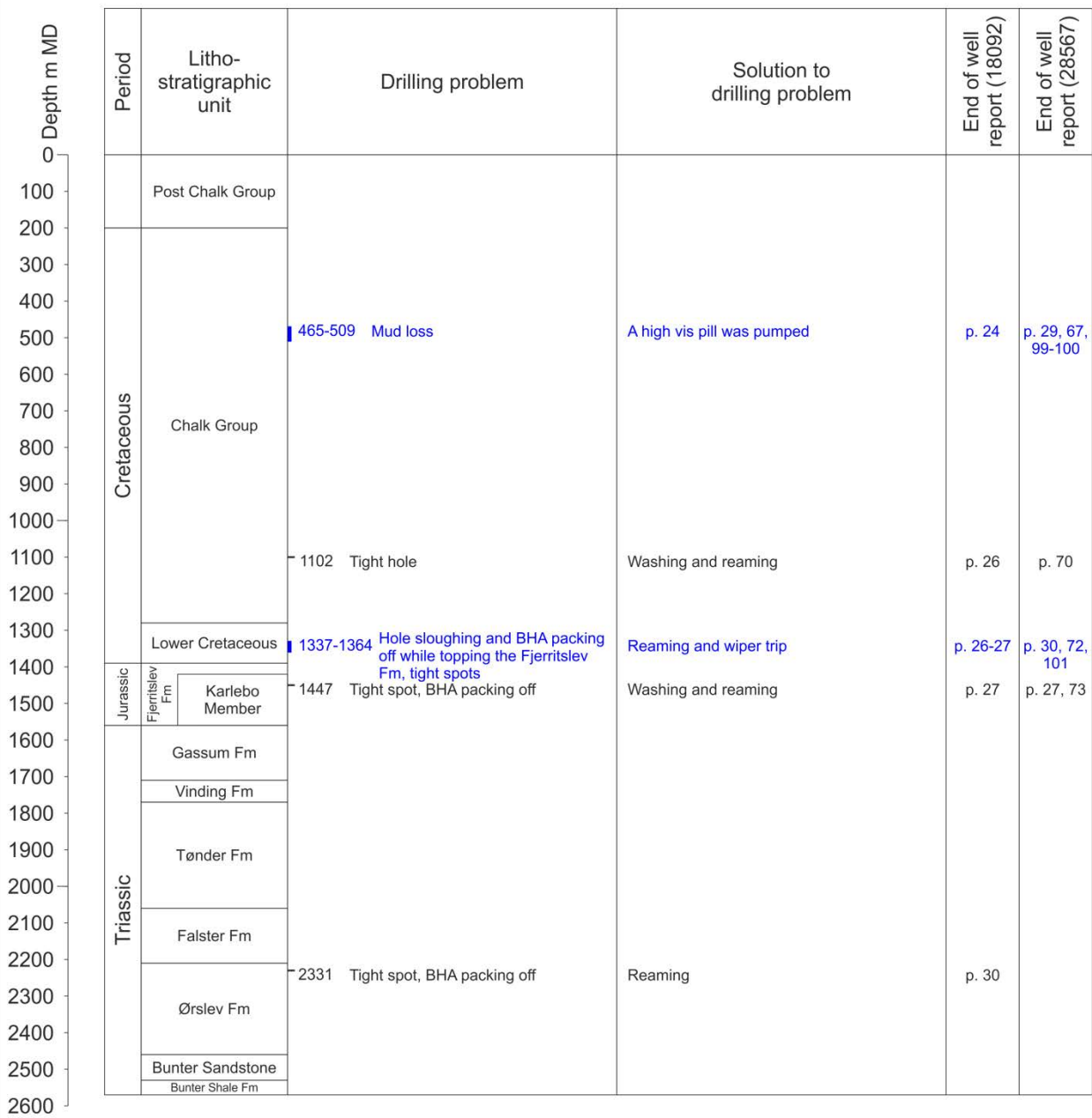


Figure 1. Overview of drilling problems related to depth and lithostratigraphic units in the Stenlille-19 well.

## Extracts from the end of well report (Report file no. 18092)

### Introduction

p. 4 core run was performed through the Gassum Formation. Drilling continued, again with a 8 ½” rotary assembly, to the second coring point at the top of the Bunter Sandstone at a depth of 2331m. The second core run ran from 2331m to 2349m and was pulled early due to poor rates of penetration. Drilling continued to the third core

### Engineering Summary

p. 24

#### 17.5 ” Hole section

Comments: The 17 ½” hole was drilled with no hole problems up to a depth of 465m, from here losses of 5 m<sup>3</sup>/hr were encountered, so the pump rate and weight on bit were reduced in attempt to minimise mud losses. Losses continued at a steady rate of 5 m<sup>3</sup>/hr to a depth of 509m. A high vis pill was pumped and losses slowed to 2 m<sup>3</sup>/hr to TD of the section at 587 m.

At section TD an 11m<sup>3</sup> Hi Vis pill was pumped and the hole was circulated clean. Total losses of 1.2m<sup>3</sup> were recorded on pulling out with the 17 ½” BHA.

The hole was cased using 50 joints of 13 3/8”, K-55/N80 grade casing. The shoe being set at 585m. No mud was lost during the cementing operations.

p. 25

#### 12 1/4” Hole section

No drilling / hole problems were encountered in this section, although the chert beds caused a considerable slower ROP in parts.

p. 26

Comments: On running in hole with the new assembly tight hole conditions were experienced at 1102m, at which time washing and reaming in the hole was performed to a depth of 1180m. From 1180m to 1240m, the hole was logged whilst washing and reaming at a rate of 45m/hr.

From 1240m the hole was directionally drilled and logged to 1337m, where adverse hole conditions became apparent, after topping the Fjerritslev formation such as hole sloughing and BHA packing off.

p. 27 In order to stop the tight hole and sloughing conditions, the hole was reamed from 1337m to 1364m several times. After working through the tight spots the hole conditions improved dramatically.  
A wiper trip was performed from 1364m to 1255m, again tight spots were encountered while pulling out from 1359m up to 1328m. There were no tight spots or bridges going back in the hole. Directionally drilled and logged to 1447m, where another tight spot occurred and again the hole was washed and reamed over the tight spot. While reaming the tight spot, the BHA would pack off causing an increase in pump pressure and also causing the drill string to lift. Hence another wiper trip was performed from 1447m up to 1255m. Going back in hole a tight spot was encountered at 1424m, so the hole was reamed back to bottom. No hole problems were encountered drilling to section TD at 1551m, with a hole inclination of 2.07°. On reaching TD a 5m<sup>3</sup> High Vis Viscosity sweep was pumped and the mud was circulated and conditioned. Tight spots were encountered whilst pulling out of hole between 1518m to 1160m, with overpull ranging between 10 – 25 Tons. The 9 5/8" and 10 3/4" Casing was run with no problems with the shoe being set at 1548m. No losses occurred during the displacement of the cement.

p. 29

#### 8.5 " Hole section

Comments: The coring assembly was run in and the core was cut from 1630m to 1665.5m. ROP in the clay section was up to 5m/hr whilst the sand produced 60m/hr. 89% recovery was obtained. The string was pulled to surface with no problems.

p. 30

Comments: Bit #5 was made up and re-run into the hole and the core section was reamed out to 1665.5m. Drilling continued to 1859m without directional control due to MWD failure. A TOTCO survey was then run and drilling continued to 1942m after which MWD resumed operation. The well was then directionally drilled to the second coring point at 2331m. Problems occurred when pulling out and the pipe had to be reamed through some tight spots. This was mainly due to the hole packing off.

p. 31

Comments: Core bit #6RR was run in and had to be washed and reamed down to bottom. During coring extremely low penetration rates (averaging < 1m/hr) were obtained due to the presence of hard claystone at the top of the run. No sandstone was found in the cuttings samples and the decision to pull the bit after 17.9m was made.

## Extracts from the final well report (Report file no. 28567)

### Operations Summary

p. 29

**17.5 " section**                      **123-587 m**

The drilling was very rough from 123 to 158 m where an excessive bounce in the drillstring was experienced. Chert was encountered from 240 to 475 m.

Mud losses of 5 m<sup>3</sup>/hr were experienced from 465m to TD. LCM was pumped which minimised the losses to 2 m<sup>3</sup>/hr.

p. 30

**12 1/4" section**                      **587-1551 m**

Chert was encountered in the base of the Chalk Group. Before entering the Fjerritslev Formation the mudweight and KCl content were increased and 3% glycol added to reduce problems with hole instability in the reactive clays.

Adverse hole conditions, including hole sloughing and BHA packing off were encountered after drilling through the top of the Fjerritslev Formation.

Tight hole conditions were encountered while running in and out of the hole on the second BHA run. Overpulls up to a maximum of 33 MT were experienced between 1100 and 1550 m.

p. 31

**8.5 " Hole section**                      **1551-2570 m**

The mud weight was gradually increased from 1.20 to 1.26 sg to compensate for problems related to hole stability (tight hole, sloughing shales and hole fill).

## Daily Drilling Summary

p. 67

Drilled 17 1/2" hole from 494m to 501m with reduced bit weight, and reduced pump rate. Slowed the pump rate to 2500 l/m and reduced the bit weight to 5 ton in an attempt to minimize mud losses. Sent a Hi Vis LCM pill around also. Losses did not immediately slow.

Shut down and cleaned the LCM out of the screens in the pumps.

Drilled 17 1/2" hole from 501m to 509m. The mud losses were steady at 5m<sup>3</sup>/hr. Drilling parameters were 2500 l/m, 5 ton wob, 74 bar, and 80 rpm. Continued to mix LCM into the active system. A visual check was made on the LCM content in and out. Going in the LCM content was approximately 4% by volume, and out was just a trace.

Shut down and cleaned the LCM out of the pumps.

Drilled 17 1/2" hole from 509m to 587m. The mud losses slowed to 2m<sup>3</sup>/hr. As stated above, the drilling parameters were reduced in order to minimize mud losses.

p. 70

**Note:** There were traces of Chert in the samples from 1090m and increasing up to as much as 50% at 1100m. Reduced the rotary rpm to 20 after seeing the chert.

p. 71

Experienced some tight hole conditions at 1102m at which time, started washing and reaming in the hole at 500 m/h or less. Washed and reamed at this rate to a depth of 1180m.

p. 72

Worked tight hole from 1337m up to 1332m. Reamed this section 4 times then the tight hole and sloughing stopped. Made a connection.

Directionally drilled and logged 12 1/4" hole from 1337m to 1349m.

Worked tight hole from 1349m to 1345m. Again, after reaming 4 times, the sloughing and tight hole conditions stopped.

Directionally drilled and logged 12 1/4" hole from 1349m to 1364m.

Worked tight hole from 1364m to 1359m. After working through tight spots, hole conditions improved dramatically.

Made a wiper trip from 1364m up to 1255m. Tight spots were encountered while pulling out from 1359m up to 1328m. Above 1328m the hole conditions were good. There were no bridges or tight spots going back in the hole. Maximum overpull was 22 ton.

Washed and reamed tight hole from 1447m to 1420m. The bottom hole assembly would pack off causing an increase in pump pressure and would lift the drill string. Also saw sloughing causing excessive rotary torque. After reaming this section 4 times, hole conditions improved dramatically.

Normal rotary torque was 7000 to 11000 Nm. While reaming tight hole, the torque would increase to 11000 to 15000 Nm. Normal off bottom pump pressure at 200 spm was 185 bar. When the bottom hole assembly would pack off, the pump pressure would increase to as much as 210 bar.

Made a wiper trip from 1447m up to 1255m. The maximum overpull was 12 to 18 ton at 1376m, 1374m, and 1325m. Encountered tight hole when going back in hole at 1424m. Reamed back to bottom from 1424m.

## Drilling Fluids Summary

**17.5 " section**                      **123-587 m**

- p. 99        The 17-1/2" hole was drilled to 465 m, where losses were observed. A  
p. 100      10 m<sup>3</sup> LCM pill was pumped. The LCM pill was incorporated into the  
              system to control losses to an acceptable level. Pumped high visc pill to  
              clean the hole at TD.

This mud system turned out to work well and it is recommended for future wells in this area.

- p. 100      At 465 m, losses occurred. Losses were controlled by additions of  
              Nutplug and Mica in different sizes.

**12 1/4" section**                      **587-1551 m**

- p. 101      Adverse hole conditions, including hole sloughing and BHA packing  
              off, were encountered after drilling the top of the Fjerritslev Formation.

Tight hole conditions were encountered while running in and out of the hole on the second BHA run. Overpull at maximum 33 MT was experienced between 1100 and 1550 m.

The casing got stuck at TD after stopping reciprocation. The casing was freed again with 30 MT overpull.

**8.5 " Hole section**                      **1551-2570 m**

- p. 103      The mud weight was gradually increased from 1.20 s.g. to 1.26 s.g. to  
              compensate for problems related to hole stability (tight hole, sloughing  
              shale and hole fill). KCl was maintained at 140 kg/m<sup>3</sup> throughout the  
              section.



**Enclosure 2: Well log panel covering the Gassum Fm – Fjerritslev Fm (including Karlebo Mb) interval, showing sequence stratigraphic key surfaces, lithology in wells and position of samples collected for bulk- and clay mineralogy analysis. Positions of wells are shown in Figures 1.1.**

